Photocatalytic Carbon – Carbon Bond Formations with Visible Light

Dissertation

Zur Erlangung des Doktorgrades

Dr. rer. nat.

der Fakultät für Chemie und Pharmazie

der Universität Regensburg

vorgelegt von

Paul Simon Kohls

aus Aalen

Regensburg 2015

Die Arbeit wurde angeleitet von: Prof. Dr. Oliver Reiser

Promotionsgesuch eingereicht am: 16.02.2015

Promotionskolloquium am: 04.03.2015

Prüfungsausschuss: Vorsitz: Prof. Dr. Sigurd Elz

1. Gutachter: Prof. Dr. Oliver Reiser

2. Gutachter: Prof. Dr. Kirsten Zeitler

3. Gutachter: Prof. Dr. Manfred Scheer

Der experimentelle Teil der vorliegenden Arbeit wurde in der Zeit von Oktober 2010 bis April 2014 unter der Gesamtleitung von Prof. Dr. O. Reiser am Lehrstuhl für Organische Chemie der Universität Regensburg angefertigt. Zusätzlicher Betreuer war von Januar 2012 bis April 2012 Dr. Ganesh Pandey am National Chemical Laboratory, Pune (IN).

Besonders bedanken möchte ich mich bei Herrn Prof. Dr. O. Reiser für die Aufnahme in seinen Arbeitskreis, die Überlassung des interessanten Themas, die anregenden Diskussionen und die stete Unterstützung.

Meiner Familie

"Experience is what you get when you didn´t get what you wanted."

Randy Pausch (computer scientist)

Table of Content

A. Introduction

Photoredox catalysis with visible light[1, 2] may not yet be a chemist's first choice to tackle synthetic problems because of old prejudices deriving from UV photochemistry and an unawareness of its possibilities. However, using visible light offers a variety of advantages, starting from unique reactivities, the ease of handling the reactions and the ubiquitous availability of solar or artificial light. For most reactions a small LED or ordinary light bulb is sufficient; no special glassware or safety procedures are required.

Most organic molecules do not absorb light in the visible region and therefore a photoredox catalyst is required to transfer the energy of the photon to the reagent. This offers the advantage that the target molecule itself is not excited and cannot undergo undesired side reactions without activation by the catalyst. The energy is either transferred by sensitization or electron transfer, whereof the later will be discussed here. Many metal complexes, mostly containing a ruthenium, iridium or copper central ion, and some organic molecules offer this trait. [3, 4, 5]

The most prominent one is tris(bipyridine)ruthenium(II) (**1**) (Figure 1)[2, 6, 7, 8] and this article will give an overview of its manifold applications in photoredox catalysis.

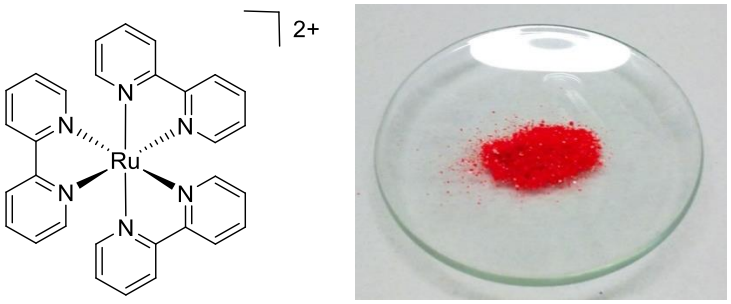

Figure 1. Tris(bipyridine)ruthenium(II) (**1**).

This complex is mostly used as dichloride hexahydrate salt which is commercially available. Other commonly used anions are $(PF_6)^-$ and $(BF_4)^-$. The complex was first reported by Burstall *et al.* back in 1936 and can be synthesized starting from $RuCl_3$ according to a procedure by Young *et al.*[2, 9]

Many organic molecules can be activated by **1,** and the number of reactions utilizing this is growing every day. First reports using $Ru(bpy)_3Cl_2$ date back to the late 70s, when this concept was known as photo sensitized reactions, but has not received much attention until recent years when the field was revived by David MacMillan, [10] Tehshik Yoon[11] and Corey Stephenson.[12]

Table 1. Photophysical and electrochemical properties of $Ru(bpy)_3^{2+}$ (**1**).

excitation λ_{max}	452 nm	**$E_{1/2}^{a)}(Ru^{II}*/Ru^{I})$**	+ 0.77 V
emission λ_{max}	615 nm	**$E_{1/2}^{a)}(Ru^{II}/Ru^{I})$**	- 1.33 V
excited state lifetime	1100 ns	**$E_{1/2}^{a)}(Ru^{III}/Ru^{II}*)$**	- 0.81 V
		$E_{1/2}^{a)}(Ru^{III}/Ru^{II})$	+ 1.29 V

a) Measurements conducted in acetonitrile at room temperature and values are given in Volt *vs.* a saturated calomel electrode (SCE).

An explanation for the current increased interest in photochemistry are the demand for novel, environmental begin reaction and new developments in the field of lighting devices such as LEDs and fluorescent light bulbs. LEDs have a narrow emission peak and can therefore excite the catalyst at or close to its maximum absorption and no energy is wasted in the generation of photons that cannot be absorbed by the catalyst and may cause side reactions.

The simplest setup for a photoreaction consists of a vessel, e.g. a round-bottom flask or a snap cap vial, containing the reaction solution which is irradiated by an external lighting source, such as a light bulb, a LED or the sun.

A better option to transfer light directly into the reaction solution is *via* an optical fiber (Figure 2). Applying such a setup minimizes the amount of light that is lost through absorption by the glass wall of the vessel and therefore more of the emitted photons can excite the photocatalyst compared to a classical setup. In addition, it is possible to heat or cool the solution to any desired temperature without taking precautions for the light source.

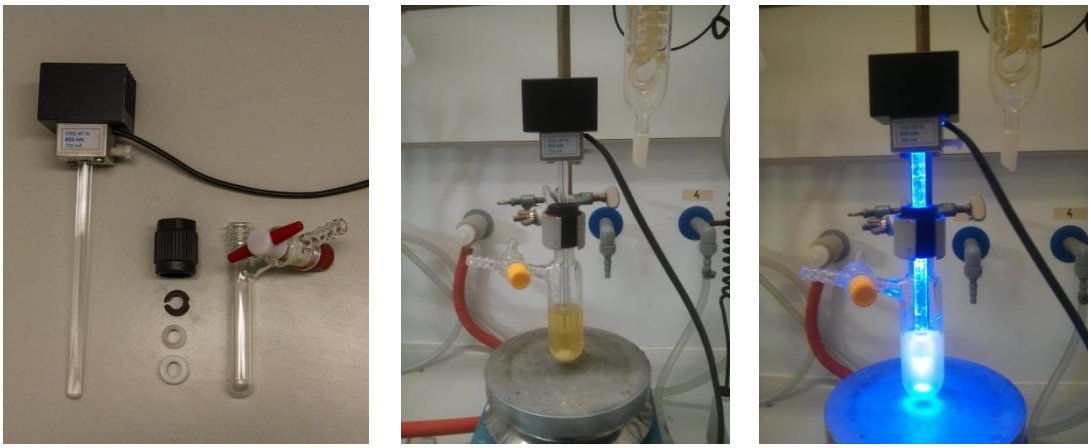

Figure 2. Irradiation systems using optical fibers.

A convenient setup developed by Reiser *et al.* is depicted in figure 2.[13] A LED with an appropriate wavelength to activate the catalyst channels light into a glass rod whose other end is inside a Schlenk tube containing the reaction solution.

Because of its maximum absorption at 452 nm blue LEDs are most efficient to excite $Ru(bpy)_3^{2+}$ (**1**). In general, photoredox catalysts have a very high extinction coefficient. The molar absorptivity of $Ru(bpy)_3^{2+}$ (**1**) at 452 nm is $\varepsilon = 14.6\ mM^{-1}\ cm^{-1}$.[6]

$$A_\lambda = \lg\left(\frac{I_0}{I}\right) = \varepsilon\ c\ d \qquad \text{(Eq. 1)}$$

$$d = \frac{\lg(\frac{I_0}{I})}{\varepsilon\ c} \qquad \text{(Eq. 2)}$$

A_λ: molar absorbance; I_0: intensity of the incident light; I: intensity of the transmitted light; ε: molar absorptivity; c: molar concentration ; d: depth of penetration.

Solving the Beer-Lambert law (Eq. 1) for a typical photoredox reaction with a concentration of 1 mmol/l $Ru(bpy)_3^{2+}$ (1 mol% $Ru(bpy)_3^{2+}$ at a substrate concentration of 0.1 mol/l) reveals that 99% of the incident light are absorbed within 1.4 mm and 99.9% do not penetrate the flask further than 2.1 mm.

Employing 5 mol% of catalyst at the same substrate concentration of 0.1 mol/l resulting in a catalyst concentration of 5 mmol/l, 99% of the incident light are already absorbed within 0.3 mm. Therefore a high surface area is beneficial in order to excite as many catalyst molecules at the same time as possible. This can for example be achieved by employing a micro reactor (Figure 3). These systems consist of glass or plastic plate containing a long, thin channel through which the reaction solution is pumped at a defined speed. The reactor is irradiated from above with an appropriate light source. This offers a variety of advantages. Because the channels are very thin, nearly every catalyst molecule can be excited by the incident light. The speed of pumping and therefore the reaction time can be controlled very precisely with the help of a syringe or HPLC pump. Exposure of the reaction mixture to the light source before and after passing the reactor is avoided, thus preventing decomposition and side reactions. Also the temperature can be controlled and changed rapidly due to the small dimensions of the micro reactor. The disadvantages of this system are the high costs of the reactors and the pump system. In addition the channels can be blocked easily by precipitates which are difficult to remove.

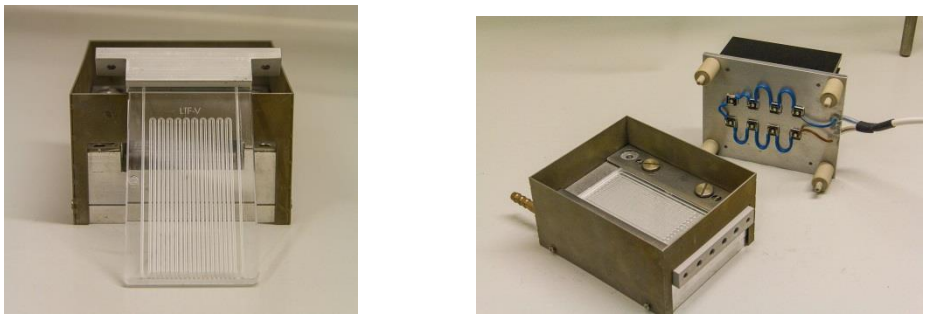

Figure 3. Micro reactor system for photocatalysis.

A more cost efficient alternative are FEP (fluorinated ethylene propylene copolymer) tube reactors. They can be assembled by wrapping a FEP tube around a cylinder, for example a beaker, and putting the light source inside. By changing the length of the tube, the internal volume of the reactor can be adjusted to the demands of the reaction. Stephenson *et al.* and Zeitler *et al.* demonstrated the advantages of micro reactors and tube reactors compared to batch systems.[14, 15]

At first a simplified picture of the mode of actions of tris(bipyridine)ruthenium(II) (**1**) is given in Scheme 1; a more detailed discussion can be found below.

By absorption of a photon $Ru(bpy)_3^{2+}$ is transferred to the excited state $Ru(bpy)_3^{2+}$*. Depending on the other reactants present, the excited photocatalyst can undergo either reductive or oxidative quenching. Reductive quenching is found when the catalyst accepts an electron from a donor **D** and lowers thereby its oxidation state to Ru^{I}. $Ru(bpy)_3^{2+}$ is regenerated by donation of an electron to a suitable acceptor **A**.

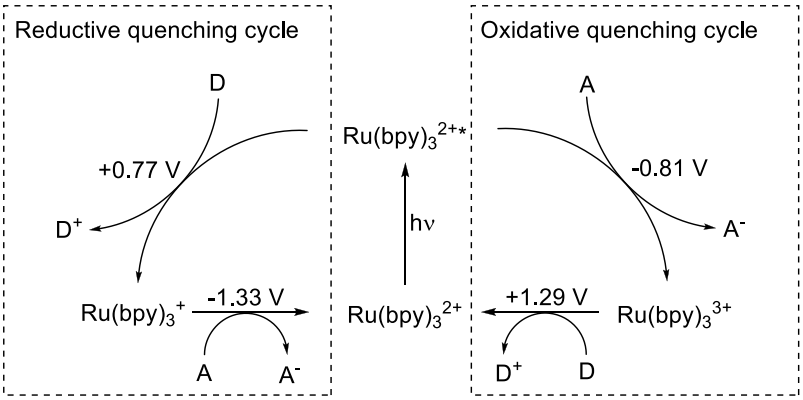

Scheme 1. Photocatalytic reaction of $Ru(bpy)_3^{2+}$ (**1**) (D: electron donor, A: electron acceptor).

The oxidative quenching cycle operates in the opposite way. By donation of an electron from excited $Ru(bpy)_3^{2+}$* to an acceptor **A** the oxidation state is raised to Ru^{III}. Regeneration of the ground state $Ru(bpy)_3^{2+}$ takes place by accepting an electron from a present donor **D**.

More information about each step can be obtained by applying quantum mechanics and taking a look at the Jablonski diagram (Scheme 2). Powered by the absorption of a photon a metal centered electron is transferred to an unoccupied ligand orbital resulting in the S_1 state (Scheme 2, B). This is called a metal to ligand charge transfer (MLCT), resembling a formal oxidation of the metal core and a single electron reduction (SET) of the ligand. Instead of losing its energy by fluorescence or thermal vibration, $Ru(bpy)_3^{2+}$ undergoes intersystem crossing (ISC) to a more stable triplet state (Scheme 2, C).

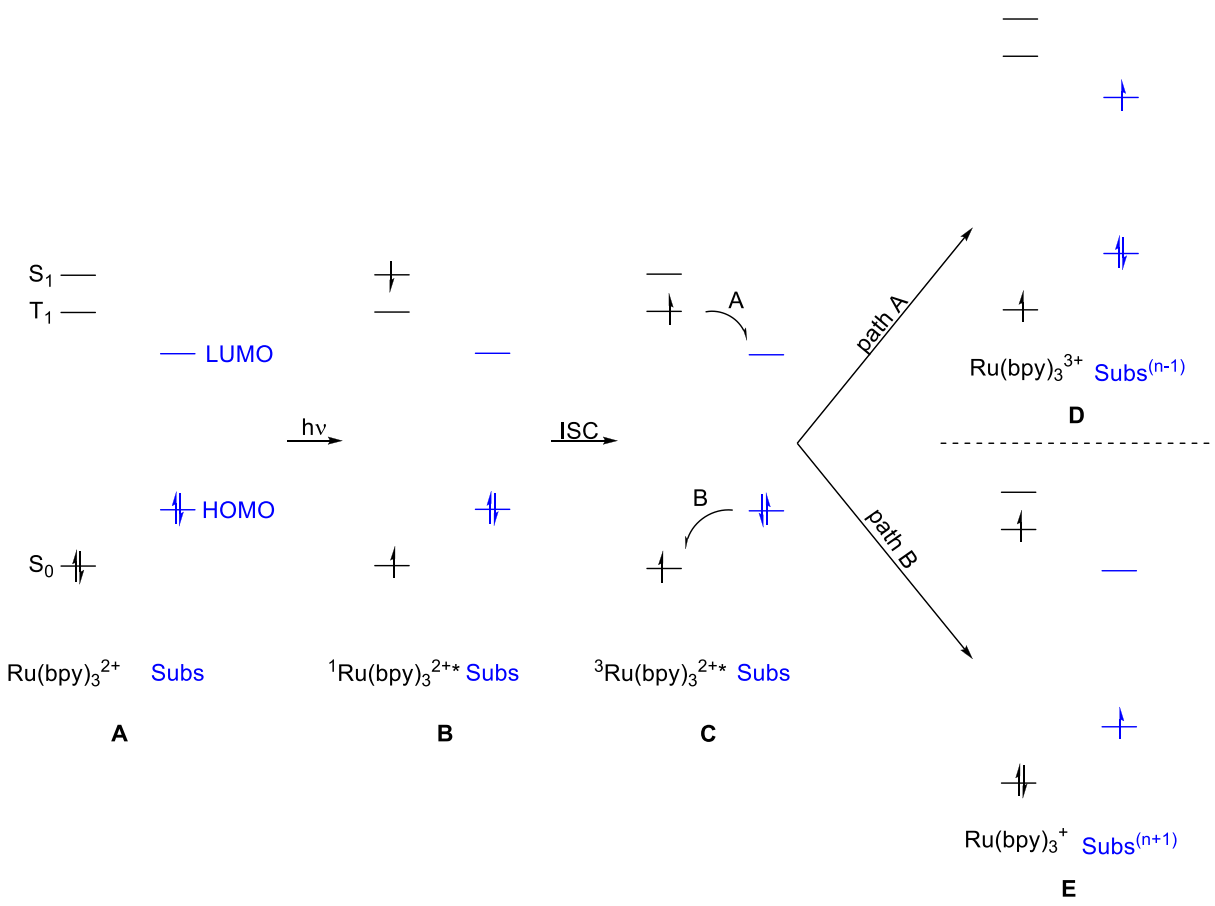

Scheme 2. Jablonski diagram of a photocatalyst interaction with another molecule.

This triplet state with a metal centered hole and a ligand centered additional electron is the catalytic active species. The catalyst can donate the additional ligand centered electron to an acceptor (Scheme 2, path A, oxidative quenching cycle) or accept an electron leading to a reduction of the metal core (Scheme 2, path B, reductive quenching cycle).

$Ru(bpy)_3^{2+}$ in its ground state is regenerated either by accepting an electron from a donor into a metal centered orbital (path A) or by donating one from the ligand to an acceptor (path B).

In general, tris(bipyridine)ruthenium(II) (**1**) serves as an electron pump, shuttling electrons from a donor to an acceptor. It is commercially available at a reasonable price or can be synthesized starting from $RuCl_3$. The catalyst is excited by blue light (λ_{max} = 452 nm) and can undergo, starting from its excited triplet state, either reductive or oxidative quenching.

1. Photocatalytic Reactions Proceeding *via* the Reductive Quenching Cycle of $Ru(bpy)_3^{2+}$

The most utilized reaction pathway is the reductive quenching cycle, where excited $Ru(bpy)_3^{2+*}$ in its triplet state accepts an electron from a substrate molecule which is oxidized at the time (Scheme 3). The oxidation potential of this step is $E_{1/2}$ (Ru^{II}*/Ru^{I}) = + 0.77 V *vs.* SCE in acetonitrile.[6] A more detailed picture is given in chapter 1.1.

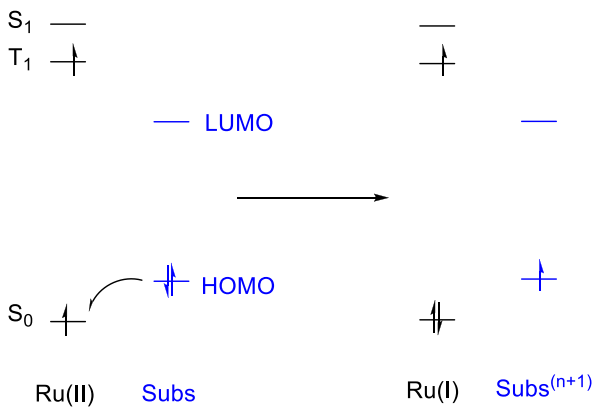

Scheme 3. Jablonski diagram of the transition $Ru(bpy)_3^{2+}$* → $Ru(bpy)_3^{+}$.

By donating an electron from a ligand centered orbital to a substrate molecule $Ru(bpy)_3^{+}$ is oxidized to $Ru(bpy)_3^{2+}$ regenerating the initial state of the catalyst (Scheme 4) and reducing the substrate. The reduction potential of this step is $E_{1/2}$ (Ru^{II}/Ru^{I}) = - 1.33 V *vs.* SCE in acetonitrile.[6] More information on this transformation is found in chapter 1.2.

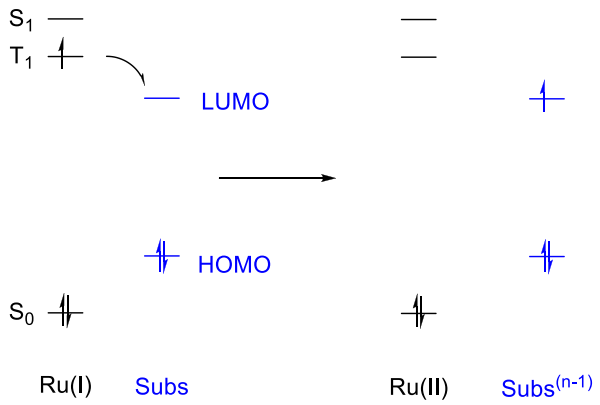

Scheme 4. Jablonski diagram of the transition $Ru(bpy)_3^{+}$ -> $Ru(bpy)_3^{2+}$.

1.1 Reactions initiated by Substrate Oxidation

The reactions discussed in this chapter have in common that the photochemical transformation is initiated by the oxidation of a substrate. Most molecules addressable in this step have in common that they contain a nitrogen atom. These are for example tetrahydroisoquinoline derivatives (Scheme 5, 7, 9, 10, 11, 12, 14, and 17), dihydroacridine derivatives (Scheme 15), aniline derivatives (Scheme 14), imine derivatives (Scheme 19), hydrazones (Scheme 20) and *N*-α-centered radicals (Scheme 28). Some of the reactions only require the oxidation of the substrate (Scheme 5, 8, 9, 10, 17, 18, 19 and 20). In those cases the catalyst is regenerated by a sacrificial electron acceptor. Oxygen is used most frequently as electron acceptor and also molecules with an activated carbon-bromine bond, e.g. bromotrichloromethane (**8**). On the other hand there are reactions that require, after the initial oxidation, a reduction to finish the transformation (Scheme 11, 13 and 14). These processes are overall redox neutral and often very atom economic.

Stephenson *et al.* were the first to report a photocatalytic oxidation of tetrahydroisoquinoline **2a** to the corresponding iminium ion **6a**.[16] This cation is trapped subsequently by deprotonated nitromethane (**3**) in an *aza*-Henry type reaction giving rise to nitro compound **4a** in up to 81% yield using $Ru(bpy)_3Cl_2$ (**1**·Cl_2) (Scheme 5).

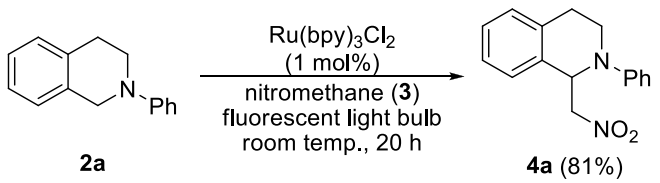

Scheme 5. Photocatalytic *aza*-Henry reaction.

The first step of the proposed reaction mechanism is the transfer of an electron from isoquinoline **2a** into a metal orbital of excited $Ru(bpy)_3^{2+}$* following the Jablonski diagram shown in Scheme 3. Arising $Ru(bpy)_3^{+}$ is reoxidized with the help of a sacrificial electron donor, in this case molecular oxygen (Scheme 4). The reduced donor O_2^- abstracts a hydrogen atom from **5a** leading to the formation of iminium ion **6a**, the proposed key intermediate. In the final step **6a** is attacked by deprotonated nitromethane **23** forming the final product **4a** (Scheme 6).

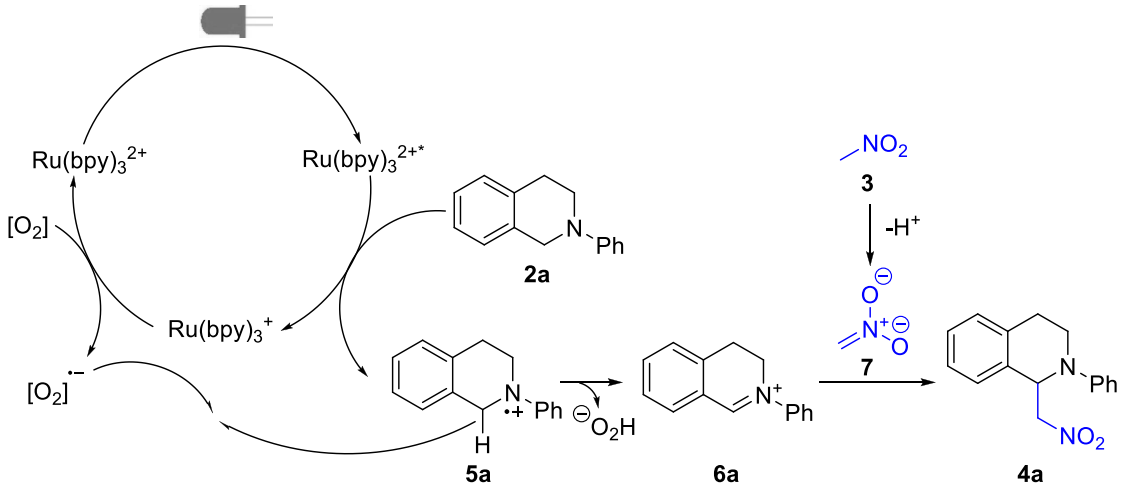

Scheme 6. Mechanism of a photocatalytic *aza*-Henry reaction.

Two years later the group of Corey Stephenson developed a method to generate the stable isoquinoline iminium ion [**6a**·Br] with the help of bromotrichloromethane (**8**).[17] In the first step one electron from isoquinoline **2a** is transferred to excited $Ru(bpy)_3^{2+}$* forming radical cation **5a**. In contrast to the mechanism in Scheme 5, where $Ru(bpy)_3^{2+}$ (**1**) is regenerated by O_2, **1** is regenerated by reduction of bromotrichloromethane to radical anion **9** which splits into a bromide ion and trichloromethane radical **10**.

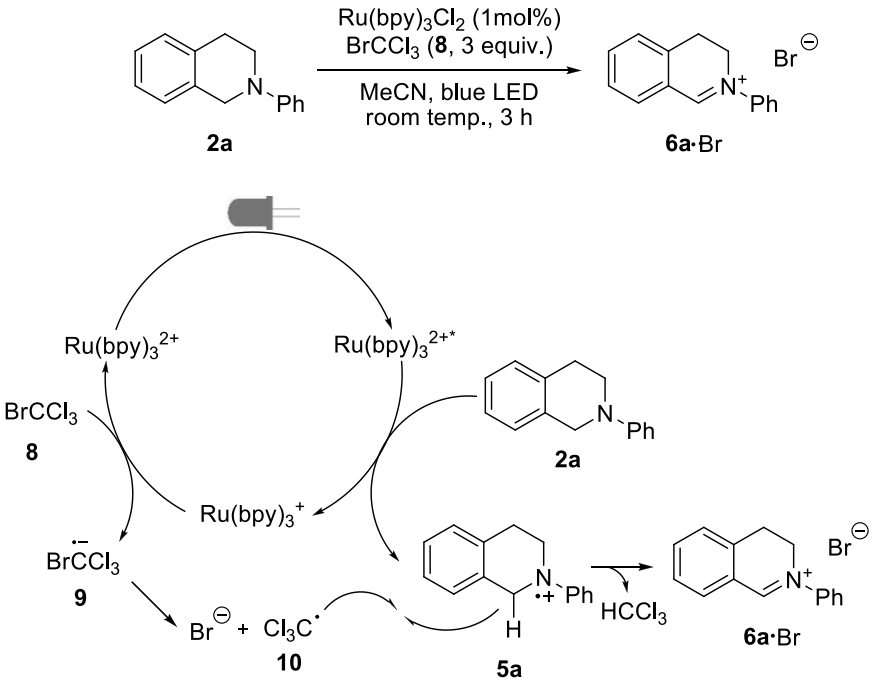

Scheme 7. Generation of stable isoquinoline iminium ions (**6a**·Br).

Radical **10** abstracts a hydrogen atom from the *N*-α-position of **5a** resulting in the formation of chloroform and iminium ion **6** which is stabilized by bromide (Scheme 7). When **2a** was fully converted to stable [**6a**·Br], the light was switched off and a nucleophile was added.

This method enabled Stephenson et *al*. to broaden the scope of nucleophiles because no interaction of the active catalyst or other reactive species generated during the irradiation process and the nucleophile can take place. Apart from nitromethane (**3**) they were able to use, amongst others, allyl silane **12**, siloxyfurane **13** and malonate **14**. Most interestingly, also a photocatalytic alkynylation was performed by addition of alkyne **15** and copper(I)bromide as co-catalyst (Scheme 8).

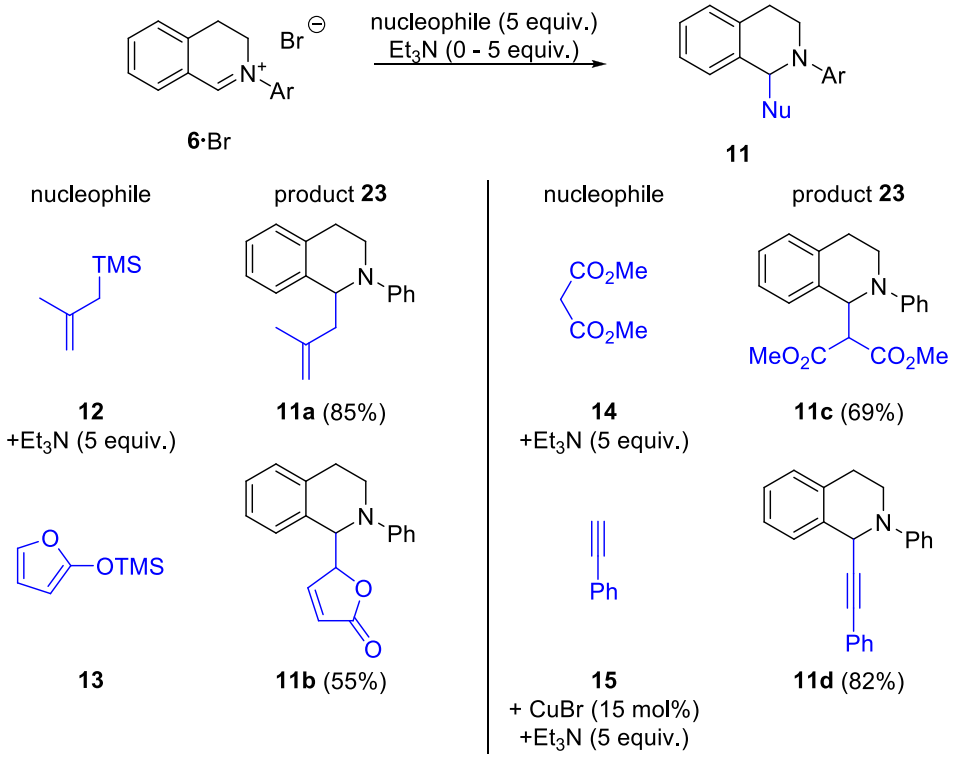

Scheme 8. Scope of nucleophilic trapping of iminium ion **22a**·Br.

By combining this method with asymmetric anion binding catalysis, Stephenson and Jacobsen showed that silyl ketene acetal **16** can be enantioselective coupled to the preformed iminium ion [6**a**·Cl].[18] Chiral thiourea derivative **17** proofed to be the right co-catalyst for this reaction. The stoichiometric oxidant and the counterion had to be changed to CCl_4 and Cl^- respectively. In addition the solvent was changed from acetonitrile to the less polar solvent methyl *tert*-butyl ether (MTBE) after the initial conversion of isoquinoline **2a** (Scheme 9) to [**6a**·Cl]. This step was necessary to enhance the formation of the chiral catalyst-counterion-substrate transition complex.

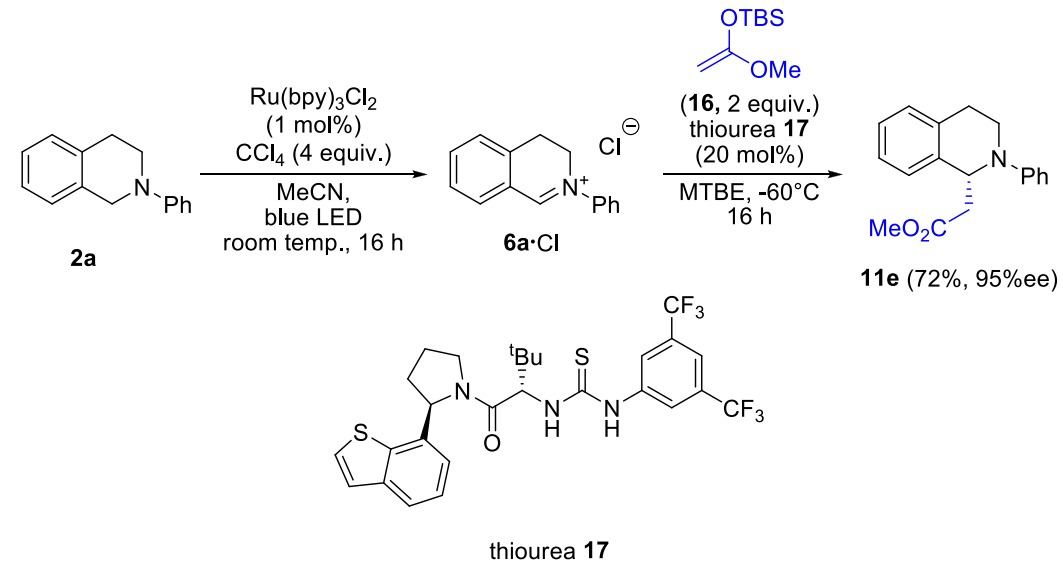

Further examples:

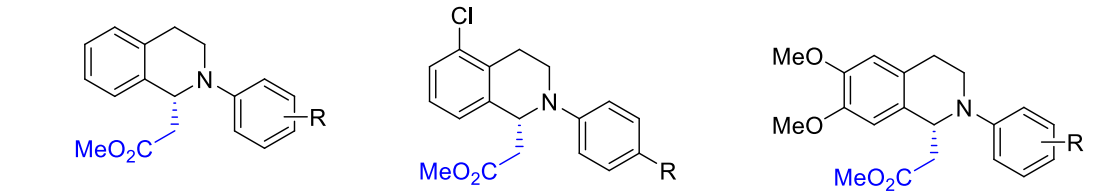

11f (R = 2-OMe) (62%, 99%ee)
11g (R = 4-OMe) (60%, 84%ee)
11h (R = 2,4-OMe) (52%, 96%ee)
11i (R = 4-Br) (69%, 86%ee)
11j (R = 4-Cl) (62%, 99%ee)

11k (R = H) (58%, 92%ee)
11l (R = Cl) (48%, 82%ee)

11m (R = H) (14%, 67%ee)
11n (R = 4-Cl) (44%, 42%ee)
11o (R = 2-OMe) (11%, 79%ee)

Scheme 9. Enantioselective synthesis of β-amino esters.

The position of a substituent on the *N*-aryl moiety had a greater influence on the enantioselectivity of the reaction than its electronic nature. In general *ortho* substituted *N*-aryl isoquinolines let to higher enantioselectivities compared to *para* substituted ones (*cf.* **11f** and **11g**). On the other hand, the electronic nature of substituents on the tetrahydroisoquinoline ring had a severe influence on the enantioselectively. Electron poor substrates usually gave higher yields and/or higher selectivity than electron rich ones (*cf.* **11k** and **11m**) (Scheme 9).

The concept of photoredox catalysis was combined with organocatalysis by Rueping *et al*. in order to perform photocatalytic Mannich reactions.[19] They were able to couple acetone with isoquinoline **2** using $Ru(bpy)_3(PF_6)_2$ (**1**·$(PF_6)_2$) and L-proline (**18**) as catalysts (Scheme 10). The key intermediate in this step is iminium ion **6** and the pathway for its formation is the same as proposed by Stephenson et *al*. (Scheme 6).[16] **6** is trapped by enamine **19** which is formed from acetone and L-proline (**18**) yielding product **20** in excellent yield.

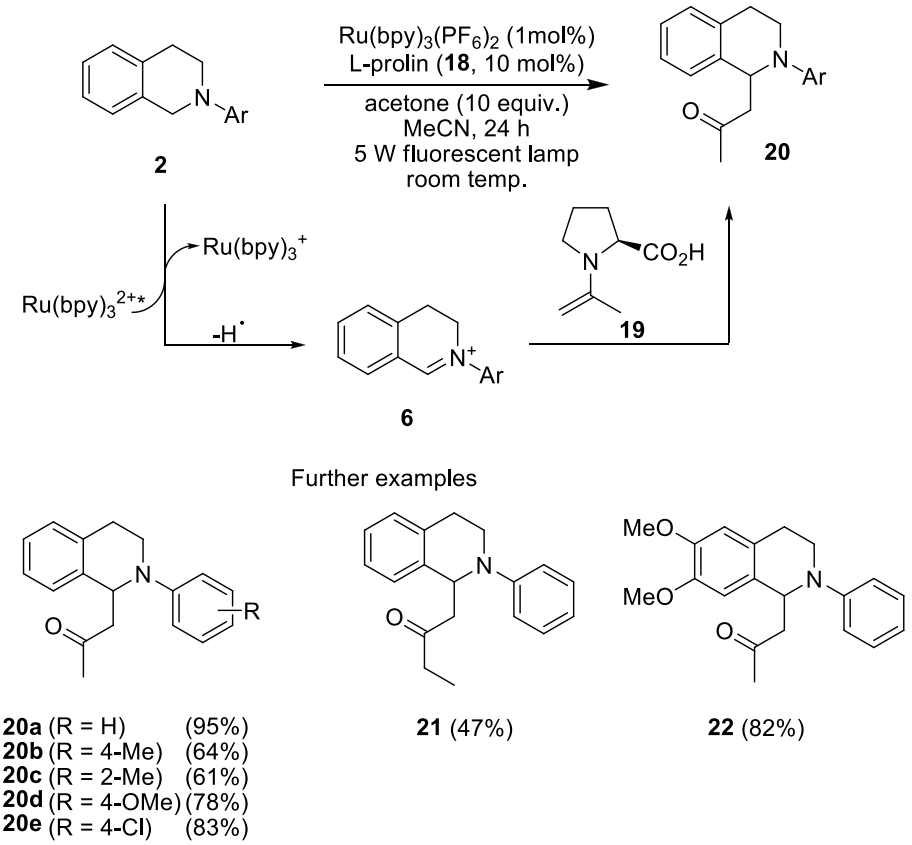

Scheme 10. Photocatalytic Mannich reaction.

Interestingly, the yield of the reaction decreases if a more powerful light source, like a LED, is used. This observation suggests that iminium ion **6a** decomposes under these conditions and its concentration has to be low in comparison to the nucleophile in order be trapped immediately after its generation. Modifications on the *N*-aryl moiety of isoquinoline **2** reduce the yield of **20b-e** as well as modifications on the tetrahydroisoquinoline core (*cf.* **22**). The reaction works best with acetone, switching to butanone nearly bisects the yield of **21**. (Scheme 10)

Reiser *et al.* were able to show that not only iminium ions can be generated with the help of $Ru(bpy)_3^{2+}$ (**1**) but also *N*-α-radicals (Scheme 11).[20] These radicals were trapped by enone **23** *via* a photocatalytic conjugate addition. The proposed reaction mechanism uses the oxidative power of $Ru(bpy)_3^{2+}$* as well as the reductive power of $Ru(bpy)_3^{+}$. No sacrificial electron donor or acceptor is needed in this reaction and the molecular formula of the product is the same as the combination of isoquinoline **2** and enone **23** making the reaction atom economic. However, oxygen has to be excluded to block the reaction pathway for reoxidation of $Ru(bpy)_3^{+}$ by the latter, contrasting reactions discussed earlier (*cf.* Scheme 6, 7).

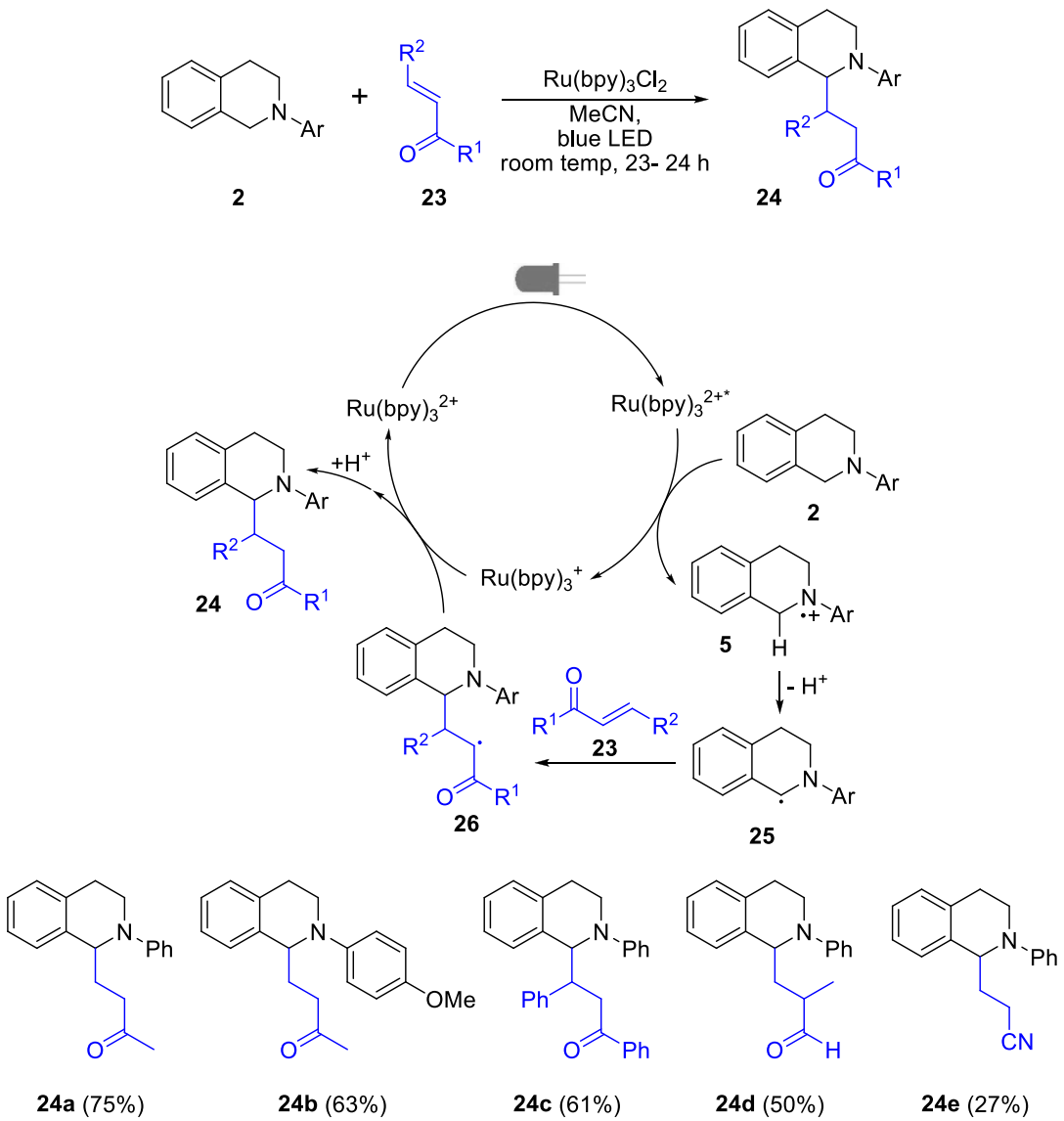

Scheme 11. Photocatalytic conjugate addition.

At first excited $Ru(bpy)_3^{2+*}$ is reduced by isoquinoline **2** to $Ru(bpy)_3^{+}$ generating radical cation **5** following the Jablonski diagram shown in Scheme 3. *N*-α-radical **25** is then generated by loss of a proton. **25**, being a nucleophilic radical, is able to attack an enone such as **23** in β-position. The resulting α-carbonyl radical **26** is reduced by $Ru(bpy)_3^{+}$ regenerating the photoredox catalyst. After a subsequent protonation product **24** is formed (Scheme 11).

The applicable enones range from ketone and chalcone, giving **24a-c**, to aldehydes and nitriles, giving **24d-e**.

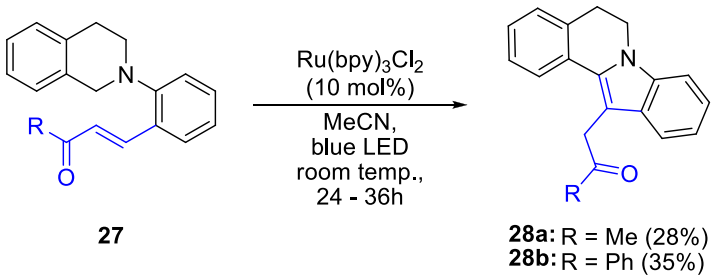

Scheme 12. Photocatalytic formation of dihydroindolo isoquinoline derivatives **52**.

Also two intramolecular examples were realized where not only a photocatalytic conjugate addition takes place but also a dehydrogenation leading to dihydroindolo isoquinoline moieties (Scheme 12).

Yoon *et al.* showed that the yield of product **24a** can be increased to 90% and that the reaction time can be shortened to 5 h by the addition of trifluoroacetic acid (TFA) and elevated temperatures of 50 °C.[21] They found that Brønsted acids with a pKa value close to 1 increase the yield significantly due to protonation of the enone. In addition they were able to identify the rate determining step of this reaction by kinetic isotope effect (KIE) studies.

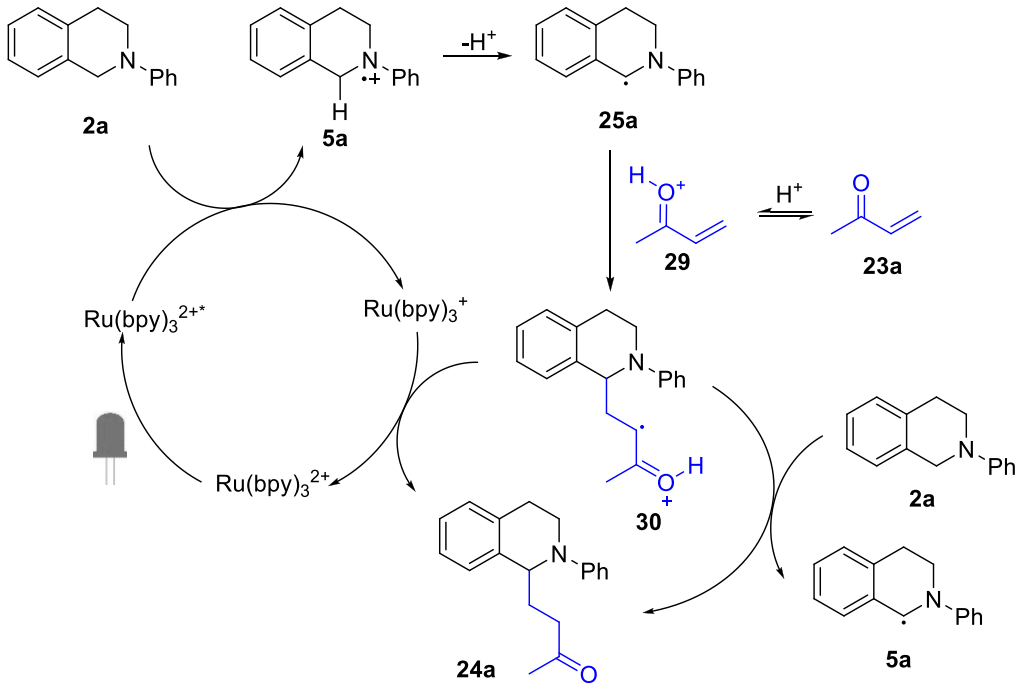

Scheme 13. Reaction mechanism of a photocatalytic conjugate addition with Brønsted acid co-catalyst.

Without the addition of TFA the rate determining step is the addition of *N*-α-radical **25a** to enone **23a**. By protonating enone species **29**, TFA is accelerating this step so it is no longer rate determining. With the help of the KIE studies they could rule out that the oxidation of isoquinoline **2a** by the excited photocatalyst is a dominant pathway in this process. The authors suggest that the new rate

determining step is the radical chain propagation by α-keto radical **30** abstracting a hydrogen atom from isoquinoline **2a** (Scheme 13).

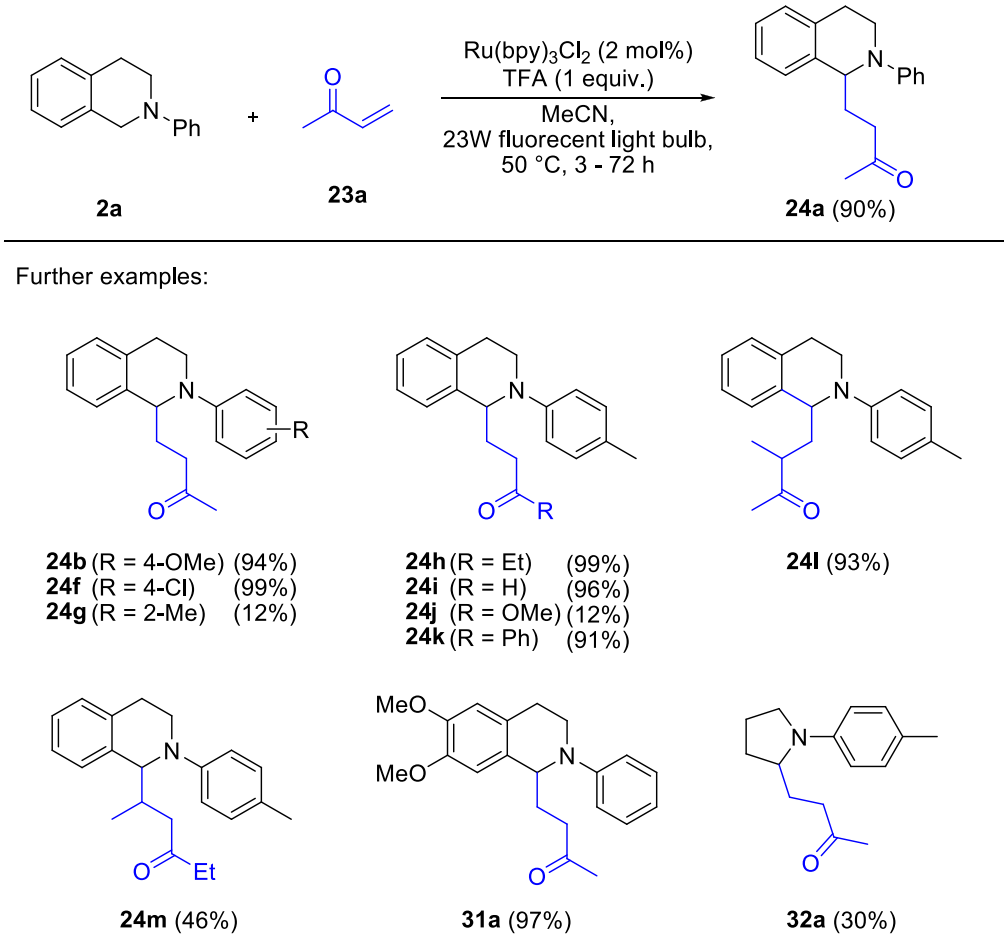

Scheme 14. Photocatalytic conjugate addition with Brønsted acid co-catalyst.

The reaction tolerates electron donating as well as electron withdrawing substituents on the *N*-aryl moiety of **2** though ortho substitution decreases the yield (*cf*. **24a**, **24b**, **24f**, **24g**). The isoquinoline moiety can bear groups of various electronic natures with little effect on the yield (*cf*. **31**). On the other hand, *N*-alkyl substituted isoquinolines do not react at all and other aniline derivatives such as **32** at diminished reaction rates. With respect to the enone system **23** the reaction proceeds well with aliphatic as well as aromatic substituents on the enone (*cf*.**24h-k**). Due to the poor electrophilicity of acrylic acid esters the yield of **24j** decreases. α-Substituted enones lead to good yields in this reaction while β-substituted ones decrease it (*cf.* **24l**, **24m**) (Scheme 14).

The γ-C-H activation of acridine derivatives was discovered by Pandey *et al*.[22] They were able to oxidize dihydroacridine **33** with excited $Ru(bpy)_3^{2+}$*. The formed radical cation **34** rearranges under loss of a proton to the corresponding *N*-γ-radical **35** which can be trapped with an enone system or nitrostyrene yielding radical **36** (Scheme 15).

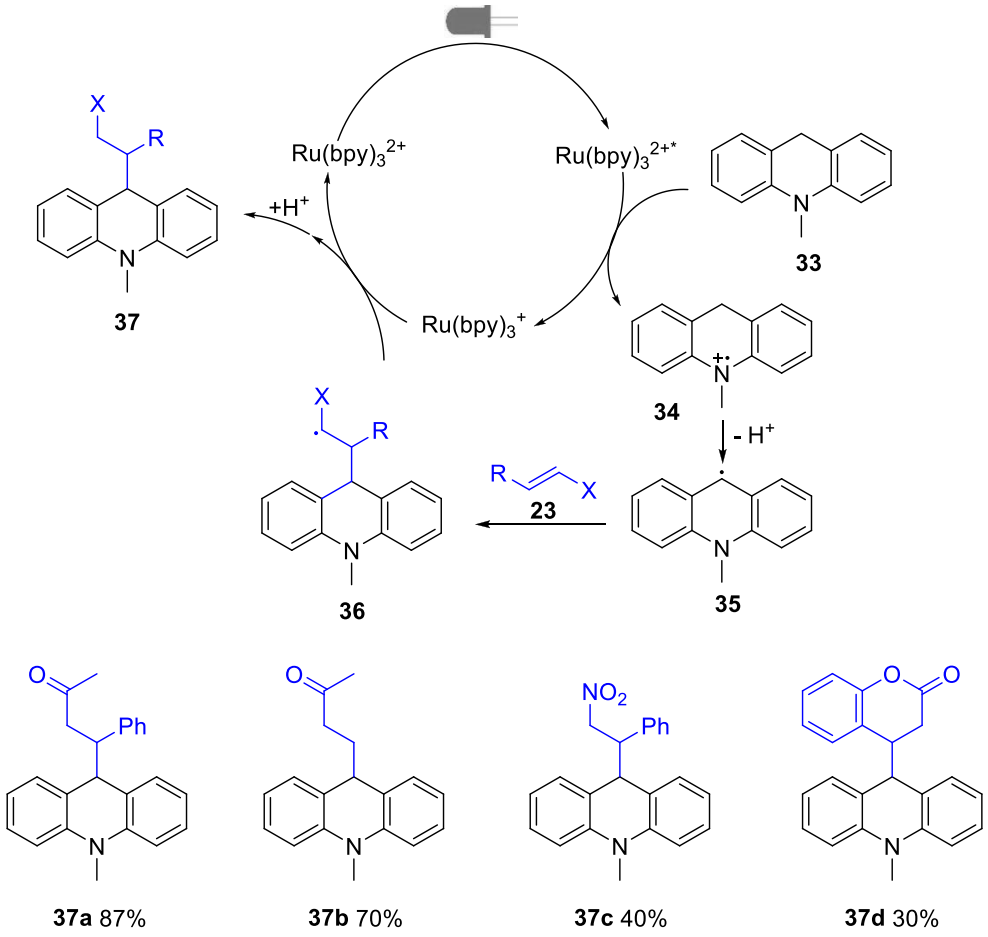

Scheme 15. Photocatalytic γ-C-H alkylation of acridine derivatives.

After reduction of **36** by $Ru(bpy)_3^+$ and subsequent protonation, the final product **37** is obtained and the catalyst is regenerated. The yields range from 87% if methyl cinnamate is used as enone to 30% employing coumarin (Scheme 15).

In 2011 Xiao *et al.* extended the concept of photocatalytical iminium ion generation by their further transformation to 1,3-dipols **41**.[23] They were able to trap these 1,3-dipols with electron poor olefins **42** in a [3+2] photocycloaddition yielding **44** (Scheme 16).

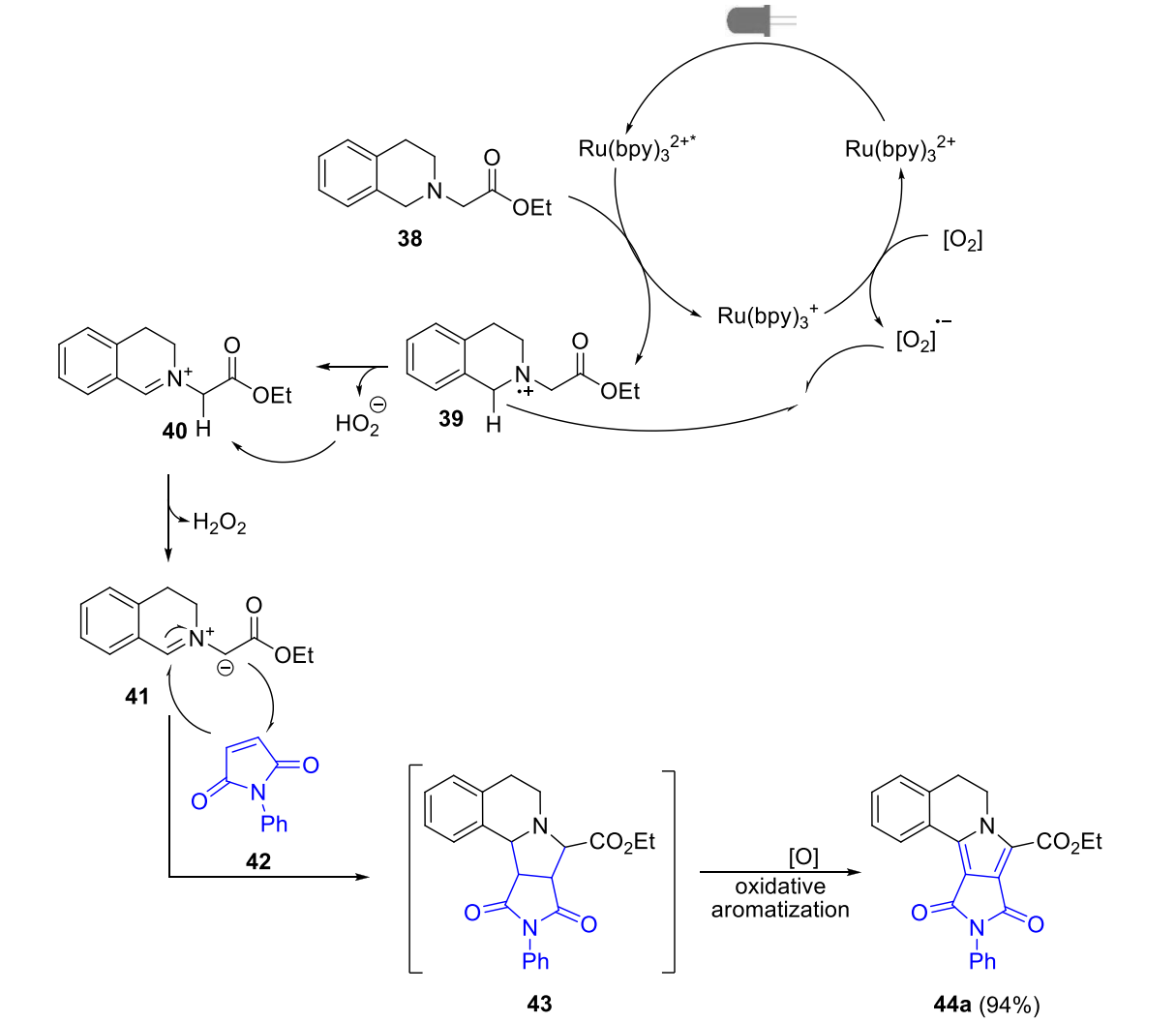

Scheme 17. Photocatalytic [2+3] cycloaddition.

In the first step excited $Ru(bpy)_3^{2+}$* (**1***) oxidizes tetrahydroisoquinoline **38** to radical cation **39**. An oxygen radical anion $O_2^{\bullet-}$, generated by the oxidation of $Ru(bpy)^+$, subsequently abstracts a proton from the radical cation **39** leading to iminium ion **40** following the mechanism shown in Scheme 5. The formation of iminium ion **40** is followed by an abstraction of another proton at the α-carbonyl position of **40,** generating zwitterion **41**. This zwitterion couples with the electron deficient olefin **42** in a [3+2] cycloaddition. A subsequent oxidative aromatization of **43** leads to the final product **44**. The reaction works well with maleimide (*cf.* **44a-c**) and styrene derivatives (*cf.* **45a-c**) as dipolarophiles. Also some alkynes (*cf.* **46**) and maleic anhydride (*cf.* **47**) can be used however with decreased yield (Scheme 17).

The C-C bond of 1,2-diamines can be cleaved with the help of $Ru(bpy)_3Cl_2$ (**1**·Cl_2). Wang *et al.* utilized this concept to perform *aza*-Henry reactions.[24] Diamine **48** is oxidized to a radical cation by excited $Ru(bpy)_3^{2+}$* which cleaves afterwards into amine radical **49** and iminium ion **50**. The catalyst is regenerated by oxygen as shown in Scheme 5. **50** is attacked by a deprotonated nitro compound, giving rise to product **53** (Scheme 18).

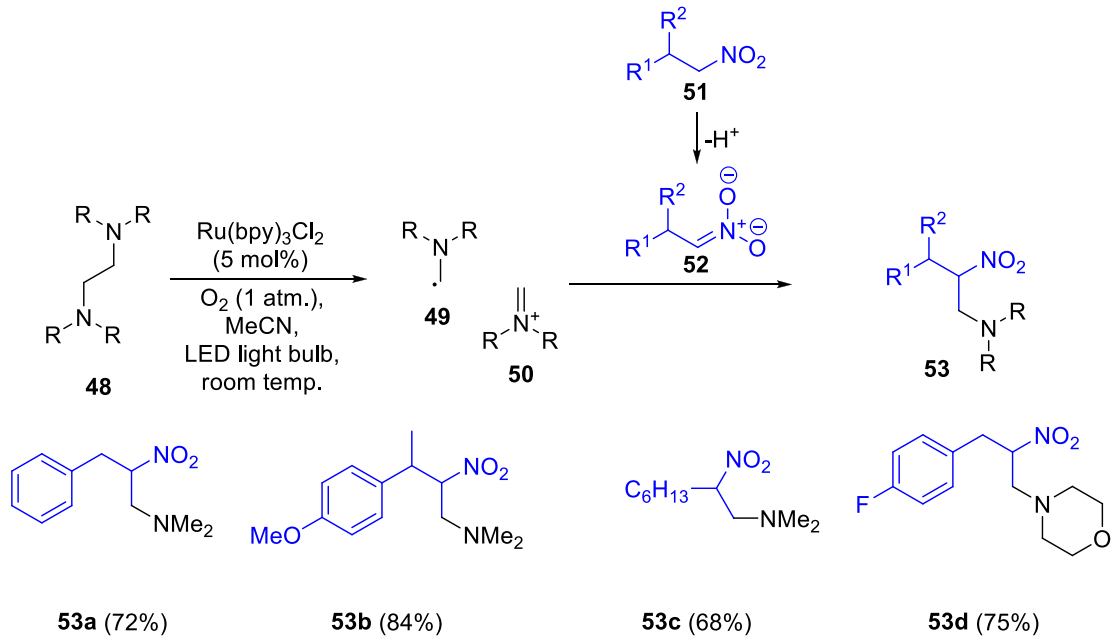

Scheme 18. Photocatalytic oxidative cleavage of C-C bonds and subsequent *aza*-Henry reaction.

Nitro compounds with aromatic as well as aliphatic moieties can be used giving rise to **53a-c**. Also other *tert.* 1,2-diamines are applicable in good to excellent yields (*cf.* **53d**) (Scheme 18).

Another example combining organo catalysis with photoredox catalysis is the oxidative cleavage of C-C bond in aldehydes 54 performed by Xia *et al.*[25]

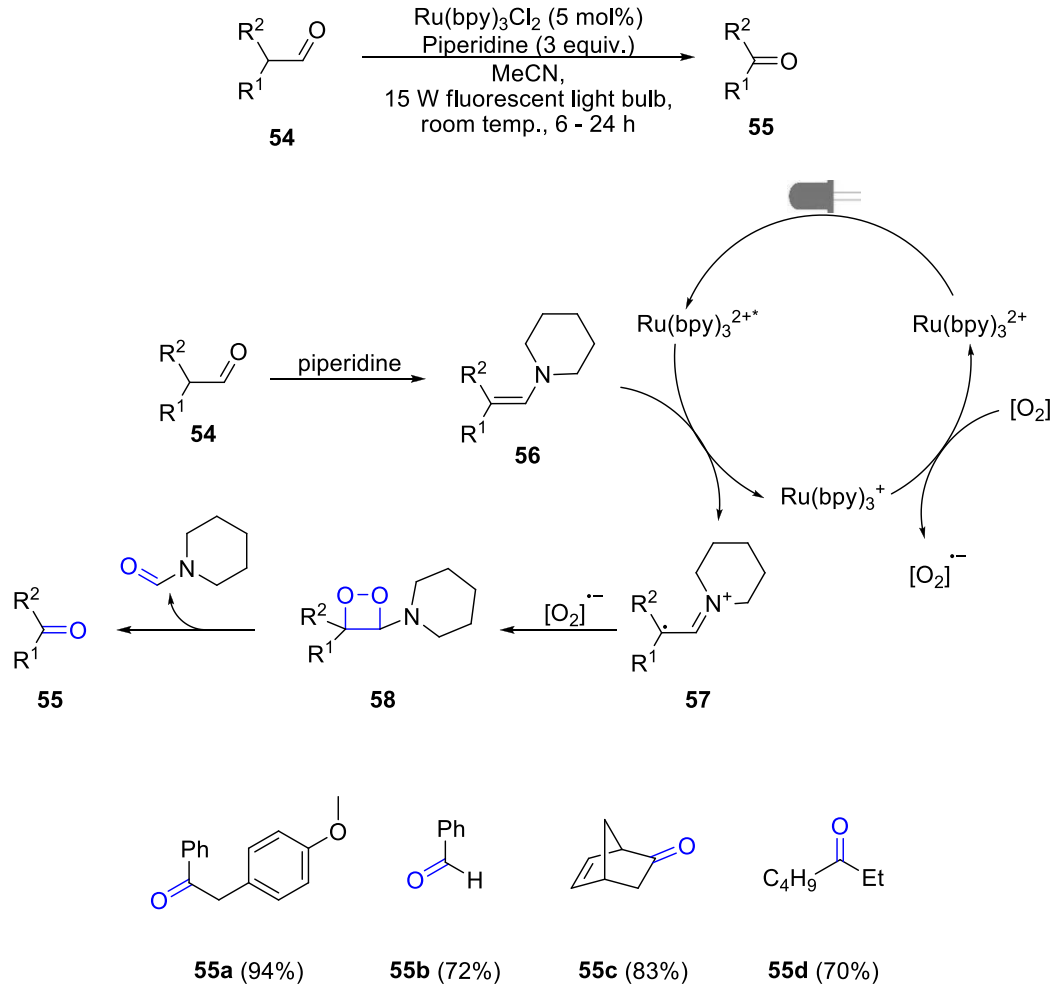

Scheme 19. Photocatalytic cleavage of aldehydes.

Piperidine served as organocatalyst converting aldehyde **54** to enamine **56**. This enamine is oxidized by excited $Ru(bpy)_3^{2+}$* to the corresponding radical cation **57**. $Ru(bpy)_3^{2+}$ is regenerated by reducing molecular oxygen to $O_2^{\bullet-}$, which combines with **57** to form 1,2-dioxetane **58**. After fragmentation of **58** by cycloreversion, carbonyl compound **55** is obtained truncated by one carbon compared to aldehyde **54** (Scheme 19).

In most of the suitable substrates R^1 is aromatic. Also some aliphatic examples, like carbocylces or alkyl chains, have been used, however, demanding prolonged reaction times (Scheme 19).

So far, all presented reactions involving amines led to the activation of a carbon in close proximity to a nitrogen atom. The first photochemical generation of *N*-centered radical **62** in hydrazones catalyzed by $Ru(bpy)_3^{2+}$ (**1**) was achieved by Xiao *et al*.[26] They were able to add these radicals in an intramolecular 5-exo-trig cyclization to an allyl moiety forming pyrazoline derivative **60** (Scheme 20). In the first step of the proposed reaction mechanism, hydrazone **59** is deprotonated by NaOH. The resulting anion **61** is oxidized to the corresponding *N*-centered radical **62** by excited $Ru(bpy)_3^{2+*}$. This radical attacks the allyl system in a 5-*exo*-trig cyclization leading to the formation of radical **63** that abstracts a hydrogen atom from a solvent molecule to give rise to the final product **60**. Proof for the assumed mechanism was obtained by trapping radical **63** with TEMPO.

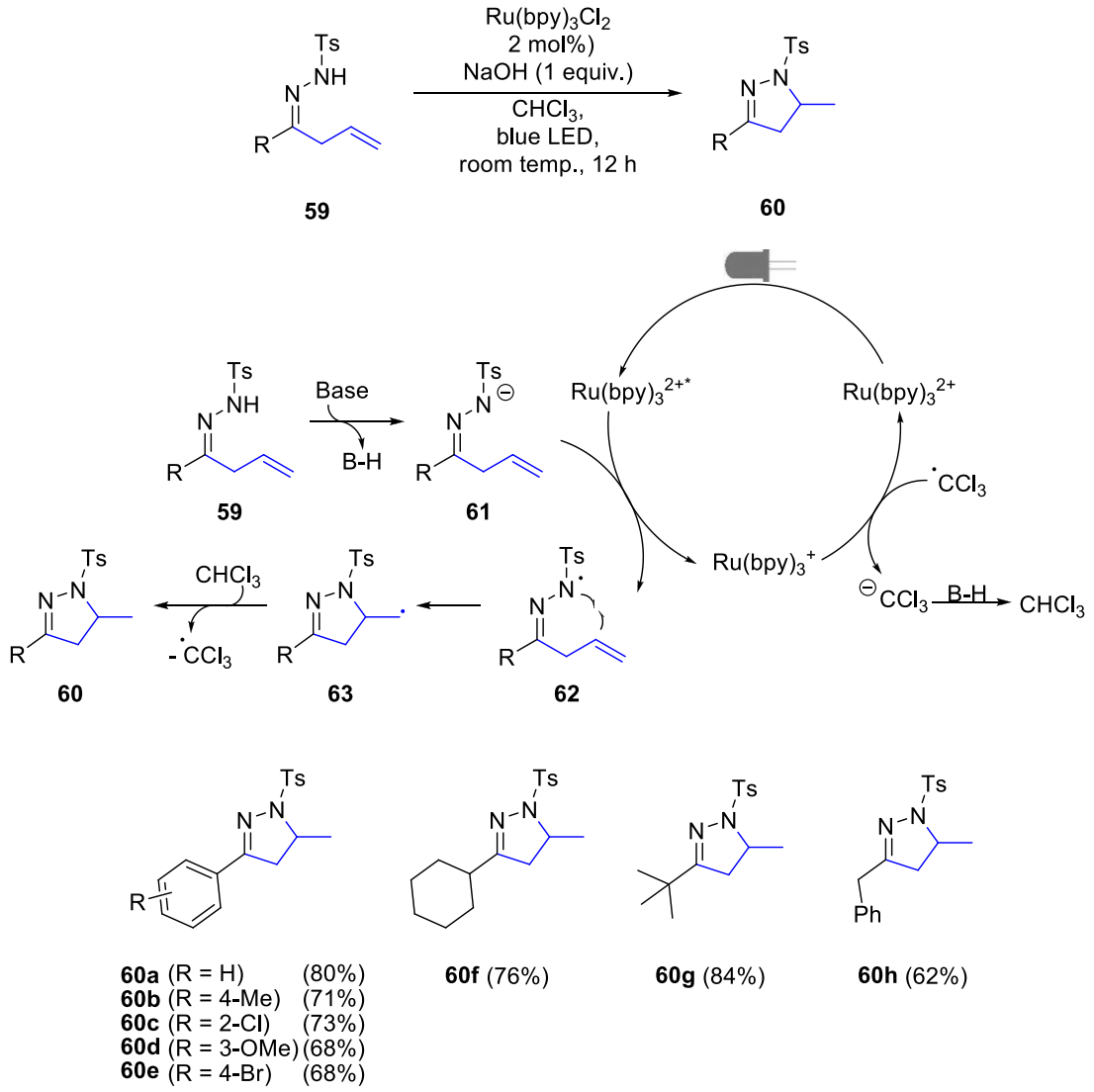

Scheme 20. Photocatalytic generation of *N*-centered hydrazonyl radicals and formation of pyrazoline derivatives.

The reaction can be conducted with a broad variety of aryl hydrazones **59** and both steric as well as electronic variations of the aryl moiety have little influence on the reaction (*cf.* **60a-e**). Other suitable residues are cyclohexyl, *tert*-butyl and benzyl moieties (*cf.* **60f-h**) (Scheme 20).

1.2 Reactions initiated by Substrate Reduction

The reactions discussed in this chapter have in common that the photochemical transformation is initiated by the reduction of a substrate. $Ru(bpy)_3^+$ can reduce a variety of activated carbon halogen bonds (Scheme 21, 23, 25, 26, 27 and 29) forming carbon centered radicals and halogen anions. Another class of substrates are carbonyl compounds with a functionality at the α-carbonyl position (scheme 30, 31). Some of the reactions discussed in this chapter only require a reduction. In those cases excited $Ru(bpy)_3^{2+}$* is reduced to $Ru(bpy)_3^+$ by a sacrificial electron donor (Scheme 21, 23, 24, 25, 26, 27 and 30). Commonly used electron donors are *tert.* amines such as triethylamine, diisopropylethylamine (DIPEA) and Hantzsch ester (**82**). On the other hand there are reactions that require, after the initial reduction, an oxidation to lose the additional electron and to finish the transformation (Scheme 28, 31, 32 and 33).

One of the first examples of a photochemical dehalogenation of activated carbon-halogen-bonds was reported by Kellogg *et al.* in 1985.[27] They were able to reduce C-X bonds α to carbonyl positions in **64a**, **64c**, **64d** and α to nitriles in **64b** (Scheme 21). In addition also the C-Cl bond in **64e** could be cleaved.

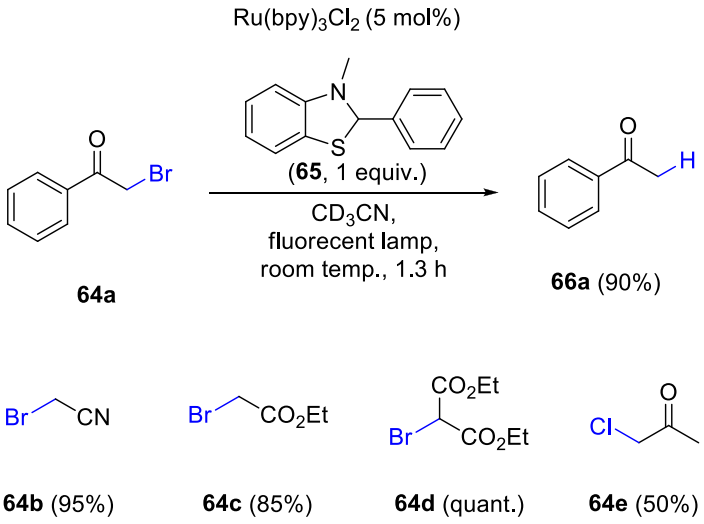

Scheme 21. Photocatalytic dehalogenation of activated carbon halogen bonds.

In the first step of the catalytic cycle, excited $Ru(bpy)_3^{2+*}$ oxidizes **65**, which serves here as sacrificial electron donor, to its corresponding radical cation **68**. $Ru(bpy)_3^{+}$ is then capable of reducing the C-Br bond of acetophenone **64a** leading to the formation of carbon centered radical **67** and a bromide anion. This radical abstracts a hydrogen atom from **68** giving rise to product **66** (Scheme 22).

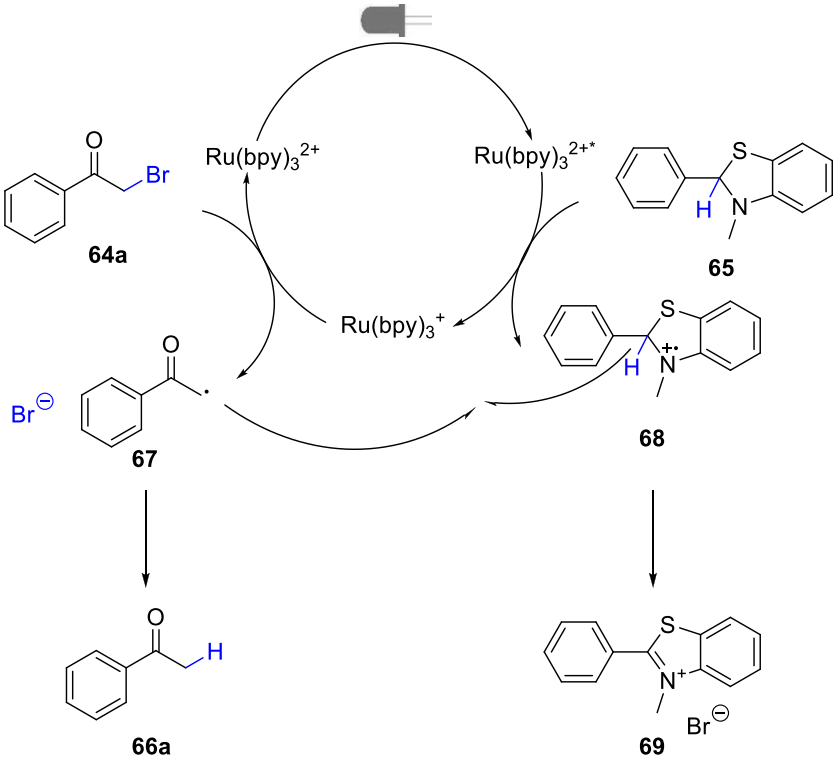

Scheme 22. Proposed reaction mechanism of a reductive dehalogenation.

Another dehalogenation of activated C-X bonds was developed by Stephenson *et al*.[12] With the help of this reaction bromopyrroloindoline **70** and α-carbonyl compounds **72** and **73** could be selectively dehalogenated (Scheme 23).

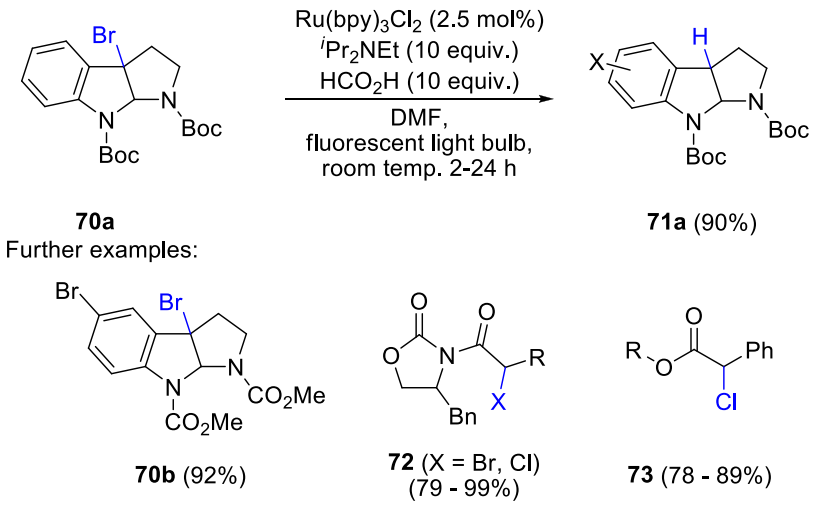

Scheme 23. Photocatalytic reductive dehalogenation.

By accepting an electron from DIPEA, $Ru(bpy)_3^+$ is generated as catalytic active species. $Ru(bpy)_3^+$ is then capable of reducing an activated C-X bond giving rise to radical anion **74** which splits into carbon centered radical **75** and a halogen anion. The radical is trapped by formic acid furnishing the final product **76** (Scheme 24).

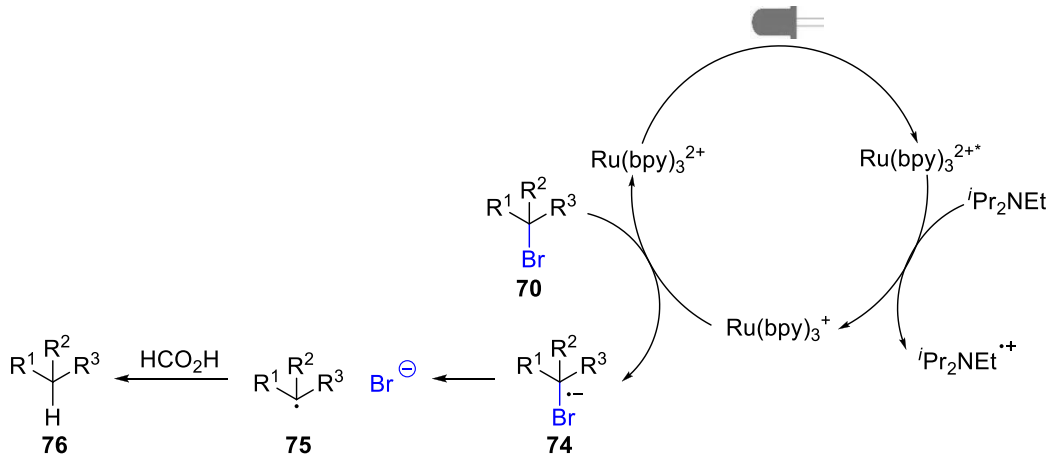

Scheme 24. Proposed reaction mechanism for a reductive dehalogenation.

A year later Stephenson *et al.* presented a method to trap and transfer the carbon radicals **75** generated by cleavage of a C-X bond.[28] They showed that 2-bromomalonate (**64d**) can be reduced to its corresponding radical anion which cleaves to a malonate radical **75d** and a bromide ion as depicted in the mechanism in Scheme 24. **75d** can add to a variety of electron rich heterocycles leading to the formation of a new C-C bond. Apart from indoles (*cf.* **79a-c**) also pyrrole (*cf.* **79d**) and furan (*cf.* **79e**) are suitable substrates. The yield was significantly increased by substituting Et_3N with 4-methoxy-*N,N*-diphenylaniline (Scheme 25).

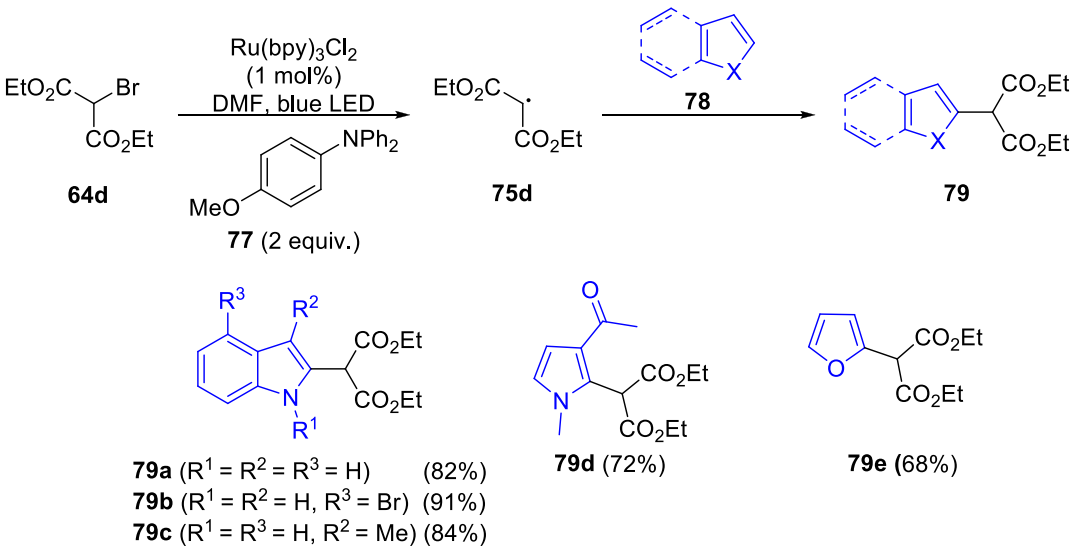

Scheme 25. Functionalization of electron rich heterocycles.

Gagné *et al.* showed that glycosyl halide **80** can be cleaved with a similar method as presented above.[29] Excited $Ru(bpy)_3^{2+}$* is reduced by DIPEA. Afterwards $Ru(bpy)_3^{+}$ reduces **80** to glycosyl radical **84** which was trapped by alkene **81** leading to the formation of radical **85**. This radical abstracts a hydrogen atom from Hantzsch ester (**82**) forming product **83** (Scheme 26).

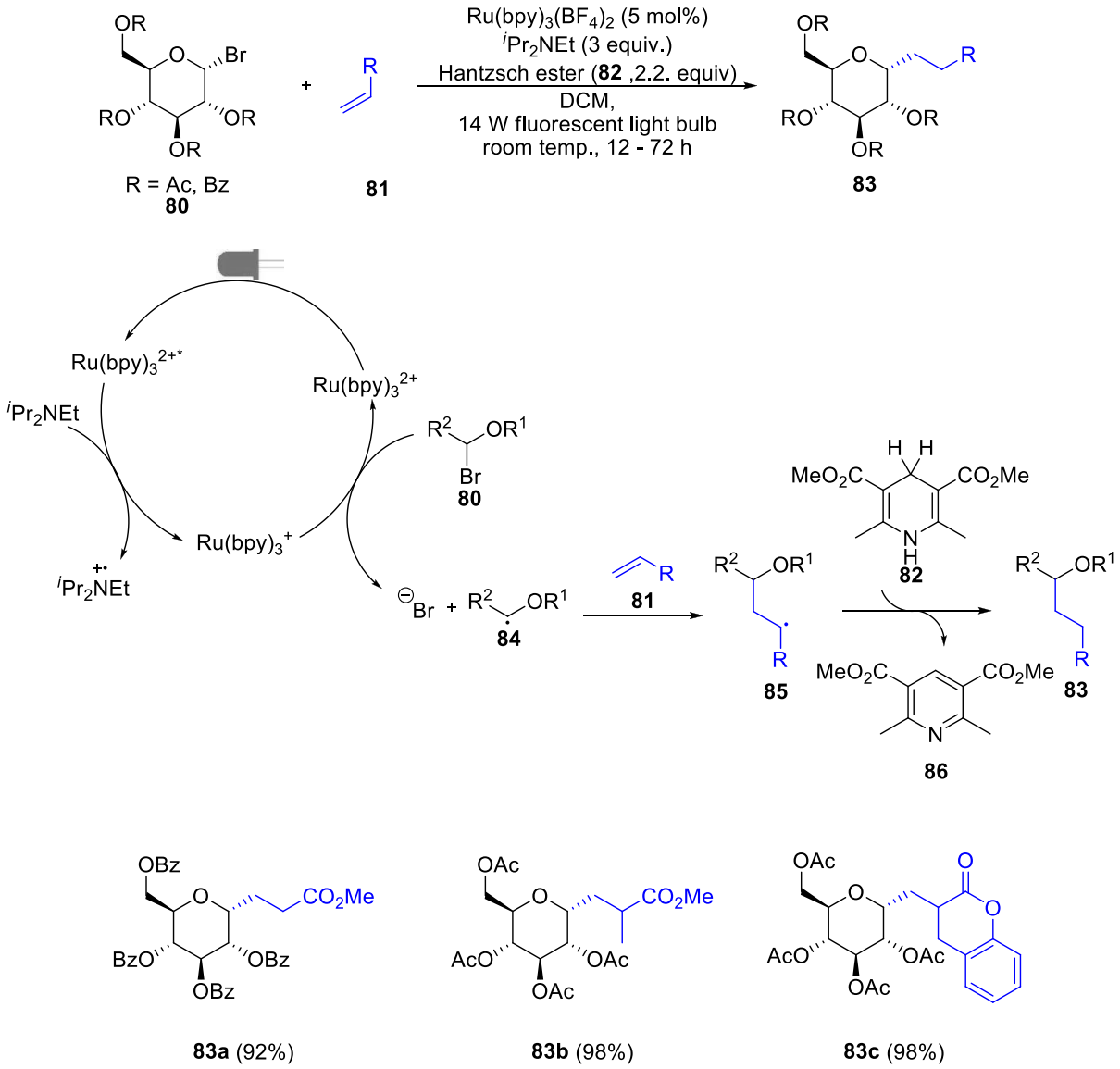

Scheme 26. Addition of glycosyl halides (**66**) to alkenes.

A double dehalogenation of vicinal bromides was performed by Reiser *et al.* utilizing visible light photoredox catalysis.[30] In this case an unusual redox mediator was used to generate $Ru(bpy)_3^{+}$ in order to have a not nucleophilic electron donor: a combination of 1,5-dimethoxynaphthalene (DMN) as mediator and ascorbate as sacrificial electron donor. Under these conditions a variety of enones could be synthesized. In the assumed reaction mechanism excited $Ru(bpy)_3^{2+}$* oxidizes DMN to a radical cation which will accept an electron from ascorbate. $Ru(bpy)_3^{+}$ on the other hand reduces

vicinal dibromide **87**, leading to radical anion **88**. After rapid elimination of one halogen the resulting α-acyl radical **89** is further reduced to the corresponding enolate **90**, which eliminates once more a bromide leading to enone **91** in good yields (Scheme 27).

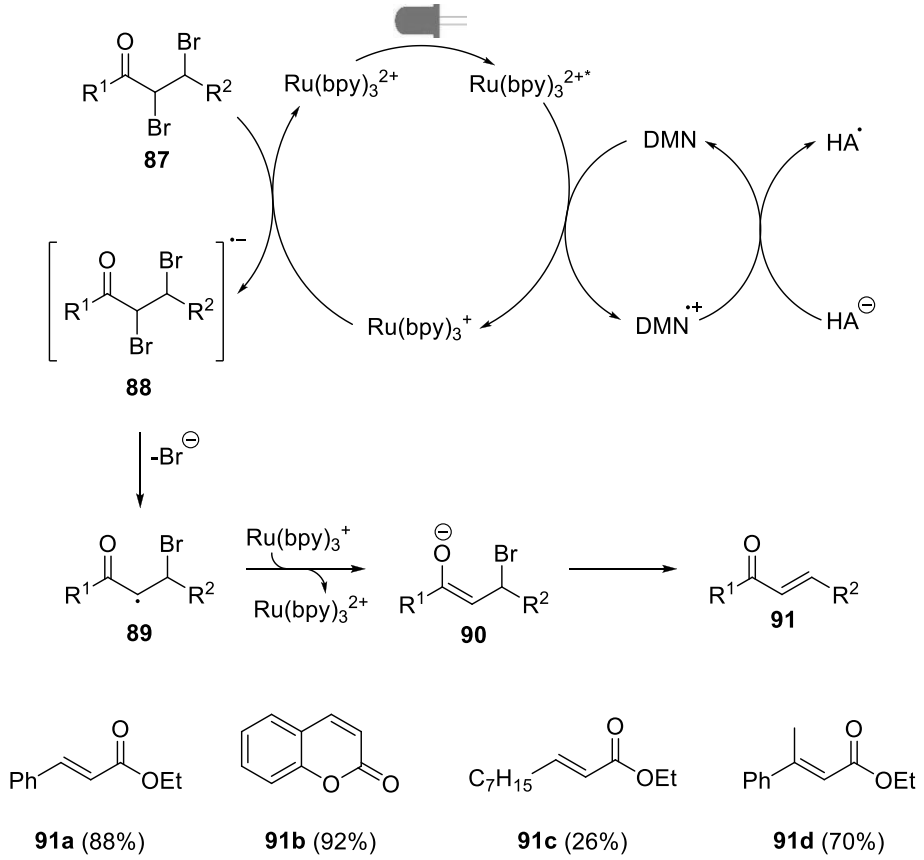

Scheme 27. Reductive double dehalogenation (HA = ascorbic acid).

Good yields were obtained for cinnamate **91a**, chromanone **91b** and ester **91d**. Substrates without an aromatic moiety can also be applied but with reduced yields. The debromination of α-bromo and α,α-dibromo carbonyl compounds is also possible *via* this method (Scheme 28).

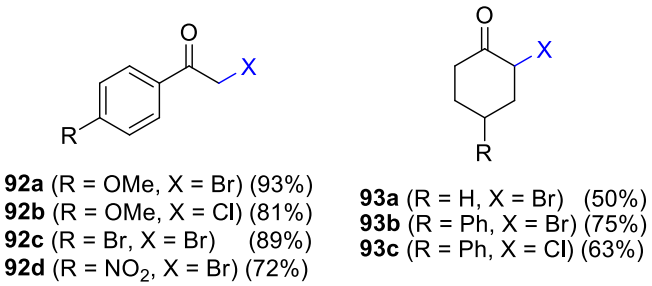

Scheme 28. Reductive dehalogenation of α-bromo carbonyl compound.

MacMillan and his co-workers were able to combine enamine catalysis and photoredox catalysis to achieve an enantioselective alkylation of aldehydes (Scheme 29).[10] This report received great attention in the organic community and marked in 2008 the starting point of todays increased interest in this field.

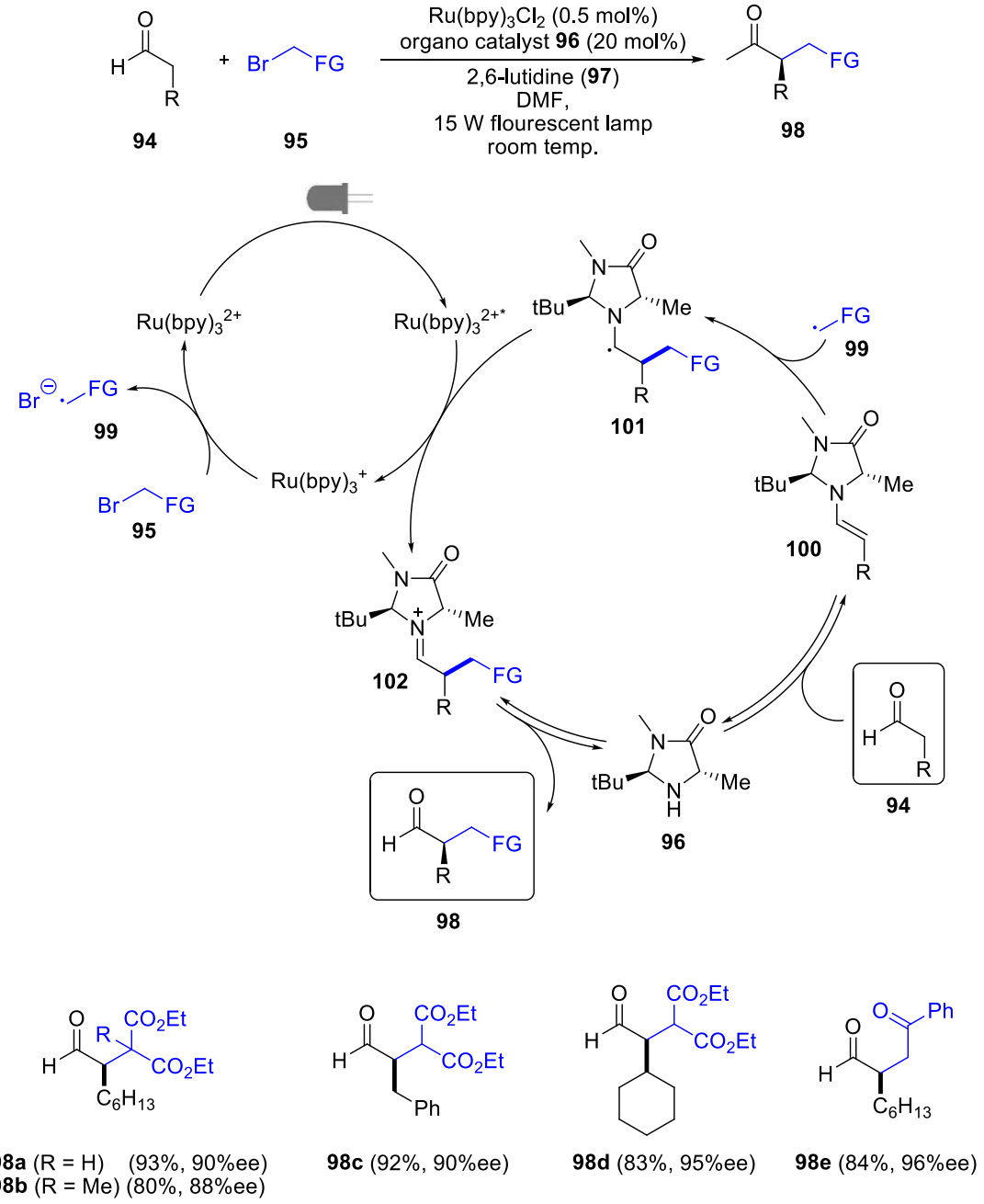

Scheme 29. Enantioselective alkylation of aldehydes. (FG: functional group)

This reaction involves an oxidation of the substrate but the transformation is initiated by the reduction of halocarbon **95**. After the reduction by $Ru(bpy)_3^+$, which was previously generated by an sacrificial electron donor like 2,6-lutidine (**96**), **95** splits into a bromide ion and carbon radical **99**. This

radical will attack chiral enamine **100** formed by organo catalyst **96** and aldehyde **94**. Only the *si*-face is accessible for radical **99**. The resulting *N*-α-radical **101** is oxidized to the corresponding iminium ion **102** by excited $Ru(bpy)_3^{2+}$*. Upon hydrolysis the final product **98** is released (Scheme 29).
Suitable aldehydes **94** for this reaction are bearing mostly long alkyl chains, but also benzyl or cyclohexyl moieties can be used (*cf.* **98a-e**). All precursor **95** bear a bromine substituent in the α-carbonyl position, for example α-bromo malonates or phenacyl bromide have been successfully utilized.

A photocatalytic epoxide and aziridine opening was developed by Fensterbank *et al*.[31] By employing the reductive quenching cycle and using DIPEA as reducing agent for $Ru(bpy)^{2+}$*, they were able to transfer an electron into the carbonyl moiety of **103**. This radical anion is rearranging to an oxygen or nitrogen centered anion and an α-carbonyl radical in **105**.

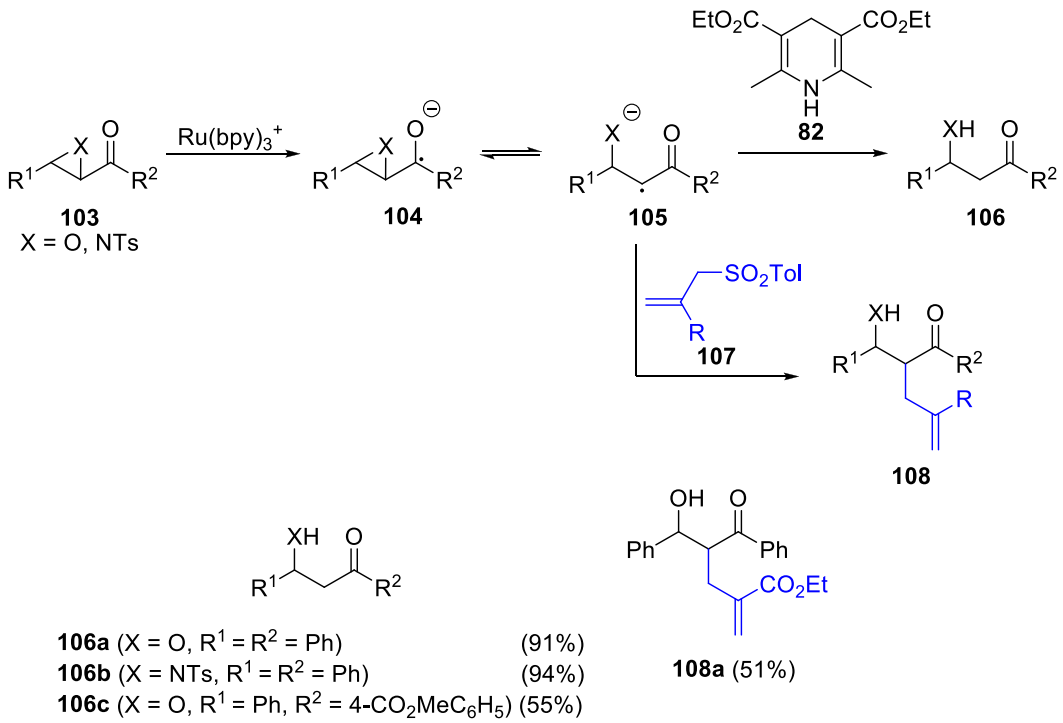

Scheme 30. Photocatalytic opening of epoxides and aziridines.

Radical **105** can be trapped either by a proton source like Hantzsch ester (**82**) or by allyl sulfonides (**107**) (Scheme 30). No full conversion could be reached with sterically hindered α,β-epoxy ketones.

Using classic photocatalysis hard UV light is required to excite an alkene directly to perform a [2+2] cycloaddition. Photosensitized radical reactions using 9,10-dicyanoanthracene as catalyst were developed by Pandey *et al.* in the middle of the 90´s.[32] Employing $Ru(bpy)_3Cl_2$ (**1**·Cl_2) as catalyst, the

group of Tehshik Yoon was able to activate linked (bis)-enone system **109**.[11] With the help of this reaction they were able to build up bicyclic heptanes **110** very efficiently.

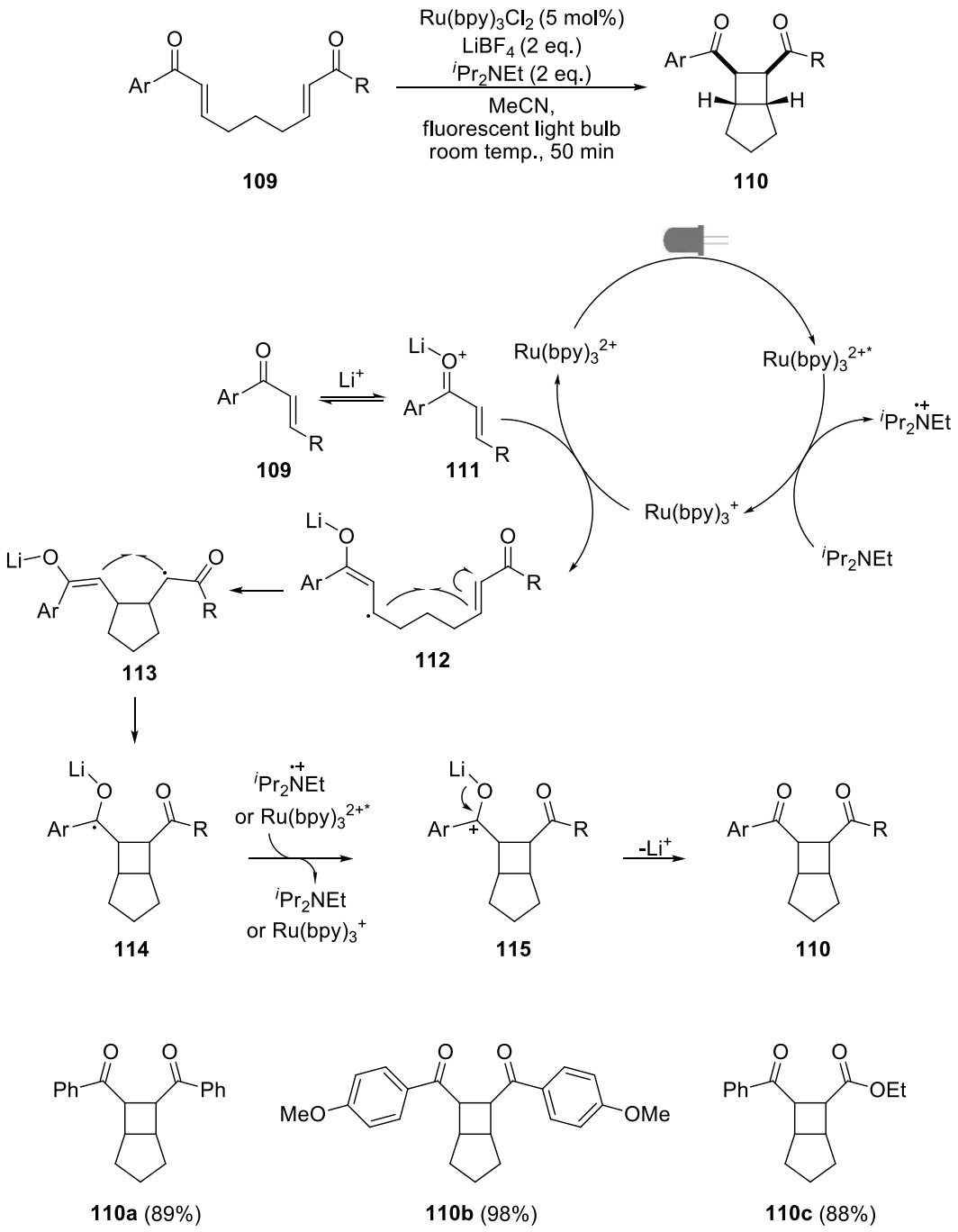

Scheme 31. Proposed reaction mechanism of a [2+2] photocycloaddition reaction.

At first, excited $Ru(bpy)_3^{2+}$* is reduced to $Ru(bpy)_3^{+}$ with the help of DIPEA. In the next step enone **109** is activated by a Lewis acid making the reduction by $Ru(bpy)_3^{+}$ more feasible. The resulting radical **112** attacks an adjacent enone leading to a five membered ring **113**. Under formation of a

cyclobutane moiety a second C-C bond in **115** is formed. The additional electron is either donated to a DIPEA radical cation or the excited $Ru(bpy)_3^{2+*}$ resulting in a radical propagation (Scheme 31).
The reaction works very well if at least one substituent is aromatic giving rise to **110a-c**. No product can be obtained if no α-aryl substituent is present (Scheme 31).

A year later, Yoon *et al.* were able to photocatalytically couple unlinked enones yielding cyclobutanes.[33] Recently, Yoon *et al.* reported an enantioselective version of this reaction by replacing $LiBF_4$ with a chiral Lewis acid.[34] The best results were obtained using a combination of $Eu(OTf)_3$ and ligand **118**. This way product **119** could be obtained with an enantiomeric excess of 93%ee (Scheme 32).

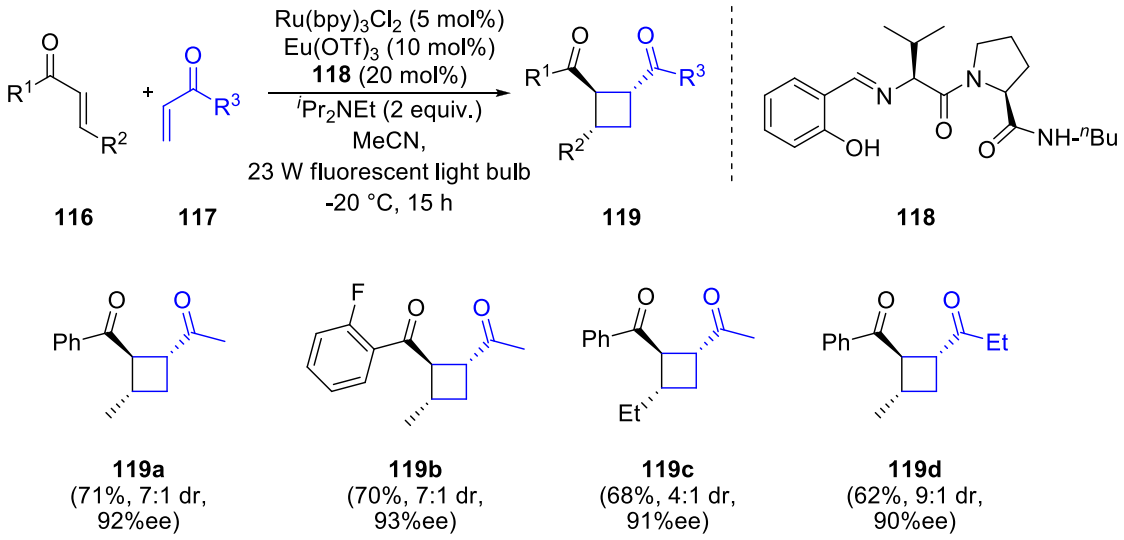

Scheme 32. Enantioselective photocatalytic [2+2] cycloaddition reaction.

Not only enones proofed to be good substrates, also α,β-cyclopropyl ketones **120** are feasible for this reaction. Yoon *et al.* were able to develop a photocatalytic [3+2] cycloaddition employing these substrates (Scheme 33).[35]

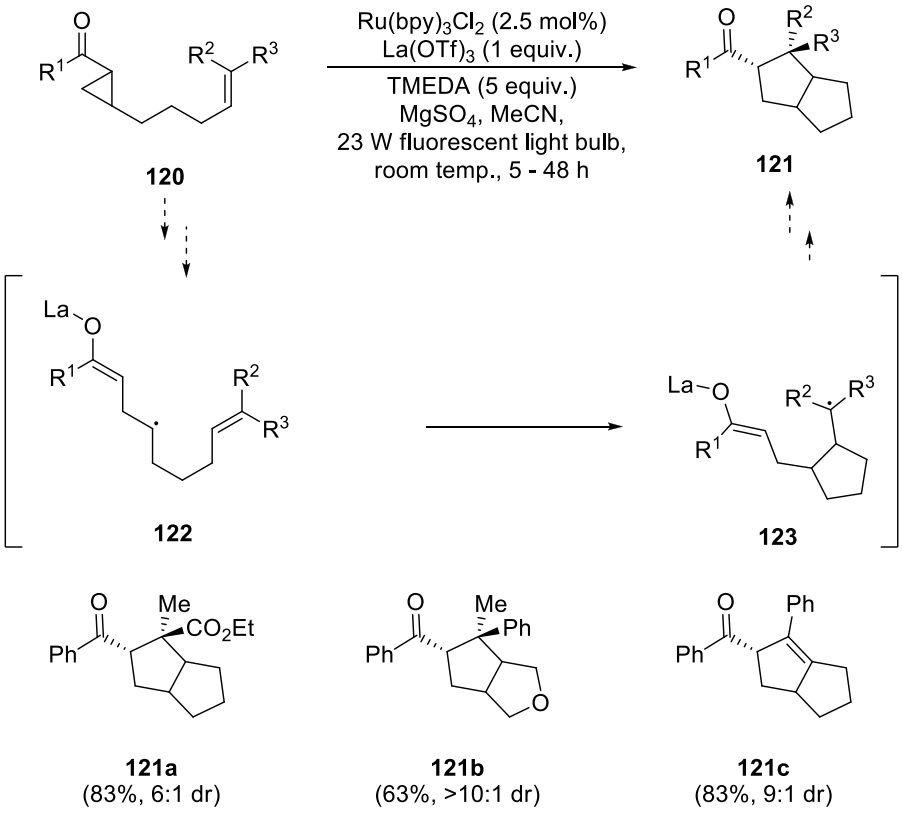

Scheme 33. Photocatalytic [3+2] cyclization reaction.

The proposed reaction mechanism is similar to the one for [2+2] cycloadditions. Excited $Ru(bpy)_3^{2+}$* is reduced by tetramethylethylenediamine (TMEDA) to $Ru(bpy)_3^{+}$ which reduces a Lewis acid activated enone **120** to a radical. Upon epoxide opening an attack of the γ-carbonyl radical to the adjacent alkene takes place in intermediate **122**. The second C-C-bond is formed between the aliphatic radical and the enole system in **123** generating the second ring system (Scheme 33). The alkene moiety can also be an alkyne, furnishing a cyclopentene – cyclopentane framework (*cf.* **121c**).

An example combining transition metal catalysis and photoredox catalysis was reported by Sanford *et al.*[36] They were able to substitute boronic acid moieties into trifluoromethyl groups with the help of a copper(I) acetate and $Ru(bpy)_3Cl_2$ (**1**·Cl_2). In the first step excited $Ru(bpy)_3^{2+}$* oxidizes $copper^{I}$ to $copper^{II}$. The photocatalyst is regenerated by reducing CF_3I (**124**) to a radical anion which splits into CF_3 radical (**127**) and I^-. Radical **127** adds to the $copper^{II}$ species **128** raising the oxidation state to

copper^{III} in **129**. By ligand exchange one of the ligands is substituted with an aryl residue resulting out of boronic acid **124**. In the last step a reductive elimination gives rise to product **126** (Scheme 34).

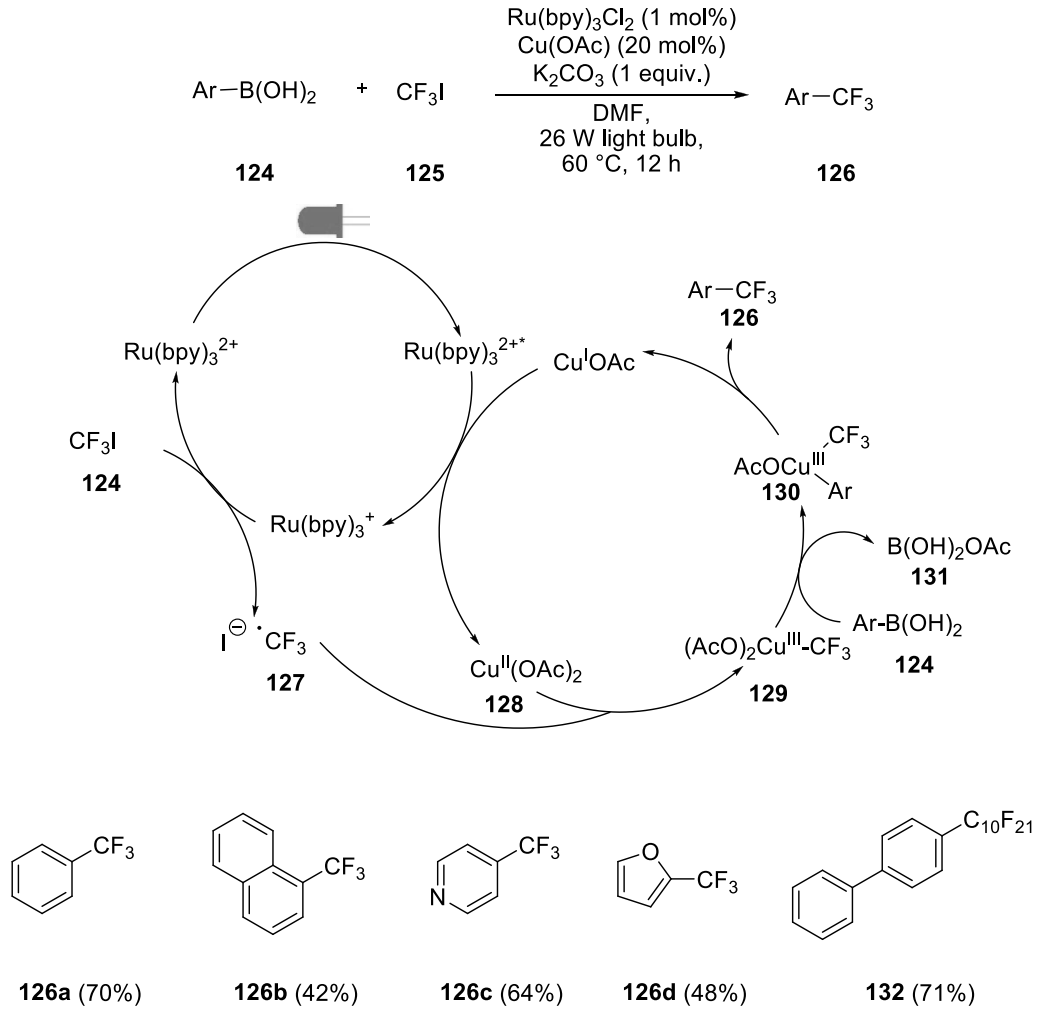

Scheme 34. Photocatalytic trifluoromethylation of boronic acids.

The substrate scope of **124** ranges from phenyl and naphthyl derivatives to pyridines and furans (*cf.* **126a-d**). In addition not only trifluoromethyl groups (**125**) can be incorporated *via* this method but also longer perfluorinated alkyl chains (*cf.* **132**).

Overall, most photoredox reactions utilize the reductive reaction pathway of $Ru(bpy)_3^{2+}$ described in chapter 1.1 and 1.2. Often applied molecules addressable with these redox potentials are *tert.* amines and carbonyl compounds bearing either a halogen atom or an alkene in α-carbonyl position.

2. Photocatalytic Reactions Proceeding *via* the Oxidative Quenching Cycle of $Ru(bpy)_3^{2+}$

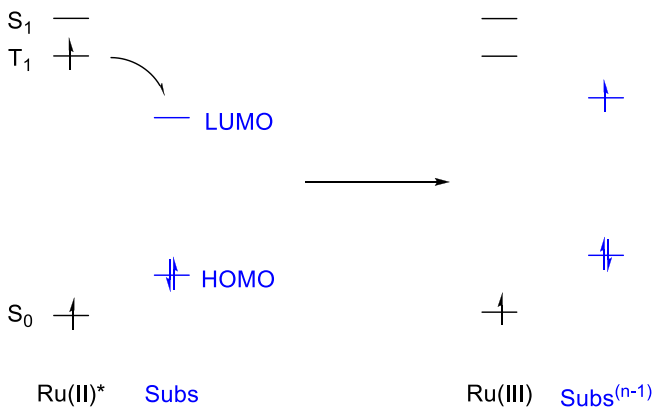

Scheme 35. Jablonski Diagram of the transition $Ru(bpy)_3^{2+}$* -> $Ru(bpy)_3^{3+}$.

Apart from accepting an electron, leading to the reductive quenching cycle, excited $Ru(bpy)_3^{2+}$* can also donate an electron to another molecule *via* the oxidative pathway (Scheme 35).
$Ru(bpy)_3^{2+}$* is a moderate reducing agent, the half-wave potential is $E_{1/2}$ (Ru^{III}/Ru^{II}*) = -0.81 V *vs.* SCE in acetonitrile. In comparison the reduction potential of $Ru(bpy)_3^{+}$ is $E_{1/2}$ (Ru^{II}/Ru^{I}) = - 1.33 V *vs.* SCE in acetonitrile.[6] However, excited $Ru(bpy)_3^{2+}$* can still reduce some activated carbon halogen bonds, e.g. tetrabromomethane (**140**) or Umemoto's reagent (**150**), whereas α-carbonyl radicals can no longer be reduced. In addition, the reductive power of $Ru(bpy)_3^{2+}$* is can be used to generate aryl radicals from diazonium salts, sulfonyl chlorides or diaryl iodonium salts (Scheme 42-44).

In order to regenerate $Ru(bpy)_3^{2+}$, $Ru(bpy)_3^{3+}$ has to accept an electron from a substrate molecule into the metal centered HOMO. At the same time the oxidation state of the substrate is raised by one (Scheme 36).

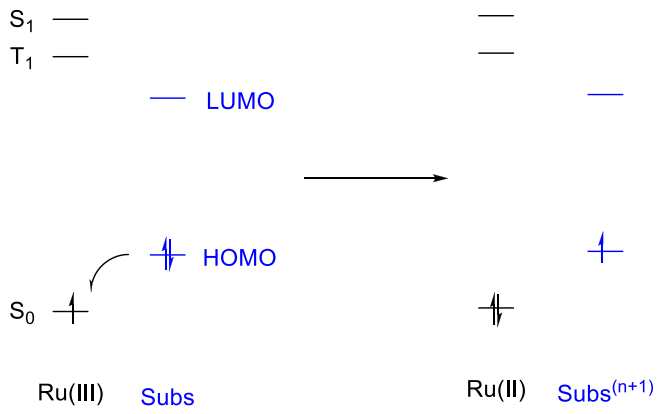

Scheme 36. Jablonski Diagram of the transition $Ru(bpy)_3^{3+}$ -> $Ru(bpy)_3^{2+}$.

It is the oxidation potential of $E_{1/2}$ (Ru^{III}/Ru^{II}) = +1.29 V *vs.* SCE in acetonitrile, compared to $E_{1/2}$ ($Ru^{II}*/Ru^{I}$) = + 0.77 V *vs.* SCE in acetonitrile for $Ru(bpy)_3^{2+}*$, that makes the oxidative quenching cycle appealing to synthetic chemists.[6] In contrast to excited $Ru(bpy)_3^{2+}*$, which can, in general, oxidize tert. amines and hydrazones, $Ru(bpy)_3^{3+}$ is also capable of oxidizing benzylic radicals to cations (Scheme 41 and 42).

2.1 Reactions initiated by Substrate Reduction

The reactions discussed in this chapter have in common that the photochemical transformation is initiated by the reduction of a substrate. Most of the reactions require after the initial reduction an oxidation to lose the additional electron and finish the transformation. These processes are therefore overall redox neutral and no sacrificial electron donor is required.

One early example proceeding via the oxidative quenching cycle using a sacrificial electron donor was given by Willner *et al*.[37] They were able to conduct the debromination of 1,2-dibromo-1,2-diphenylethane (**133**) with the help of di-octyl viologen (C_8V, **134a**) as redox mediator and $Ru(bpy)_3Cl_2$ (**1**·Cl_2) (Scheme 37).

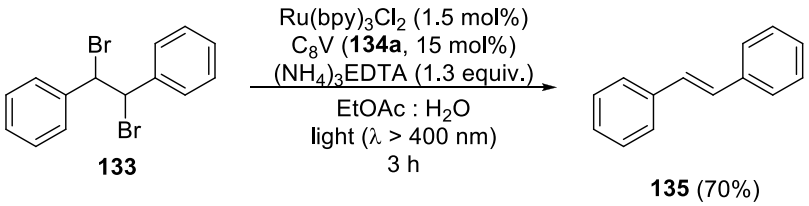

Scheme 37. Photocatalytic debromination of 1,2-dibromo-1,2-diphenylethane (**133**).

A biphasic system of water and ethyl acetate was used as reaction media. In the proposed reaction mechanism excited $Ru(bpy)_3^{2+}*$, located in the aqueous phase, reduces **134a** to radical cation **137a**. An electron transfer between two radical cations **137a** generates neutral C_8V (**138a**) and **134a**. **138a** will than transfer two electrons to 1,2-dibromo-1,2-diphenylethane (**133**) initiating the formation of stilbene (**135**) (Scheme 38).

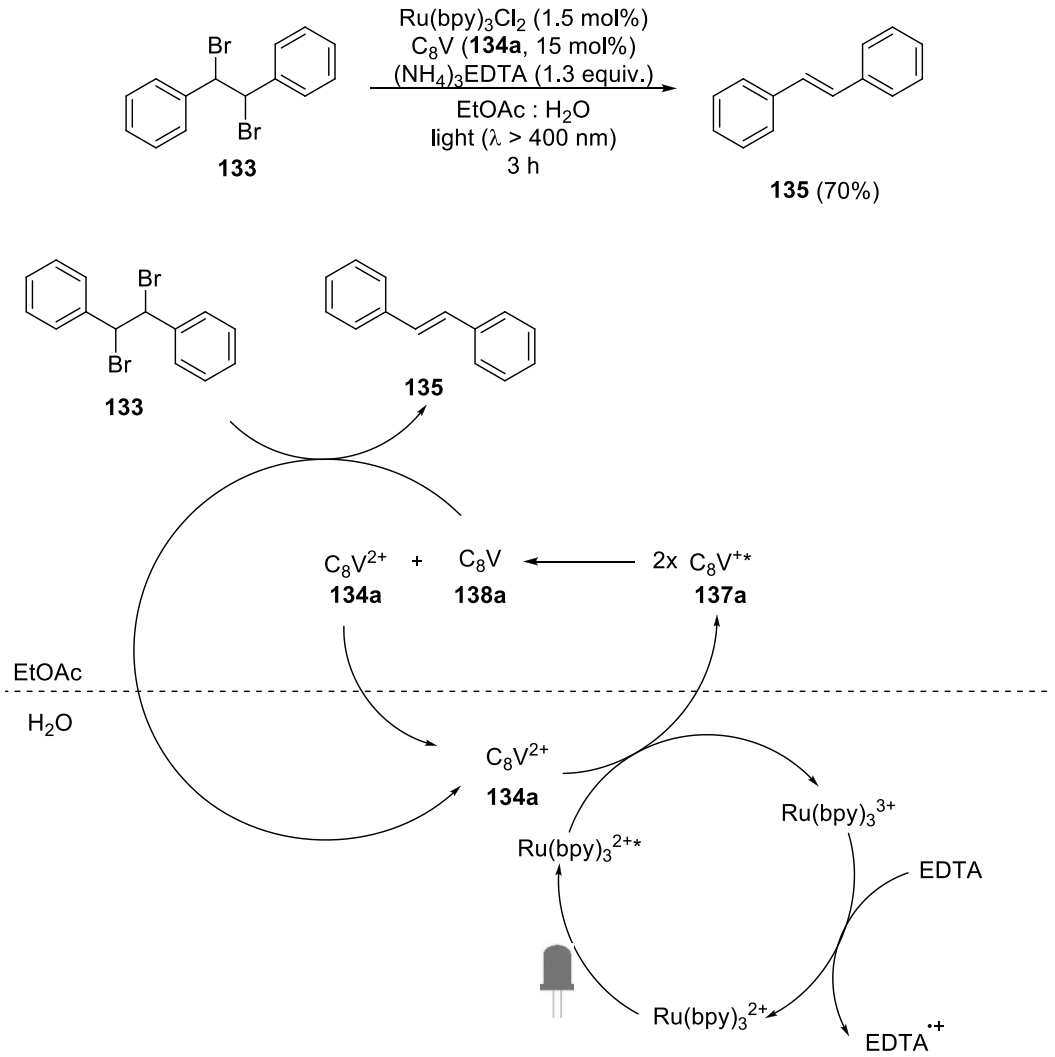

Scheme 38. Reaction mechanism of a photocatalytic debromination of 1,2-dibromo-1,2-diphenylethane (**133**).

A remarkable reaction employing the oxidative pathway was developed by Stephenson *et al.* in 2011.[38] They were able to convert many alcohols to halides with the help of a photochemically generated Vilsmeier-Haack reagent (**147**) (Scheme 39).

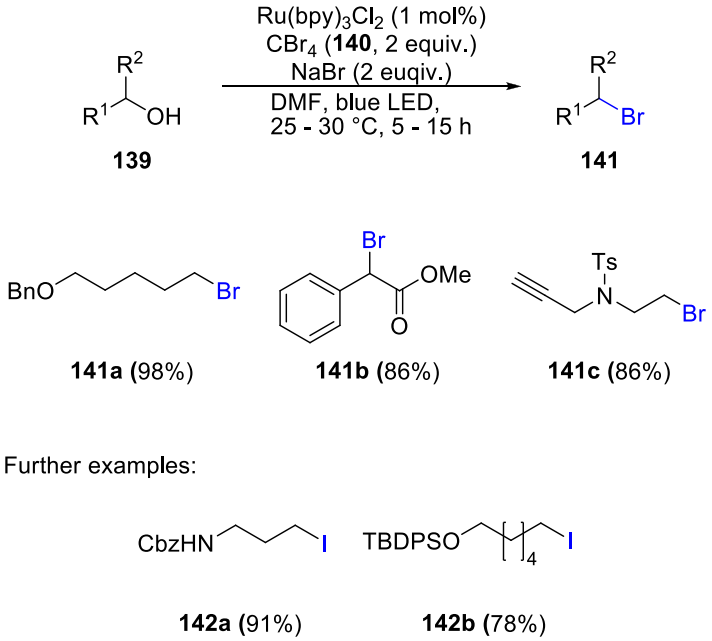

Scheme 39. Photocatalytic conversion of alcohols to halides.

The reaction tolerates many functional groups like amino, ether, tosly, carboxybenzyl, silyl groups or esters (*cf.* **141a-c**). Phenols cannot be transformed to halides *via* this reaction. In addition, not only the conversion of alcohols to bromides is possible *via* this route but also to iodides (*cf.* **142a-b**). In this case CBr_4 (**140**) is replaced with iodoform (Scheme 39).

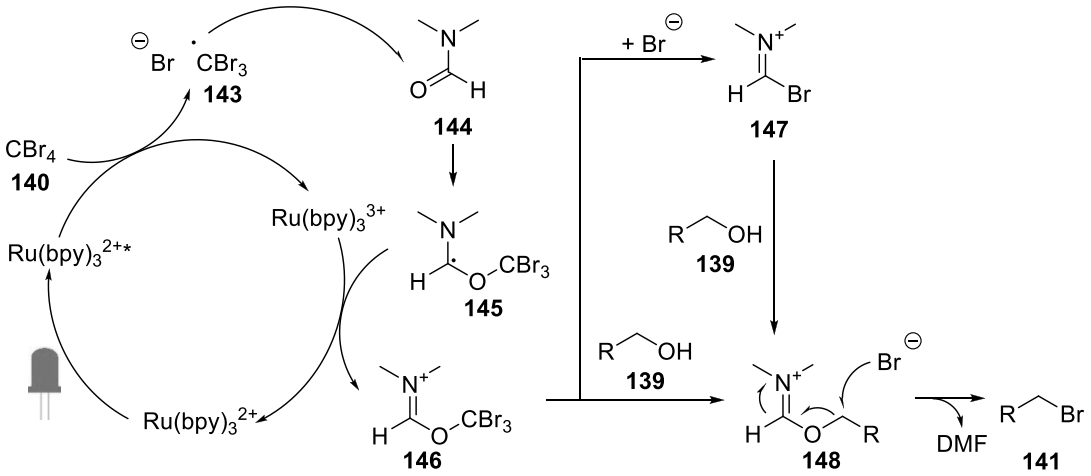

Scheme 40. Mechanism of a photocatalytic conversion of alcohols to halides.

In the proposed reaction mechanism, excited $Ru(bpy)_3^{2+}$* reduces CBr_4 (**140**) to a bromide ion and CBr_3 radical **143**. This radical couples with DMF (**144**) leading to *N*-α-radical **145** which is oxidized by $Ru(bpy)_3^{3+}$ to the corresponding iminium ion **146**. The later can be either attacked directly by alcohol **139** giving rise to **148** or a bromide forming **147** which is converted to **148** by an attack of alcohol **139**. By the attack of a bromide ion, **148** splits into DMF and the final product **141** (Scheme 40).

A versatile reaction sequence to functionalize styrene derivatives **149** with trifluoromethyl groups was developed by Atika *et al.*[39] Also an aminotrifluoromethylation can be performed using this reaction, enabling them to functionalize styrene **149** with a trifluoromethyl group and an amide moiety.[40]

In the proposed reaction mechanism, Umemoto´s reagent (**150**) is reduced by excited $Ru(bpy)_3^{2+*}$, generating a CF_3 radical (**152**). This radical adds to a styrene derivative leading to the more stable benzylic radical **153**. Upon oxidation to the corresponding cation **154**, a Ritter type reaction takes place, furnishing the desired product **151** (Scheme 41).

As substrates served a variety of styrene derivatives **149** bearing differently functionalized aromatic systems (*cf.* **151a-e**). Also dihydronaphthalene, cinnamic ester, steroids and protected amino acids can be used (Scheme 41).

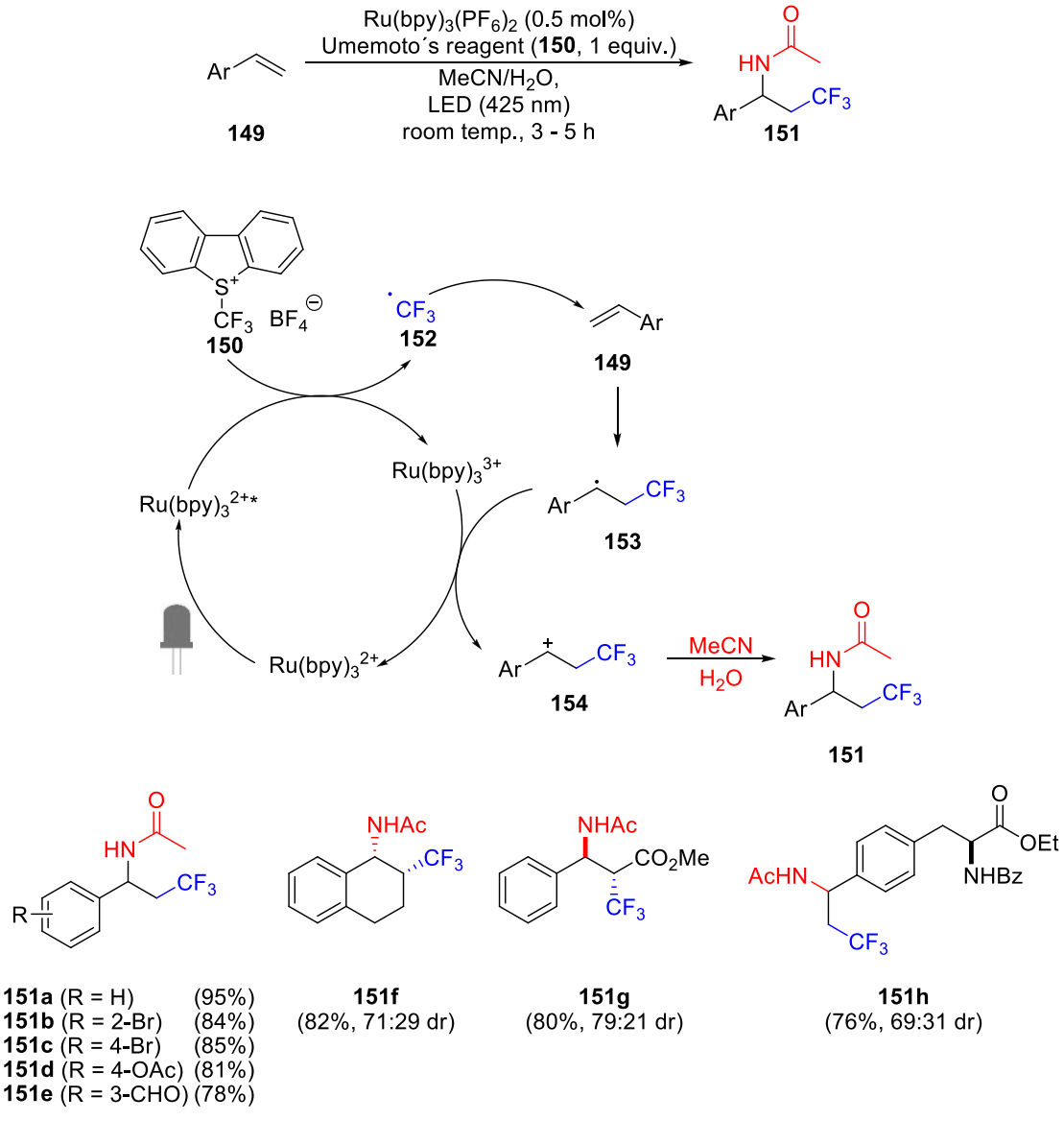

Scheme 41. Photocatalytic aminotrifluoromethylation reaction.

A photocatalytic version of the Meerwein arylation was reported by König *et al*. This reaction enables the chemist to couple aryl diazonium salts to alkenes or aryl moieties. In the first step diazonium salt **155** is reduced by excited $Ru(bpy)_3^{2+*}$ to radical anion **156**. After decomposition, aryl radical **157** adds to olefin **158**. Newly formed radical **159** is oxidized by $Ru(bpy)_3^{3+}$ leading to the formation of cation **160**. In a Meerwein arylation addition reaction, a nucleophile adds to cation **160**. Using the later pathway König *et al.* developed a photocatalytic amino-arylation of styrene (Scheme 42).[41]

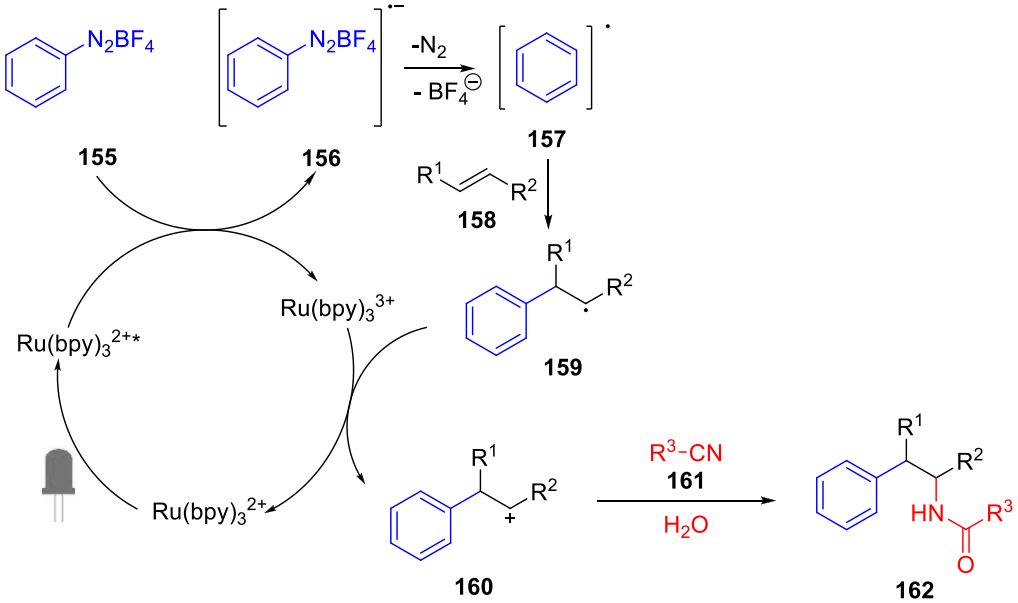

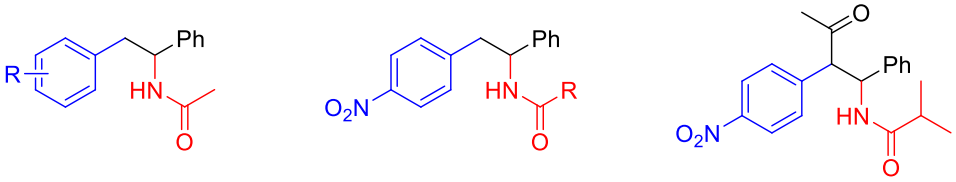

162a (R = H) (82%)
162b (R = 2-NO_2) (87%)
162c (R = 3-NO_2) (70%)
162d (R = 4-NO_2) (92%)
162e (R = 4-OMe) (70%)
162f (R = 2,3,4-Cl) (50%)
162g (R = 4-CF_3) (73%)

162h(R = Et) (84%)
162i (R = C_3H_5) (65%)
162j (R = ^{i}Pr) (71%)

162k (43%)

Scheme 42. Photocatalytic Meerwein arylation reactions.

The reaction can be conducted with functionalized diazonium salts. Functional groups tolerated on the diazonium salt are: nitro groups, ethers, halides and trifluoromethyl groups (*cf.* **162a-g**). Aliphatic nitriles like acetonitrile serve as R-CN source **161** in this reaction (Scheme 42). Other photocatalytic Meerwein arylation reactions were reported by Deronzier *et al.*,[42] Sanford *et al.*,[43] Glorius *et al.*[44] and König *et al.*[45]

Another way to generate aryl radicals *via* photoredox catalysis was explored by Li *et al.*[46] Subjecting aryl sulfonyl chloride **163** to visible light irradiation in the presence of $Ru(bpy)_3^{2+}$ as catalyst cleaves the Ar-SO_2Cl bond and forms an aryl radical **167** after reduction of **163** to the corresponding radical anion **166** (Scheme 43).

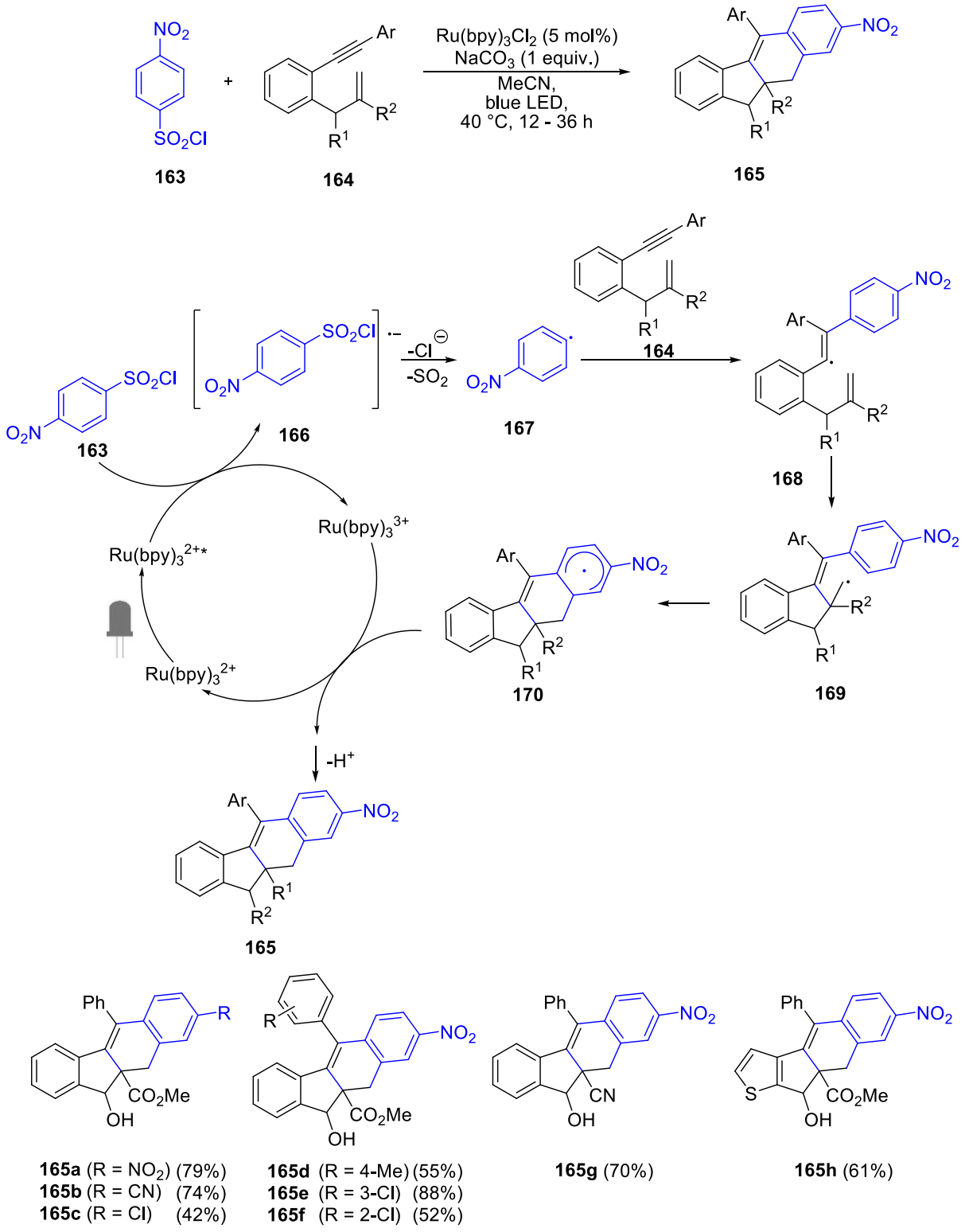

Scheme 43. Tandem cyclization of 1,6-enynes with arylsulfonyl chlorides.

This aryl radical attacks alkyne **164** which undergoes two cyclizations leading to the formation of product **165**.

Nitro and nitrile groups increase the reactivity of the sulfonyl chloride; halogens like chloro decrease it. The reaction works well with many benzylated alkynes giving rise to different substituted benzo[b]fluorenes **165a-h** (Scheme 43).

Aryl radicals **176** can also be generated photocatalytically starting from diaryliodonium salt **171**. Xiao *et al.* developed a method to couple those aryl radicals **176** to arenes and heteroarenes.[47]

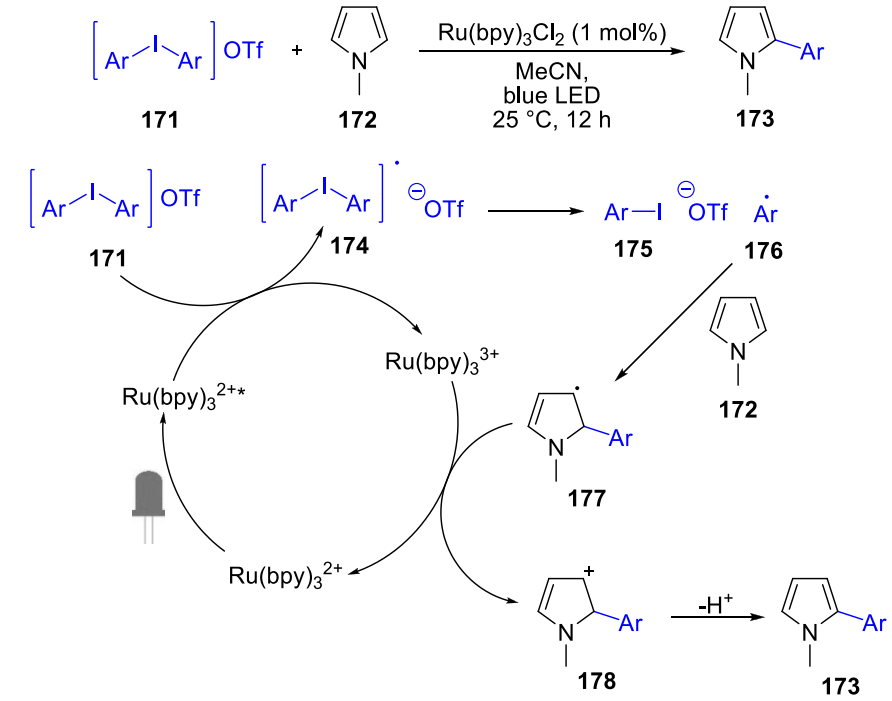

Further examples:

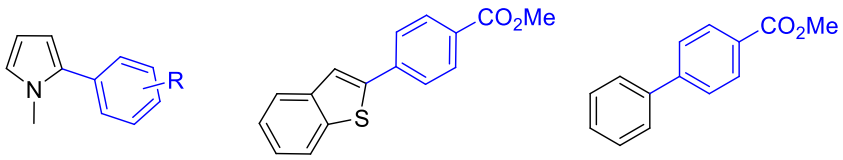

173a (R = H) (87%)
173b (R = 2-F) (91%)
173c (R = 3-F) (85%)
173d (R = 4-F) (91%)
173e (R = 4-CF_3) (89%)
173f (R = 4-CO_2Me) (78%)
173g (R = 4-OMe) (40%)

179 66%

180 50%

Scheme 44. Photocatalytic arylation of aromatic compounds.

The assumed reaction mechanism is similar to the two previous reports, only the leaving group differs. Diaryliodonium salt **171** is reduced in the first step by excited $Ru(bpy)_3^{2+}$*. This leads, after

cleavage of radical **174**, to the formation of iodoarene **175** and the desired aryl radical **176**. The thus obtained radical **176,** adds to N-methylpyrrole (**172**). The intermediate radical **177** is subsequently oxidized by $Ru(bpy)_3^{3+}$ to the corresponding cation **178**. The aromaticity is restored by elimination of a proton forming the final product **173** (Scheme 44).The reaction works best with N-methylpyrrole (**172**), but also other (hetero)arenes like benzothiophene and benzene can be used. A broad variety of differently substituted diaryliodonium salts **171** can be applied. The position of the substituent has no significant influence on the yield of the reaction. On the other hand, the electronic nature of the substituent has a sever influence on the yield; electron withdrawing substituents lead to higher yields than electron donating ones (*cf.* **173a-g**) (Scheme 44).

The most employed photocatalytic way to generate aryl radicals is by using diazonium salts. Its chemistry is well explored and the preparation of many diazonium salts is known.[48] Using aryl sulfonyl chlorides as aryl source enables the chemist to functionalize alkynes and synthesize complex polycyclic compounds. Diaryliodonium salts are useful to functionalize heteroaromatic compounds like pyrroles and benzothiophene.

2.2 Reactions initiated by Substrate Oxidation

As was already shown in Scheme 37, a well-established way to generate $Ru(bpy)_3^{3+}$ selectively is by addition of a viologen derivative **134** as electron acceptor. Yoon *et al.* used this mechanism for a photocatalytic [2+2] cycloaddition of bis-styrene derivatives **181** (Scheme 45).[49]

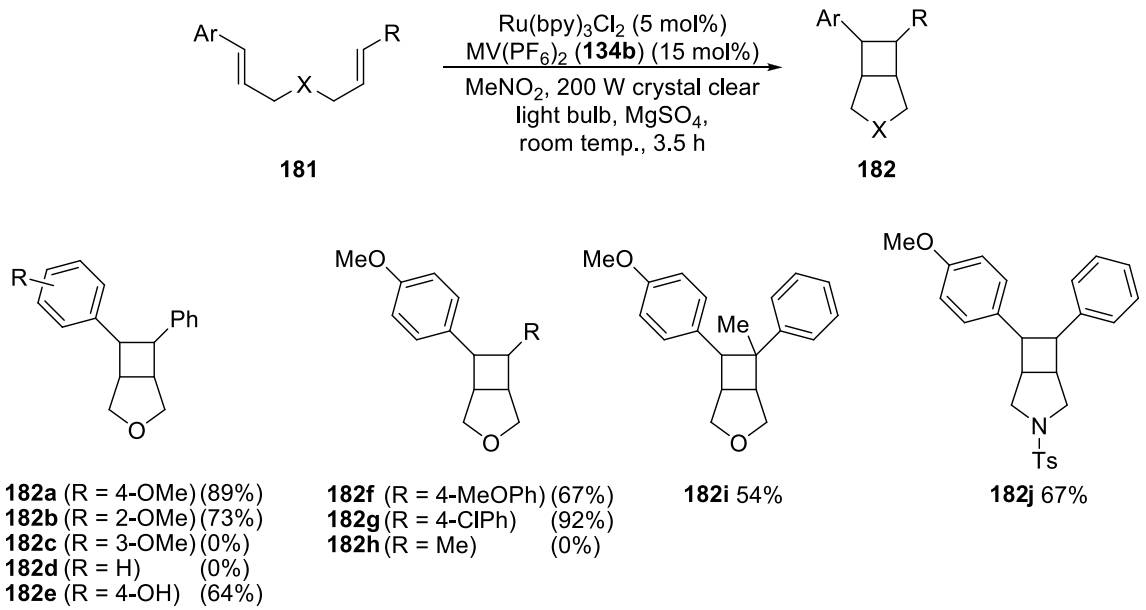

182a (R = 4-OMe) (89%)
182b (R = 2-OMe) (73%)
182c (R = 3-OMe) (0%)
182d (R = H) (0%)
182e (R = 4-OH) (64%)

182f (R = 4-MeOPh) (67%)
182g (R = 4-ClPh) (92%)
182h (R = Me) (0%)

182i 54%

182j 67%

Scheme 45. Photocatalytic [2+2] cycloadditions of (bis)-styrene derivatives.

The styrene moiety has to bear an electron donating substituent in *para* or *ortho* position in order to be electron rich enough to conduct this reaction. At least two styrene moieties have to be present in the molecule (*cf.* **182h**). Styrenes with substituents in *meta* position are not electron rich enough. Formation of **182c** could not be observed. The highest yield was obtained for **182g** where one styrene moiety was electron rich and one was electron poor and decreased when two electron rich styrenes were present as in **182f**. In addition not only styrenes linked *via* oxygen could be applied in this reaction but also ones linked *via* nitrogen yielding **182j**.

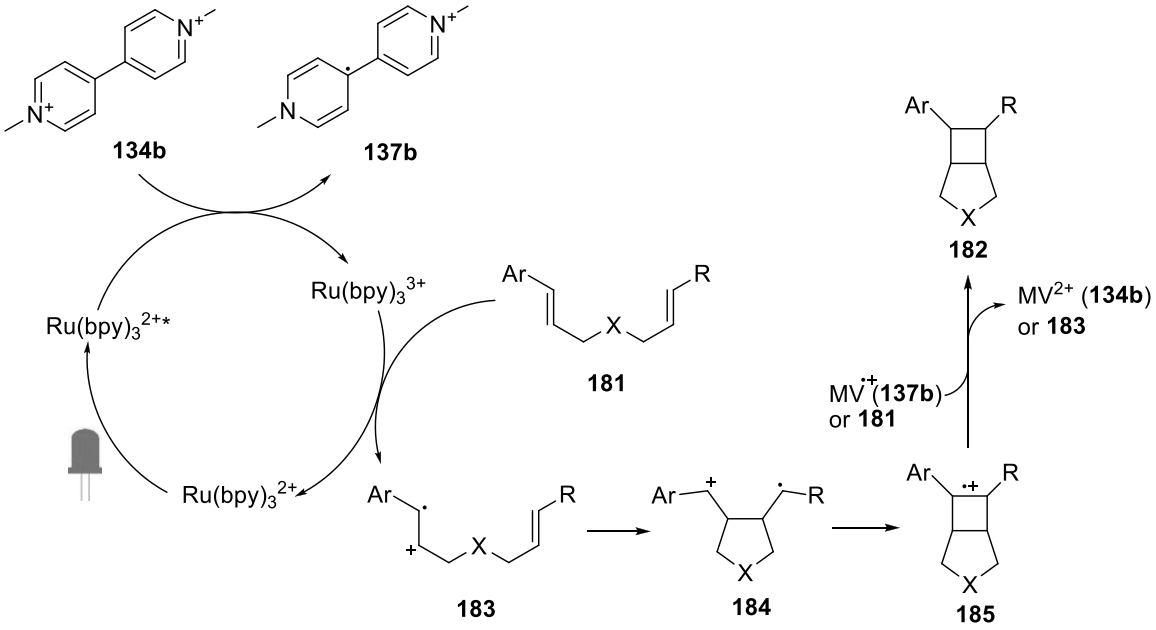

Scheme 46. Mechanism of a photocatalytic [2+2] cycloadditions of (bis)-styrene derivatives.

In contrast to the previously reported [2+2] addition which works by reducing an enone system to a corresponding radical anion, this time radical cation **183** is generated as active intermediate. **183** attacks the opposite styrene systems and the reaction proceeds as depicted in Scheme 46.

As could be shown in Chapter 1 and 2, many interesting and synthetically viable transformations can be conducted using $Ru(bpy)_3^{2+}$ as visible light photoredox catalyst and its number is growing every day. Many reactions require only oxygen or cheap amine bases like Et_3N as stoichiometric reagent or they are redox neutral making photoredox catalysis an economical as well as ecological benign process. Some enantioselective reactions are known. However, so far always in combination with a co-catalyst that introduces the chirality. One of the great challenges for the future will be the development of photoredox catalysts that can introduce chirality on their own without the need for a co-catalyst. A chiral photocatalyst with an iridium center that can be used for enantioselective C-C bond formations was developed recently by Meggers *et al*.[50]

3. References

[1] *Chemical Photocatalysis* König B. Ed.; Walter de Gruyter: Berlin, Boston, **2013.**

[2] Teply, F. *Collect. Czech. Chem. Commun.* **2011**, *76*, 859.

[3] Prier, C. K.; Rankic, D. A.; MacMillan, D. W. C. *Chem. Rev.* **2013**, *113*, 5322.

[4] Nicewicz, D. A.; Nguyen, T. M. *ACS Catalysis* **2014**, *4*, 355.

[5] Paria, S.; Reiser, O. *ChemCatChem* **2014**, *6*, 2477.

[6] Kalyanasundaram, K. *Coord. Chem. Rev.* **1982**, *46*, 159.

[7] Juris, A.; Balzani, V.; Barigelletti, F.; Campagna, S.; Belser, P.; von Zelewsky, A. *Coord. Chem. Rev*. **1988**, *84*, 85.

[8] Yoon, T. P. *ACS Catalysis* **2013**, *3*, 895.

[9] Broomhead, J. A.; Young, C. G. *Syntheses* **1990**, *28*, 338.

[10] Nicewicz, D. A.; MacMillan, D. W. C. *Science* **2008**, *322*, 77.

[11] Ischay, M. A.; Anzovino, M. E.; Du, J.; Yoon, T. P. *J. Am. Chem. Soc.* **2008**, *130*, 12886.

[12] M. R. Narayanam, J. W. Tucker, C. R. J. Stephenson, *J. Am. Chem. Soc.* **2009**, *131*, 8756.

[13] Rackl, D.; Kais, V.; Kreitmeier, P.; Reiser, O. *Beilstein J. Org. Chem.* **2014**, *10*, 2157.

[14] Tucker, J. W.; Zhang, Y.; Jamison, T. F.; Stephenson, C. J. R. *Angew. Chem. Int. Ed.* **2012**, *51*, 4144.

[15] Neumann, M.; Zeitler, K. *Org. Lett.* **2012**, *14*, 2658.

[16] Condie, A. G.; González-Gómez, J. C.; Stephenson, C. R. J. *J. Am. Chem. Soc.* **2010**, *132*, 1464.

[17] Freeman, D. B.; Furst, L.; Condie, A. G.; Stephenson C. R. J *Org. Lett.* **2012**, *14*, 94.

[18] Bergonzini, G.; Schindler, C. S.; Wallentin, C.-J.; Jacobsen, E. N.; Stephenson, C. J. R. *Chem. Sci.* **2014**, *5*, 112.

[19] Rueping M.; Vila, C.; Koenigs, R. M.; Poscharny K.; Fabryet D. C. *Chem. Commun.* **2011**, *47*, 2360.

[20] Kohls, P.; Jadhav, D.; Pandey G.; Reiser O. *Org. Lett.* **2012**, *14*, 672.

[21] *Ruiz Espelt, L.; Wiensch, E. M.; Yoon T. P. J. Org. Chem.* **2013**, *78*, 4107.

[22] Pandey, G.; Jadhav, D., Tiwari, S. K.; Singh, B. *Adv. Synth. Catal.* **2014**, *356*, 2813.

[23] Zou, Y. Q.; Lu, L. Q.; Fu, L.; Chang, N. J.; Rong, J.; Chen, R. J.; Xiao W. J. *Angew. Chem. Int. Ed.* **2011**, *50*, 7171.

[24] Cai, S.; Zhao, X.; Wang, X.; Liu, Q.; Li, Z.; Wang, D. Z. *Angew. Chem. Int. Ed.* **2012**, *51*, 8050.

[25] Sun, H.; Yang, C.; Gao, F.; Li, Z.; Xia, W.*Org. Lett.* **2013**, *15,* 624.

[26] Hu, X.-Q.; Chen, J.-R.; Wei, Q.; Liu, F.-L.; Deng, Q.-H.; Beauchemin, A. M.; Xiao, W.-J. *Angew. Chem. Int. Ed.* **2014**, *53*, 12163.

[27] Mashraqui S. H.; Kellogg R. M. *Tetrahedron Lett.* **1985**, *26*, 1453.

[28] Furst, L.; Matsuura, B. S.; Narayanam, J. M. R.; Tucker, J. W.; Stephenson, C. R. J. *Org. Lett.* **2010**, *12*, 3104.

[29] Andrews, R. S.; Becker, J. J.; Gagné, M. R. *Angew. Chem. Int. Ed.* **2010**, *49*, 7274.

[30] Maji, T.; Karmakar, A.; Reiser, O. *J. Org. Chem.* **2011**, *76*, 736.

[31] Larraufie, M.-H.; Pellet, R.; Fensterbank, L.; Goddard, J.-P.; Lacôte, E.; Malacria, M.; Ollivier, C. *Angew. Chem., Int. Ed.* **2011**, *50*, 4463.

[32] Pandey, G.; Hajra, S.; Ghorai, M. K.; Kumar, K. R. *J. Am. Chem. Soc.*, **1997**, *119*, 8777.

[33] Du, J.; Yoon, T. P. *J. Am. Chem. Soc.* **2009**, *131*, 14604.

[34] Du, J.; Skubi, K. L.; Schultz, D. M.; Yoon, T. P. *Science* **2014**, *344*, 392.

[35] Lu, Z.; Shen, M.; Yoon, T. P. *J. Am. Chem. Soc.* **2011**, *133*, 1162.

[36] Ye Y.; Sanford, M. S. *J. Am. Chem. Soc.* **2012**, *134*, 9034.

[37] Maidan, R.; Goren, Z.; Becker, J. Y.; Willner, I. *J. Am. Chem. Soc.* **1984**, *106*, 6217.

[38] Dai, C.; Narayanam, J. M. R.; Stephenson, C. R. J. *Nat. Chem.* **2011**, *3*, 140.

[39] Yasu, Y.; Koike, T.; Akita, M. *Chem. Commun.* **2013**, *49*, 2037.

[40] Yasu, Y.; Koike, T.; Akita, M. *Org. Lett.* **2013**, *15*, 2136 (and references therein).

[41] Hari, D. P.; Hering, T.; König, B. *Angew. Chem. Int. Ed.* **2014**, *53*, 725.

[42] Cano-Yelo, H.; Deronzier, A. *J. Chem. Soc. Perkin Trans. 2* **1984**, 1093.

[43] Kalyani, D.; McMurtrey, K. B.; Neufeldt, S. R.; Sanford, M. S.; *J. Am. Chem. Soc.* **2011**, *133*, 18566.

[44] Sahoo, B.; Hopkinson, M. N.; Glorius, F. *J. Am. Chem. Soc.* **2013**, *135*, 5505.

[45] Schroll, P.; Hari, D. P.; König, B. *Chemistry Open* **2012**, *1*, 130.

[46] Deng, G. B.; Wang, Z.-Q.; Xia, J.-D.; Qian, P.-C.; Song, R.-J.; Hu, M.; Gong, L.-B.; Li, J. H. *Angew. Chem. Int. Ed.* **2013**, *52*, 1535.

[47] Liu, Y.-X.; Xue, D.; Wang, J.-D.; Zhao, C.-J.; Zou, Q. Z.; Wang, C.; Xiao, J. *Synlett* **2013**, *24*, 507.

[48] Hari, D. P.; König, B. *Angew. Chem. Int. Ed.* **2013**, *52*, 4734.

[49] Ischay, M. A.; Lu, Z.; Yoon, T. P. *J. Am. Chem. Soc.* **2010**, *132*, 8572.

[50] Huo, H.; Shen, X.; Wang, C.; Zhang, L.; Röse, P.; Chen, L.-A.; Harms, K.; Marsch, M.; Hilt, G.; Meggers, E. *Nature* **2014**, *515*, 100.

B. Main Part

1. Photocatalytic Conjugate Additions

1.1 Initial Position

In the course of my Master thesis, Deepak Jadhav and I were able to develop a novel photocatalytic conjugate addition driven by visible light.[51] With this unprecedented reaction, we were able to couple a variety of Michael acceptors **23** with *N*-aryltetrahydroisoquinoline derivatives **2** in moderate to good yields (Table 2).

Table 2. $Ru(bpy)_3Cl_2$ (**1**·Cl_2) catalyzed photocatalytic conjugate additions.

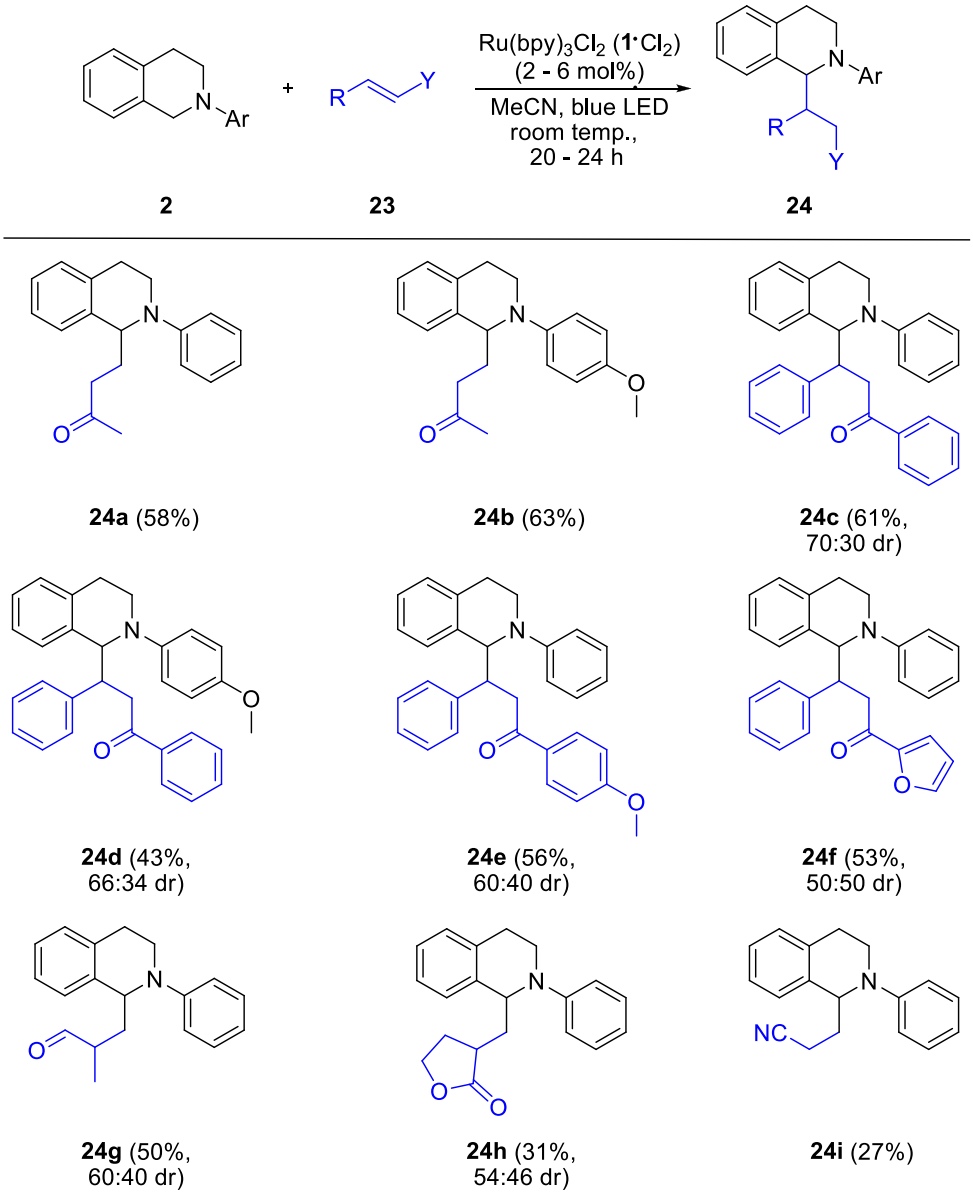

Other groups working with isoquinoline derivative **2** propose an iminium ion **6** as active intermediate in their reaction mechanisms.[52] Exemplary a Lewis base catalyzed Mannich reaction developed by Rueping *et al.* is displayed in Scheme 47 (*cf.* Introduction, Scheme 10).[53]

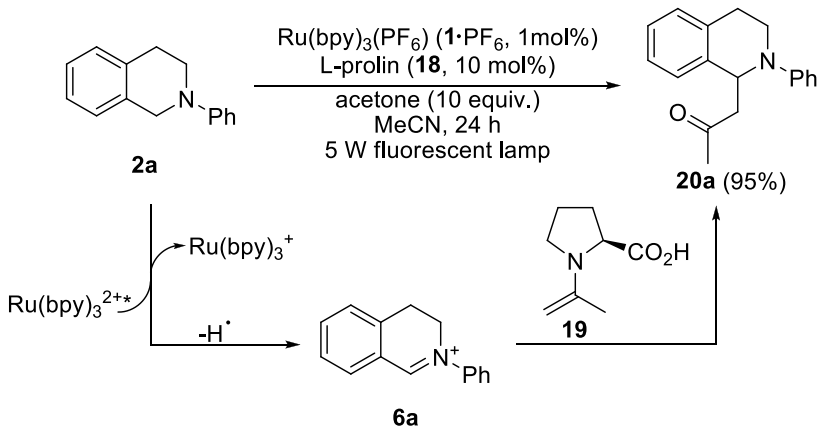

Scheme 47. Photocatalytic Mannich reaction.

In contrast to the above mentioned reaction, it is unlikely that the conjugate addition discovered by our group is proceeding *via* intermediate **6**. In case of the depicted Mannich reaction (Scheme 47) **2** is coupled with a nucleophile, while in our case **2** is coupled with an electrophile. Therefore it is more likely that the reaction proceeds *via* *N*-α-radical **25** (Scheme 48), instead of an iminium ion **6**.

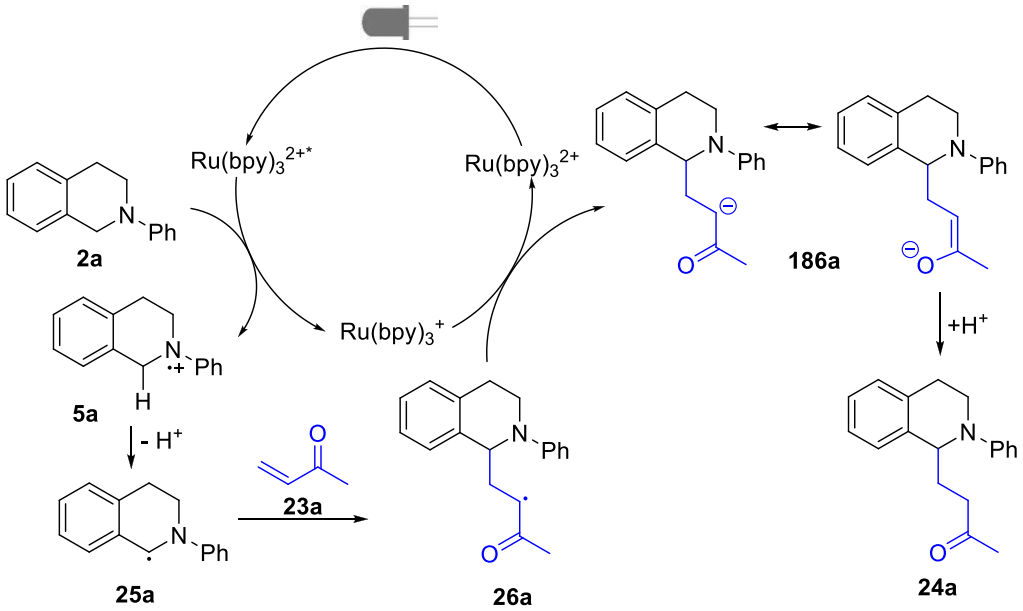

Scheme 48. Proposed mechanism for the photocatalytic *N*-α-functionalization.

In the first step, excited $Ru(bpy)_3^{2+*}$ accepts an electron from isoquinoline **2a** forming radical cation **5a** (Scheme 48). By loss of a proton, the postulated *N*-α-radical **25a** is generated which attacks enone

23a subsequently. The resulting α-carbonyl radical **26a** is reduced by $Ru(bpy)^{+}$, forming anion **186a** which is protonated to yield the final product **24a**.

In addition to the studied intermolecular *N*-α-functionalizations, molecules **27a** and **27b** were synthesized to investigate intramolecular cyclizations. Instead of the expected 1,4 addition products, the dihydroindolo isoquinoline derivatives **28a** and **28b** were obtained (Scheme 49). This means that the initial 1,4 addition is followed by a dehydrogenation merging the two aryl groups to one extended π-system. The different electronic properties of **27** and the additional dehydrogenation step are most likely the reason for the low obtained yields of **28a** in 28% and **28b** in 35%, respectively.

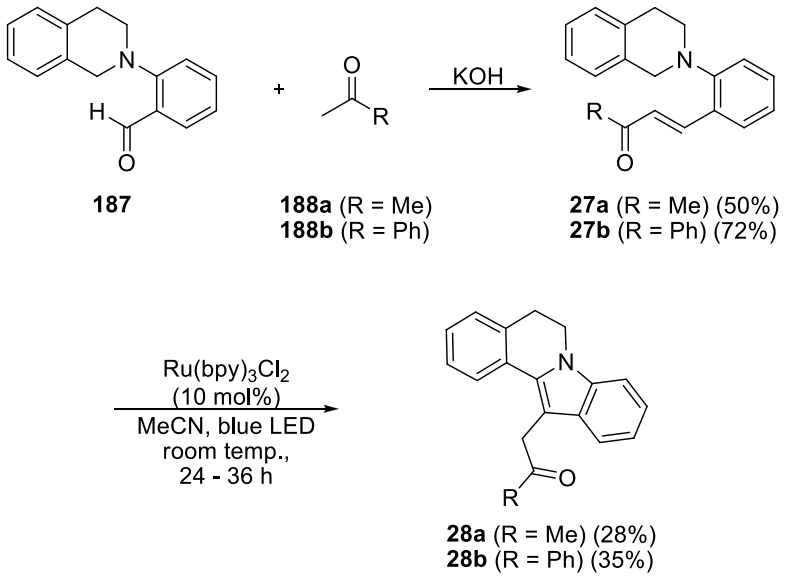

187 **188a** (R = Me) **27a** (R = Me) (50%)
188b (R = Ph) **27b** (R = Ph) (72%)

28a (R = Me) (28%)
28b (R = Ph) (35%)

Scheme 49. Synthesis of dihydroindolo isoquinoline derivatives **28a** and **28b**.

In conclusion, a novel photocatalytic reaction to functionalize isoquinolines at the *N*-α-position was discovered. A variety of Michael acceptors was applicable in this reaction. Small modifications of the isoquinoline were also tolerated but led in most cases to a reduced yield. Besides, the reaction is completely atom economical; every single atom of the reactants can be found in the product and no sacrificial electron donor or acceptor is required.

The aim of the following investigations is to gain a deeper insight in the *N*-α-activation of *tert.* amines and the coupling of Michael acceptors to the resulting radicals. In the beginning different known photoredox catalysts were screened. The first one, tetra-butylammonium decatungstate (TBADT, **190**) is activated by UV light and was used successfully by Albini *et al.* in similar reactions (Chapter 1.2).[54] Our group discovered that $Cu(dap)_2Cl$ (**195**) can be activated by visible light, driving forward ATRA reactions (Chapter 1.3).[55] The photoredox catalyst $[Ir(ppy)_2(dtbbpy)]PF_6$ (**204**·PF_6) is well established in the photochemical community possessing similar reactivities as $Ru(bpy)_3Cl_2$ (**1**·Cl_2) (Chapter 1.4).[56] $[Ir\{dF(CF_3)ppy\}_2(dtbbpy)]PF_6$ (**216**·PF_6) has a great oxidation and reduction potential and was therefore appealing for the transformation of *tert.* amines with greater oxidation potentials compared to isoquinolines (Chapter 1.7).

It was envisioned to enhance the rate of the reaction and the yield with the help of additives. Therefore the influence of different Brønsted bases (Chapter 1.4), Lewis acids (Chapter 1.7) and combinations of proton donors and acceptors (Chapter 1.6) for the reaction was investigated.

In Chapter 1.5 novel amines were examined for their applicability in this transformation and in Chapter 1.6 micro reactors as irradiation devices are described.

1.1 TBADT as photocatalyst for *N*-α-activation

Polyoxometalates (POM) are metal oxide clusters that form in self-assembly in the presence of a chelating counter ion. POM´s contain at least three metal atoms that are coordinated octahedral. These octahedrons are linked together by shared oxygen atoms. Due to ligand to metal charge transfer (LMCT) from the oxygen to the metal these complexes exhibit large absorption bands, usually in the ultra violet (UV) regime of the electromagnetic spectrum. Therefore they have been used numerous times as photocatalysts.[57]

One prominent example for a polyoxometalate based catalyst is tetra-butylammonium decatungstate (TBADT, (n-$Bu_4N)_4W_{10}O_{32}$, **190**) which is activated by UV-light.[58] It can be easily prepared by stirring sodium tungstate in oxygen enriched water for 12 h. After slow acidification with hydrochloric acid, the product can be precipitated through addition of (n-Bu)$_4$NCl.[59] The absorption maxima of the LMCT band is located at 323 nm with an extinction coefficient of $\varepsilon = 1.35 \times 10^4$ l mol^{-1} cm^{-1}.[60]

The group of Angelo Albini used this catalyst for alkylations of electrophilic alkenes (Scheme 50),[61] acylations of electrophilic olefins,[62] radical C-H functionalization of amides[63] and the synthesis of 2-substituted 1,3-benzodioxoles[64].

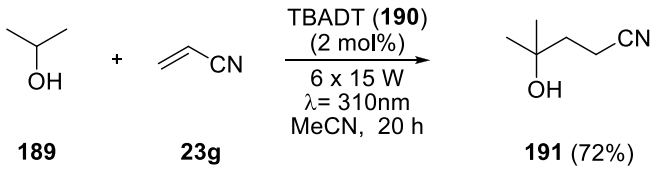

Scheme 50. Photocatalytical alkylation of acrylonitrile (**23g**).[54]

The mechanism for this reaction, depicted in Scheme 51, is similar to the mechanism we propose for the photocatalytic conjugate addition (Chapter 1.1, Scheme 48).

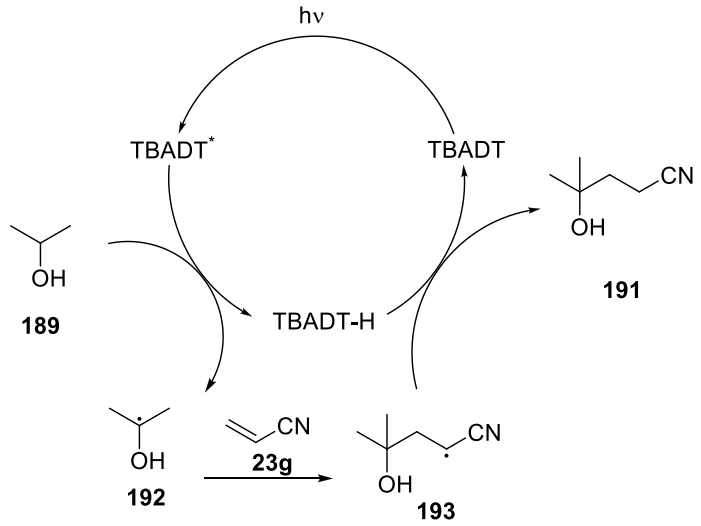

Scheme 51. Reaction mechanisms for the alkylation of alkenes with the help of TBADT (**190**).

Based on this similarity it was envisioned to use TBADT (**190**) as UV-photoredoxcatalyst for the *N*-α-activation of *tert.* amine. A 6 W fluorescent tube with a maximum emission at λ_{max}=360 nm. Was chosen as light source Therefore an experiment was conducted if the catalyst can be activated with this light source. To our delight, product **191** was furnished when acrylonitrile (**23i**) (1 equiv.) was mixed with isopropyl alcohol (**189**) (5 equiv.) in degassed acetonitrile (Scheme 52 A)) even though the reaction time had to be extended to 3.5 d. Those conditions should be suitable to test if TBADT can be used for the *N*-α-activation of **2a**. If these experiments would yield any product, further reactions will be conducted with a more appropriate light source.

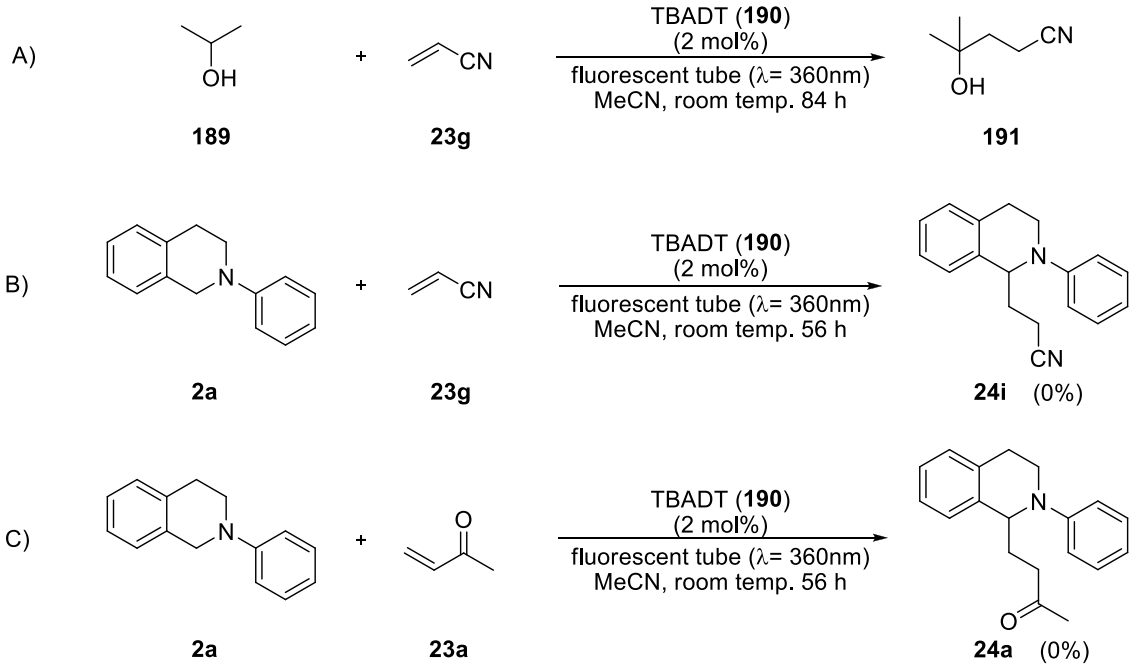

Scheme 52. Photocatalytic N-α-activation with TBADT (**190**).

Changing the substrate from isopropyl alcohol (**189**) to isoquinoline **2a** in degassed acetonitrile, no conversion and no product formation could be detected within 2.5 d according to TLC and NMR analysis, so the reaction was terminated (Scheme 52 B)). Using methyl vinyl ketone (**23a**), instead of acrylonitrile, (**23i**) led also to no conversion (Scheme 52 C)). Only isoquinoline **2a** was detectable *via* ^{1}H-NMR after removing solvent and **23a** *in vacuo*.

Additionally the same experiments were conducted without degassing the reaction mixture. Also in this case, nearly no conversion and no product formation could be observed when **2a** and either **23a** or **23g** were irradiated in the presence of TBADT (**190**) in acetonitrile for 24 h.

With the help of these experiments it could be proven, that TBADT is not a suitable catalyst for photocatalytic *N*-α-activation of amines under UV-light irradiation.

1.2 $Cu(dap)_2Cl$ as photocatalyst for *N*-α-activation

In search for another visible light photoredoxcatalyst, capable of enhancing the *N*-α-activation of *tert.* amines, $Cu(dap)_2Cl$ (dap = 2,9-bis(p-anisyl)-l, 10-phenanthroline) (**195**) was investigated. This complex was first reported in literature 1987 by Sauvage *et al.* for C-C bond formations under photocatalytic conditions (Scheme 53).[65]

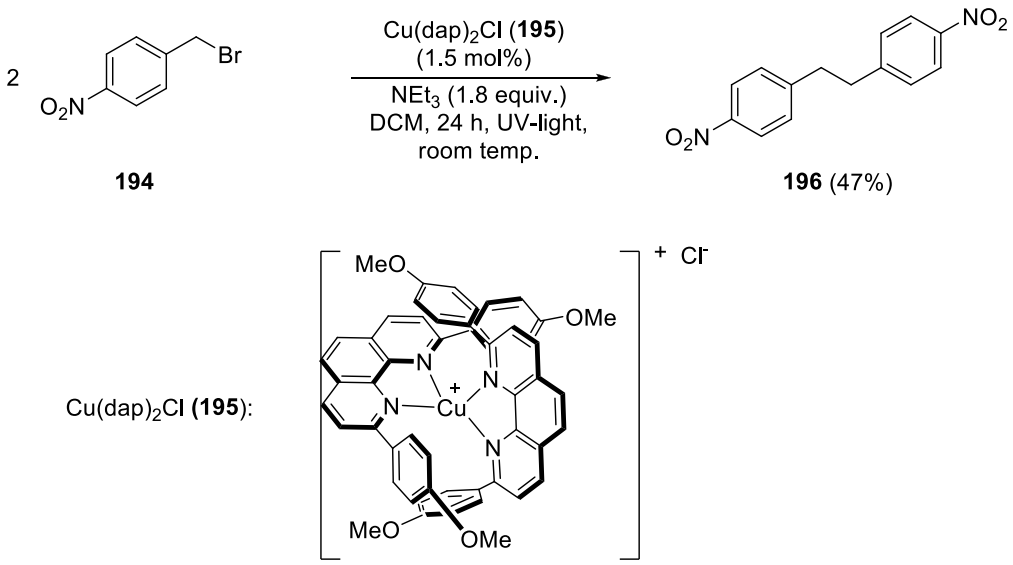

Scheme 53. Photocatalytic dimerization of nitrobenzene derivative **194** in the presence of catalyst $Cu(dap)_2Cl$ (**195**).[65]

Michael Pirtsch from our group discovered that electron transfer from **195** is not only possible under UV-irradiation, but also visible light irradiation can be utilized. Reiser *et al.* were able to apply this concept to a variety of ATRA reactions (Scheme 54).[55]

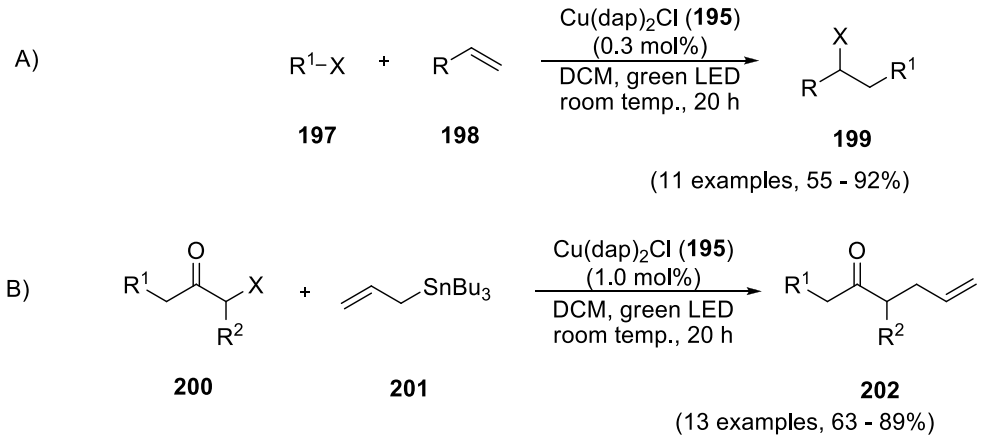

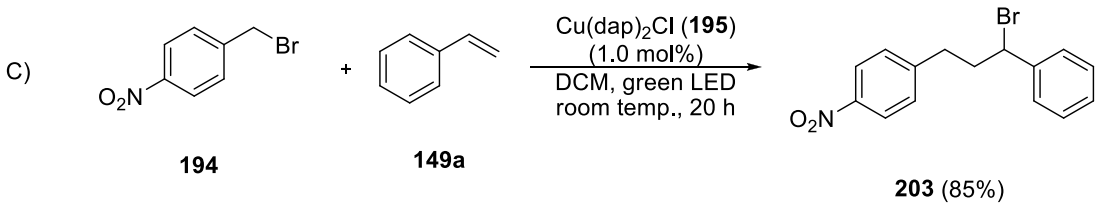

Scheme 54. Photochemical ATRA reactions driven by Cu(dap)$_2$Cl (**195**).[55]

Due to these promising results, Cu(dap)$_2$Cl (**195**) was applied in photocatalytic conjugate additions. **195** has a broad absorption band in the range of 400 – 600 nm and the excited state lasts for 270 ns. $[Cu(dap)_2]^{+}$* has a reduction potential of $E_{1/2}(Cu^{II}/Cu^{I}*)$ = -1.43 V *vs.* SCE and is therefore a better reductant than $Ru(bpy)_3^{+}$ ($E_{1/2}(Ru^{II}/Ru^{I})$ = -1.33 V *vs.* SCE).[66] The oxidation potential has a value of $E_{1/2}(Cu^{II}/Cu^{I})$ = 0.62 V *vs.* SCE and is therefore in the range of the isoquinoline derivative **2a** (E_{ox} = 0.66 V *vs.* SCE).[65] So far, no reaction using an oxidation by $Cu(dap)_2^{2+}$ as step in catalysis is known.[67] But in summer 2011, after Michael Pirtsch´s discovery that **195** can be excited by visible light, hopes were high that also a substrate oxidation can be performed. The catalytic cycle should be initiated by the reduction of the enone generating $Cu(dap)_2^{2+}$ which should be able to oxidize isoquinoline **2** to its radical cation and from there on the mechanism would be the same as postulated above (Scheme 48).

In order to investigate this idea, isoquinoline **2a** (1 equiv.), Cu(dap)$_2$Cl (**195**) (5 mol%) and either methyl vinyl ketone (**23a**, 3 equiv.) or chalcone (**23b**, 1.1 equiv.) were dissolved in acetonitrile and degassed by the freeze pump thaw method.

Table 3. Photocatalytic *N*-α-activation with Cu(dap)$_2$Cl (**195**).

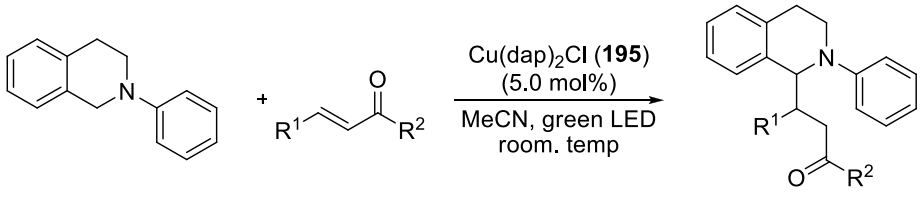

2a **23** **24**

entry	R^1	R^2	time [h]	conversion	yield
1	H	H	20	7%	0%
2	Ph	Ph	20	2%	0%

In both cases no product formation could be observed according to TLC and crude ^{1}H-NMR analysis with p-nitrobenzaldehyde as NMR internal standard (Table 3). Because the results in the presence of photocatalyst $Ru(bpy)_3Cl_2$ (**1**·Cl_2) were superior compared to **195**, no further studies using **195** for photocatalytic *N*-α-activation were conducted.

1.3 $[Ir(ppy)_2(dtbbpy)]PF_6$ as photocatalyst for *N*-α-activation

Not only octahedral ruthenium complexes exhibit an important class of visible light photoredox catalysts. Also complexes with iridium as central atom find broad application.[56] One prominent example is $[Ir(ppy)_2(dtbbpy)]PF_6$ (**204**·PF_6) (ppy = 2-phenylpyridine; dtbbpy = 4,4'-di-*tert*-butyl-2,2'-bipyridine) (Figure 4).

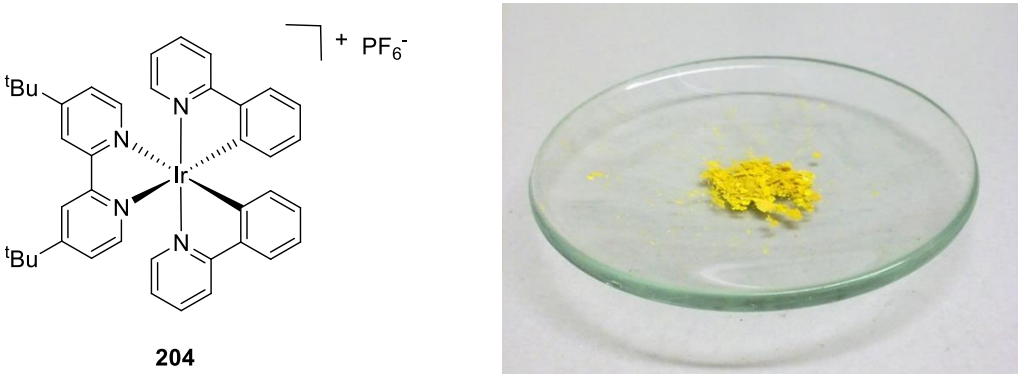

204

Figure 4. $[Ir(ppy)_2(dtbbpy)]PF_6$ (**204**·PF_6): Structure and powder.

It was first synthesized and characterized by Malliaras *et al.* in 2004. Its emission maximum is located at 581 nm which corresponds to 2.13 eV.[68] The redox potentials *vs.* a saturated calomel electrode (SCE) in acetonitrile are depicted in Scheme 55.

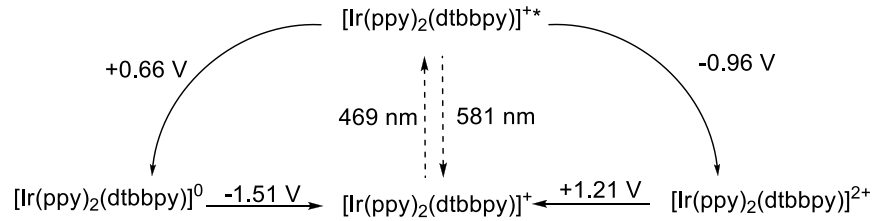

Scheme 55. General reaction pathway and redox potentials of $[Ir(ppy)_2(dtbbpy)]PF_6$ (**204**).[52b)]

MacMillan *et al.* reported the use of this complex for the enantioselective addition of trifluoromethyl groups to aldehydes in 2009.[69] In the first step aldehyde **94** and chiral organocatalyst **96** form enamine **100** which is enantioselectively attacked by a CF_3-radical (**127**), generated previously through photo-catalytic electron transfer and subsequent cleavage of trifluoroiodomethane (**125**). The final product **205** is formed by oxidation of intermediate **206** and subsequent hydrolysis of the organocatalyst product complex (Scheme 56).

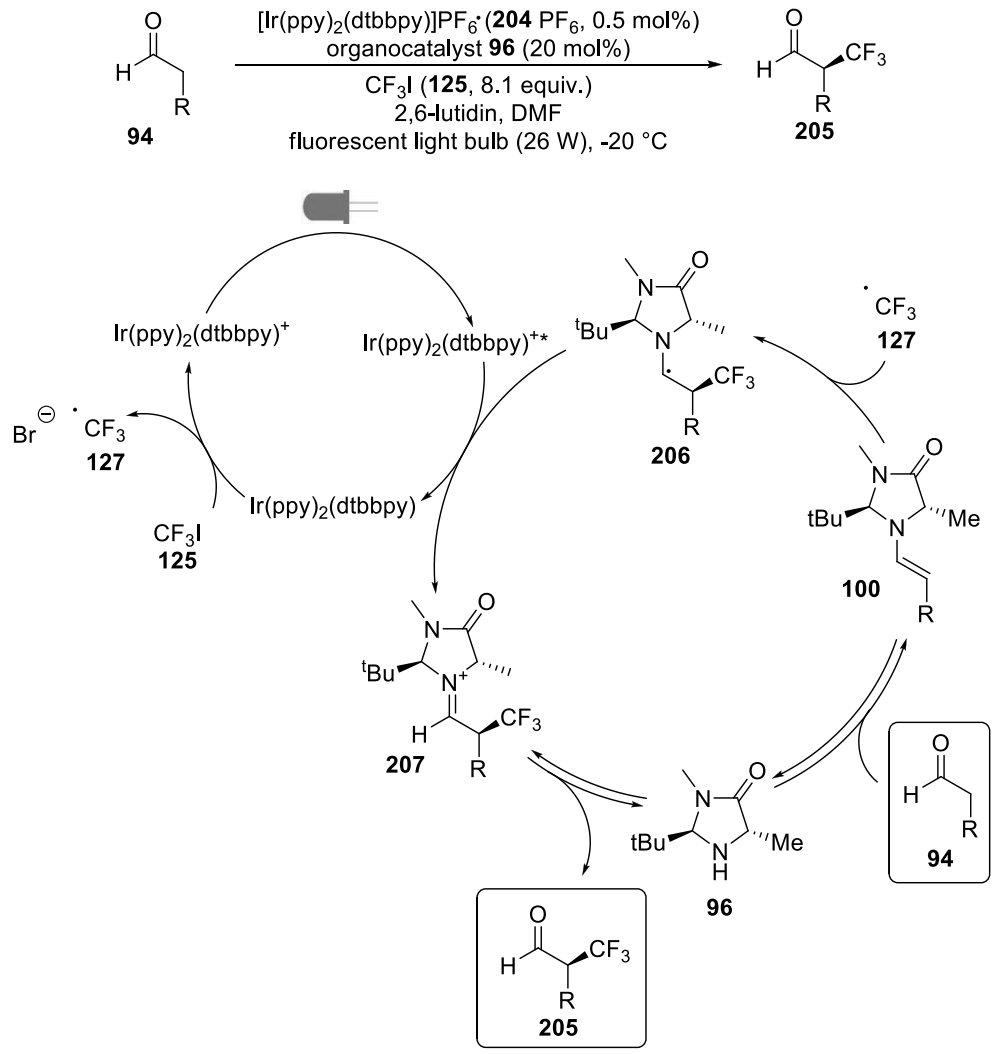

Scheme 56. Reaction pathway of the enantioselective trifluoromethylation of aldehydes.[69]

With the help of this reaction, MacMillan *et al.* were able to enantioselectively add different fluoroalkyl radicals to a variety of aldehydes.

As already discussed in the introduction, Stephenson *et al.* were able to develop a photocatalytic *aza*-Henry reaction. This reaction can not only be conducted using $Ru(bpy)_3Cl_2$ (**1**·Cl_2) as photoredox catalyst but also with $[Ir(ppy)_2(dtbbpy)]PF_6$ (**204**·PF_6). This finally led to the full establishment of **204** as photocatalyst in the synthetic community. Applying $Ru(bpy)_3Cl_2$ (**1**·Cl_2) as photocatalyst for the

aza-Henry reaction with **2a** gave rise to product **4a** in up to 73% yield (*cf.* Introduction, Scheme 5). Through the use of photocatalyst $[Ir(ppy)_2(dtbbpy)]PF_6$ (**204**·PF_6) the yield could even be increased to 92%.[52b)]

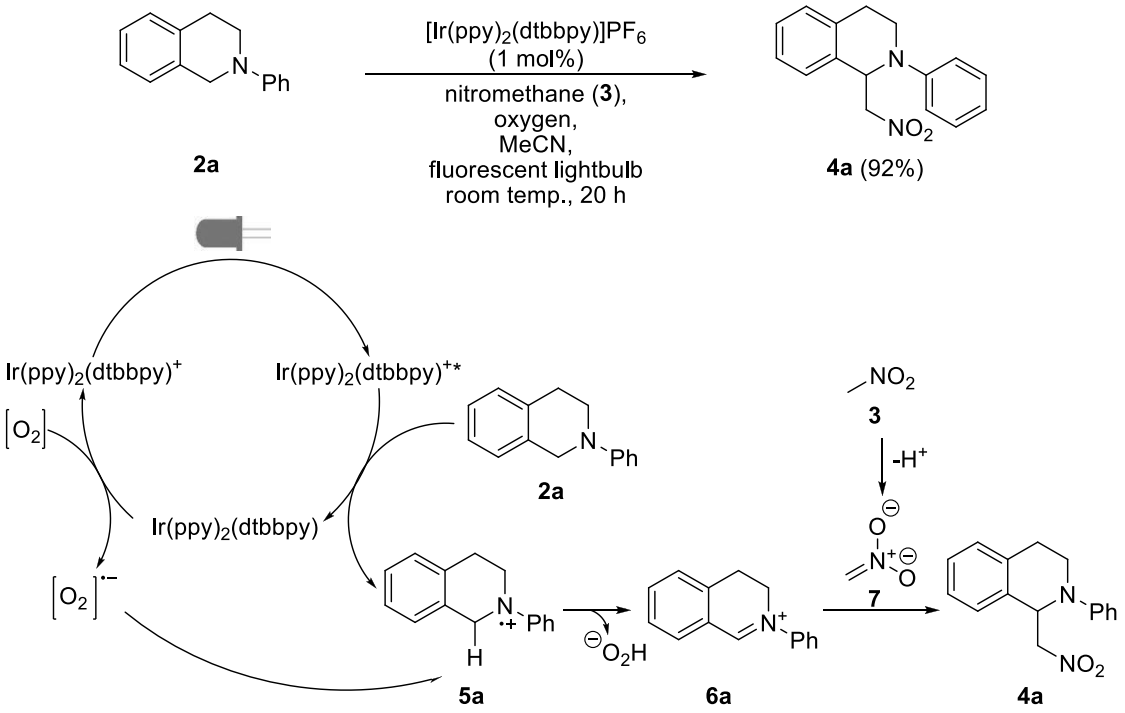

Scheme 57. Proposed reaction mechanism of a photocatalytic *aza-Henry* reaction.[52b)]

With this method Stephenson *et al.* were able to functionalize a variety of *N*-aryltetrahydro-isoquinoline derivative **2** with nitromethane (**3**) or nitroethane in good to excellent yields, forming a basis for a variety of other photochemical transformations using **2** as substrate.

Due to its interesting redox properties, $[Ir(ppy)_2(dtbbpy)]PF_6$ (**204**·PF_6) was employed in a photocatalytic conjugate addition reaction (Scheme 58). The catalyst was prepared according to literature procedures.[68] If not otherwise stated, all conjugate additions reactions were degassed using three freeze pump thaw cycles prior to irradiation. This was necessary to exclude oxygen, which is known to oxidize Ir^{II} to Ir^{III} and lead to the formation of iminium ion **6** (*cf.* Scheme 47)

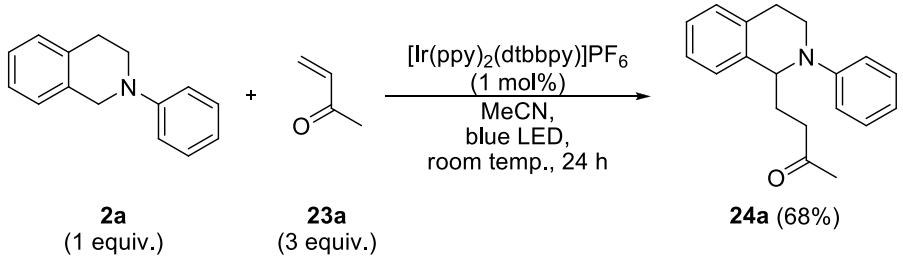

Scheme 58. Photocatalytic conjugate addition using $[Ir(ppy)_2(dtbbpy)]PF_6$ (**204**·PF_6).

To our delight, when methyl vinyl ketone (**23a**) was used as Michael acceptor, product **24a** could be isolated in 68% yield within 24 h using 2 mol% of catalyst **204** compared to 58% yield using $Ru(bpy)_3Cl_2$ (**1**·Cl_2) (Scheme 58).[51]

A screening regarding catalyst loading and the influence of additives was performed to determine the best reaction conditions.

To find the optimal catalyst loading the reaction was conducted using 0.5 mol%, 1 mol% and 2 mol% of the new catalyst **204**. When 0.5 mol% of catalyst **204** was employed 38% of product **24a** was formed within 24 h (entry 1, Table 4). Using 1 mol% of catalyst **204** increased the yield of **24a** to 66% (entry 2, Table 4) and 2 mol% furnished conjugate addition product **24a** in 68% yield within 24 h. As the yield was not significantly increased when 2 mol% instead of 1 mol% of **204** were used, further optimization experiments to determine the influence of bases on the reaction were performed in the presence of 1 mol% of the iridium photoredox catalyst **204**.

Table 4. Optimization of the photocatalytic *N*-α–activation using **204**.

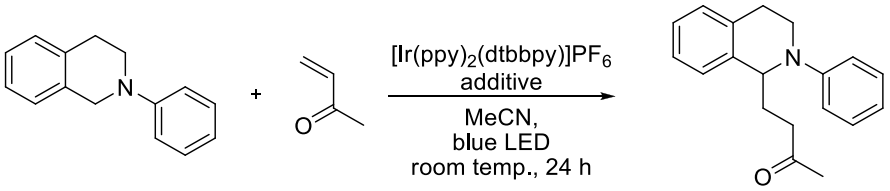

2a **23a** **24a**

entry	2a	23a	additive	catalyst loading / [mol%]	yield[a] 24a
1	1 equiv.	3 equiv.	-	0.5	38%
2	1 equiv.	3 equiv.	-	1.0	66%
3	**1 equiv.**	**3 equiv.**	**-**	**2.0**	**68%**
4	1 equiv.	3 equiv.	NaOAc 1.1 equiv	1.0	64%
5	1 equiv.	3 equiv.	K_2CO_3 1.1 equiv.	1.0	46%
6	1 equiv.	3 equiv.	imidazole 1.1 equiv.	1.0	0%

a) Yield determined by ^{1}H-NMR-analysis using 1,2 dicyanobenzene as internal standard.

One of the key steps in the proposed reaction mechanism is the deprotonation of isoquinoline radical cation **5** to radical **25** (Chapter 1.1, Scheme 48). Therefore it was explored if the addition of different bases could further increase the yield. Addition of 1.1 equiv. of sodium acetate had no influence on the reaction (64% yield, entry 4, Table 4). Potassium carbonate (1.1 equiv.) on the other hand decreased the yield to 46% (entry 5, Table 4) and no product formation was observed when 1.1 equiv. of imidazole were employed (entry 6, Table 4). This observation might not only be caused by the basicity of imidazole. It is also possible that this *N*-heterocycle is causing a ligand exchange in catalyst **204**. Overall, the addition of a base to promote deprotonation of intermediate radical cation **5** has no beneficial effect on the reaction.

Next the influence of water in the reaction media was investigated. Water can serve as proton shuttle and therefore accelerate the deprotonation of the radical cation intermediate and the protonation of the final product. This screening was conducted in a micro reactor purchased from LTF with an internal volume of 1.7 mL. More information about this micro reactor system is given in Chapter 1.6. The reaction solution was pumped through the reactor at a speed of 1 mL/h, which corresponds to a retention time in the system of 1 h 50 min. Catalyst **204** (2 mol%) was employed and 0% (v/v), 5% (v/v) and 10% (v/v) of water were added to obtain a fully dissolved and clear the solvent.

Table 5. Water as additive for photocatalytic conjugate additions.

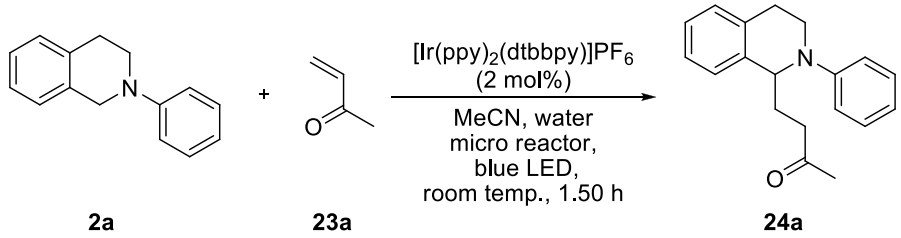

2a **23a** **24a**

entry	2a	23a	water / [% (v/v)]	yield[a] 24a
1	1 equiv.	3 equiv.	0	46%
2	1 equiv.	3 equiv.	5	46%
3	1 equiv.	3 equiv.	10	0%

a) Yield determined by ^{1}H-NMR-analysis using 1,2 dicyanobenzene as internal standard.

As depicted in entry 1 (Table 5) product **24a** could be obtained in 46% yield within 2 h using a micro reactor system. The same yield was obtained when the solvent contained 5% (v/v) water (entry 2,

Table 5). No product formation was observed when the solvent mixture contained more than 5% (v/v) water (entry 3, Table 5). These experiments showed that up to 5% (v/v) water is neither increasing nor decreasing the yield and beyond this the yield decreases.

In further experiments the substrate scope of the reaction using catalyst **204** was determined. Due to the different electronic and steric properties, compared to methyl vinyl ketone (**23a**), chalcone **23b** was investigated next. To find the optimal reaction conditions first the catalyst loading and afterwards the ratio of **2a** to chalcone **23b** was optimized. In contrast to methyl vinyl ketone (**23a**), which polymerizes upon irradiation with visible light, **23b** is photostable, only a E/Z isomerization of the double bond can be observed.

Table 6. Photocatalytic conjugate addition using chalcone **23b** and catalyst **204**.

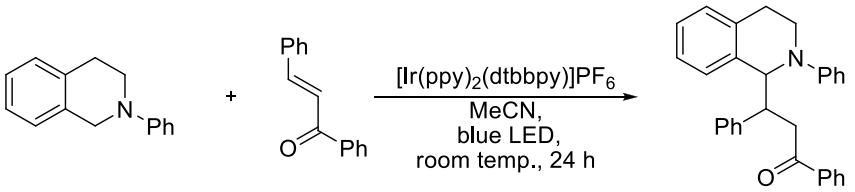

2a **23b** **24c**

entry	2a	23b	catalyst loading /[mol%]	yield 24c
1	1 equiv.	1.1 equiv.	1.0	48%[a]
2	1 equiv.	1.1 equiv.	2.0	73%[a]
3	**1 equiv.**	**1.1 equiv.**	**5.0**	**91%[a] / 83%[b]**
4	1 equiv..	1.1 equiv	10.0	34%[a]
5	2 equiv.	1.0 equiv.	5.0	76%[a]
6	1 equiv.	1.5 equiv.	5.0	83%[a]
7	1 equiv.	3.0 equiv.	5.0	67%[a]

a) Yield determined by ^{1}H-NMR-analysis using 3-nitrobenzaldehyde as internal standard; b) isolated yield.

Using 1 mol% and 2 mol% of **204** product **24c** was formed in 48% and 73% yield (entry 1 - 2, Table 6). To our delight, employing 5 mol% of catalyst **204** furnished product **24c** in an increased yield of 91% (entry 3, Table 6). Subsequent isolation yielded 83% of **24c**. Thus, yields obtained in the presence of iridium catalyst **204** are significantly better than using $Ru(bpy)_3Cl_2$ (**1**·Cl_2). However, the yield decreased dramatically when 10 mol% of catalyst **204** were employed (entry 4, Table 6). Therefore this coupling works best in the presence of 5 mol% of $[Ir(ppy)_2(dtbbpy)]PF_6$ (**204**·PF_6).

In another set of experiments the optimal ratio of isoquinoline **2a** to chalcone **23b** was determined (entry 3 and 5 – 7, Table 6). Using an excess of 2.0 equiv. of isoquinoline **2a** led to a decreased yield of 76% (entry 5, Table 6) compared to the use of a slight excess of 1.1 equiv. of chalcone **23b** (entry 3, Table 6). Further increasing the amount of chalcone **23b** to 1.5 equiv. (entry 6, Table 6) and 3.0 equiv. (entry 7, Table 6) resulted in reduced yields of 83% and 67% of product **24c**. Thus a ratio of **2a** to **23b** of 1:1.1 and a catalyst loading of 5 mol% are regarded to be the optimal reaction conditions, resulting in the formation of 91% of product **24c**. In conclusion, the same reaction conditions that proofed to be best using $Ru(bpy)_3Cl_2$ (**1**·Cl_2) as catalyst are also the optimized conditions for $[Ir(ppy)_2(dtbbpy)]PF_6$ (**204**·PF_6).

Photocatalytic conjugate additions using $[Ir(ppy)_2(dtbbpy)]PF_6$ (**204**·PF_6) as catalyst were performed with the same substrates that were applicable using $Ru(bpy)_3Cl_2$ (**1**·Cl_2). The optimized reaction conditions are shown in Table 7.

Product **24a** could be obtained in 68% yield using 1 equiv. of **2a**, 3 equiv. of **23a** and 2 mol% of **204** (entry 1, Table 7). Performing the same reaction with the more electron rich 2-(4-methoxyphenyl)-1,2,3,4-tetrahydroisoquinoline (**2b**), 5 mol% of catalyst **204** were necessary to obtain 37% of **24b** (entry 2, Table 7). The same trend was observed when Michael acceptor **23b** instead of **23a** was employed. As shown in Table 7, product **24c** could be obtained in 83% isolated yield using 1.0 equiv. of **2a**, 1.1 equiv. of **23b** and 5 mol% of catalyst [**204**·PF_6] (entry 3, Table 7). Exchanging the isoquinoline to **2b** reduced the yield to 33% (entry 4, Table 7) compared to 43% using [**1**·Cl_2] as catalyst. The same trend was observed for the coupling of **2b** with **23a** where the yield decreased from 61% using catalyst [**1**·Cl_2] to 43% using catalyst **204**. Thus, catalyst **204** is regarded not to be optimal to activate isoquinoline **2b**. Product **24e** was furnished in 93% yield (entry 5, Table 7), the highest isolated yield in this conjugate addition. Chalcone **23d** bearing a furan moiety could be coupled to isoquinoline **2a** in 60% (entry 6, Table 7). Using methacrolein (**23e**) led to 50% of product **24g** using only 2 mol% of catalyst (entry 7, Table 7). Coupling product **24h** could be furnished in 34% yield using 3 equiv. of γ-butyrolactone and 5 mol% of catalyst (entry 8, Table 7). Employing 3 equiv. of acrylonitrile (**23g**) in this reaction yielded product **24i** in 31% (entry 9, Table 7). A comparison of these results with the results obtained using $Ru(bpy)_3Cl_2$ (**1**·Cl_2) is given in Chapter 1.8.

Table 7. Photocatalytic conjugate additions using $[Ir(ppy)_2(dtbbpy)]PF_6$ (**204**·PF_6).

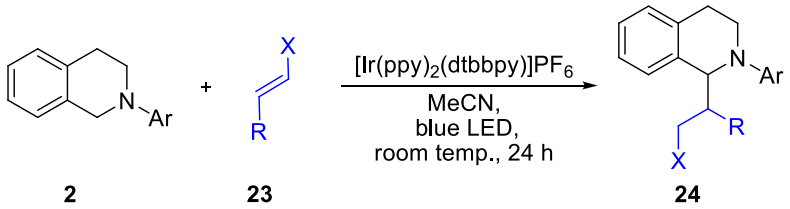

2 **23** **24**

entry	2	23	cat. loading / [mol%]	24
1	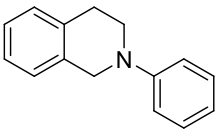 **2a** 1 equiv.	 **23a** 3.0 equiv.	2.0	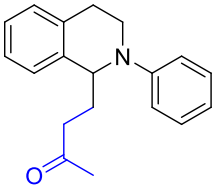 **24a** 68%
2	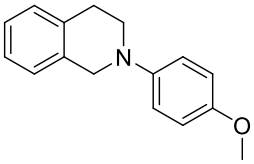 **2b** 1 equiv.	 **23a** 3.0 equiv.	5.0	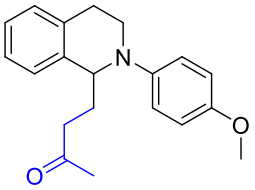 **24b** 37%
3	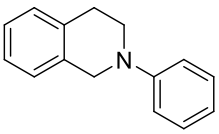 **2a** 1 equiv.	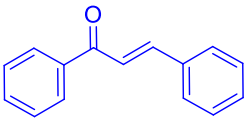 **23b** 1.1 equiv.	5.0	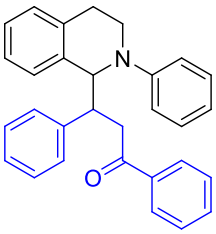 **24c** 83% (70:30 dr)
4	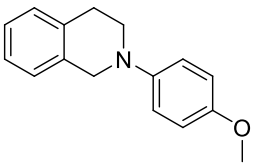 **2b** 1 equiv.	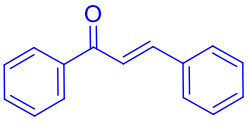 **23b** 1.4 equiv	5.5	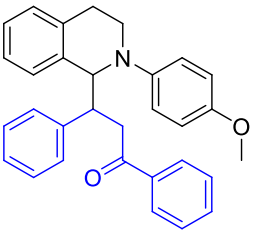 **24d** 33% (66:34 dr)
5	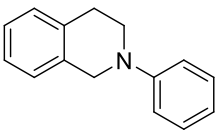 **2a** 1 equiv.	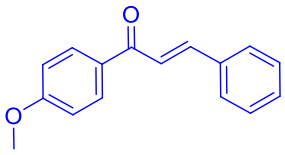 **23c** 1.4 equiv.	7.0	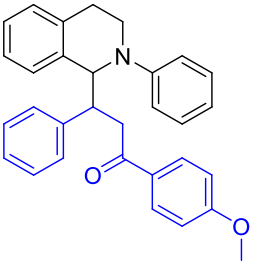 **24e** 93% (60:40 dr)

entry	2	23	cat. loading / [mol%]	24
6	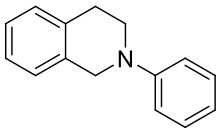 **2a** 1 equiv.	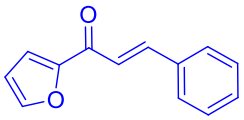 **23d** 1.1 equiv.	5.0	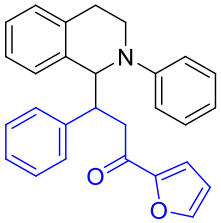 **24f** 60% (1:1 dr)
7	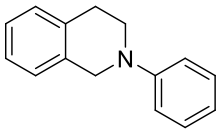 **2a** 1 equiv.	 **23e** 3.0 equiv.	2.0	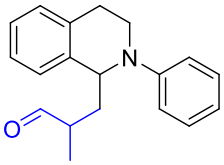 **24g** 50% (7:3 dr)
8	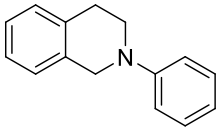 **2a** 1 equiv.	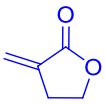 **23f** 3 equiv.	5.0	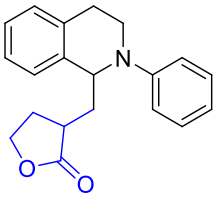 **24h** 34% (54:46 dr)
9	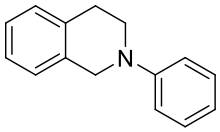 **2a** 1 equiv.	 **23g** 3.0 equiv.	5.0	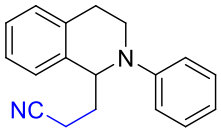 **24i** 31%

In addition to the above depicted intermolecular examples, two intramolecular examples were applied in a conjugate addition using [**204**·PF_6] as photocatalyst that have also worked with $Ru(bpy)_3Cl_2$ (**1**·Cl_2) (Scheme 59). Molecules **27** were obtained by an aldol condensation using KOH starting from acetone (**188a**) or acetophenone (**188b**) and 2-(3,4-dihydro-isoquinolin-2(1H)-yl)benzaldehyde (**187**) as reported before (Chapter 1.1 Scheme 49).[51]

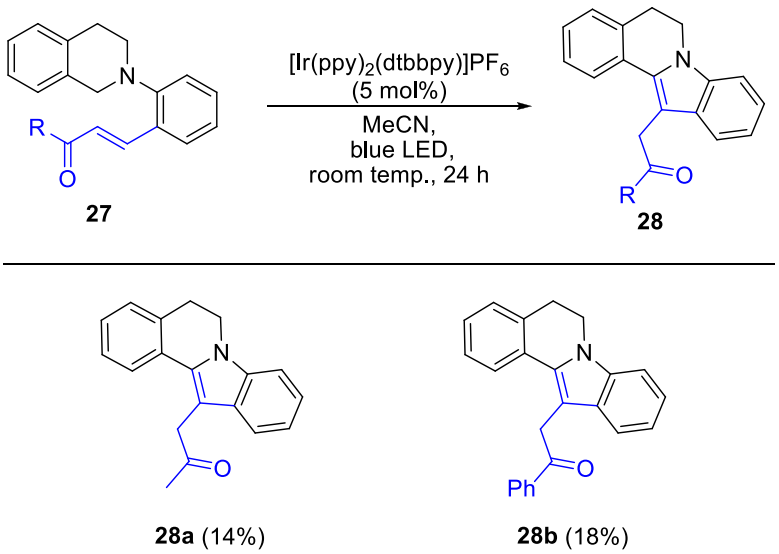

Scheme 59. Intramolecular photocatalytic conjugate additions.

The reaction did not proceed well which was similar to our report for $Ru(bpy)_3Cl_2$ (**1**·Cl_2). Most likely this is due to the fact that not only a photocatalytic conjugate addition takes place but also a dehydrogenation, leading to an extended, single π-system. No full conversion could be obtained even after prolonged reaction times of 48 h. Due to very similar R_f values of product and starting material, separation *via* column chromatography was very difficult. The best isolated yield of 14% for product **28a** and 18% for product **28b** was obtained using 5 mol% [$Ir(ppy)_2(dtbbpy)$]PF_6 (**204**·PF_6) after 24 h.

1.5 Screening for novel suitable amines

In contrast to the broad scope of applicable enone systems, so far only isoquinoline derivatives could be used as *tert.* amines. Therefore other phenyl bearing *tert.* amines were investigated in combination with catalyst **204** to see if the desired conjugate addition products are obtained. Dimethyl aniline **208** and diethyl aniline **210** are commercially available; whereas phenylpyrrolidine **212** and phenylpiperidine **214** were synthesized according to a procedure by Buchwald *et al*.[70]

Table 8. Aniline derivatives as substrates for photocatalytic conjugate additions.

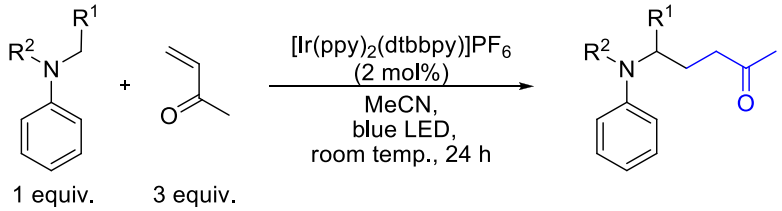

entry	aniline derivative	product	yield
1	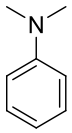 **208**	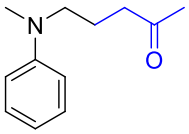 **209**	12%
2	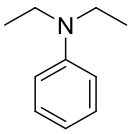 **210**	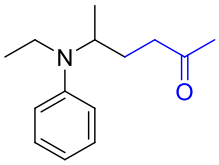 **211**	0%
3	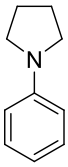 **212**	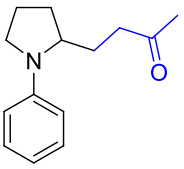 **213**	28%
4	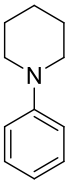 **214**	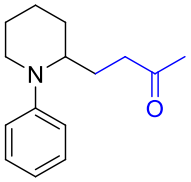 **215**	0%

Product **209** could be isolated in 12% yield using 1 equiv. of dimethyl aniline (**208**), 3 equiv. of methyl vinyl ketone (**23a**) and 2 mol% of catalyst **204** after 24 h of external irradiation with a blue LED (entry 1, Table 8). Employing diethyl aniline **210** under otherwise identical conditions did not lead to the formation of product **211** (entry 2, Table 8). To our delight, product **213** was furnished in up to 28% yield when a mixture of 1 equiv. of **212**, 3 equiv. of **23a** and 2 mol% of **204** was irradiated for 24 h (entry 3, Table 8). When switching from pyrrolidine **212** to piperidine **214,** again no conjugate addition product could be observed (entry 4, Table 8).

1.6 Micro reactor systems

Due to the low yields obtained, when the reaction mixture was irradiated from the outside using a snap-cap vial and a single LED, it was envisioned to increase the yield by conducting the reactions in a micro reactor.

Photocatalysts have a high extinction coefficient, for example, $[Ir(ppy)_2(dtbbpy)]PF_6$ (**204**·PF_6) has an extinction coefficient of $\varepsilon = 4920\ M^{-1}\ cm^{-1}$.[71] At a catalyst concentration of 2 mmol/l, which corresponds to the standard reaction conditions using 2 mol% of catalyst, 99% of the incident light is absorbed after 2 mm and less than 1‰ penetrates further than 3 mm. Therefore close to no catalyst molecules are excited beyond this layer making round bottom flasks and snap –cap vials unfavorable. On the other hand, increasing the surface area and decreasing the depth of the solution at the same time would allow the light to penetrate the whole solution and excite all available catalyst molecules. Both can be achieved with the help of a micro reactor.

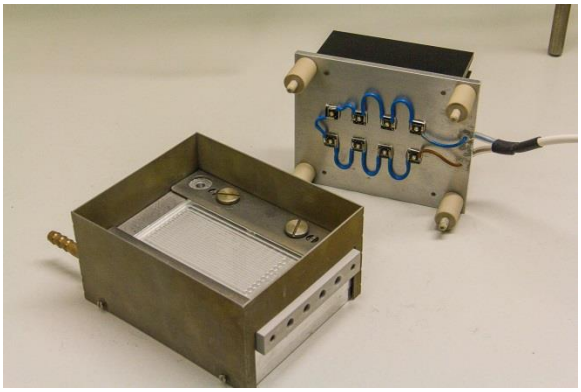

Figure 5. LTF-V micro reactor system with irradiation unit in metal frame.

All of the following experiments were performed in a LTF-V reactor developed by LTF GmbH. The reactor consists of two borosilicate glass plates in which a semicircular channel is carved. These two glass plates are glued together so one round channel is created (Figure 5). In- and outlet are mounted to the glass plate *via* a 1/4" UNF fitting. The channel has a diameter of 1 mm and a volume of 1.7 mL. The glass plates fit into a metal frame. Through tubing underneath this frame external cooling or heating can be applied. On top an array of eight LEDs of any color can be installed for irradiation (Figure 5). The reaction solution is pumped through the reactor by a syringe pump and collected in a Schlenk flask with an attached bubbler to exclude oxygen and prevent excess pressure.

The coupling of phenyl pyridine (**212**) and methyl vinyl ketone (**23a**) was chosen as model reaction. The ratio of substrates was kept constant for all experiments using 1 equiv. of **212** and 3 equiv. of **23a**. Catalyst and retention time, which corresponds to the pump speed, were varied.

Table 9. Micro reactor studies.

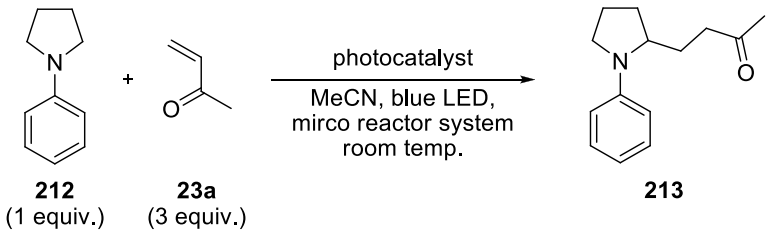

entry	catalyst	catalyst loading	pump speed	retention time	additives	yield 213
1	**1**·Cl_2	5 mol%	0.33 mL/h	5 h 10 min	-	17%[a]
2	**1**·Cl_2	5 mol%	0.33 mL/h	5 h 10 min	CsF (1.0 equiv.) ^{i}PrOH (10 equiv.)	28%[a]
3	**1**·Cl_2	5 mol%	0.25 mL/h	6 h 50 min	CsF (1.0 equiv.) ^{i}PrOH (10 equiv.)	7%[a]
4[c]	**1**·Cl_2	5 mol%.		15 h	CsF (1.0 equiv.) ^{i}PrOH (10 equiv.)	15%[a]
5	**204**·PF_6	5 mol%	0.50 mL/h	3 h 30 min	-	27%[a]
6	**204**·PF_6	5 mol%	0.33 mL/h	5 h 10 min	-	32%[b]
7	**204**·PF_6	2 mol%	1.00 mL/h	1 h 50 min	-	44%[a]
8[c]	**204**·PF_6	2 mol%		24 h	-	28%[a]

1·Cl_2: $Ru(bpy)_3Cl_2$; **204**·PF_6: $[Ir(ppy)_2(dtbbpy)]PF_6$. a) isolated yield; b) yield determined by ^{1}H-NMR-analysis using 3-nitrobenzaldehyde as internal standard; c) reaction conducted in a snap-cap vial.

According to the proposed reaction mechanism the initially formed radical cation of the *tert.* amine is deprotonated in order to form the radical intermediate. But as depicted in Chapter 1.4, Table 4, entry 4 – 6, the sole addition of a base does not increase the yield. Later on in the reduction step an anion is generated which is protonated giving rise to the final product. Therefore the addition of a base might be beneficial for the deprotonation step and the presence of a proton source for the protonation of the carbanion. In order to confirm this assumption, caesium fluoride (CsF) as mild base and isopropyl alcohol (^{i}PrOH) as proton source were added in some reactions.

The reactions were conducted using 1 equiv. of **212**, 3 equiv of **23a**, an additive if indicated and catalyst **1** or **204** in acetonitrile. The solution was degassed using three freeze pump thaw cycles, taken up in a syringe and pumped through the micro reactor at the indicated speed.

Pumping a solution containing **212**, **23a** and 5 mol% of **1** through a micro reactor at a speed of 0.33 mL/h yielded already 17% of product **213** (entry 1, Table 9). The yield could be further increased to 28% by the addition of 1 equiv. of CsF and 10 equiv. of isopropyl alcohol under otherwise identical conditions (entry 2, Table 9). Increasing the reaction time by decreasing the pumping speed to 0.25 mL/h lowered the yield to 7% (entry 3, Table 9). This indicates that the product might not be stable under photochemical conditions. Due to these results, a control experiment was conducted in a snap cap vial using CsF (1.0 equiv.) and ^{i}PrOH (10 equiv.). In this case, product **213** could be isolated in 15% after 15 h (entry 4, Table 9). In conclusion, with a yield of 28% the best results with **1** as catalyst were obtained using 1 equiv. of CsF and 10 equiv. of ^{i}PrOH in a micro reactor at a pump rate of 0.33 mL/h.

Changing the catalyst to $[Ir(ppy)_2(dtbbpy)]PF_6$ (**204**·PF_6), product **213** could be isolated in 27% yield when the reaction solution was pumped through the micro reactor at a speed of 0.5 mL/h (entry 5, Table 9). This is already very close to the result obtained using a snap-cap vial for this reaction (entry 8, Table 9). Decreasing the pump rate to 0.33 mL/h, the optimal rate using $Ru(bpy)_3Cl_2$ (**1**·Cl_2), had close to no influence on the yield of the reaction (entry 6, Table 9). On the other hand the yield could be increased to 44% when the pump rate was increased to 1 mL/h and the catalyst loading was reduced to 2 mol% (entry 7, Table 9).

Therefore the best yields in order to synthesize 4-(1-phenylpyrrolidin-2-yl)butan-2-one (**213**) were obtained using a micro reactor and $[Ir(ppy)_2(dtbbpy)]PF_6$ (**204**·PF_6). The yield increases from 28% using a snap cap vial to 44% using a micro reactor system. Employing a proton source and a base at the same time was shown to have a beneficial effect in combination with $Ru(bpy)_3Cl_2$ (**1**·Cl_2). Overall the product seems to be unstable under photochemical conditions; hence a short retention time and low catalyst loading are beneficial.

Due to these promising results, an experiment was conducted to test if *N*-phenylpiperidine (**214**) can be activated by **204** in a micro reactor. The best conditions for the synthesis of **213** were applied and *N*-phenylpiperidine (**214**) (1 equiv.) was mixed with 3 equiv of **23a** and 2 mol% of **204** in acetonitrile, degassed and pumped through a micro reactor but again no product formation could be observed (Scheme 60).

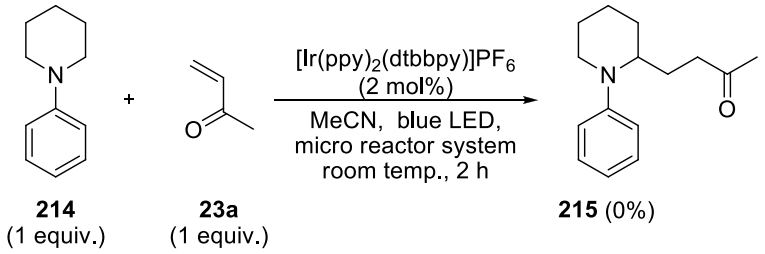

Scheme 60. Phenylpiperidine (**214**) as substrate for photocatalytic conjugate additions in a micro reactor.

1.7 [Ir{dF(CF$_3$)ppy}$_2$(dtbbpy)]PF$_6$ as photocatalyst for N-α-activation

Due to its great oxidation as well as reduction potential, [Ir{dF(CF$_3$)ppy}$_2$(dtbbpy)]PF$_6$ (**216**·PF$_6$) (dtbbpy: 4,4'-di-tert-butyl-2,2'-bipyridine; dF(CF$_3$)ppy: 2-(2,4-difluoro-phenyl)-5-trifluoromethyl-pyridine) was another promising catalyst for photocatalytic conjugate additions. Especially the reductive catalytic pathway with an oxidation potential of $E_{1/2}(Ir^{III}*/Ir^{II})$ = +1.21 V *vs.* SCE in MeCN and a reduction potential of $E_{1/2}(Ir^{III}/(Ir^{II})$ = -1.37 V *vs.* SCE in MeCN is very appealing. **216** was developed by Malliaras *et al.* in 2005 and can be synthesized according to a procedure in the same publication (Scheme 61).[72] Stephenson *et al.* first reported its use as photoredox catalyst for the ATRA reaction of bromomalonates and olefins.[73]

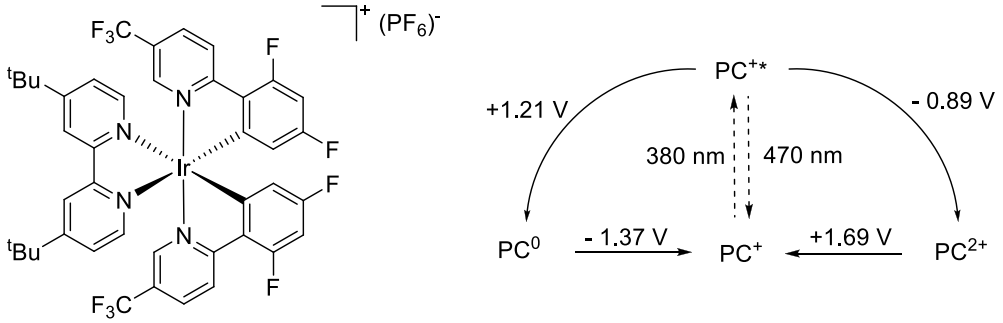

Scheme 61. Structure and photocatalytic properties of [Ir{dF(CF$_3$)ppy}$_2$(dtbbpy)]$^+$ (**216**) (dtbbpy: 4,4'-di-tert-butyl-2,2'-bipyridine; dF(CF$_3$)ppy: 2-(2,4-difluorophenyl)-5-trifluoro-methylpyridine).[72]

With the help of the new, powerful catalyst it was intended to further increase the yield of the conjugate addition of phenylpyrrolidine (**212**) and methyl vinyl ketone (**23a**). The reactions were conducted using 1 equiv. of **212**, 3 equiv. of **23a** and catalyst [**216**·PF$_6$] in acetonitrile. The solution was degassed using three freeze pump thaw cycles, taken up in a syringe and pumped through the micro reactor at the indicated speed.

At first, the optimal catalyst loading was determined. Using 1 mol% of catalyst **216** at a pump rate of 0.33 mL/h already let to the formation of 20% of **213** (entry 1, Table 10). Doubling the catalyst loading to 2 mol% at the same speed yielded 35% of product **213** (entry 2, Table 10). Increasing the catalyst loading to 5 mol% furnished product **213** only in 39% yield (entry 3, Table 10) which is only slightly higher than using 2 mol% catalyst. If oxygen was present in the reaction mixture, no product formation could be observed (entry 4, Table 10). The catalyst loading was not further increased because the catalyst is very costly and the yield obtained using 5 mol% was only slightly better than the one using 2 mol%. Overall the catalyst could not fulfill the high expectations that arose from its redox properties. The yields were in the same range as using [Ir(ppy)$_2$(dtbbpy)]PF$_6$ (**204**·PF$_6$) but the preparation of **216** is more complex and the costs are higher.

Table 10. Micro reactor studies using catalyst [**216**·PF_6].

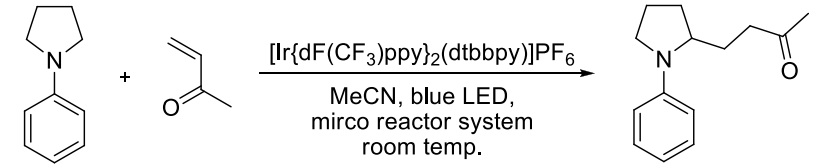

212 (1 equiv.) **23a** (3 equiv.) **213**

entry	catalyst loading	pump speed	retention time	additive	yield 213
1	1 mol%	0.33 mL/h	5 h 10 min h	-	20%
2	2 mol%	0.33 mL/h	5 h 10 min	-	35%
3	5 mol%	0.33 mL/h	5 h 10 min	-	39%
4	5 mol%.	0.16 mL/h	10 h 20 min	air	0%
5	2 mol%	0.50 mL/h	3 h 30 min	$LiBF_4$ (1.2 equiv.)	traces
6	2 mol%	0.33 mL/h	5 h 10 min	$ZnCl_2$ (1.3 equiv.)	traces
7	2 mol%	0.33 mL/h	5 h 10 min	$AlCl_3$ (1.3 equiv.)	traces
8	2 mol%	0.33 mL/h	5 h 10 min	$Ce(SO_4)_2$ (1.3 equiv.)	traces

By screening different catalysts and additives, a yield of 44% was obtained for the coupling of phenylpyrrolidine (**212**) with methyl vinyl ketone (**23a**) (entry 7, Table 9, Chapter 1.6). In order to improve the yields, the influence of Lewis acids on the reaction was investigated. Lewis acids are known to activate carbonyl systems and their application in photoredox catalysis has been shown, amongst others, by Yoon *et al.*[74] Therefore a variety of Lewis acids were added to the above described reaction solution. Independent of the Lewis acid, only trace amounts of product could be identified when they were applied as additive in photocatalytic conjugate additions (entry 5 – 8, Table 10). Thus, Lewis acids are not capable of enhancing the yield of this reaction; in fact they impede the reaction.

1.8 Conclusion and Outlook

To increase yield and scope of the conjugate addition developed by our group, the influence of different additives, new photoredox catalysts, new amine species as well as a mircoreactor system was investigated.

In order to facilitate the deprotonation step of the radical cation to an *N*-α-radical, different bases were added to the reaction mixture (Chapter 1.4, Table 4, entry 4 – 6). However, none of these bases could enhance the yield. The ampholyte water was tolerated in the reaction mixture in up to 5% (v/v), whereas higher concentrations of water decreased the yield (Chapter 1.4, Table 5). No positive influence could be observed when water was added. The yield of the coupling of phenylpyrrolidine (**212**) and methyl vinyl ketone (**23a**) was increased moderately by the addition of caesium fluoride (1 equiv.) and isopropyl alcohol (10 equiv.) in combination with the catalyst $Ru(bpy)_3Cl_2$ (**1**·Cl_2) (Chapter 1.6, Table 9, entry 1 – 4). With this strategy the yield was only slightly improved and therefore this path was no longer pursuit. In order to active the enone system, different Lewis acids were added to the reaction mixture. However, all of them stopped the reaction almost completely.

Tetrabutylammonium decatungstate (TBADT, **190**), $Cu(dap)_2Cl$ (**195**), $[Ir(ppy)_2(dtbbpy)]PF_6$ (**204**·PF_6) and $[Ir\{dF(CF_3)ppy\}_2(dtbbpy)]PF_6$ (**216**·PF_6) were tested as novel photoredox catalyst for the *N*-α-activation of *tert.* amines. The first two catalysts, **190** and **195**, could not drive the reaction forward at all. The latter two, **204** and **216**, were successfully used in this reaction. Catalyst **216** let to comparable results as catalyst **204** but is more complex to prepare and more expensive. Depending on the substrate either $Ru(bpy)_3Cl_2$ (**1**·Cl_2) or $[Ir(ppy)_2(dtbbpy)]PF_6$ (**204**·PF_6) proofed to be the best catalyst.[75] The best obtained yields using each catalyst are displayed in Table 11.

The yield decreased when catalyst **204** was employed instead of **1** for the coupling of 2-(4-methoxyphenyl)-1,2,3,4-tetrahydroisoquinoline (**2b**) and isoquinoline derivatives **27a**, **27b** (*cf.* Table 11, **24b**, **24d**, **28a** and **28b**). Using **204** for the reaction of **2a** with aliphatic enones or nitriles, the yields stay the same or increased slightly (*cf.* Table 11, **24a**, **24g**, **24h** and **24i**). To our delight, a moderate to great increase in product formation was observed for catalyst **204** in combination with chalcone derivatives (*cf.* Table 11, **24c**, **24e** and **24f**). In one case the yield could be boosted from 56% using $Ru(bpy)_3Cl_2$ (**1**·Cl_2) to 93% using $[Ir(ppy)_2(dtbbpy)]PF_6$ (**204**·PF_6) (*cf.* Table 11, **24e**).

Table 11. Comparison of the best results obtained using $Ru(bpy)_3Cl_2$ (**1**·Cl_2) and $[Ir(ppy)_2(dtbbpy)]PF_6$ (**204**·PF_6)

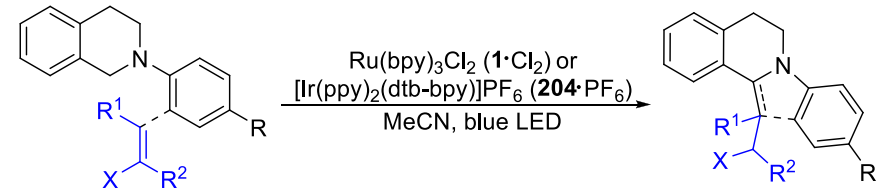

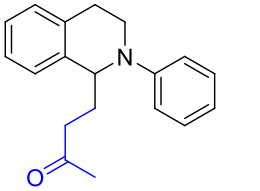

24a:
Cat **1**: 58%
Cat **204**: 68%

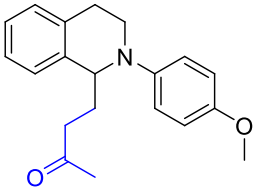

24b:
Cat **1**: 63%
Cat **204**: 37%

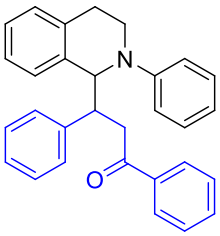

24c:
Cat **1**: 61%
Cat **204**: 83%

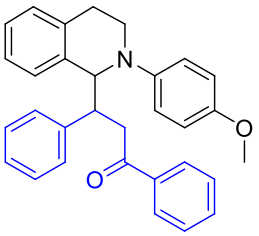

24d:
Cat **1**: 43%
Cat **204**: 33%

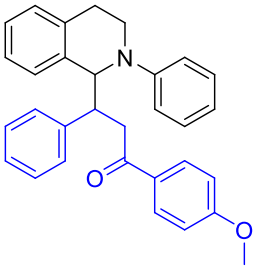

24e:
Cat **1**: 56%
Cat **204**: 93%

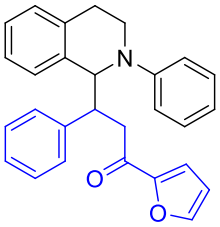

24f:
Cat **1**: 53%
Cat **204**: 66%

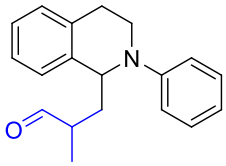

24g:
Cat **1**: 50%
Cat **204**: 50%

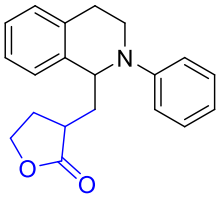

24h:
Cat **1**: 31%
Cat **204**: 33%

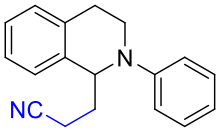

24i:
Cat **1**: 27%
Cat **204**: 31%

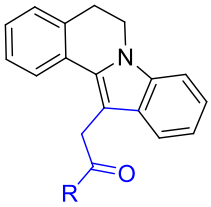

28a (R = Me):
Cat **1**: 28%
Cat **204**: 14%

28b (R = Ph):
Cat **1**: 35%
Cat **204**: 18%

The substrate dependency of the catalysts can be explained by the different redox potentials of **204** and **1**. **204** has a lower initial oxidation potential, therefore the oxidation of the isoquinoline **2** to a radical cation **5** is less feasible. On the other hand it has a greater reduction potential, improving the reduction of the α-carbonyl radical **26** to an anion **186** (Scheme 62).

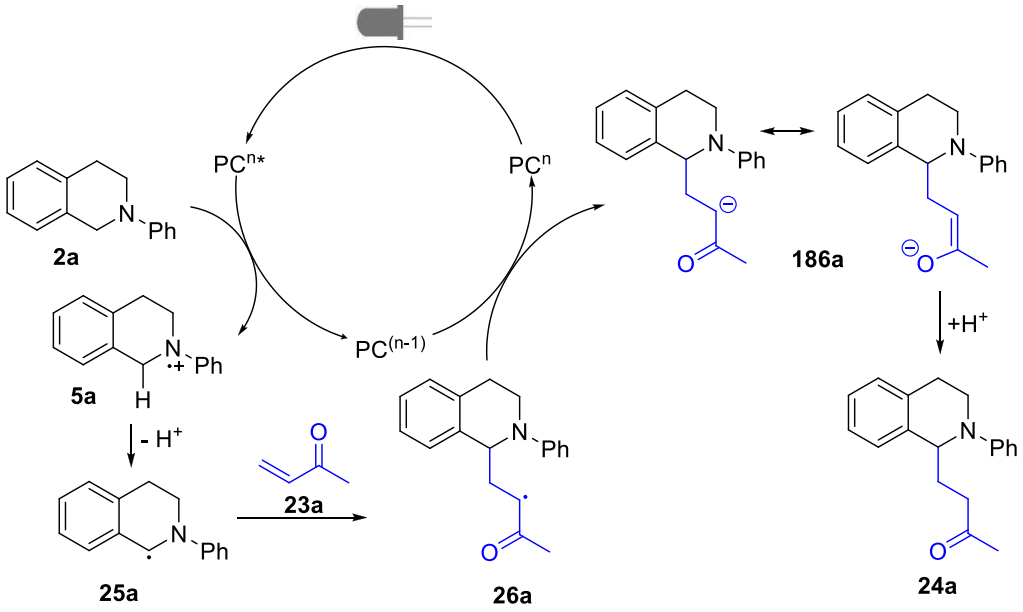

Scheme 62. Proposed reaction mechanism of a photocatalytic conjugate addition.

Aniline derivatives **208** and **212** could be identified as suitable substrates for this coupling but the yields stayed low, even when the reaction was conducted in a micro reactor system. For both of them $[Ir(ppy)_2(dtbbpy)]PF_6$ (**204**·PF_6) proofed to be the best catalyst (Scheme 63).

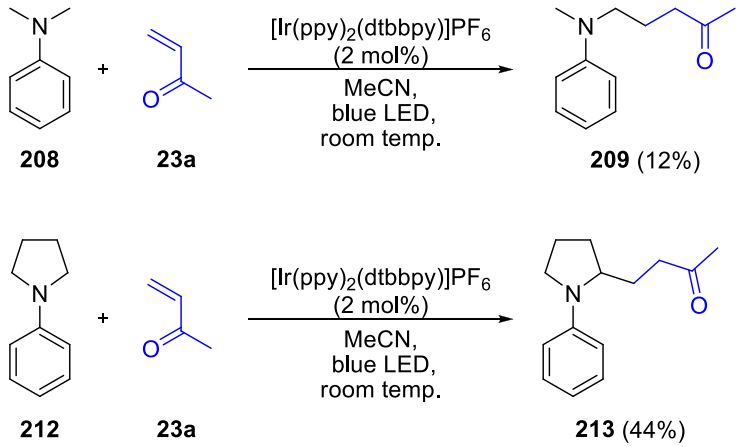

Scheme 63. Photocatalytic conjugate addition using aniline derivatives.

In conclusion we were able to further enhance this unprecedented photocatalytic *N*-α-activation of *tert.* amines and their coupling to Michael acceptors. The yields were in a moderate to good range using 2-phenyl-tetrahydroisoquinoline (**2a**) but decreased when other *tert.* amines were applied.

All reactions discussed in chapter 1.2 to 1.5 were conducted between the end of 2010 and the end of 2011. To the best of my knowledge there was no report on *N*-α-radicals generated by visible light photoredox catalysis without pre-functionalization until we submitted the manuscript covering this work to Organic Letters (Sunday, Oct, 23rd, 2011),[75] apart from one report by MacMillan *et al.* that appeared online three days earlier (Thursday, Oct, 20th, 2011).[76] We got aware of this publication later during the revision process. All other groups working in this field like Stephenson *et al.*,[52b] Rueping *et al.*[53] or König *et al.*[77] proposed at that time an iminium ion as key intermediate.

As mentioned before, MacMillan *et al.* were the first to report *N*-α-radicals generated by visible light photoredox catalysis as intermediate in their coupling of aniline derivative **212** and cyanobenzene **217** (Scheme 64).[76]

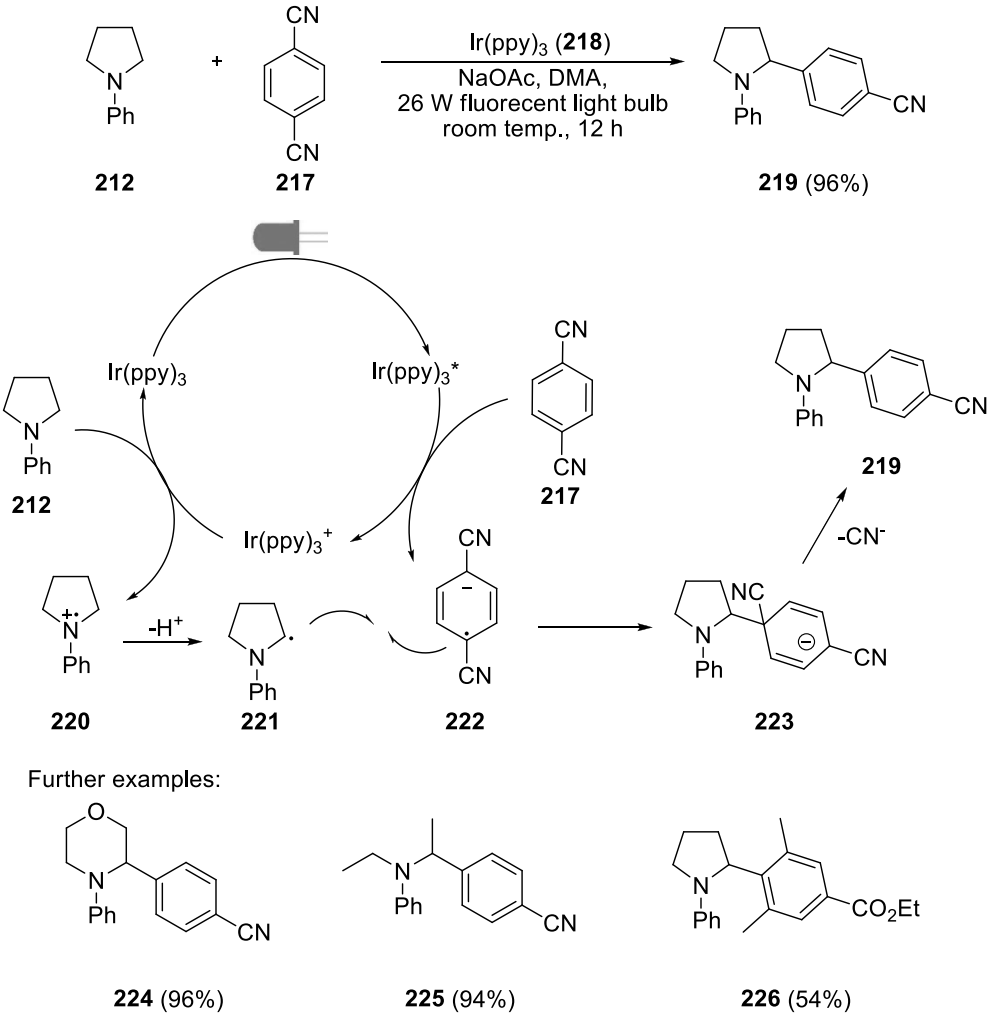

Scheme 64. Photocatalytic arylation of aniline derivative **xx**.

In the proposed reaction mechanism 1,4-Dicyanobenzene (**217**) is reduced to the corresponding radical anion **222** by excited $Ir(ppy)_3$*. $Ir(ppy)_3^+$ on the other hand oxidizes *tert*. amine **212** to radical

cation **220**. After deprotonation, radical **221** is formed which is similar to our proposed intermediate **25** (*cf.* Scheme 62). Radical **221** recombines with radical anion **222** forming anion **223** which leads to product **219** after cleaving off a cyanide anion (Scheme 64).

Right after our publication, Nishibayashi *et al.* reported the photocatalytic generation of α-amino radicals and their addition to electron deficient alkenes **227** (Scheme 65).[78] The proposed reaction mechanism is the same as we propose for the photocatalytic conjugate addition (*cf.* Scheme 62). However, the reported substrate scope differs.

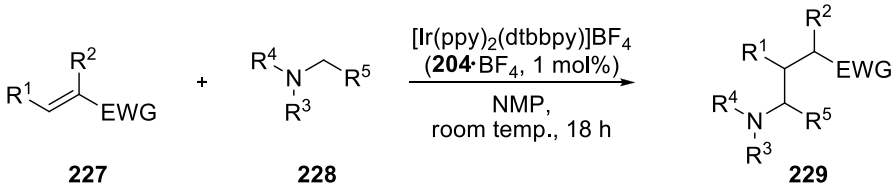

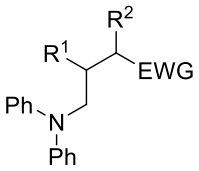

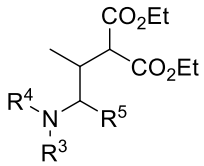

229a (R^1 = Me, R^2 = EWG = CO_2Et)	(90%)	**229f** (R^3 = R^4 = Ph, R^5 = Me)	(89%)
229b (R^1 = Ph, R^2 = EWG = CO_2Et)	(89%)	**229g** (R^3 = 4-$MeOC_6H_4$, R^4 = Ph, R^5 = Me)	(80%)
229c (R^1 = ^{n}Pr, R^2 = EWG = CO_2Et))	(91%)	**229h** (R^3 = 4-ClC_6H_4, R^4 = Ph, R^5 = Me)	(79%)
229d (R^1 = Ph, R^2 = CO_2Me, EWG = CO_2Et)	(79%)	**229g** (R^3 = 4-$MeOC_6H_4$, R^4 = Ph, R^5 = Me)	(80%)
229e (R^1 = Ph, R^2 = EWG = CO_2Me)	(36%)	**229i** (R^3 = R^4 = ^{i}Pr, R^5 = He)	(94%)

Scheme 65. Trapping of photocatalytically generated *N*-α-radicals **228** with electron deficient alkenes **227**.

The best yields were obtained using *N*-methylpyrrolidone (NMP) as solvent and $[Ir(ppy)_2(dtbbpy)]PF_6$ (**204**·PF_6) as catalyst. Conducing experiments in MeCN or MeOH let to no product formation. In contrast to this, we obtained the best yields using MeCN as solvent and did not obtain any yield when the reaction was conducted in NMP. All reactions were conducted with [**204**·PF_6] as catalyst and the formation of product **229a** decreased dramatically from 90% to 35% when $Ru(bpy)_3BF_4$ (**1**·BF_4) was employed. In contrast to this some of our conjugate additions gave higher yields using **1** as catalyst, primarily when isoquinolines other than **2a** where used (*cf.* Table 11). Suitable alkenes for this reaction are electron deficient ethylidenemalonate **228** while our best yields were obtained with electron rich chalcones (*cf.* **229a** *vs.* **24e**). In the presented reaction, all applicable alkenes contain at least one ester moiety (Scheme 65). In contrast to this, esters, apart from lactone **23f**, do not lead to any product formation employing our reaction conditions. The reaction worked well using aniline derivatives (*cf.* **229f-g**) and aliphatic *tert.* amine (*cf.* **229i**). A trend that was also visible in our

experiments using **204** as catalyst was, that methoxy substituents on the *N*-aryl moiety decrease the yields (*cf.* **229g** *vs.* **24d** and **24d**). Overall, Nishibayashi[78] and our group[75] discovered nearly the same reaction at nearly the same time but under different reaction conditions and a different substrate scope.

More than one year after our report[75] of this reaction, Yoon *et al.* were able to accelerate the rate of this reaction and further increase the yields through the addition of 1 equiv. of trifluoroacetic acid (TFA) (Scheme 66).[79]

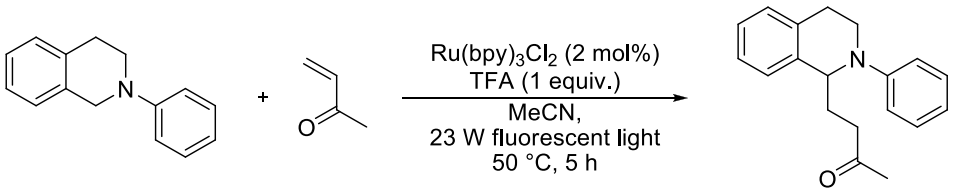

2a **23a** **24a** (90%)

Scheme 66. TFA as co-catalyst in photocatalytic conjugate additions.

In this publication they showed that only acids with a pKa value very close to 1, e.g. TFA, can enhance this reaction by activating methyl vinyl ketone (**23a**). All other acids decrease the yield or stop the reaction completely. TFA is used to protonate the Michael system and activate it to be attacked by an isoquinoline radical (*cf.* Introduction Scheme 31).

In the following years more reports on the photochemical generation of *N*-α-radicals got published. These reports are summarized, amongst others, by Xia *et al.*[80] and, more recently, by Zhu *et al*.[81]

2. Photocatalytic Oxidative Mannich Reactions

Mannich reactions have proven to be a useful tool in synthetic organic chemistry, being applied in many total syntheses.[82]

In 2011 the group of Magnus Rueping developed a photocatalytic variant of the Mannich reaction (*cf.* Introduction, Scheme 10).[53] They were able to couple tetrahydroisoquinoline derivative **2a** and acetone with the help of the photoredox catalyst $Ru(bpy)_3PF_6$ (**1**·PF_6) and L-proline (**18**) as co-catalyst. As key intermediate they propose an isoquinoline iminium ion which is attacked by an enamine. The same iminium ion intermediate has also been proposed by other groups using **2a** as substrate in photoredox catalysis.[52b)]

Not only Mannich reactions, but also vinylogous Mannich reactions are an important tool in organic synthesis. For example Doyle *et al***.** were able to show this with their synthesis of γ-aminoalkyl butenolides (**232**) under mild reaction conditions (Scheme 67).[83] The γ-butyrolactone motif is found in nearly 10% of all natural products and therefore new ways to synthesize and functionalize these structures are of great interest to the synthetic community.[84]

In the proposed reaction mechanism, dirhodium complex **231** oxidizes dimethylaniline (**208**) to iminium ion **233** which is subsequently attacked by furan derivative **230**, a vinylogous enole, to form the desired product **232**. *tert*-Butyl hydroperoxide (TBHP) serves as stoichiometric oxidizing agent, regenerating dirhodium complex **231** (Scheme 67).

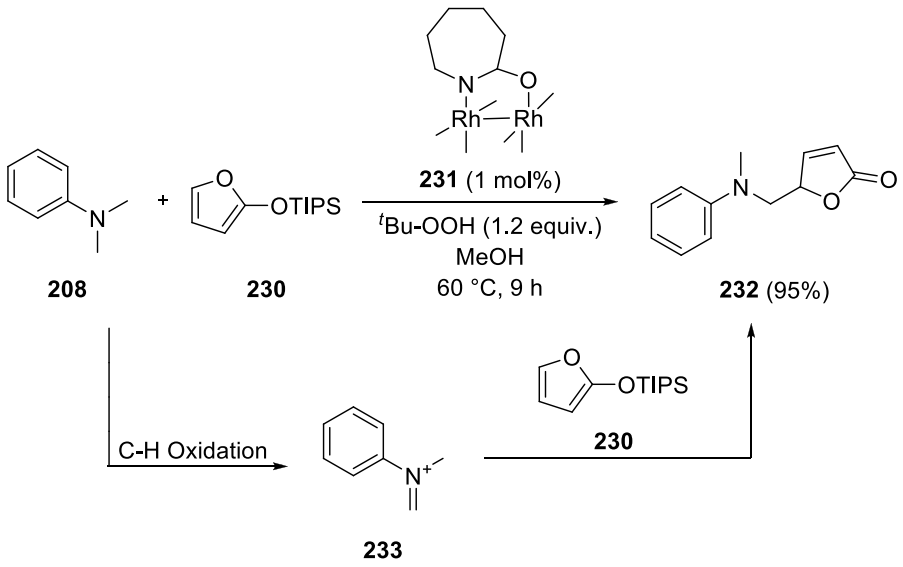

Scheme 67. Vinylogous Mannich reaction by Doyle *et al*.[83]

With these literature examples in mind we set out in fall 2011 to develop a photocatalytic vinylogous Mannich reaction. **230** was synthesized according to a procedure by Rosso *et al.* and tested afterwards for its photostability.[85] Neither by TLC nor NMR analysis any conversion could be detected when **230** and $Ru(bpy)_3Cl_2$ (**1**·Cl_2) were mixed in degassed acetonitrile and irradiated for 24 h with blue LEDs. Therefore it can be concluded that in the envisioned reaction **230** will not be activated by the catalyst itself and should only be attacked by the photochemically generated iminium ion.

As shown in the previous chapter, dimethylaniline (**208**) was successfully deployed as substrate in photocatalytic conjugate additions and therefore also the iminium ion of **208** should be accessible by photoredox catalysis. The yields using **208** in the previous chapter were not satisfactory and therefore the reactions were conducted in an LTF-V micro reactor system as employed in chapter 1.6.

In the first experiments the feasibility of this reaction was tested. Therefore different conditions for the reaction of dimethylaniline (**208**) and (furan-2-yloxy)triisopropylsilane (**230**) were screened. Several catalysts, different modes of action, additives and light sources were examined as well as the influence of oxygen on the reaction.

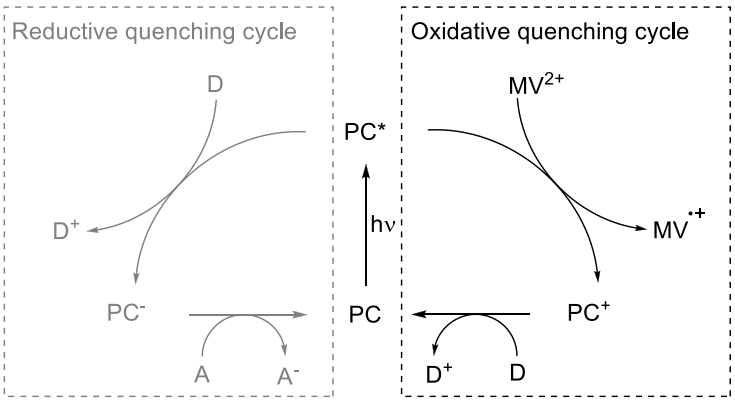

Scheme 68. Oxidative quenching cycle of a photoredox catalyst (PC: photoredox catalyst, MV: methyl viologen (**134b**), D: electron donor).

In the first two experiments it was envisioned to address the oxidative reaction pathway of $Ru(bpy)_3Cl_2$ (**1**·Cl_2) or $[Ir(ppy)_2(dtbbpy)]PF_6$ (**204**·PF_6) with the help of methylviologen **134b**. **134b** is used to oxidize the excited photocatalyst; in case of **1** a Ru^{III} species is generated, in case of **204** an Ir^{IV} species. These oxidized catalysts exhibit strong oxidation potentials. In case of **204** the potential is $E_{1/2}(Ir^{IV}/Ir^{III})$ = 1.21 V *vs.* SCE in MeCN and **1** offers even a slightly higher potential of $E_{1/2}(Ru^{III}/Ru^{II})$ = 1.26 V *vs.* SCE, in MeCN (Scheme 68).[86] This reaction pathway was, for example, successfully used by

Yoon *et al.* to perform [2+2] photocycloaddition reactions with styrene derivatives (*cf.* Introduction, Scheme 45).[87]

Table 12. Photocatalytic vinylogous Mannich reaction

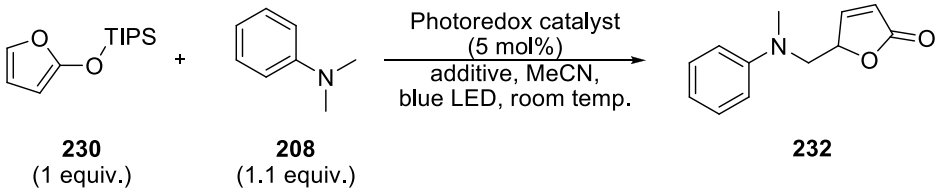

230 (1 equiv.) **208** (1.1 equiv.) **232**

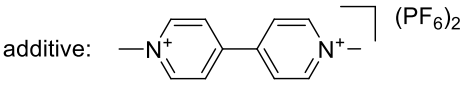

134b

entry	catalyst	additive	degassed	irradiation device	time	yield
1	$Ru(bpy)_3Cl_2$ (**1**·Cl_2)	**134b**	yes	micro reactor	3 h 30 min	0%
2	$[Ir(ppy)_2(dtbbpy)]PF_6$ (**204**·PF_6)	**134b**	yes	micro reactor	3 h 30 min	0%
3	$[Ir(ppy)_2(dtbbpy)]PF_6$ (**204**·PF_6)	none	yes	micro reactor	3 h 30 min	0%
4	$[Ir(ppy)_2(dtbbpy)]PF_6$ (**204**·PF_6)	none	no	LED plate	22 h	Product detectable

Applying Yoon´s reaction conditions[87] to this system, **230** (1 equiv.) and **208** (1.1 equiv.) were mixed with methylviologen (**134b**) (15 mol%) and 5 mol% photocatalyst in acetonitrile. The solution was degassed by freeze pump thaw, taken up in a syringe and pumped through a LTF micro reactor with a retention time of 4 h. Full conversion but no product formation could be detected employing this pathway using either $Ru(bpy)_3Cl_2$ (**1**·Cl_2) or $[Ir(ppy)_2(dtbbpy)]PF_6$ (**204**·PF_6) (entry 1 – 2, Table 12).
Using **204** as catalyst in degassed acetonitrile utilizing the reductive quenching cycle led to no product formation as displayed in entry 3, Table 12. On the other hand, a promising first hit was found when the reaction mixture was not degassed; this implies that oxygen functions as reducing agent to regenerate the initial catalyst. In this case small amounts of product **232** could be detected *via* NMR analysis (entry 4, Table 12).

All of the above depicted reactions did not work well or at all. It was assumed that this is due to a poor iminium ion generation which might be caused by a to high oxidation potential. Therefore p-methyl-N,N-dimethylaniline (**234**) was chosen as new substrate instead of dimethylaniline (**208**). **234** has an oxidation potential of E_{ox}= 0.65 V[88] *vs.* SCE in MeCN which is roughly 0.1 V lower compared to dimethylaniline (**208**) (E_{ox}= 0.76 V *vs.* SCE, in MeCN).[89]

Promising results were obtained right away when p-methyl-N,N-dimethylaniline (**234**) was employed as substrate and **204** as catalyst. The reaction mixtures were not degassed, utilizing the reductive pathway and pumped through a LTF micro reactor.

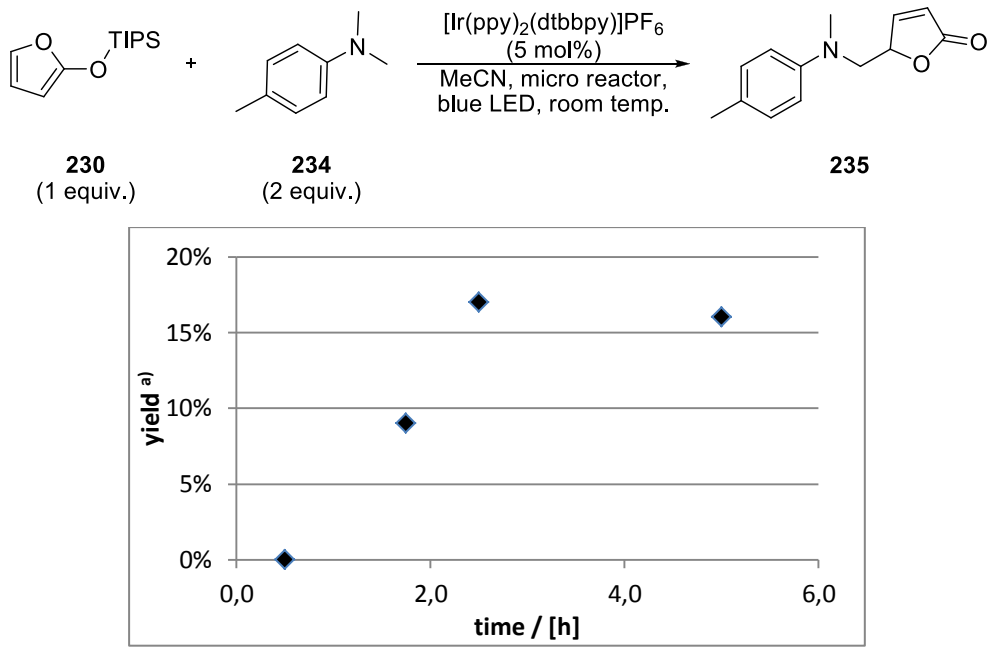

Scheme 69. Optimization of the reaction time of photocatalytic vinylogous Mannich reaction. a) Yields determined by ^{1}H-NMR analysis using p-nitrobenzaldehyde as internal standard.

Within one hour already 8% product formation could be observed and after 3 h 16% of **235** could be detected by ^{1}H-NMR analysis. Unfortunately the reaction did not proceed any further after 3 h. The maximum obtainable yield was 17% with respect to **230** (Scheme 69).

Based on the so far obtained results we propose the following mechanism, proceeding via the reductive pathway, for this reaction:

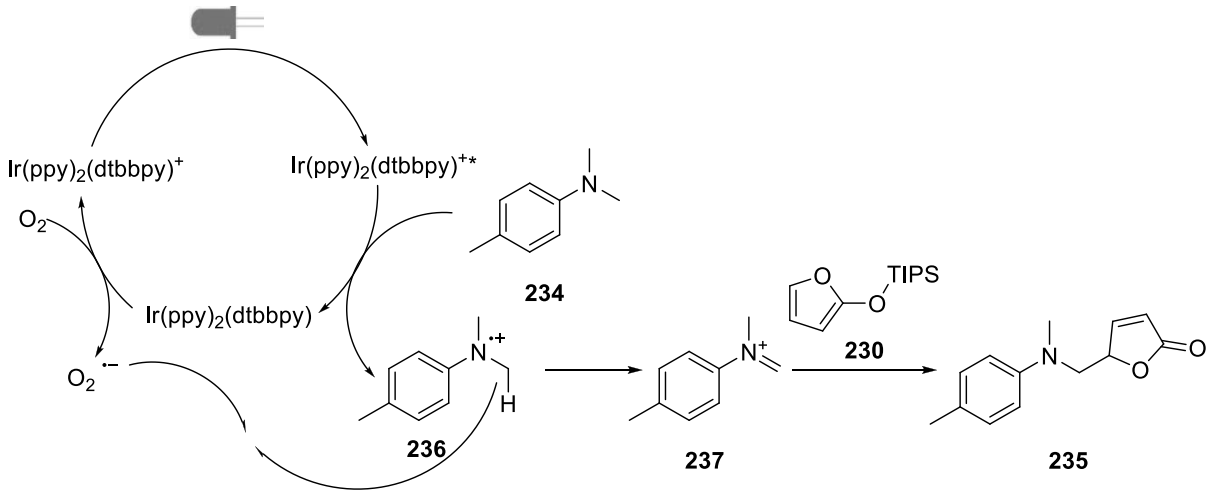

Scheme 70. Proposed reaction mechanism of the Photocatalytic Vinylogous Mannich Reaction.

It is assumed that trimethylaniline **234** in the first step reductively quenches the excited state of **204**, forming radical cation **236** and an Ir^{II} species. This Ir^{II} complex has a reduction potential of $E_{1/2}(Ir^{III}/Ir^{II})$ = -1.51 V (*vs.* SCE, in MeCN) and is therefore capable of reducing molecular oxygen.[56b] The resulting radical anion abstracts in the next step a hydrogen atom from radical cation **236**, forming iminium ion **237**. Cation **237** is subsequently attacked by vinylogous enole **230**, giving rise to γ-aminoalkyl butenolide **235** (Scheme 70).

In order to increase the yield, the influence of sterically different silyl protection groups was investigated. TMS protected furan derivative **13** was prepared according to a procedure by Boeckmann *et al*.[90] The following experiments were conducted using (furan-2-yl-oxy)trimethylsilane **13** (1 equiv.), dimetyhlanilne (**208**) or trimethylaniline (**234**) (2 equiv.) and 5 mol% of $[Ir(ppy)_2(dtbbpy)]PF_6$ (**204**·PF_6) in acetonitrile. The clear yellow solution was pumped through a LTF micro-reactor at different rates and irradiated with eight royal blue LEDs (1 W). The results are summarized in Table 13.

Table 13. Photocatalytic Vinylogous Mannich reaction with (furan-2-yloxy)trimethylsilane (**13**).

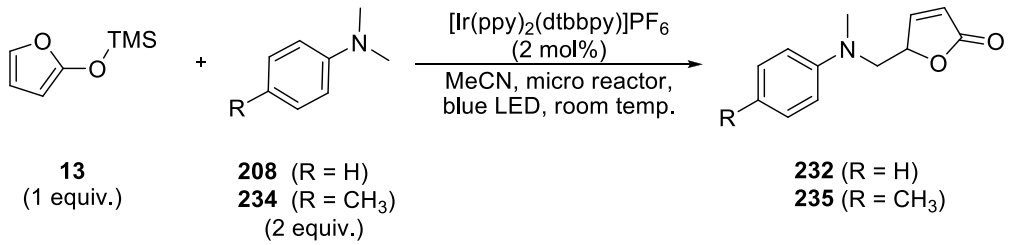

entry	amine	time	yield[a)]
1	**208**	50 min	5%
2	**234**	50 min	6%
3	**234**	3 h 30 min	12%

a) Yield determined by ^{1}H-NMR analysis using p-nitrobenzaldehyde as internal standard.

Using dimethylaniline (**208**) in this reaction yielded 5% of product within one hour (entry 1, Table 13). Conducting this experiment with trimethylaniline (**234**) led to the formation of 6% of product (entry 2, Table 13). Prolonging the reaction time to 4 h gave rise to 12% product (entry 3, Table 13,).

Additionally to this, *tert*-butyl(furan-2-yloxy)dimethylsilane (**238**) was synthesized according to a procedure published by Casiraghi *et al*.[91] TBS-ethers offer a much higher stability towards acid and base hydrolysis or oxidations and reductions than TMS-ethers but a lower one than TIPS ethers. In case of stability towards acid hydrolysis the relative rates ($1/k_{rel}$) are: TMS (1) < TBS (20 000) < TIPS (700 000).[92]

For this screening we used the conditions determined for substrate **234** in the experiments before and varied the amount of photocatalyst used. The experiments were conducted using *tert*-butyl(furan-2-yloxy)dimethylsilane (**238**) (1 equiv.), trimethylaniline (**234**) (2 equiv) and $[Ir(ppy)_2(dtbbpy)]PF_6$ (**204**·PF_6) as photocatalyst in acetonitrile. The clear yellow solution was pumped through a LTF micro reactor at a rate of 0.66 mL/h, which corresponds to a retention time of 2 h 40 min, and was irradiated with eight royal blue LEDs (1 W).

Table 14. Photocatalytic Vinylogous Mannich Reaction with *tert*-butyl(furan-2-yloxy)dimethylsilane (**238**).

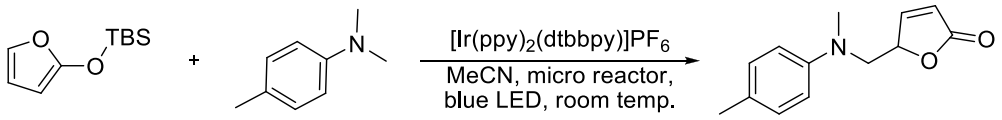

238 (1 equiv.) **234** (2 equiv.) **235**

entry	catalyst loading	time	yield[a)]
1	1 mol%	2 h 40 min	18%
2	2 mol%	2 h 40 min	18%
3	5 mol%	2 h 40 min	28%

a) Yield determined by ^{1}H-NMR analysis using p-nitrobenzaldehyde as internal standard.

Using 2 mol% $[Ir(ppy)_2(dtbbpy)]PF_6$ (**204**·PF_6) led to the same yield as using 1 mol% (entry 1 – 2, Table 14). To our delight 28% of 5-((methyl(p-tolyl)amino)methyl)furan-2(5H)-one (**235**) were generated when 5 mol% catalyst were employed in the reaction (entry 3, Table 14).
Having the economic and ecological viability of the reaction in mind, the amount of catalyst was not further increased.

After these promising first results, Stephenson *et al.* were able to publish a synthetically useful method to perform photocatalytic vinylogous Mannich reactions (Scheme 71).[93]

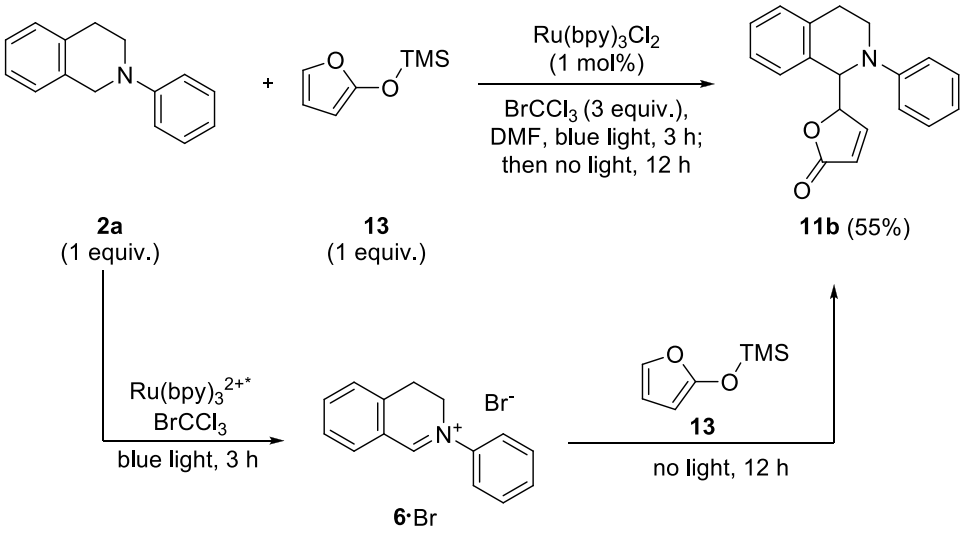

Scheme 71. Photocatalytic vinylogous Mannich reaction developed by Stephenson *et al.*[93]

They developed an interesting method to generate a stable iminium ion of isoquinoline **2a** with the help of $BrCCl_3$ and were able to trap this ion with a variety of nucleophiles, amongst others with TMS-Furan **13** (*cf.* Introduction, Scheme 7-9).

In conclusion a new way to functionalize γ-butyrolactones was established and investigated. We were able to obtain up to 28% yield when TBS-furan (**238**) (1 equiv.), trimethylaniline (**234**) (2. equiv) and $[Ir(ppy)_2(dtbbpy)]PF_6$ (**204**·PF_6, 5 mol%) as photocatalyst were mixed and irradiated without degassing in a micro reactor at a pumping rate of 0.66 mL/h which correlates to a retention time of 2 h 40 min.
Stephenson et al. published a very similar approach regarding the same class of substrates right after these promising first results; therefore this topic was not further pursued. In contrast to the method developed by Stephenson *et al.* and the Rhodium catalyzed reaction developed by Doyle *et al*. our approach does not need a sacrificial electron donor or acceptor apart from ubiquitous oxygen, making this process environmentally begin.

3. Studies towards the Synthesis of Jamtine

3.1 Introduction and Retrosynthetic Analysis

In this chapter, I would like to focus on our efforts to synthesize jamtine, which I undertook with Puneet Desai a Bachelor student from Bhopal, India.

Jamtine (**239**) is a natural product occurring in the climbing shrub *Cocculus hirsutus*, that growth in the south east of Pakistan (Figure 6).[94]

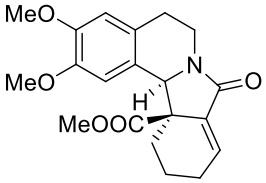

239

Figure 6. Structure of jamtine and climbing shrub *Cocculus hirsutus*.

The plant has various applications in the traditional local medicine. It is known to lower the level of blood sugar due to its antihyperglycemic activity.[95] The structure was resolved by Rehman *et al.* in 1987 by complex 2D-NMR studies.[96] Padwa *et al.* published the first total synthesis of (±)-jamtine. The key step of their synthesis is an unselective thionium/*N*-acyliminium ion cascade leading to jamtine (**239**) in 13 linear steps.[97]

The first asymmetric synthesis was reported a year later by Simpkins *et al.* They were able to introduce chirality by desymmetrization of a ring fused imide with the help of a chiral lithium amine base.[98] With this method they could synthesize jamtine (**239**) in six linear steps with an overall yield of 20%.

Due to our interest in photochemistry, especially the photoredox catalysis with isoquinoline derivatives, we intended to develop a new synthetic route for jamtine (**239**) with a photocatalytic key step. Our retrosynthetic analysis is shown in Scheme 72.

Opening of the lactam and protection of the amine would lead to structure **240** which can be furnished in a Tsuji-Trost-type reaction from previously formed triflate **241**. The key step is the

photocatalytic coupling of isoquinoline **243** and cyclohexanone derivative **244** leading to molecule **242**.

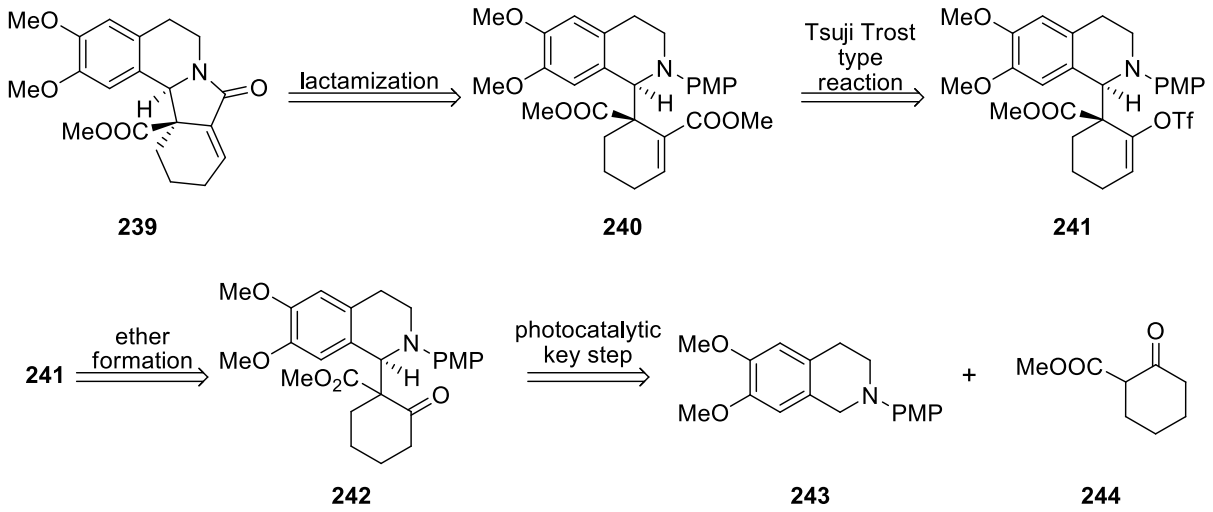

Scheme 72. Retrosynthetic analysis of jamtine (1) with photocatalytic key step.

In the envisioned forward synthesis, the first step will be a photocatalytic coupling of isoquinoline **243** and cyclohexanone **244** in a Mannich-type fashion to give rise to addition product **242**. Similar reactions have been performed by König *et al.* (Scheme 73)[99] and Stephenson *et al*. (Scheme 74).[93]

The group of König was able to couple dimethyl malonate **14** and isoquinoline **2a** with the help of eosin Y (**245**) as photocatalyst under green light irradiation giving **11c** in excellent yields (Scheme 73).[99]

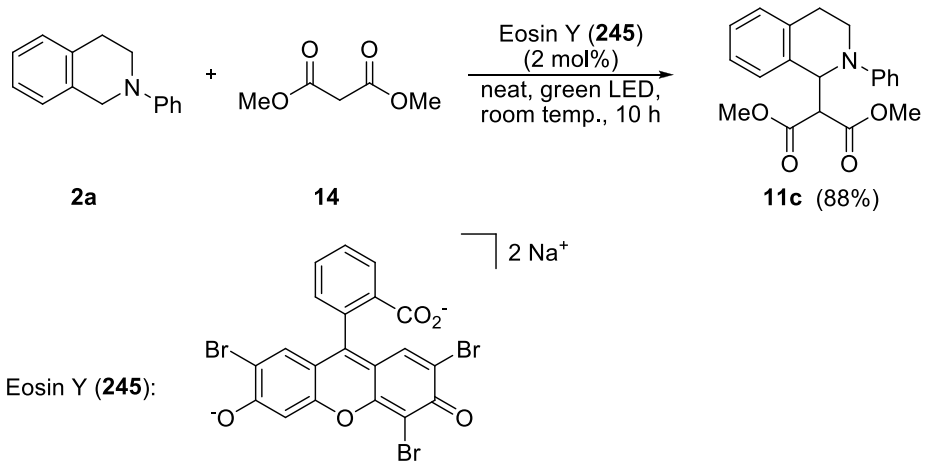

Scheme 73. Oxidative coupling reaction of isoquinoline **2a** and malonate **14**.

Stephenson on the other hand used the same method as described earlier to preform iminium ions to perform such couplings (*cf.* Introduction, Scheme 7-9).[93] The addition of either dimethyl malonate (**14**) or methyl acetoacetate (**246**) to the preformed iminium ion [**6**·Br] furnished the desired products in good yields (Scheme 74).

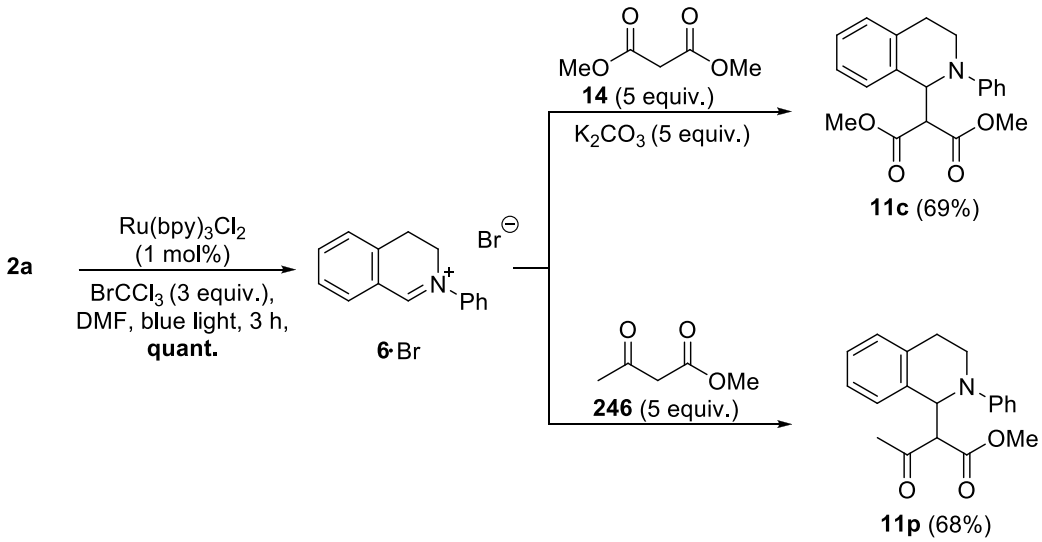

Scheme 74. Photocatalytic Mannich reaction with preformed iminium ions.

Based on these literature examples the oxidative coupling of isoquinoline **243** and cyclohexanone **244** under photocatalytic conditions should be possible. The only difference would be that in this reaction a quaternary carbon center is formed compared to tertiary ones in the reports by König and Stephenson.

The next step, the formation of the triflic ether, would be analogous to a method published by de Lera *et al.* (Scheme 75).[100] *N*-phenyl triflimide (**248**) was used to transfer the triflate moiety.

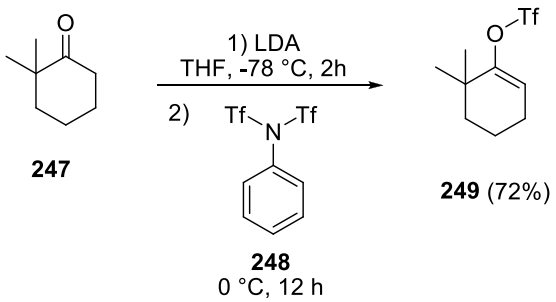

Scheme 75. Generation of triflate enolate **248** reported by de Lera.[100]

The Tsuji-Trost reaction of molecule **241** to furnish ester **240** would be another key step of this total synthesis (Scheme 76 A). Similar reactions have been successfully performed in the synthesis of a

variety of other natural products. Exemplary, a synthesis by Williams *et al.* is shown in Scheme 76 B).[101]

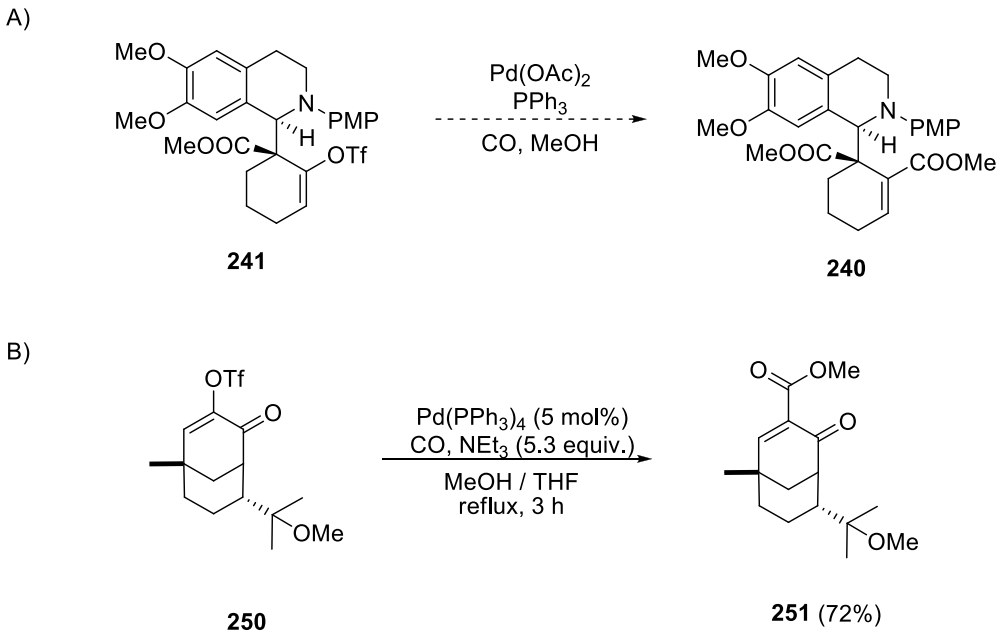

Scheme 76. Tsuji Trost type reactions in natural product synthesis.

This would be followed by the removal of the PMP group with ceric ammonium nitrate (CAN), which has been demonstrated for example by Buchwald *et al*.[102] The synthesis of jamtine (**239**) would be concluded by the formation of lactam **239** in overall 5 sequential steps (Scheme 77).

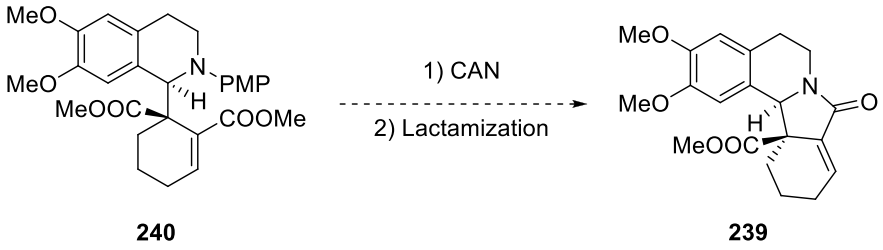

Scheme 77. Envisioned deprotection and lactamization to obtain jamtine **239**.

3.2 Photocatalytic oxidative coupling reactions

It was envisioned to generate the iminium ion of isoquinoline **2a** and trap it with a cyclohexanone derivative in a similar fashion as König *et al*. did.[99] As model substrates 2-phenyl-1,2,3,4-tetra-hydroisoquinoline (**2a**) and ethyl 2-oxocyclohexanecarboxylate (**252**) were chosen.

By screening different photoredox catalysts the optimal catalyst for this reaction should be determined first (Table 15). In further experiments the right solvent and the right choice of additives will be investigated.

Table 15. Catalyst, solvent and additive screening for suitable reaction conditions.

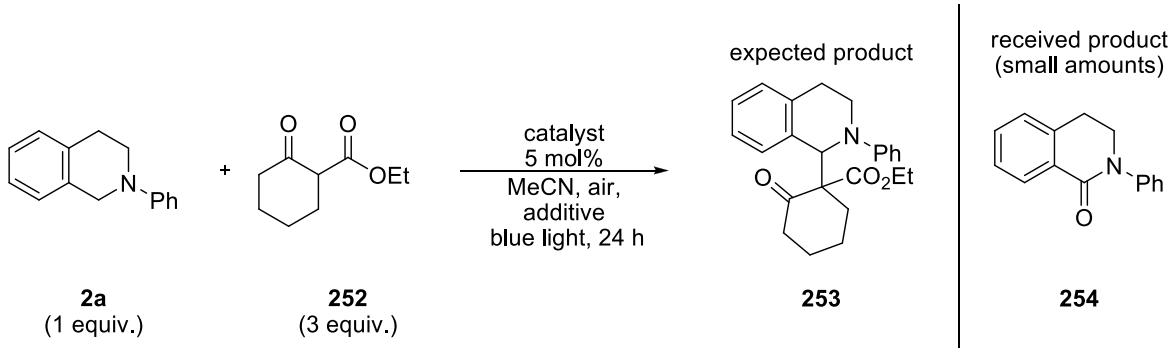

entry	catalyst	solvent	additive	yield 253	obtained product
1	Eosin Y (**245**)	MeCN	-	0 %	**254**
2	$Ru(bpy)_3Cl_2$ (**1**·Cl_2)	MeCN	-	0 %	**254**
4	$Cu(dap)_2Cl$ (**195**)	MeCN	-	0 %	**254**
3	$[Ir(dtb\text{-}bpy)(ppy)_2]PF_6$ (**204**·PF_6)	MeCN	-	0 %	**254**
5	$[Ir(dtb\text{-}bpy)(ppy)_2]PF_6$ (**204**·PF_6)	DMF	-	0 %	-
6	$[Ir(dtb\text{-}bpy)(ppy)_2]PF_6$ (**204**·PF_6)	DCM	-	0 %	-
7	$Ru(bpy)_3Cl_2$ (**1**·Cl_2)	MeCN	5 % (v/v) H_2O	0 %	**254**
8	$Ru(bpy)_3Cl_2$ (**1**·Cl_2)	MeCN	$NaCO_3$ (1.3 equiv.)	0 %	**254**
9	$Ru(bpy)_3Cl_2$ (**1**·Cl_2)	MeCN	$Cu(OTf)_2$ (1.3 equiv.)	0 %	-
10	$Ru(bpy)_3Cl_2$ (**1**·Cl_2)	MeCN	NaOH (1.3 equiv.)	0 %	**254**
11	$Ru(bpy)_3Cl_2$ (**1**·Cl_2)	MeCN	TFA (1.3 equiv.)	0 %	-
12[a]	$Ru(bpy)_3Cl_2$ (**1**·Cl_2)	DMF	$BrCCl_3$ (3 equiv.)	0 %	-

a): **2a**, $BrCCl_3$ (**8**) and $Ru(bpy)_3Cl_2$ (**1**·Cl_2) were irradiated in DMF for 3 h to preform the iminium ion.[93] Then irradiation was stopped and **252** added.

The conditions applied by König *et al.* were used (Scheme 73),[99] therefore the reaction solution was not degassed. All of the employed catalysts in acetonitrile led not to the desired product **253** (entry 1 – 4, Table 15). Only amide **254** could be identified as side product. This product was also obtained in the photocatalytic conjugate additions if oxygen was present in the reaction mixture.[75] Using [**204**·PF_6] as catalyst and changing the solvent from MeCN to DMF or DCM did not yield any product (entry 5 – 6, Table 15). In fact in those cases not even oxidized product **254** was identifiable. Also the additions of Lewis or Brønsted acids and bases in combination with [**1**·Cl_2] as catalyst and MeCN as solvent did not give rise to the desired product (entry 7 – 11, Table 15).
In another experiment the conditions used by Stephenson *et al.* were applied (entry 12, Table 15).[93] The stable iminium ion [**6**·Br] was preformed with the help of $BrCCl_3$ (**8**) and $Ru(bpy)_3Cl_2$ (**1**·Cl_2) as photocatalyst (*cf.* Introduction, Scheme 7). After complete consumption of starting material **2a**, the light was switched of and cyclohexanone **252** was added. No product formation could be observed.

A non photocatalytic attempt for the synthesis of jamtine **239** was also considered. Therefore a cross dehydrogenative coupling (CDC), developed by Li *et al.*, seemed to be most promising. In one report they were able to couple dimethyl malonate **244** to isochroman using $Cu(OTf)_2$ and 2,3-Di-chloro-5,6-dicyano-1,4-benzoquinone (DDQ);[103] in another report they coupled **2a** and malonate **14** by employing CuBr as catalyst and *tert*-butyl hydroperoxide (TBHP) as oxidant.[104]

Table 16. Cross dehydrogenative coupling reactions.

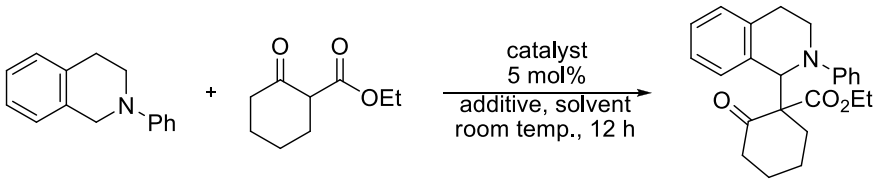

2a (1 equiv.) **252** (1.2 equiv.) **253**

entry	catalyst	additive	solvent	yield
1	$Cu(OTf)_2$	DDQ (1.2 equiv.)	DCM	No reaction
2	CuBr	TBHP (1.3 equiv.)	MeCN	No reaction

In a first attempt, $Cu(OTf)_2$ was used as catalyst and DDQ as oxidant, but no reaction took place (entry 1, Table 16). In another experiment, CuBr and the oxidant TBHP were used to couple **2a** and **252**, but also in this case, no product formation could be observed (entry 2, Table 16).

Most likely, product **253** could not be obtained due to sterical hindrances. In general it is easier to generate tertiary carbon centers, as reported in literature, than quaternary.

3.3 Photocatalytic [3+2] Cycloaddition Reactions

Due to the results obtained in the previous chapter, the whole strategy was revised and changed towards photocatalytic [3+2] additions. Xiao *et al.* reported a novel photocatalytic method to furnish pyrrole derivatives by [3+2] addition (*cf.* Introduction, Scheme 17).[105] In this reaction isoquinoline derivative **38** was oxidized to the corresponding iminium ion **40** and by abstraction of a proton zwitterion **41** was generated. Zwitterion **41** reacts with the electron deficient olefin **255** in a [3+2] cycloaddition to give **256** which is further oxidized to **45a** in an overall yield of 64% within 15 h. Interestingly, if no NBS is added to the reaction mixture, also intermediate **256** is isolable, however only in 49% yield within 10 h (Scheme 78).

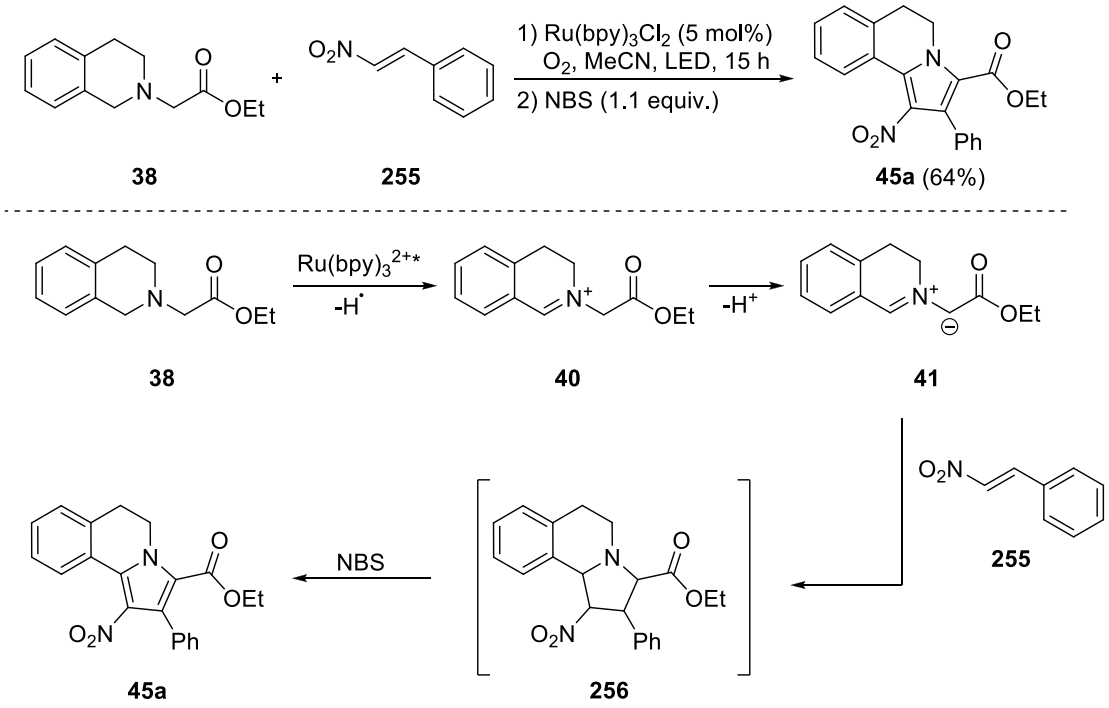

Scheme 78. Photocatalytic [3+2] addition reported by Xiao *et al.*

Based on this publication it was intended to synthesize isoquinoline derivative **257**, which is commercially available[106] and was employed by Xiao for the above depicted reaction. It should be coupled with cyclohexene derivative **258** furnishing the core structure **259** of jamtine (**239**) in one step.

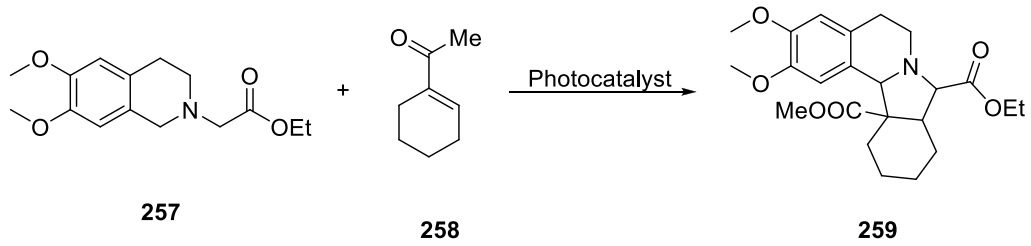

257 **258** **259**

Scheme 79. Formation of the jamtine core structure **259** by photocatalytic [3+2] addition.

From there on it was envisioned to finish jamtine (**239**) in 2 more steps, making this route the shortest reported synthesis (Scheme 80).

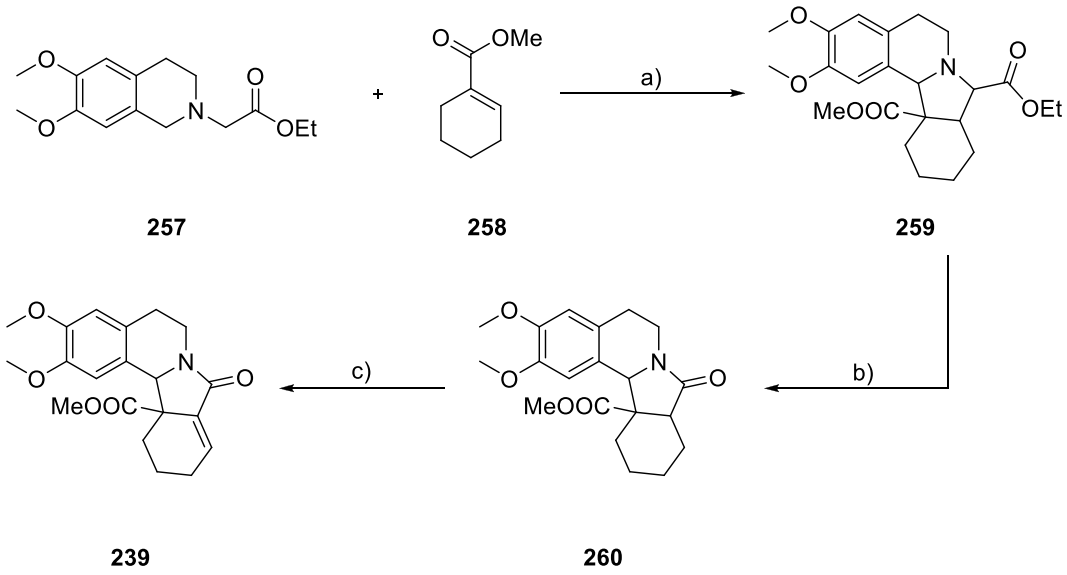

257 **258** **259**

239 **260**

Scheme 80. Synthesis of jamtine (**239**) via [3+2] photocycloaddition reaction. Reactions: a) photocatalytic key step with commercially available substrates; b) oxidation with IBX and TEAB; c) oxidation with HMDS and PhSeBr.

The transformation of ethyl ester **259** to ketone **260** would be conducted similar to a report by Akamanchi *et al.* who utilized IBX and TEAB as oxidizing agent.[107] Then jamtine (**239**) would be finished by introducing the double bond with the help of HMDS and phenylselenyl bromide. A similar reaction was performed by Brocksom *et al.* to generate α,β-unsaturated ketone **262** (Scheme 81).[108]

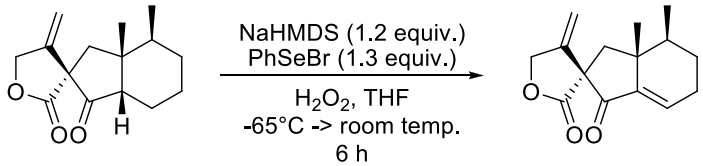

261 **262** (77%)

Scheme 81. Introduction of a double bond performed by Brocksom *et al.*[108]

As model substrates isoquinoline **38** and tiglinic acid **263a** were chosen. **38** was prepared by refluxing 1,2,3,4-tetrahydroisoquinoline and ethyl 2-bromoacetate in THF with $NaCO_3$ as catalyst in 48% yield similar to a procedure by Rueping *et al*.[109] **38** and **263a** were mixed with $Ru(bpy)_3Cl_2$ (**1**·Cl_2, 5 mol%) in MeCN and irradiated with blue LEDs. No reaction could be detected after 24 h (Scheme 82).

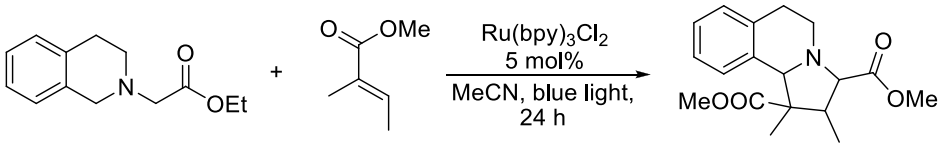

38 **263a** **264a** (0%)

Scheme 82. [3+2] Addition of ethyl 2-(6,7-dimethoxy-3,4-dihydroisoquinolin-2(1H)-yl)acetate (5) with (E)-methyl 2-methylbut-2-enoate (**263**).

Additionally it was tried to preform iminium ion **40** by Stephenson's method and deprotonate it with the help of a base to obtain zwitterion **41** prior to the addition of the olefin (entry 1, Table 17).[93] Again no product formation could be observed. Also changing the olefin to methyl acrylate (**263b**) did not succeed (entry 2 – 3, Table 17).

Table 17. Preformation of the iminium ion and subsequent [3+2] photocycloaddition.

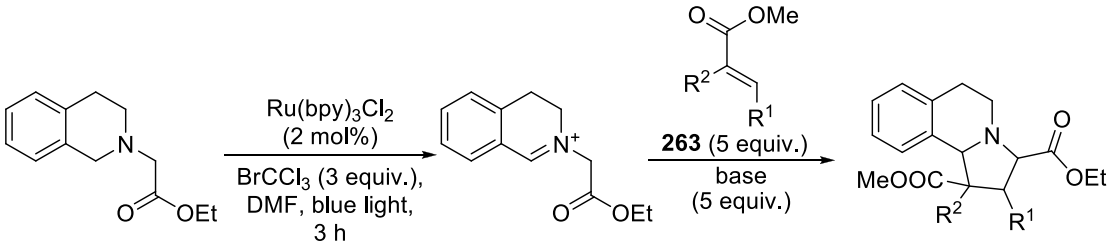

38 **40** **264**

entry	R^1	R^2	base	yield (264)
1	Me	Me	NEt_3 (5 equiv.)	0 %
2	H	H	NEt_3 (5 equiv.)	0 %
3	H	H	K_2CO_3 (5 equiv.)	0 %

At the same time as Xiao *et al.* reported their addition reaction,[105] the group of Rueping *et al.* developed a similar [3+2] photocycloaddition shown in Scheme 77.[109] In this report they were able to couple isoquinoline derivative **265** with maleimide **266** under photocatalytic conditions in good yield (Scheme 83). Because addition product **264** could not be furnished by the Xiao´s method the strategy was adapted to use the reaction developed by Rueping *et al*.

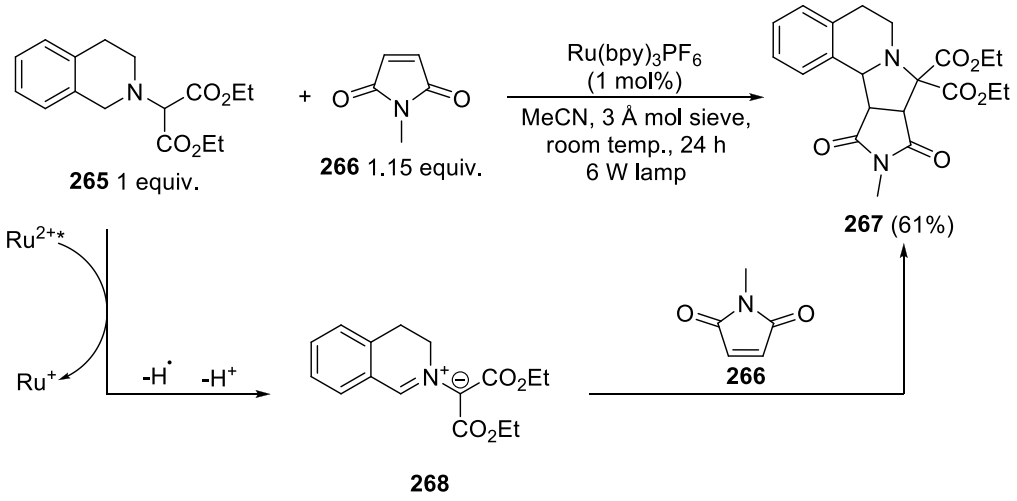

Scheme 83. Photocatalytic [3+2] addition developed Rueping *et al*.[109]

Isoquinoline **265** was synthesized according to Rueping´s procedure,[109] mixed with acrylate **263** and $Ru(bpy)_3Cl_2$ (**1**·Cl_2) (2 mol%) in MeCN and irradiated with blue LEDs for 24 h.

Table 18. Photocatalytic [3+2] photocycloaddition reactions.

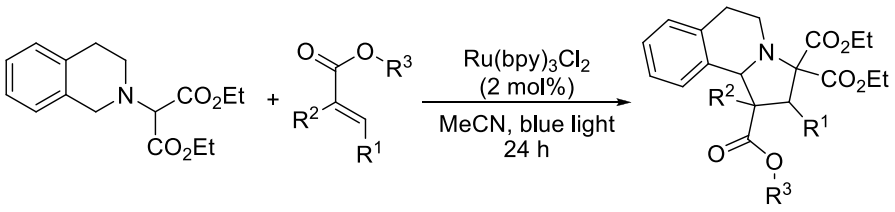

entry	R^1	R^2	R^3	yield (192)	obtained product
1	H	H	Me	0 %	**270**
2	H	H	Et	0 %	-
3	Me	Me	Me	0 %	**270**

identifyable product:

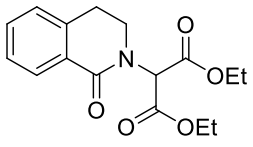

270

Figure 7. Structure of diethyl 2-(1-oxo-3,4-dihydroisoquinolin-2(1H)-yl)malonate (**270**).

In all reactions no product formation could be observed, only trace amounts of the amide species **270**. This product was also obtained by Rueping *et al.* if no suitable dipolarophile was present.

In conclusion it can be stated that no Mannich-type method could be developed to oxidatively couple an isoquinoline species with a β-ketoester to yield an intermediate for the synthesis of jamtine, neither under photocatalytic condition nor under non photocatalytic conditions (Scheme 84 A).

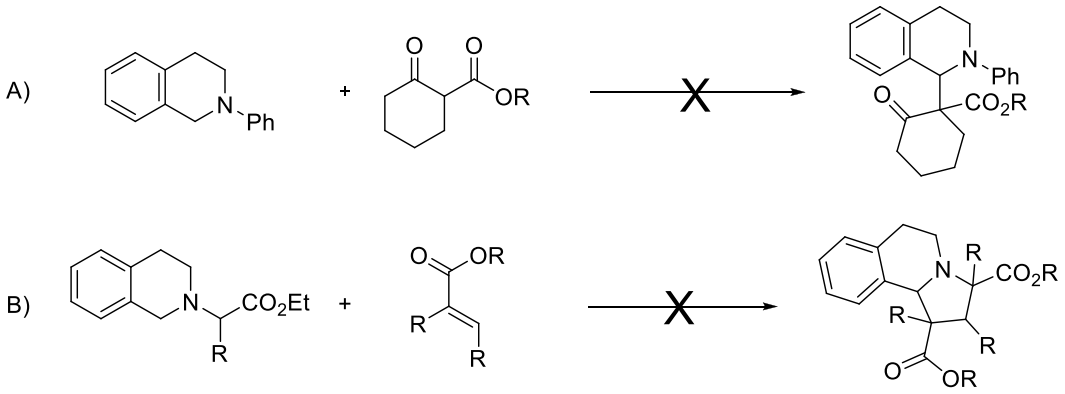

Scheme 84. Envisioned photocatalytic key steps for the synthesis of jamtine (**239**).

Also revising the strategy to [3+2] photocycloadditions using either Xiao´s or Rueping´s conditions did not succeed (Scheme 84 B) and therefore no novel synthesis for jamtine (**239**) could be developed. Most likely steric hindrances and the formation of quaternary carbon centers are the reason for this. Further considerations to synthesize jamtine let to longer reaction sequences. Because Simpkins *et al.* were already able to furnish this natural product enantioselective in six steps, no more efforts were made to synthesize jamtine.

4. Photocatalytic Cyclopropane Functionalization

Cyclopropanes are important intermediates in synthetic organic chemistry and a structural motive in many natural products. The group of Reiser *et al.* has developed a whole toolbox of enantioselective cyclopropane chemistry which is often applied in natural product synthesis or the synthesis of biological active compounds, for example unnatural amino acids.[110]

In the course of his studies, Ludwig Pilsl synthesized the furan and pyrrole derived cyclopropanes depicted in Figure 8. To generate these compounds, furan or Boc-protected pyrrole was cyclopropanated with *tert*-butyldiazoacetate, catalyzed by a chiral copper aza-bisoxazoline complex, yielding the desired products in up to 52% yield and 99%ee after recrystallization. [111]

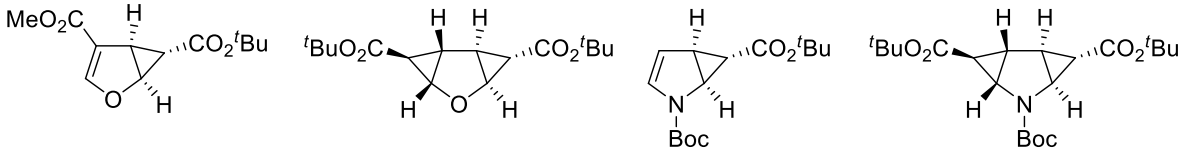

271 **272** **273** **274**

Figure 8. Structure of (1S,5R,6S)-6-tert-butyl 4-methyl 2-oxabicyclo[3.1.0]hex-3-ene-4,6-dicarboxylate (**271**), (1S,2S,3S,4S,6S,7S)-tri-tert-Butyl-2-oxatricyclo[4.1.0.0^{3,5}]heptane-4,7-dicarboxylate (**272**), (1S,5S,6S)-di-tert-Butyl-2-azabicyclo[3.1.0]hex-3-ene-2,6-dicarboxylate (**273**) and (1S,2S,3S,4S,6S,7S)-tri-tert-Butyl-5-azatricyclo[4.1.0.0^{2,4}]heptane-3,5,7-tricarboxylate (**274**)

Due to our interest in developing new methods to modify and transform cyclopropanes it was envisioned to initiate a single electron transfer (SET) from the catalyst to the target molecule. This should, *via* a radical mechanism, lead to an opening of the cyclopropane moiety. The thus generated radical should be trapped by a suitable reagent, opening up a novel way to modify cyclopropanes.

At first, the cyclic voltammogram (CV) of cyclopropanes **271** – **274** was measured. All spectra were recorded in degassed acetonitrile; tetra-*n*-butylammonium tetrafluoroborate was used as supporting electrolyte in a concentration of 0.1 M. The set up consisted of an undivided cell, a glassy carbon working electrode, a platinum wire as the counter electrode and a silver wire as pseudo reference electrode. The measurements ranged from -2.0 V to 2.5 V at a sweep rate of 0.05 V/s. Ferrocene was used as internal standard. With the help of Fick´s law of diffusion and the Nernst equation the reactions in the vicinity of the working electrode can be described. A process is called chemically reversible if both oxidized and reduced forms are stable during the time scale of the CV measurement. Then a reduction peak at the cathodic peak potential E_{pc} and an oxidation peak at the anodic potential E_{pa} is observable. According to equation 3 the mean value of E_{pc} and E_{pa} correspond

to the half wave potential $E_{1/2}$ which is associated with the thermodynamic equilibrium potential E° (equation 4). D_o and D_r are the diffusion constants of oxidized and reduced form.[112]

$$E_{\frac{1}{2}} = \frac{E_{pa}+E_{pc}}{2} \quad (3)$$

$$E_{\frac{1}{2}} = E^0 + \left(\frac{RT}{nF}\right)\ln\left(\frac{D_r}{D_o}\right)^{\frac{1}{2}} \quad (4)$$

Thus in a chemical reversible process, the species formed during the anodic sweep can be reduced in the back scan. In a chemical irreversible process, the generated species is rapidly transformed into a redox-inactive form in an irreversible chemical reaction and is therefore not detectable in the back-scan. The exact position of E_{Pc}, E_{Pa} and therefore $E_{1/2}$ strongly depends on the measurement conditions. Thus, no absolute values can be stated, only values relative to a reference substance.[112] All redox potentials were measured *vs.* ferrocene as internal standard. Measurements and redox potentials relative to different reference substances can be converted into each other.[113] For better comparison with literature values all redox potentials and spectra shown within this thesis are in reference to a saturated calomel electrode (SCE). Exemplary the spectrum of **273** is shown in Figure 9.

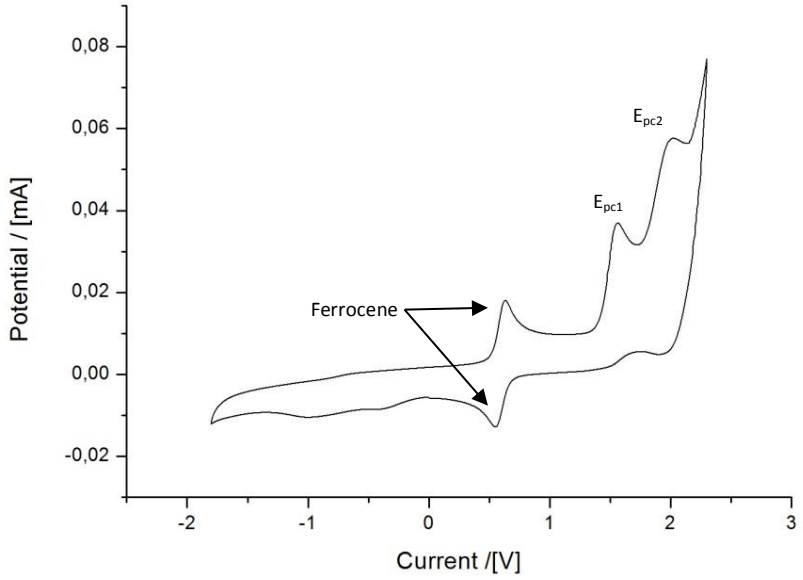

Figure 9. CV spectra of (1S,5S,6S)-di-tert-Butyl-2-azabicyclo[3.1.0]hex-3-ene-2,6-dicarboxylate (**273**) in MeCN.

The redox potentials of cyclopropanes **271** – **274** are summarized in Table 19. All electron transfer processes are irreversible which implies that the generated radical intermediates are not stable.

Table 19. Oxidation and reduction potentials of cyclopropanated furans and pyrroles.[a)]

entry	molecule		1st reduction	2nd reduction	1st oxidation	2nd oxidation
1	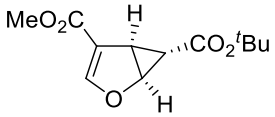	**271**	-	-	1.84 V	-
2	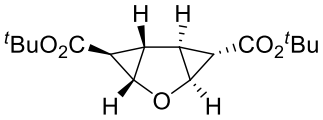	**272**	-1.84 V	-1.94 V	-	-
3	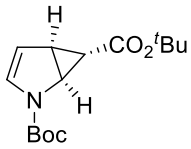	**273**	-	-	1.32 V	1.77 V
4	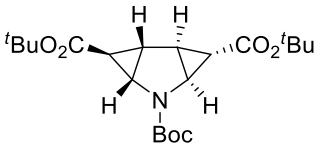	**274**	-0.82 V	-	-	-

a) All values are measured in acetonitrile and given in Volt *vs.* a saturated calomel electrode (SCE).

Judging the results, m*ono*-cyclopropanated pyrrole **273** was most promising with an oxidation potential of E_{Pc} = 1.32 V *vs.* SCE in MeCN. A molecule with this potential should be oxidizable by $Ru(bpz)_3Cl_2$ (**275**·Cl_2) (where bpz = bipyrazyl) and $[Ir(dF(CF_3)ppy)_2(dtbbpy)](PF_6)$ (**216**·PF_6) (Table 20).

Table 20. Structure and redox potentials of $Ru(bpz)_3Cl_2$ (**275**·Cl_2) and $[Ir(dF(CF_3)ppy)_2(dtbbpy)](PF_6)$ (**216**·PF_6).[86a), 114,]

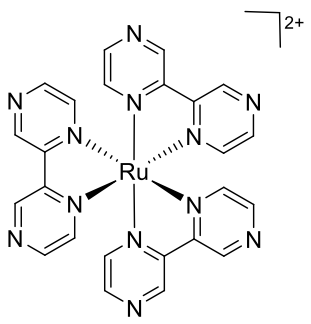

275

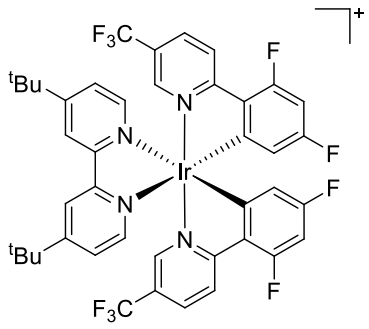

216

Redox Potentials:[a)]

	$E_{1/2}(M^*/M^-)$	$E_{1/2}(M/M^-)$	$E_{1/2}(M^+/M^*)$	$E_{1/2}(M^+/M)$
$Ru(bpz)_3^{2+}$	1.45 V	-0.80 V	-0.26 V	1.86 V

	$E_{1/2}(M^*/M^-)$	$E_{1/2}(M/M^-)$	$E_{1/2}(M^+/M^*)$	$E_{1/2}(M^+/M)$
$Ir(dF(CF_3)ppy)_2(dtbbpy)^+$	1.21 V	-1.37 V	-0.89 V	1.69 V

a) All values were measured in acetonitrile and are given in Volt *vs.* a saturated calomel electrode (SCE).

In case of **275** the reductive pathway would be used. The oxidation potential $E_{1/2}(Ru^{II*}/Ru^{II})$ = 1.45 V is fair above the one of **273**. In case of **216** the oxidative pathway with a potential of $E_{1/2}(Ir^{IV}/Ir^{III})$ = 1.69 V will be utilized, leading to an even higher oxidation potential. As there are not many literature precedencies postulating the oxidative reaction pathway of **216**, the use of $Ru(bpz)_3Cl_2$ (**275**·Cl_2) seemed more promising.[115] Furthermore it was intended to first perform an oxidation followed by a reduction of the substrate within the course of the reaction. Thus no further additive was added as sacrificial electron donor or acceptor and the reaction mixture was degassed thoroughly in order to exclude oxygen.

Pyrrole derivative **273** (1 equiv.) was mixed with methyl vinyl ketone (MVK) (**23a**, 3 equiv.) and a photocatalyst (2 mol%) in acetonitrile. The solution was degassed using freeze pump thaw method and irradiated with a blue LED (λ_{max} = 455 nm) for 24 h.

Table 21. Photochemical cyclopropane opening.

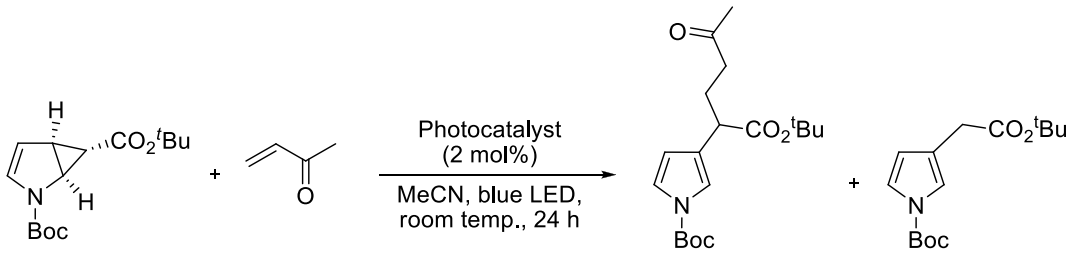

273 **23a** **276** **277**

entry	catalyst	yield 276	yield 277
1	$Ru(bpz)_3Cl_2$ (**275**·Cl_2)	0%	0%
2[a)]	$[Ir(dF(CF_3)ppy)_2(dtbbpy)](PF_6)$ (**216**·PF_6)	15%	27%

a) LED failed during experiment.

When $Ru(bpz)_3Cl_2$ (**275**·Cl_2) was employed as photocatalyst, no opening of the cyclopropane moiety and only little consumption of the starting material could be determined by TLC and ^{1}H-NMR

analysis. However, to our delight, using [Ir(dF(CF$_3$)ppy)$_2$(dtbbpy)](PF$_6$) (**216**·PF$_6$) as photocatalyst let to the formation of two new products. Product **277** deriving from an opening of cyclopropane **273** was isolated in 27% yield and product **276**, which arises from an addition of enone **23a** to the former cyclopropane moiety, in 15% yield. Due to this promising result in the presence of photoredox catalyst **216** all further reactions were conducted with this catalyst. The formation of product **276** can be explained by the following mechanism:

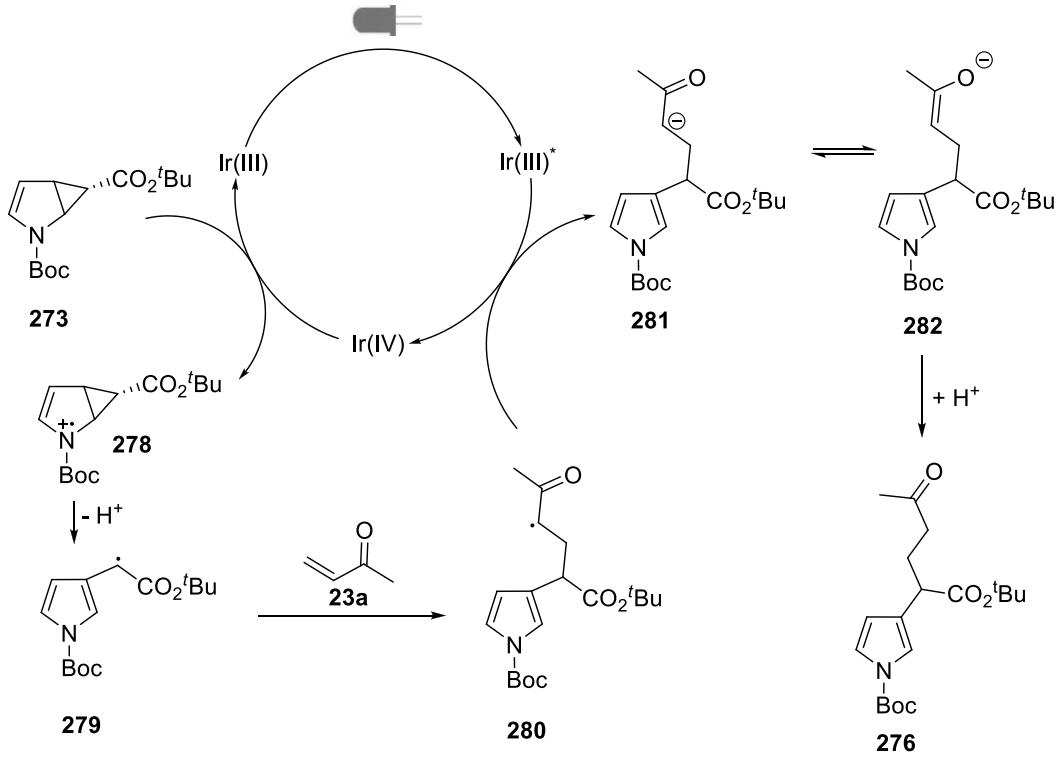

Scheme 85. Proposed mechanism for the formation of pyrrole derivative **276**.

In the first step of the assumed reaction mechanism **273** is oxidized to radical cation **278** by the oxidized species of catalyst **216**. By loss of a proton α-carbonyl radical **279** is generated. This radical can on the one hand be directly reduced by excited Ir(dF(CF$_3$)ppy)$_2$(dtbbpy) (**216**·PF$_6$) yielding ring opening product **277** after the addition of a proton. On the other hand, radical **279** can be trapped by methyl vinyl ketone **23a** giving rise to intermediate **280**. This radical can then also be reduced by excited Ir(dF(CF$_3$)ppy)$_2$(dtbbpy) (**216**·PF$_6$) yielding anion **281** which is protonated to give rise to addition product **276** (Scheme 85).

Following up these first experiments a screening for suitable solvents was conducted (Table 22).

Table 22. Screening for suitable solvents.

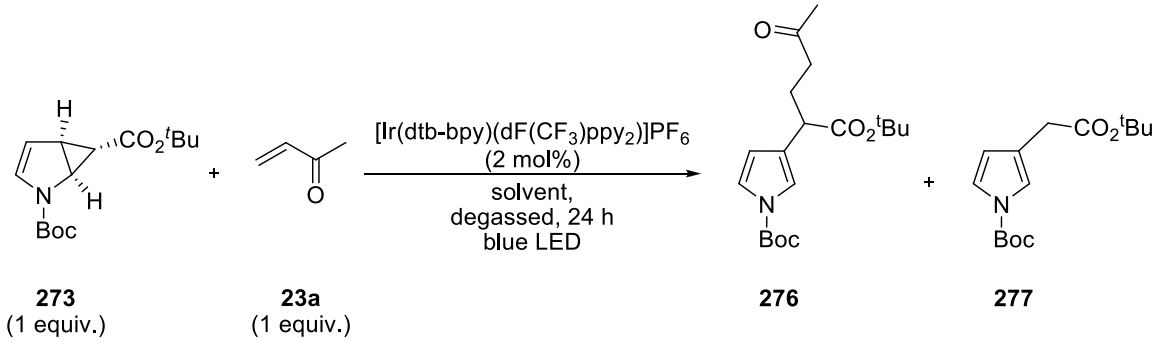

273 (1 equiv.) **23a** (1 equiv.) **276** **277**

entry	solvent	yield 276	yield 277
1	dry MeCN	27%	47%
2	MeCN with 10% H_2O	very little conversion	
3	DCM	very little conversion	
4	^{i}PrOH	no conversion	
5	DMF	no conversion	
6	DMA	no conversion	

Performing the reaction in acetonitrile, stored over molecular sieve (3 Å), increased the yield of the desired addition product to up to 27%. 47% of ring opening product **277** could be isolated (entry 1, Table 22). Adding 10% of water to acetonitrile quenched the reaction nearly completely (entry 2, Table 22). The same result was obtained when the reaction was conducted in DCM (entry 3, Table 22). Changing the solvent to *iso*-propyl alcohol, DMF or dimethylacetamide stopped the reaction completely. No conversion could be detected by TLC analysis (entry 4 – 6, Table 22). Therefore dry acetonitrile is the solvent of choice to conduct this experiment.

Following this an experiment was set up where methyl vinyl ketone (**23a**) was replaced with chalcone (**23b**) (Scheme 86).

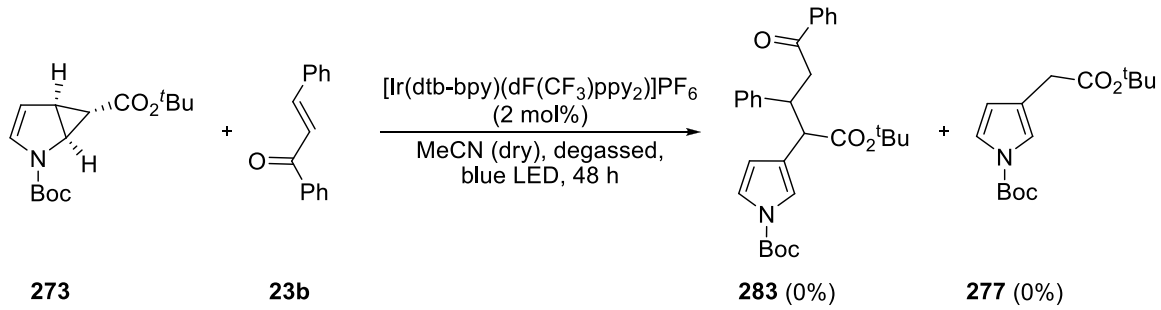

273 **23b** **283** (0%) **277** (0%)

Scheme 86. Coupling reaction with chalcone as substrate.

Performing the reaction with chalcone (**23b**) as trapping reagent did not lead to the formation of addition product **283**, nor was ring opening product **277** observed. Chalcone (**23b**) could be reisolated even after 48 h of irradiation time (Scheme 86). Only an E/Z isomerization of chalcone (**23b**) could be observed via ^{1}H-NMR analysis, proofing that an electron transfer from the catalyst to chalcone (**23b**) and vice versa is feasible. That not even ring opening is possible when MVK (**23a**) is replaced with **23b** indicates that methyl vinyl ketone plays an important role in the cyclopropane opening and the subsequent coupling. Most likely the E/Z isomerization of **23b** is initiated by the reductive quenching cycle of Ir(dF(CF$_3$)ppy)$_2$(dtbbpy) (**216**·PF$_6$). But in order to perform the epoxide opening with subsequent coupling to an enone the oxidative quenching cycle is required which is most like initiated by the reduction of MVK (**23a**).

To broaden the scope of the reaction other cyclopropanes were employed. Two experiments per cyclopropane were set up, one without any other additive except for photocatalyst **216** and one additionally containing MVK (**23a**) as trapping reagent (Table 23).

All reaction mixtures were degassed using the freeze pump thaw method and irradiated *via* an optical fiber and a blue LED (455 nm). No starting material was consumed when 1-cyclopropyl-ethanone (**284a**) was irradiated with a photocatalyst in the absence as well as in the presence of MVK (entry 1, Table 23). Changing the substrate to 3-oxabicyclo[3.1.0]hexane-2,4-dione (**284b**) gave the same result. With and without MVK as additive, no starting material was consumed (entry 3 – 4, Table 23). Employing dimethyl cyclopropane-1,2-dicarboxylate (**284c**) in this reaction led upon addition of MVK to little consumption of the starting material but neither ring opening product **285** nor addition product **286** was identifiable (entry 6, Table 23). Without MVK no starting material was

consumed (entry 5, Table 23). The same results as with **284c** were obtained conducting the experiments with 2-(ethoxycarbonyl)-3-formylcyclopropyl methyl oxalate (**284d**) as substrate.

Table 23. Screening for suitable cyclopropanes.

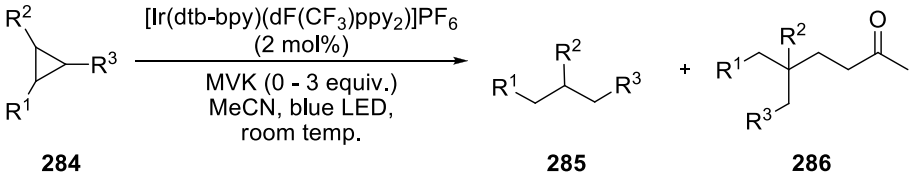

284 **285** **286**

entry	cyclopropane	MVK (23a)	time / [h]	yield 285	yield 286
1	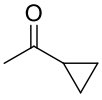 **284a**	0 equiv.	24	0%	-
2		3 equiv.	72	0%	0%
3	 **284b**	0 equiv.	24	0%	-
4		3 equiv.	72	0%	0%
5	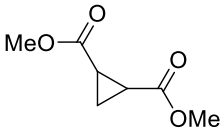 **284c**	0 equiv.	24	0%	-
6		3 equiv.	72	0%	0%
7	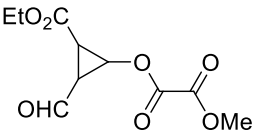 **284d**	0 equiv.	48	0%	-
8		3 equiv.	48	0%	0%

In summary it can be stated that it is possible to open pyrrole derived cyclopropane **273** photochemically and functionalize it with methyl vinyl ketone (**23a**) in an unprecedented way as shown in Scheme 87. However, currently only one example of this transformation is known. Further substrates have to be discovered.

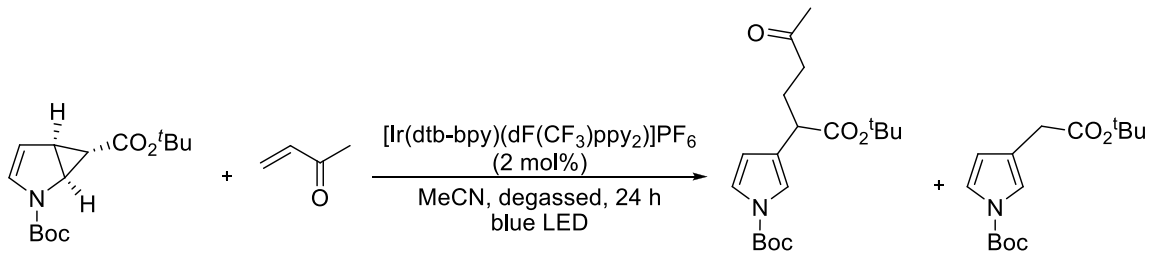

273 (1 equiv.) **23a** (3 equiv.) **276** (27%) **277** (49%)

Scheme 87. Photocatalytic cyclopropane opening and functionalization.

The best results were obtained by addition of three equivalents of MVK (**23a**) and $Ir(dF(CF_3)ppy)_2(dtbbpy)$ (**216**·PF_6, 2 mol%) as photocatalyst in dry MeCN yielding up to 27% of branched product **276** and 47% of open cyclopropane **277** (Scheme 87).

In further studies the influence of sacrificial electron acceptors should be investigated. If no enone is present in the reaction mixture this might lead to **277** as sole product. If one is present in the reaction mixture in combination with an electron acceptor the yield of coupling product **276** might be enhanced. Also other pyrrole derived cyclopropanes are of interest. One promising example is molecule **287** which was used by the Reiser group in previous studies.[116]

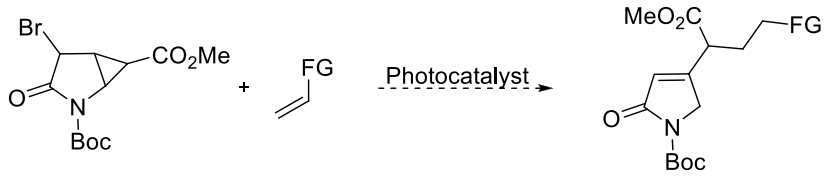

287 **288** **289**

Scheme 88. Photocatalytic functionalization of cyclopropane **287**.

Due to the structural differences of **287** compared to **273** more insight on the reaction mechanism could be gained (Scheme 88). It is also possible that an ATRA reaction will take place and the bromine can be found in the product.

5. Photoredoxcatalysts on Solid Support

5.1 Introduction

Most photoredox catalysts are octahedral transition metal complexes. The synthesis of those is often challenging and the contained metal ions, mainly ruthenium and iridium, are scarce. Therefore these catalysts are expensive and not environmentally benign. To conserve nature's recourses, it was envisioned to develop an immobilized photoredoxcatalyst on a solid support that can be easily separated after the photoreaction and recycled for a number of photoreactions. The solid support should be a transparent or white material so as less light as possible will be absorbed. In addition, the preparation and functionalization should be convenient. All these requirements are fulfilled by silica particles and therefore they were chosen as solid support for the photoredox catalyst.

The catalyst should be derived from $[Ir(ppy)_2(dtbbpy)]PF_6$ (**204**·PF_6). In order to change the active center and the electronic properties of the complex as little as possible a tether should be introduced at the *para*-position of the pyridine system. A synthesis was envisioned, in which the solid support would be functionalized with an azide and the tether should bear an alkyne moiety so both parts could be joined in a late stage of the catalyst synthesis *via* a click reaction giving rise to complex **290** (Figure 10).

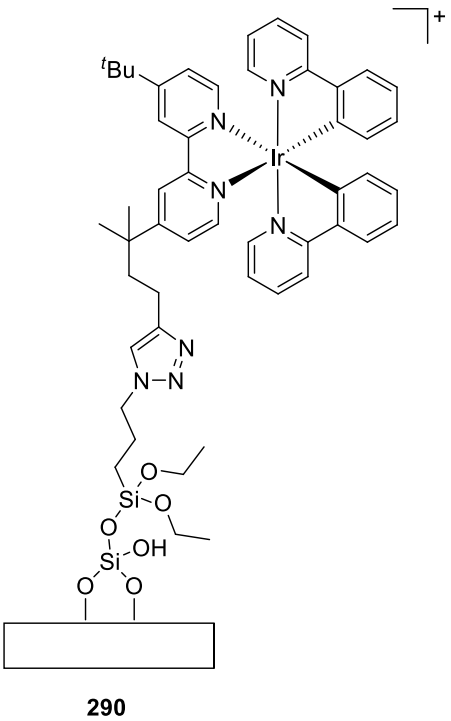

290

Figure 10. Immobilized iridium catalyst **290** on silica support.

5.2 Retrosynthetic Analysis and Initial Synthesis

The retrosynthetic analysis starts out by undoing the click reaction (Scheme 89). Photocatalyst **292** will be synthesized by the standard protocol to furnish $[Ir(ppy)_2(dtbbpy)]PF_6$ (**204**·PF_6), published by Malliaras *et al.* and complex **294** is a well-established intermediate in this synthesis.[68]

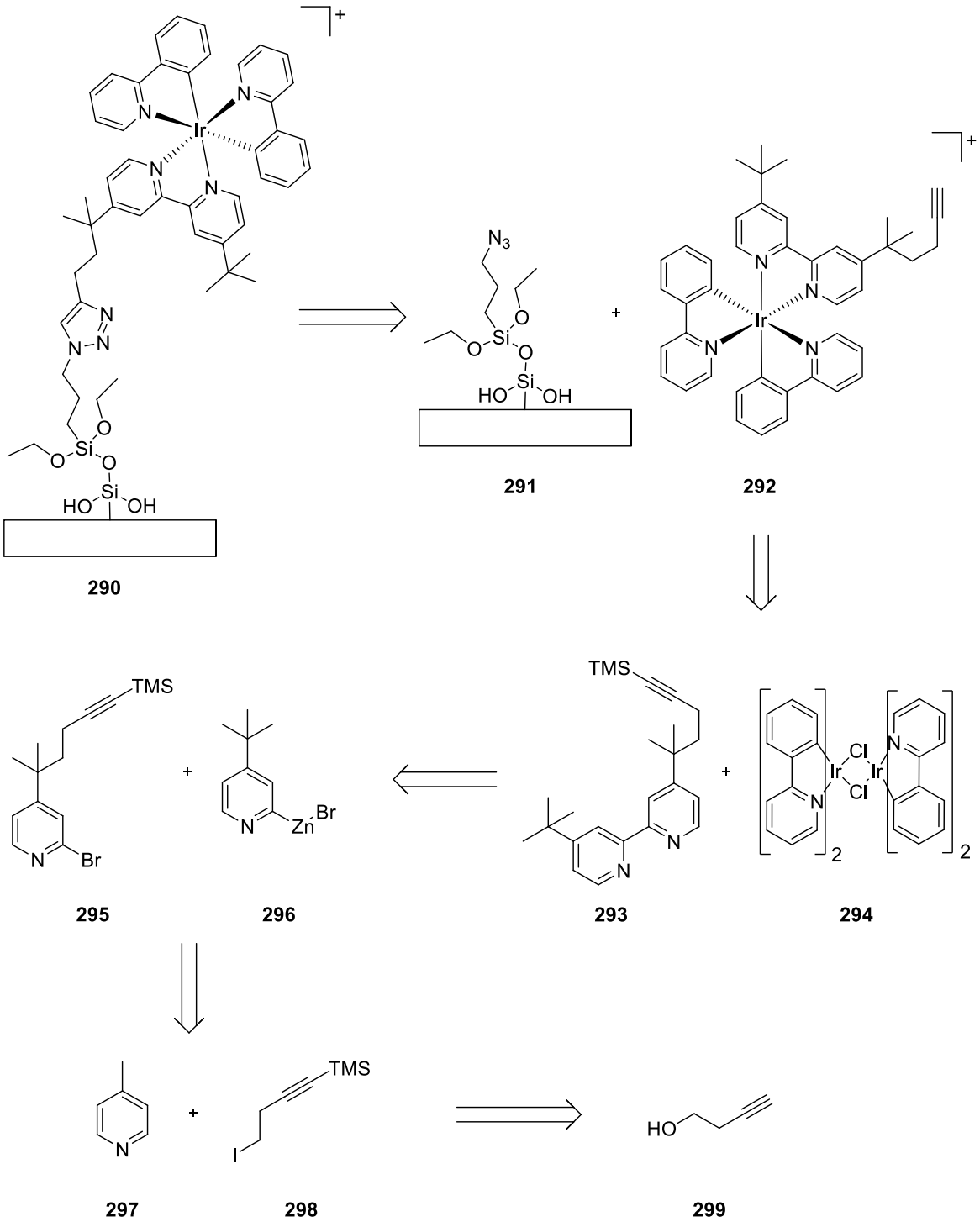

Scheme 89. Retrosynthetic analysis of the recyclable photoredoxcatalyst.

According to a publication by Jitsukawa *et al.*, who performed a Negishi type coupling on similar substrates, a coupling of bromo pyridine **295** and zinc reactant **296** to furnish bipyridine ligand **293** should be possible (*cf.* Scheme 92).[117] Pyridine derivative **295** would be synthesized by lithiation chemistry.[118]

Many established protocols are known for the synthesis of the azide functionalized silica (**291**) particles that can be employed.[119, 120]

In literature many ways are known to synthesize functionalized bipyridine derivatives and furnish ruthenium or iridium complexes apart from classical $Ru(bpy)_3Cl_2$ (**1**·Cl_2) or $[Ir(ppy)_2(dtbbpy)]PF_6$ (**204**·PF_6) respectively. These complexes are mostly used for water oxidation[121, 122] and to the best of my knowledge, nobody immobilized them on silica particles.

At first, the alkyne moiety of **299** was protected by trimethylsilyl chloride[123] and product **300** was subsequently converted to the corresponding iodine *via* a procedure published by de Meijere *et al.* as shown in Scheme 90.[124] Iodine **298** could be isolated in 65% yield (Scheme 90).

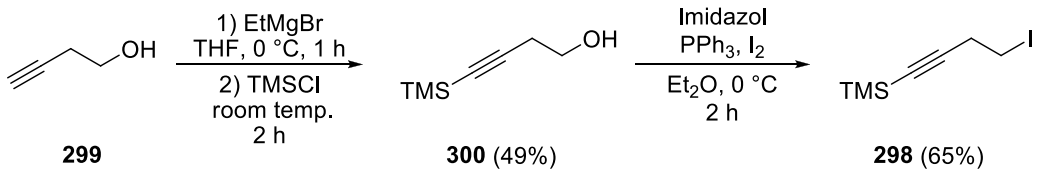

299 **300** (49%) **298** (65%)

Scheme 91. Synthesis of (4-iodobut-1-ynyl)trimethylsilane (**298**).

Following a procedure published by Quing *et al.,* 4-picoline (**297**) could be lithiated and coupled with **298** to give rise to 4-(5-(trimethylsilyl)pent-4-ynyl)pyridine (**302**) in 66% yield (Scheme 91).[118]

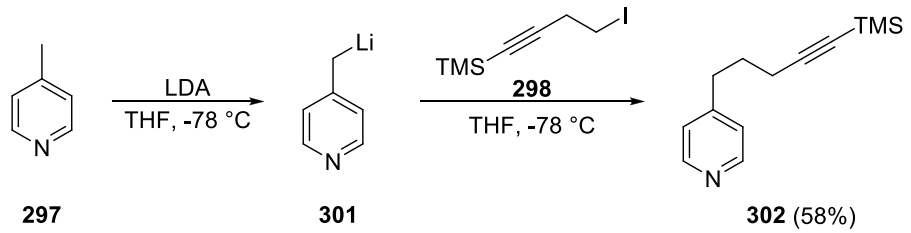

297 **301** **302** (58%)

Scheme 91. Preparation of 4-(5-(trimethylsilyl)pent-4-ynyl)pyridine (**302**) *via* lithiation.

In the next steps two methyl substituents should be introduced at the benzylic position of the pyridine moiety in order to prevent transfer of charges or radicals to the tether and further on to the solid support. However, all attempts to introduce these methyl groups with the help of LDA and methyl iodine failed. This is most likely due to the fact, that also the ortho position of the pyridine moiety can be deprotonated by LDA. Hence it was decided to introduce these groups at a later stage of the synthesis.

Jitsukawa et al. were able to synthesize bipyridyls starting from two modified pyridines. First 2-bromo pyridyl species **304** was generated out of **303** which was coupled with **305** in a Negeshi coupling yielding bipyridine **306** (Scheme 92).

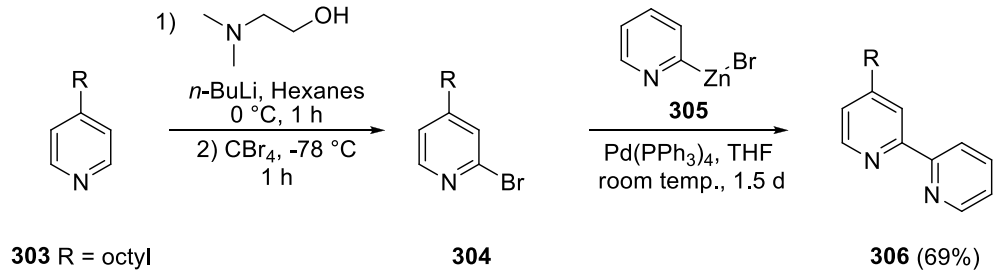

Scheme 92. Preparation of bipyridines according to *Jitsukawa et al.*[117]

All attempts to brominate **302** using this method failed and led only to decomposition of the starting material. In contrast to Jitsukawa, who used a long alkyl chain, molecule **302** is bearing an alkyne moiety with a TMS protection group.

A new route, following a procedure by *Grätzel et al.* which is displayed in Scheme 93 was examined next. In this publication an *N*-oxim is formed, emanating from a pyridine and upon treatment with $POCl_3$ a 2-chloro-pyridine species (**309**) is generated. This species can then be transformed to the corresponding bromide by addition of hydro bromic acid and acetic acid.[125]

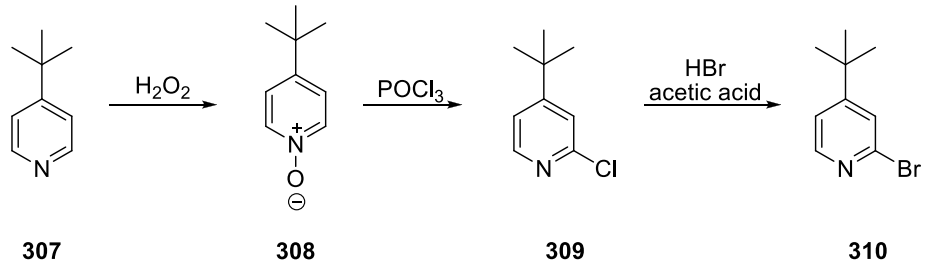

Scheme 93. Generation of 2-bromo-pyridines by *Grätzel et al.*[125]

N-oxim **311**, originating from **302**, was easily accessible by a method from *Tzschucke et al*.[126] On the other hand the corresponding chloride could not be obtained *via* the route published by *Grätzel et al.* (Scheme 94).[125]

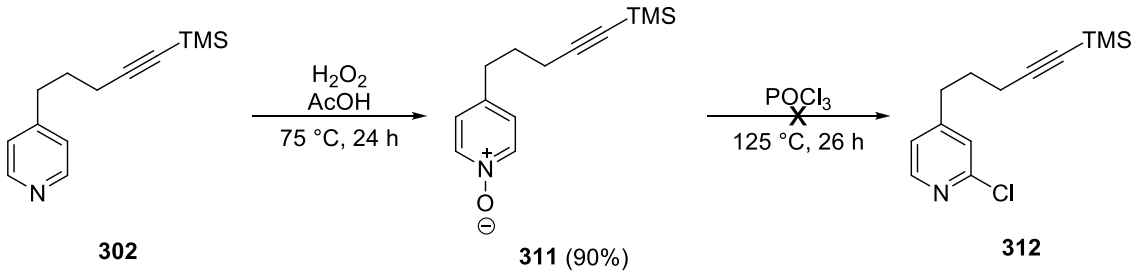

Scheme 94: Generation of N-oxim **311** and attempted chlorination.

5.3 Revised synthesis

Due to the previous difficulties the whole strategy was revised. At first a longer tether was chosen to increase the distance between the solid support and the catalyst. The TMS-protected iodine **315** could be generated in 35% yield over two steps *via* the same route as used to synthesize molecule **298** (Scheme 95).[124]

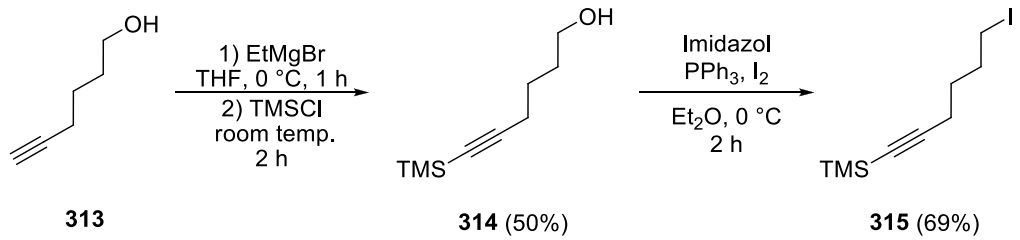

313 **314** (50%) **315** (69%)

Scheme 95. Synthesis of (6-iodohex-1-ynyl)trimethylsilane (**315**).

Second, bipyridine **316**, provided by Daniel Rackl, was used. He adapted a bipyridine synthesis by Grätzel *et al.*[125] and coupled 2-bromo-4-tert-butylpyridine (**310**) with a 4-methylpyridin-2-yl trifluoromethanesulfonate using $Pd(PPh_3)_4$ as catalyst.

Hence the tether could be introduced at a later stage of the synthesis. Ligand **317** was furnished with the help of LDA in 51% yield (Scheme 96).

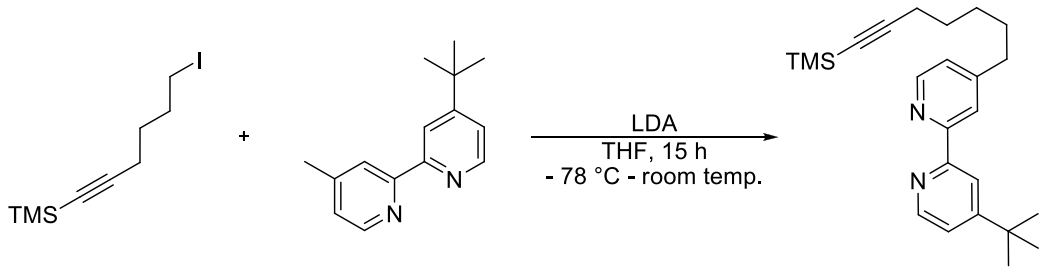

315 **316** **317** (51%)

Scheme 96. Synthesis of 4-tert-butyl-4'-(7-(trimethylsilyl)hept-6-ynyl)-2,2'-bipyridine (**317**).

In the next step the tether of **317** should be methylated in order to prevent charge transportation *via* it. To develop suitable reaction conditions before applying them to **317**, bipyridine **316** was chosen as model substrate. The best results were obtained when the methyl substituents were introduced in two separate steps including a chromatographic isolation in-between (Scheme 97). To introduce the first methyl group, ligand **316** was deprotonated with the help of 2 equiv. of LDA. Upon treatment with 6 equiv. of methyl iodine (MeI), 4-tert-butyl-4'-ethyl-2,2'-bipyridine (**318**) could be isolated in

79% yield. Subjecting **318** to a little bit harsher conditions by using 3 equiv. of LDA and 9 equiv. of methyl iodine furnished 4-tert-butyl-4'-isopropyl-2,2'-bipyridine (**319**) in 65% yield (Scheme 97).

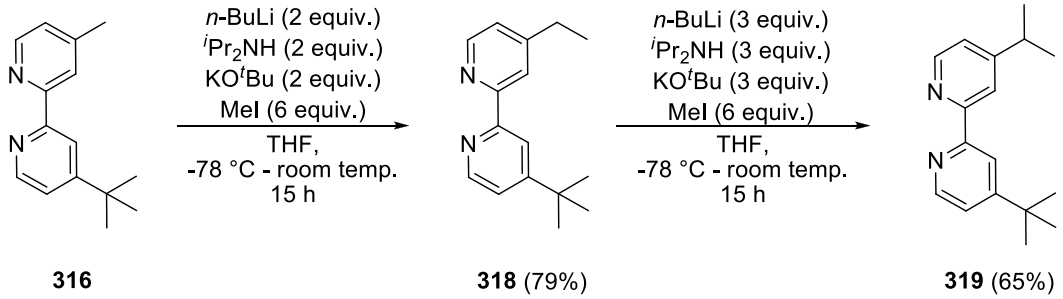

Scheme 97. Double methylation of bipyridine **316** yielding 4-tert-butyl-4'-isopropyl-2,2'-bipyridine (**319**).

Having obtained these satisfying results with model substrate **316** the same conditions were applied to ligand **317**. As depicted in Scheme 98, exposing molecule **317** to 3 equiv. of LDA and 9 equiv. of MeI subsequently resulted in the removal of the TMS group yielding 4-tert-butyl-4'-(hept-6-ynyl)-2,2'-bipyridine (**321**) in 86%.

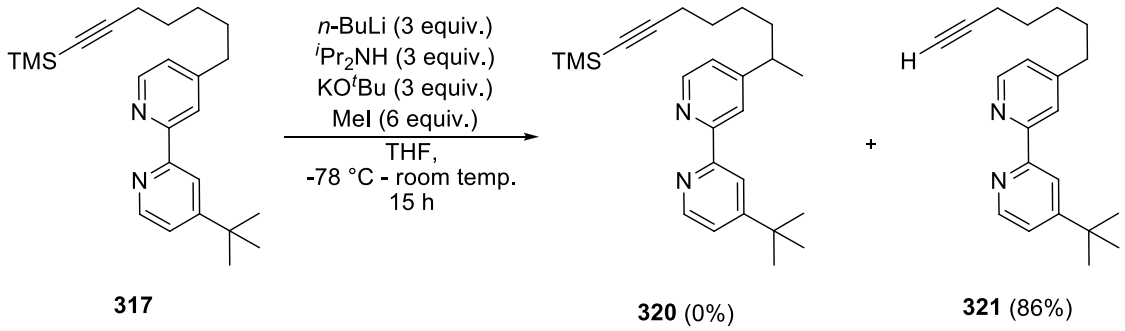

Scheme 98. Attempted methylation of bipyridine ligand **317**.

Also using only one equiv. of LDA and 3 equiv. of MeI did not lead to any formation of the desired product. Because of these results 4-tert-butyl-4'-(7-(trimethylsilyl)hept-6-ynyl)-2,2'-bipyridine (**317**) was directly used to prepare a tethered photoredoxcatalyst.

Refluxing bipyridine **317** in the presence of **294** gave rise to the TMS protected photocatalyst **322** in 79% yield (Scheme 99).[127]

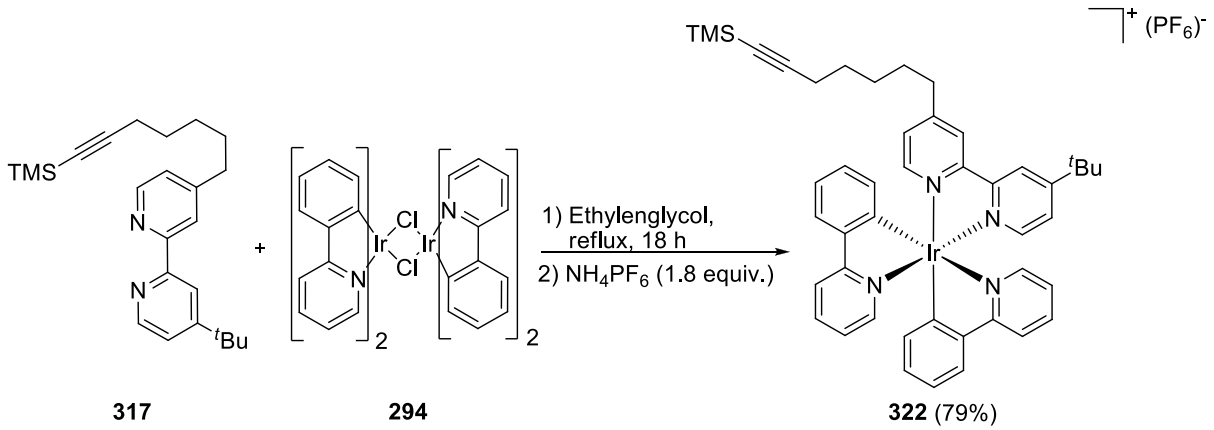

Scheme 99. Synthesis of photocatalyst **322**.

The photophysical properties of complex **322** were measured in order to evaluate if the tether had any influence and to determine its suitability as photocatalyst. As depicted in Figure 11 the absorbance spectra of complex **322** (red line) is nearly the same one as of $[Ir(ppy)_2(dtbbpy)]PF_6$ (**204**·PF_6) (black line), exhibiting the same local maxima .

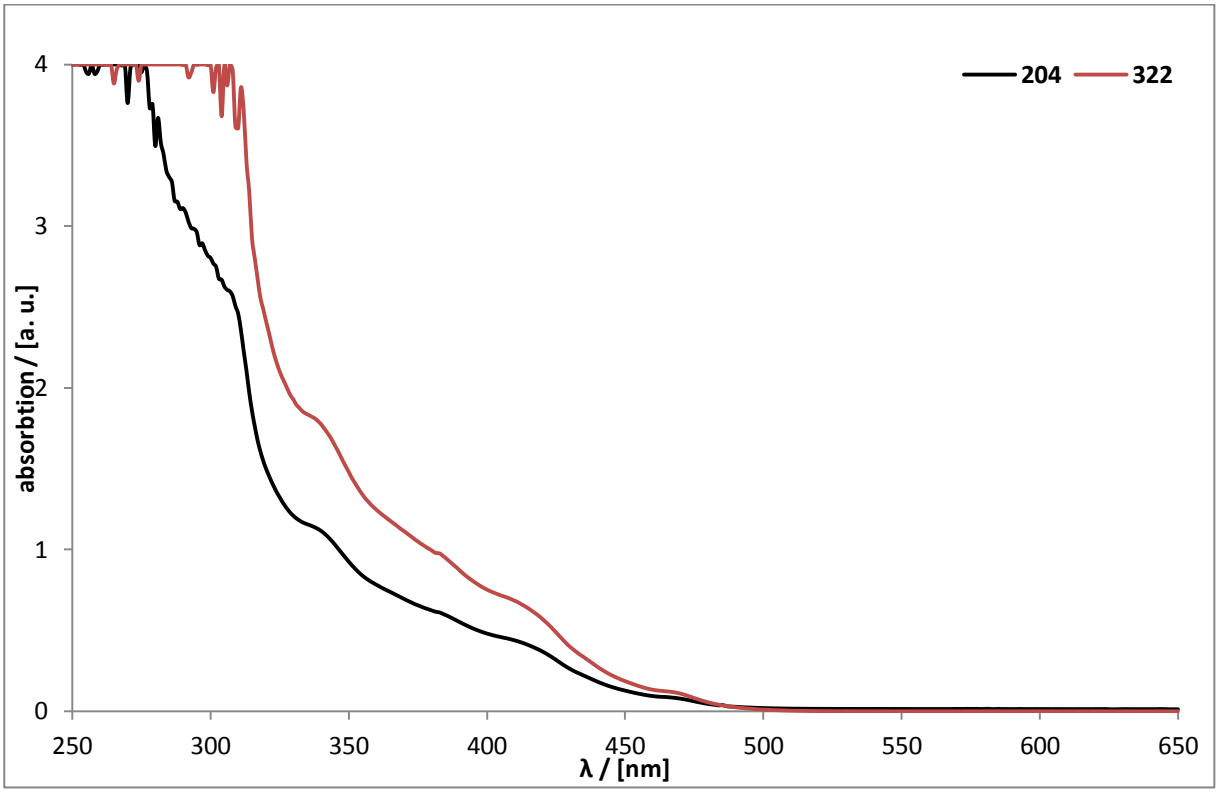

Figure 11. Absorption spectra of $[Ir(ppy)_2(dtbbpy)]PF_6$ (**204**·PF_6) and complex **322** in acetonitrile.

Also the reduction and oxidation potentials of **322** match the one of $[Ir(ppy)_2(dtbbpy)]PF_6$ (**204**·PF_6) (Table 24.).

Table 24. Redox potentials of $[Ir(ppy)_2(dtbbpy)]PF_6$ (**204**) and complex **322**.

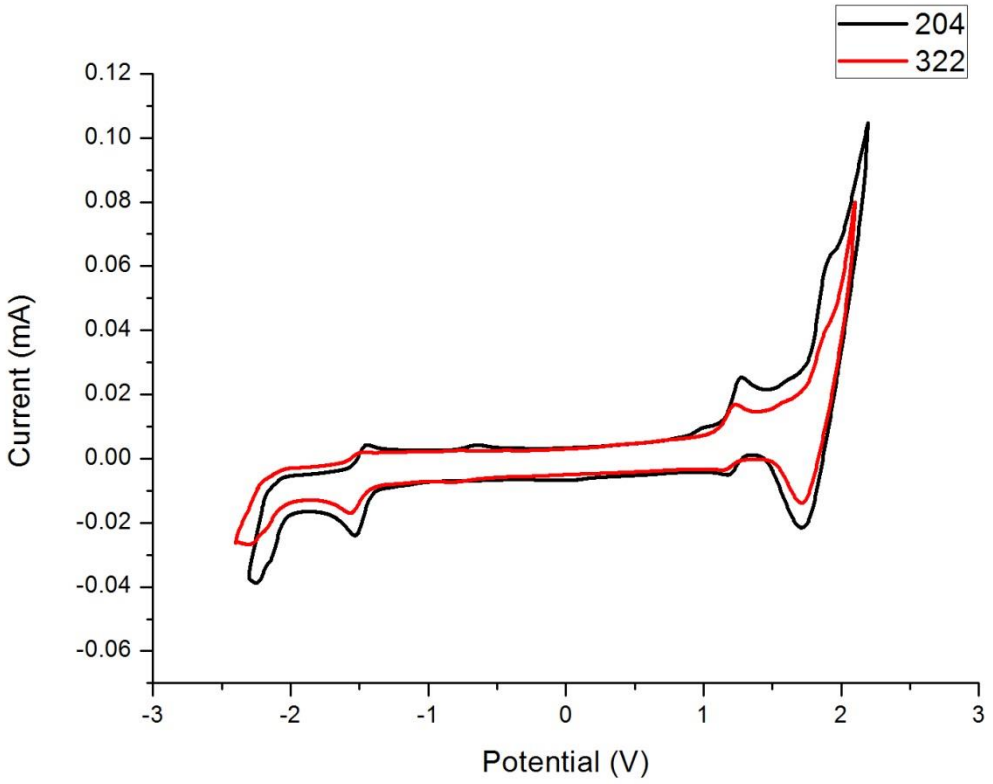

Potential[a)]	$[Ir(ppy)_2(dtbbpy)]^+$ (**204**) (literature)[86b)]	$[Ir(ppy)_2(dtbbpy)]^+$ (**204**) (measured)	complex **322** (measured)
$\mathbf{E_{1/2}(Ir^{III}/Ir^{II})}$	-1.51	-1.49 V	-1.53 V
$\mathbf{E_{1/2}(Ir^{IV}/Ir^{III})}$	1.21	1.26 V	1.25 V
$\mathbf{E_{1/2}(Ir^{V}/Ir^{IV})}$	-	1.74 V	1.67 V

[a)] Potentials recorded in acetonitrile. Ferrocene was used as internal standard. Values are given with respect to SCE. Scan rate: 0.05 V/s

As shown in Table 24 the recorded potentials of $[Ir(ppy)_2(dtbbpy)]PF_6$ (**204**·PF_6) match within a small margin the reported values in literature. Also the values of complex **322** are within this range. Therefore it can be concluded that the tether, even without a dimethyl group close to the pyridine moiety, has no influence on the redox properties.

Next complex **322** was treated with TBAF in order to remove the TMS group yielding photocatalyst **323** with a free alkyne moiety (Scheme 100).

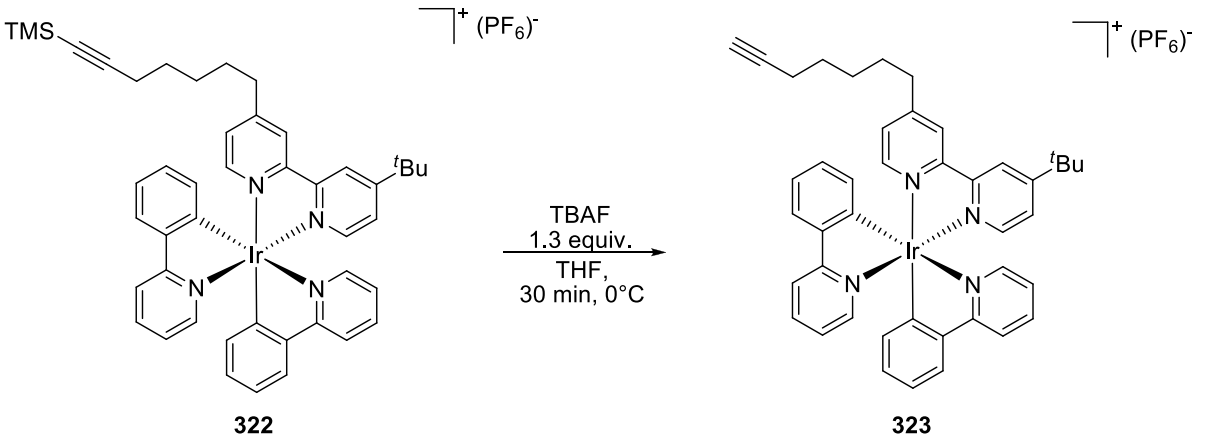

Scheme 100. Deprotection of complex **322** yielding alkyne bearing photocatalyst **323**.

The UV-Vis spectrum of complex **323** (red line) is also in good accordance with tether free complex **204** (black line) and both complexes exhibit their local maxima within close proximity (Figure 12).

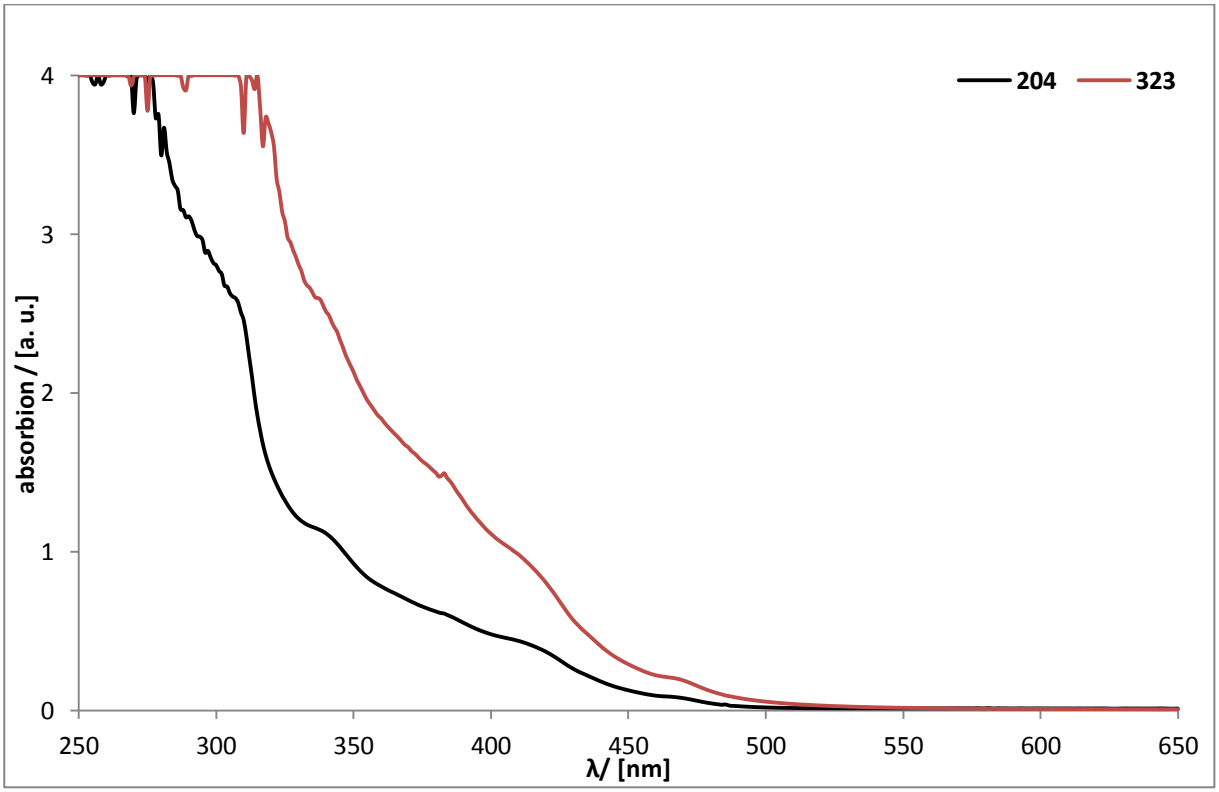

Figure 12. Absorption spectra of $[Ir(ppy)_2(dtbbpy)]PF_6$ (**204**·PF_6) and complex **323** in acetonitrile.

The reduction and oxidation peaks also match the ones recorded for $[Ir(ppy)_2(dtbbpy)]PF_6$ (**204**·PF_6) (Table 25.)

Table 25. Redox potentials and cyclic voltammogram of $[Ir(ppy)_2(dtbbpy)]PF_6$ (**204**·PF_6) and complex **323**.

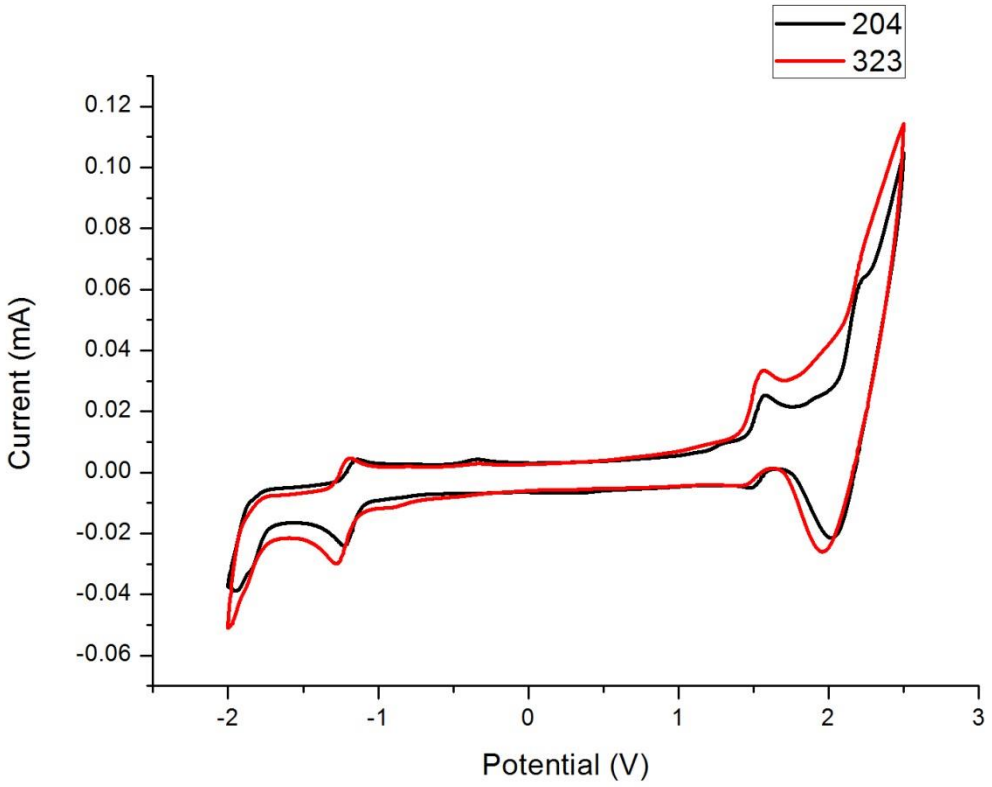

Potential[a)]	$[Ir(ppy)_2(dtbbpy)]^+$ (**204**) (measured)	complex **322** (measured)	complex **323** (measured)
$E_{1/2}(Ir^{III}/Ir^{II})$	-1.49 V	-1.53 V	-1.50 V
$E_{1/2}(Ir^{IV}/Ir^{III})$	1.26 V	1.25 V	1.29 V
$E_{1/2}(Ir^{V}/Ir^{IV})$	1.74 V	1.67 V	1.77 V

[a)] Potentials recorded in Acetonitrile. Ferrocene was used as internal standard. Values are given with respect to SCE. Scan rate: 0.05 V/s

As depicted in Table 25 photocatalyst **323** exhibits nearly the same redox values as the original catalyst **204**. The reduction potential is $E_{1/2}(Ir^{III}/Ir^{II})$ = -1.50V and the two oxidation peaks can be found at $E_{1/2}(Ir^{IV}/Ir^{III})$ = 1.29 V and $E_{1/2}(Ir^{V}/Ir^{IV})$ = 1.77 V.

In the next step a suitable solid support bearing an azide functionality was synthesized. A method provided by Adela Carillo, used for the synthesis of differently functionalized silica particles, was applied. At first azide **325** could be prepared in 53% yield starting from (3-chloropropyl)-triethoxysilane (**324**) according to a protocol published by Stack *et al.* (Scheme 101).

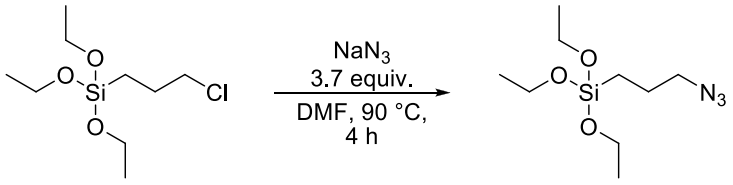

324 **325** (53%)

Scheme 101. Synthesis of (3-azidopropyl)triethoxysilane (**325**).[120]

In the next step, (3-azidopropyl)triethoxysilane (**325**) (1 equiv.) was dissolved with tetraethyl orthosilicate (TEOS) (5 equiv.) in water containing ammonia as base. After heating to 80 °C over night 890 mg of azide bearing silica particles (**326**) were obtained. The nitrogen content was analyzed by elemental analysis. An average value of 9.48% nitrogen was determined in three separate runs which corresponds to a loading of 2.26 mmol/g.

The silica particles were analyzed with the help of a phase contrast microscope. As depicted in Figure 13 the size of the particles was very heterogeneous. It ranges from 1 µm to more than 100 µm.

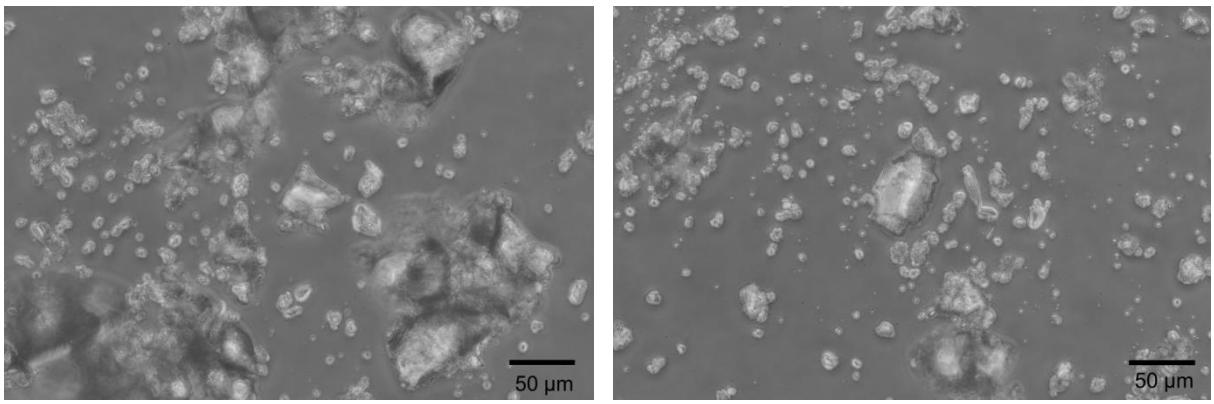

Figure 13. Azide functionalized silica particles (**326**).

These azide silica particles (**326**) were coupled with alkyne tethered photocatalyst **323** in a Huisgen cycloaddition (Scheme 102).[128]

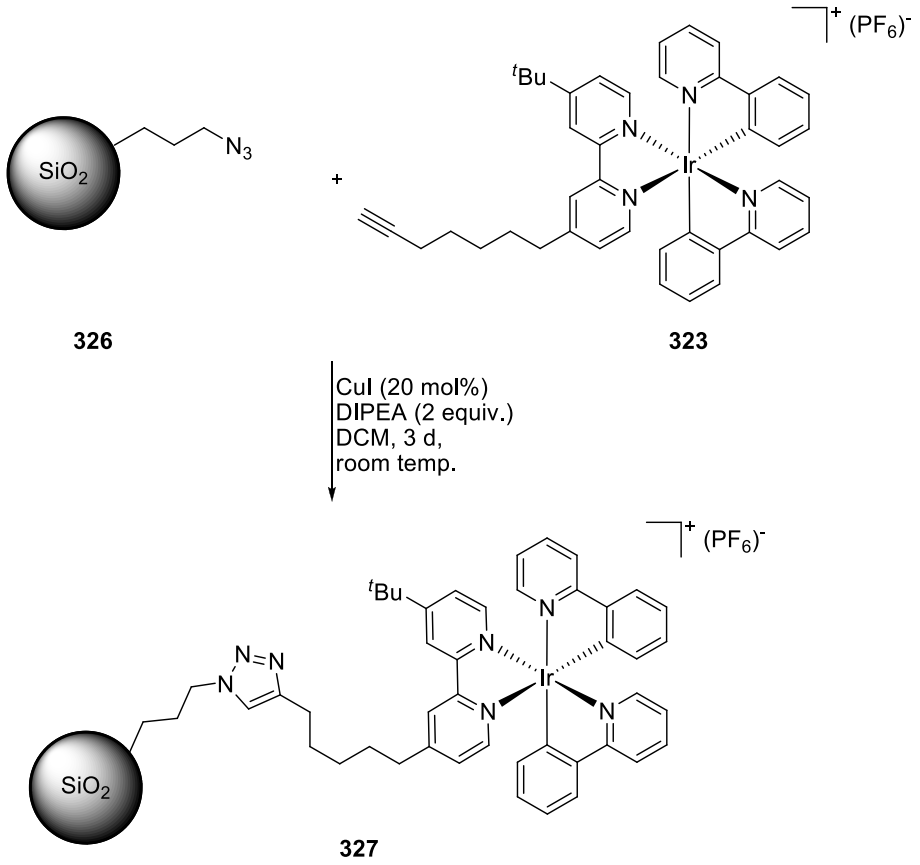

Scheme 102. Synthesis of immobilized photocatalyst **327**.

In a first experiment, one equivalent of photocatalyst **323** and two equiv. of azide particles **326** were used. Afterwards the particles were washed thoroughly with DCM. To determine the iridium content the particles were fully dissolved in aqua regia (3 mL, 64%) and analyzed by ICP-AAS measurements. An average value of 7.0 µmol/l was determined which corresponds to a catalyst loading of 35 µmol/g particles. In the following it will be referred to these as particles A.

In another experiment, equal molar amounts of photocatalyst **323** and azide particles **326** were used. Afterwards the particles were washed thoroughly with DCM. The iridium content was determined by totally dissolving the particles in aqua regia (3 mL, 64%) and analysis *via* ICP AAS. An average value of 5.6 µmol/l was found which corresponds to a catalyst loading of 18 µmol/g particles. In the following chapter it will be referred to these as particles B.

It is assumed, that azide **325** is equally distributed within the particle and therefore only a limited number of azide groups are present on the surface and utilizable for a Huisgen cycloaddition. As shown in Figure 13 the size of the particles is very heterogeneous. If we assume an average particle diameter of 10 µm, less than 1.5% of the azide groups are present on the surface. In the case of a total azide loading of 2.26 mmol/g this would correspond to 34 µmol/g. Therefore an obtained loading of 35 µmol/g and 18 µmol/g is within the expected range.

5.4 Application of Silica Bond Photoredox Catalyst

Having the silica particles with immobilized photocatalyst (**327**) in hand, the influence of unfunctionalized silica on photoreactions was investigated

The first reaction tested was the photocatalytic aza-Henry reaction developed by Stephenson *et al*. (Scheme 103).[52b] Using 0.3 mmol of **2a** yielded without silica 62% of 1-(nitromethyl)-2-phenyl-1,2,3,4-tetrahydroisoquinoline (**4a**) according to NMR analysis and with silica (50 mg) present in the reaction mixture 64% of **4a** were formed. Therefore silica has no influence on the reaction (Scheme 103).

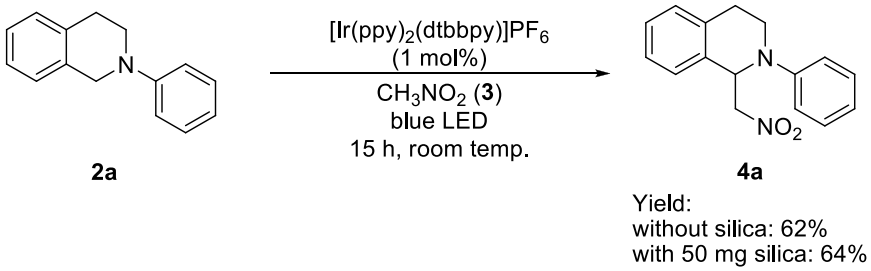

Scheme 103. Investigation of the influence on silica on photocatalytic aza Henry reactions.

Another reaction investigated was the photochemical deoxygenation of diphenylmethanol, converted to an oxalic ester. This reaction was developed by Viktor Kais who also provided substrate **328** (Scheme 104).

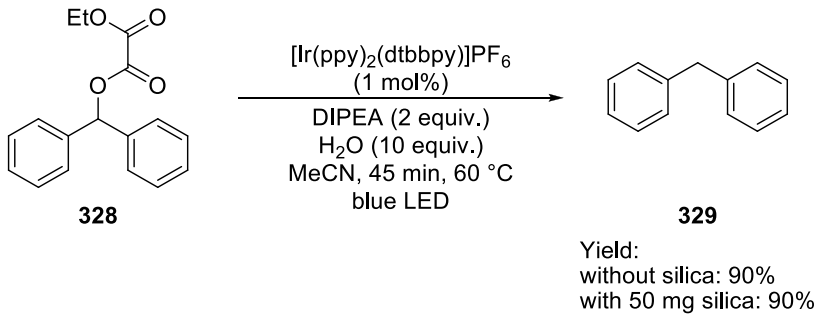

Scheme 104. Photocatalytic deoxygenation of oxalylic ester **328** in the presence of silica.

The decarboxylation was finished within 45 min at 60 °C yielding with and without silica 90% of **329**, determined by GC analysis when 0.2 mmol of **328** were used. Because of a low catalyst loading (1 mol%) and a short reaction time, this decarboxylation is a good choice to test the suitability and recyclability of the photocatalyst immobilized on silica.

For this reaction the particles with a catalyst loading of 35 µmol/g (particles A) were used. After analytic studies 16 mg of particles A were left, which corresponds to 0.55 µmol photocatalyst.

Table 26. Deoxygenation reaction and recycling studies with immobilized photoredoxcatalyst **327**.

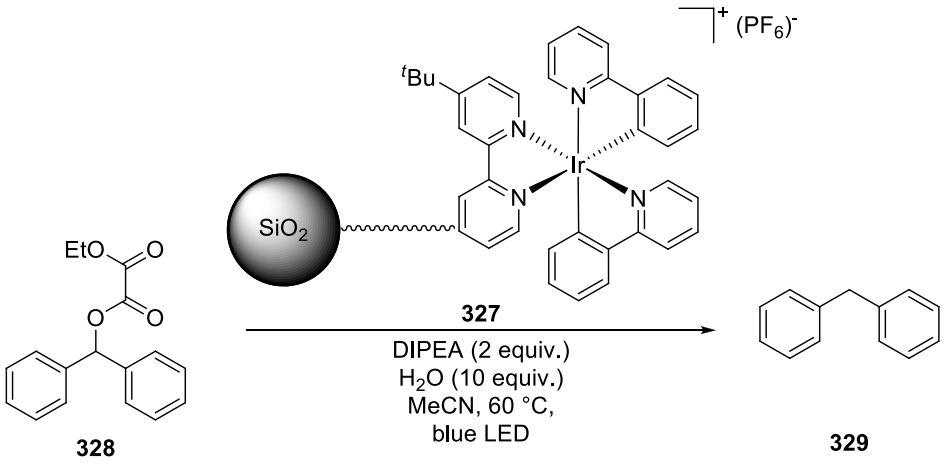

run	catalyst (mol%)	ester (mmol)	time	yield 329[a)]	catalyst recovered
1	0.5	0.11	1.5 h	0%	4 mg
2	0.1	0.14	1.5 h	48%	0 mg

[a)] Determined by GC, average of 3 measurements, naphthalene was used as internal standard.

Because of the efficiency of the reaction the amount of catalyst was bisected and the reaction time prolonged. In the first run 0.5 mol% of catalyst **327** were applied and the reaction was terminated after 1.5 h because no product formation could be detected by TLC. The same result was obtained *via* GC analysis. After filtration and washing with acetonitrile, 4 mg of silica bound catalyst **327** could be recovered. Due to the fact that the particles still had a bright yellow color, which is usually an indication for a sound photocatalyst, they were used once again.

For the second run only 0.1 mol% (4 mg) of catalyst **327** was used and within 1.5 h 48% of diphenylmethane (**329**) formed. No silica particles could be recovered after the reaction.

Surprisingly no product could be isolated in the first run but nearly 50% were obtained after the second run. With the help of these experiments the suitability of **327** as photocatalyst for deoxygenations could be proven but the recyclability was not good. That no yield was obtained in run 1 is most likely due some mistake that happened in the reaction set-up.

The loading of particles B was determined to be 18 µmol/g. After analysis, 25 mg of particles B were left which correlates to 0.45 µmol of photoredoxcatalyst. They were applied in the same deoxygenation reaction and the results are displayed in Table 27.

Table 27. Deoxygenation reaction and recycling studies with immobilized photoredoxcatalyst **327**.

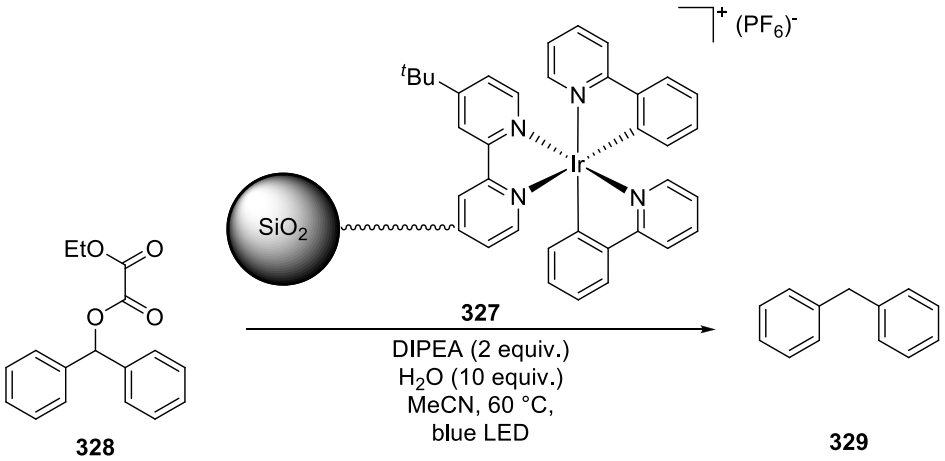

run	catalyst (mol%)	ester (mmol)	time	yield 329[a)]	catalyst recovered
1	0.1	0.45	4 h	92%	18 mg
2	0.1	0.32	4 h	29%	11 mg
3	0.1	0.2	22 h	15%	6 mg
4	0.1	0.1	22 h	0%	0 mg

[a)] Determined by GC, average of 3 measurements, naphthalene was used as internal standard.

For these reactions 0.1 mol% (25 mg) of catalyst were used and the reaction time was prolonged to 4 h. In the first run 25 mg of catalyst **327** were used and 92% of diphenylmethane (**329**) formed. After filtration and washing 18 mg (72%) of the silica particles, bearing a bright yellow color, could be recovered, which were used for the next run. In the next experiment using 18 mg of **327** only 29% product formed within 4 h and 11 mg (61%) catalyst could be recycled. Therefore, for the next run, the reaction time was extended to 22 h. Within this time 15% of **329** formed and 6 mg (55%) of photocatalyst **327** could be recovered. The recovered particles at this stage already had a brownish yellow color indicating that the catalyst on the particles is partly decomposed. Using these 6 mg of catalyst for another deoxygenation did not furnish any product within 22 h and no catalyst could be recovered after the reaction.

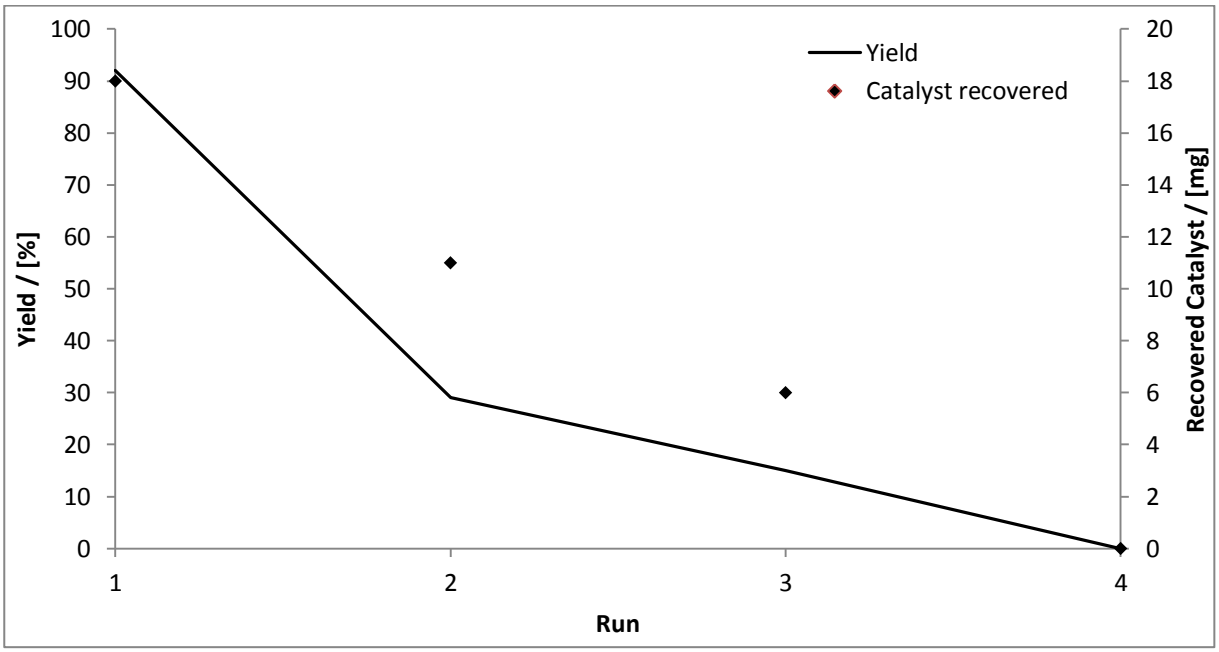

Figure 14. Product formation and recovered catalyst of deoxygenation reaction with immobilized photoredox catalyst **327**.

With the help of these experiments it could be shown that an immobilized photoredox catalyst can be synthesized *via* this route and that it is active in deoxygenation reactions with moderate recyclability.

6. References

[51] Kohls, P. Carbon – Carbon Bond Formation by Photocatalytic Conjugate Addition with Visible Light *Master Thesis*, University of Regensburg, **2010**.

[52] a) Li, C-J. *Acc. Chem. Res.* **2009**, *42*, 335; b) Condie, A. G.; González-Gómez, J. C.; Stephenson, C. J. R. *J. Am. Chem. Soc.* **2010**, *132*, 1464; c) Rueping, M.; Vila, C.; Koenigs, R. M.; Poscharny, K.; Fabry, D. C. *Chem. Commun.* **2011**, 47, 2360.

[53] Rueping M.; Vila, C.; Koenigs, R. M.; Poscharny K.; Fabryet D. C. *Chem. Commun.* **2010**, *46*, 2360.

[54] Dondi, D.; Fagnoni, M.; Albini, A. *Chem. Eur. J.* **2006**, *12*, 4153.

[55] a) Pirtsch, M.; Paria, S.; Matsuno, T.; Isobe, H.; Reiser, O. *Chem. Eur. J.* **2012**, *18*, 7336. b) Paria, S.; Pirtsch, M.; Kais, V.; Reiser O. *Synthesis* **2013**, *45*, 2689.

[56] a) Schultz, D. M.; Yoon, T. P. *Science* **2014**, *343*, 958; b) Prier, C. K.; Rankic, D. A.; Macmillan D. W. C. *Chem. Rev.* **2013**, 113, 5322; c) Narayanam, J. M. R.; Stephenson, C. R. J. *Chem. Soc. Rev.* **2011**, *40*, 102.

[57] Streb, C.; Kastner, K.; Tucher, J. Polyoxometalates in photocatalysis. In *Chemical Photocatalysis* König B. Ed.; Walter de Gruyter: Berlin, Boston, **2013,** 247.

[58] Tanielian, C. *Coord. Chem. Rev.* **1998**, *178*, 1165.

[59] Filowitz, M.; Ho, R. K. C.; Klemperer, W. G.; Shum, W. *Inorg. Chem.* **1979**, *18*, 93.

[60] Yamase, T.; Takabayashi, N.; Kaji, M. *J. Chem. Soc. Dalton Trans.* **1984**, 793.

[61] Dondi, D.; Fagnoni, M.; Molinari, A.; Maldotti, A.; Albini, A. *Chem. Eur. J.* **2004**, *10*, 142.

[62] Esposti, S.; Dondi, D.; Fagnoni, M.; Albini A. *Angew. Chem. Int. Ed.* **2007**, *46*, 2531.

[63] Angioni, S.; Ravelli, D.; Emma, D.; Dondi, D.; Fagnoni, M.; Albini, A. *Adv. Synth. Catal.* **2008** , *350*, 2209.

[64] Ravelli, D.; Albini, A.; Fagnoni M. *Chem. Eur. J.* **2011**, *17*, 572.

[65] Kern, J. M.; Sauvage, J. P. *J. Chem. Soc. Chem. Commun.* **1987**, 546.

[66] Kalyanasundaram, K. *Coord. Chem. Rev*, **1982**, *46*, 159.

[67] Paria, S.; Reiser, O. *ChemCatChem* **2014**, *6*, 2477.

[68] Slinker, J. D.; Gorodetsky, A. A.; Lowry, M. S.; Wang, J.; Parker, S.; Rohl, R.; Bernhard, S.; Malliaras G. G. *J. Am. Chem. Soc.* **2004**, *126*, 2763.

[69] Nagib, D. A.; Scott, M. E.; MacMillan, D. W. C. *J. Am. Chem. Soc.* **2009**, *131*, 10875.

[70] Kwong, F. A.; Klapars, A.; Buchwald, S. L. *Org. Lett.* **2002**, 4, 581.

[71] Neumann, M.; Zeitler, K. *Org. Lett.* **2012**, *14*, 2658.

[72] Lowry, M. S.; Goldsmith, J. I.; Slinker, J. D.; Rohl, R.; Pascal, R.A.; Malliaras, G. G.; Bernhard S. *Chem. Mater.* **2005**, *17*, 5712.

[73] Nguyen, J. D.; Tucker, J. W.; Konieczynska, M. D.; Stephenson, C. R. J. *J. Am. Chem. Soc.* **2011**, *133*, 4160.

[74] Ischay, M. A.; Anzovino, M. E.; Du, J.; Yoon, T. P. *J. Am. Chem. Soc.* **2008,** *130*, 12886.

[75] Kohls, P.; Jadhav, D.; Pandey G.; Reiser O. *Org. Lett.* **2012**, *14*, 672.

[76] McNally, A.; Prier, C. K.; MacMillan, D. W. C. *Science*, **2011**, *334*, 1114.

[77] Hari, D. P.; König, B. *Org. Lett.* **2011**, *13*, 3852.

[78] Miyake, Y.; Nakajima, K.; Nishibayashi Y. *J. Am. Chem. Soc.* **2012**, *134*, 3338.

[79] Ruiz Espelt, L.; Wiensch, E. M.; Yoon T. P. *J. Org. Chem.* **2013**, *78*, 4107.

[80] Shi, L.; Xia, W. *Chem. Soc. Rev.* **2012**, *41*, 7687.

[81] Xie, J.; Jin, H.; Xu, P.; Zhu C. *Tetrahedron Lett.* **2014**, *55*, 36.

[82] a) Kleinman, E. D. In *Comprehensi V e Organic Synthesis*; Trost, B. M., Ed.; Pergamon: Oxford, **1991**; *Vol. 2*, 893; b) Arend, M.; Westermann, B.; Risch, N. *Angew. Chem., Int. Ed.* **1998**, *37*, 1045; c) Royer, J.; Bonin, M.; Micouin, L. *Chem. Rev.* **2004**, *104*, 2311.

[83] Catino, A. J.; Nichols, J. M.; Nettles, B. J.; Doyle. M. P. *J. Am. Chem. Soc.*, **2006**, *128*, 5648.

[84] Seitz, M.; Reiser, O. *Curr. Opin. Cell. Biol.* **2005**, *9*, 285.

[85] Rosso, G. B.; Pilli, R. A., *Tetrahedron Lett.*, **2006**, *47*, 185.

[86] a) Lowry, M. S.; Goldsmith, J. I.; Slinker, J. D.; Rohl, R.; Pascal, R.A.; Malliaras, G. G.; Bernhard S. *Chem. Mater.* **2005**, *17*, 5712; b) Campagna S.; Puntoriero F.; Nastasi F.; Bergamini G.; Balzani V. *Top. Curr. Chem*. **2007**, *280*, 117.·

[87] Ischay, I. A.; Lu, Z.; Yoon, T. P. *J. Am. Chem. Soc.* **2010**, *132*, 8572.

[88] Mann, Ch. K.; Barnes, K. K. *Electrochemical Reactions in Nonaqueous Systems*; Marcel Dekker: New York, NY, **1970**.

[89] Shirota, H.; Pal, H.; Tominaga, K.; Yoshihara K. *J. Phys. Chem. A* **1998**, *102*, 3089.

[90] Boeckman, R. K.; Pero, J. E.; Boehmler, D. J. *J. Am. Chem. Soc.* **2006**, *128*, 11032.

[91] Curti, C.; Battistini, L.; Zanardi, F.; Rassu, G.; Zambrano, V.; Pinna L.; Casiraghi G. *J. Org. Chem.* **2010**, *75*, 8681.

[92] Kocienski, P. J. *Portectiong Groups;* Enders D.; Noyori R.; Trost, B. M. (Eds.) Georg Thieme Verlag, Stuttgart, **1994**.

[93] Freeman, D. B.; Furst, L.; Condie, A. G.; Stephenson C. R. J *Org. Lett.* **2012**, *14*, 94.

[94] Ahmad, V. U.; Iqbal, S. *Phytochemistry* **1993**, *34*, 735.

[95] Rao, K. V. J.; Rao, L. R. C. *J. Sci. Ind. Res.* **1981**, *20B*, 125.

[96] Ahmad, V. U.; Rahman, A.; Rasheed, T.; Rehman, H. *Heterocycles* **1987**, *26*, 1251.

[97] Padwa, A.; Danca, M. D. *Org. Lett.* **2002**, *4*, 715.

[98] Simpkins N. S.; Gill C. D. *Org. Lett.* **2003**, *5,* 535.

[99] Hari, D. P.; König, B. *Org. Lett.* **2011**, *13*, 3852.

[100] Dominguez, B.; Iglesias, B.; de Lera A. R. *J. Org. Chem.* **1998**, *63*, 4135.

[101] Gallen M. J.; Williams C. M. *Org. Lett.*, **2008**, *10*, 713.

[102] Hughes, G.; Kimura, M.; Buchwald S. L. *J. Am. Chem. Soc.*, **2003**, *125*, 11253.

[103] Zhang, Y.; Li, C. J. *Angew. Chem*. *Int. Ed.* **2006**, *45*, 1949.

[104] Li, Z; Bohle D. S.; Li, C. J. *Proc. Nat. Ac. Sci*, **2006**, *103*, 8928.

[105] Zou, Y. Q.; Lu, L. Q.; Fu, L.; Chang, N. J.; Rong, J.; Chen, R. J.; Xiao W. J.; *Angew. Chem. Int. Ed.* **2011**, *50*, 7171.

[106] Producer: Aurora Fine Chemicals LtD, Austria (http://www.aurorafinechemicals.com).

[107] Bellale, E. V.; Bhalerao,D. S.; Akamanchi K. G. *J. Org. Chem.* **2008**, *73,* 9473.

[108] Brocksom, T. J.; Coelho, F.; Deprés, J.-P.; Greene, A. E.; Freire de Lima, M. E.; Hamelin, O.; Hartmann, B.; Kanazawa, A. M.; Wang Y. *J. Am. Chem. Soc.* **2002**, *124*, 15313.

[109] Rueping, M.; Leonori D.; Poisson, T. *Chem. Commun.* **2011**, *47*, 9615.

[110] a) Kalidindi, S.; Jeong, J. W.; Schall, A.; Bandichhor, R.; Nosse, B.; Reiser O. *Angew. Chem. Int. Ed.* **2007**, *46*, 6361; b) Harrar, K.; Reiser, O. *Chem. Commun.* **2012**, *48*, 3457. c) Berlicki, L.; Pilsl, L.; Weber, E.; Mandity, I. M.; Cabrele, C.; Martinke, T. A.; Fülöp, F.; Reiser O. *Angew. Chem. Int. Ed.* **2012**, *51*, 2208; d) Koglin, N.; Zorn, C.; Beumer,R.; Cabrele, C.; Bubert, C.; Sewald, N.; Reiser, O.; Beck-Sickinger, A. G. *Angew. Chem. Int. Ed.* **2003**, *42*, 202.

[111] Pilsl, L. *Enantioselective cyclopropanation of heterocycles and the use of high-pressure techniques for the conformational analysis of peptide foldamers.* Dissertation, University of Regensburg, **2014**.

[112] a) Evans, D. H.; O'Connell, K. M.; Petersen, R. A.; Kelly, M. J. *J. Chem. Ed.* **1983**, *60*, 290; b) Heinze, J. *Angew. Chem. Int. Ed.* **1984**, *23*, 831.

[113] Pavlishchuk, V. V.; Addison, A. W. *Inorg. Chim. Acta*, **2000**, *298*, 97–102.

[114] Haga, M.; Dodsworth,E. S.; Eryavec, G.; Seymour, P.; Lever, A. B. P. *Inorg. Chem.* **1985**, *24*, 1901.

[115] Paria, S.; Reiser, O. *Adv. Synth. Catal.* **2014**, *356*, 557.

[116] Gheorghe, A.; Schulte, M.; Reiser, O. *J. Org. Chem.* **2006**, *71*, 2173.

[117] Yagyu, T.; Tonami, M.; Tsuchimoto, K.; Takahashi, C.; Jitsukawa K. *Inorg. Chim. Acta* **2012** *392* 428.

[118] Sun, J.-Y.; Qiu, X.-L.; Meng, W.-D.; Qing, F.-L. *Tetrahedron* **2006**, *62*, 8702.

[119] Stöber, W.; Fink, A.; Bohn, E. *J. Colloid and Interface Sci.*, **1968**, *26*, 62.

[120] Nakazawa, J.; Smith, B. J.; Stack, T. D. P. *J. Am. Chem. Soc.*, 2012, 134, 2750.

[121] Rau, S.; Pfeffer, M. G.; Stähle, R. Metal complexes for photohydrogenation and hydrogen evolution. In *Chemical Photocatalysis* König B. Ed.; Walter de Gruyter: Berlin, Boston, **2013**, 185.

[122] You, Y.; Nam, W. *Chem. Soc. Rev.* **2012**, *41*, 7061.

[123] Overman, E. L.; Brown, M. J.; McCann, S. F. Organic Syntheses 1990, 68, 182.

[124] Bräse, S.; Wertel, H.; Frank, D.; Vidocić, D.; de Meijere, A. *Eur. J. Org. Chem.***2005**, *19*, 4167.

[125] Barolo, C.; Nazeeruddin, M. K.; Fantacci, S.; di Censo, D., Comte, P.; Liska, P.; Viscardi, G.; Quagliotto, P.; de Angelis, F.; Ito, S.; Grätzel, M. *Inorg. Chem.* **2006**, *45*, 4642.

[126] Duric, S.; Tzschucke, C. C. *Organic Letters* **2011**, *13*, 2310.

[127] Sprouse, S.; King, K. A.; Spellane, P. J.; Watts, J. R. *J Am. Chem. Soc.***1984**, *106*, 6647.

[128] Huisgen, R. *Proc. Chem. Soc.*, **1961**, 357.

C. Summary / Zusammenfassung

1. Summary

The presented work deals with visible light photoredox catalysis. Different reactions, e. g. photocatalytic conjugate additions and oxidative Mannich reactions were investigated and an immobilizable photoredox catalyst was developed.

In the first project pursued during this thesis, the yield and scope of a photocatalytic conjugate addition, developed pervious by Deepak Jadhav and me, was increased (Scheme 105). The influence of different additives, new photoredox catalysts as well as new amine species on the reaction was investigated. Besides irradiation of the solution in snap cap vials, the reaction was also performed using a mircoreactor system.

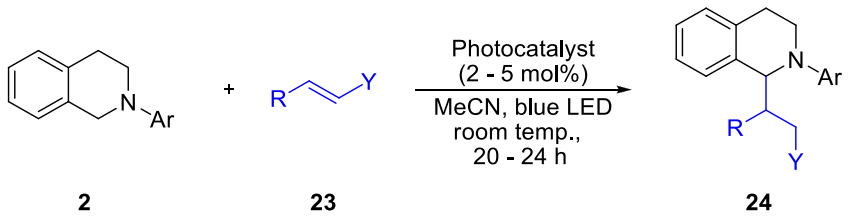

2 **23** **24**

Scheme 105. Photocatalytic N-α-functionalization.

In order to facilitate the deprotonation step of the radical cation to an *N*-α-radical (*cf.* Chapter 1.8, Scheme 62) different bases were added to the reaction mixture. However, none of these bases could enhance the yield. The ampholyte water was tolerated in the reaction mixture in up to 5% (v/v), whereas higher concentrations of water decreased the yield and therefore no positive influence on the reaction could be observed. The yield of the coupling of phenylpyrrolidine (**212**) and methyl vinyl ketone (**23a**) was increased moderately by the addition of caesium fluoride (1 equiv.) and isopropyl alcohol (10 equiv.) in combination with the catalyst $Ru(bpy)_3Cl_2$ (**1**·Cl_2). By addition of these two additives the yield was only slightly improved and therefore this path was no longer pursuit.
Tetrabutylammonium decatungstate (TBADT, **190**), $Cu(dap)_2Cl$ (**195**), $[Ir(ppy)_2(dtbbpy)]PF_6$ (**204**·PF_6) and $[Ir\{dF(CF_3)ppy\}_2(dtbbpy)]PF_6$ (**216**·PF_6) were tested as novel photoredox catalysts for the *N*-α-activation of *tert.* amines. The first two catalysts, **190** and **195**, could not drive the reaction forward at all. The latter two, **204** and **216**, were successfully used in this reaction. Catalyst **204** and **216** let to comparable results. However, **216** is more complex to prepare and more expensive, therefore no further experiments using this catalyst were performed. Depending on the substrate either

$Ru(bpy)_3Cl_2$ (**1**·Cl_2) or $[Ir(ppy)_2(dtbbpy)]PF_6$ (**204**·PF_6) proofed to be the best catalyst. The best obtained yields using each catalyst are displayed in Table 28.[129]

Table 28. Comparison of the best results obtained using $Ru(bpy)_3Cl_2$ (**1**·Cl_2) and $[Ir(ppy)_2(dtbbpy)]PF_6$ (**204**·PF_6)

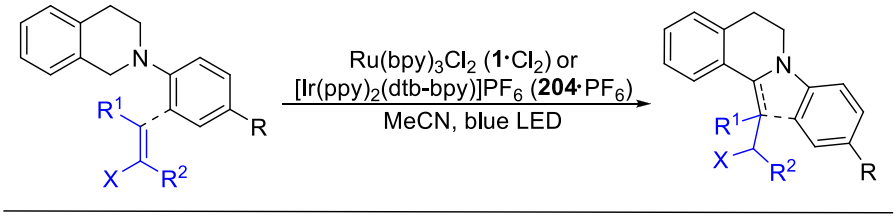

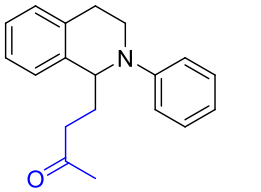

24a:
Cat **1**: 58%
Cat **204**: 68%

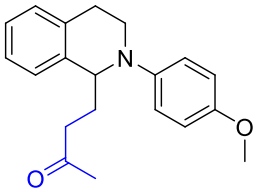

24b:
Cat **1**: 63%
Cat **204**: 37%

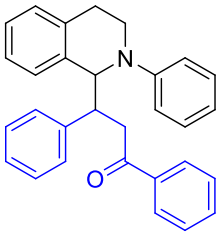

24c:
Cat **1**: 61%
Cat **204**: 83%

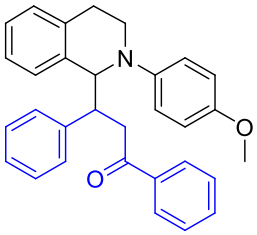

24d:
Cat **1**: 43%
Cat **204**: 33%

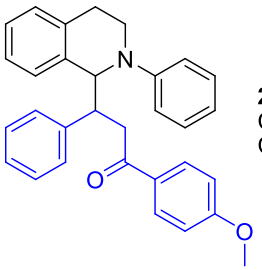

24e:
Cat **1**: 56%
Cat **204**: 93%

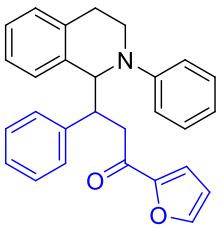

24f:
Cat **1**: 53%
Cat **204**: 66%

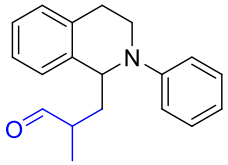

24g:
Cat **1**: 50%
Cat **204**: 50%

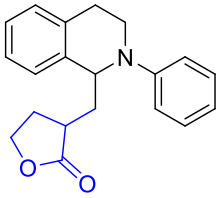

24h:
Cat **1**: 31%
Cat **204**: 33%

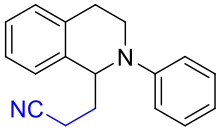

24i:
Cat **1**: 27%
Cat **204**: 31%

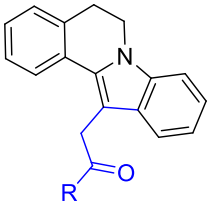

28a (R = Me):
Cat **1**: 28%
Cat **204**: 14%

28b (R = Ph):
Cat **1**: 35%
Cat **204**: 18%

The yield decreased when catalyst **204** was employed instead of **1** for the coupling of isoquinoline derivatives apart from 2-phenyl-1,2,3,4-tetrahydroisoquinoline (**2a**) with enones **23** (*cf.* Table 28 **24b**, **24d**, **28a**, **28b**). Using **204** for the reaction of **2a** with aliphatic enones or nitriles, the yields stay the same or increase slightly (*cf.* Table 28, **24a, 24c, 24g, 24h, 24i**). To our delight, a moderate to great

increase in product formation was observed for catalyst **204** in combination with chalcone derivatives (*cf.* Table 28, **24c**, **24e**, **24f**). In one case the yield could be boosted from 56% using $Ru(bpy)_3Cl_2$ (**1**·Cl_2) to 93% using $[Ir(ppy)_2(dtbbpy)]PF_6$ (**204**·PF_6) (*cf.* Table 28, **24e**).

The substrate dependency of the catalysts can be explained by the different redox potentials of **1** and **204**. **204** has a lower initial oxidation potential, therefore the oxidation of the isoquinoline to a radical cation is less feasible. On the other hand it has a greater reduction potential, improving the reduction of the α-carbonyl radical to an anion.

Two aniline derivatives, **208** and **212**, could be identified as suitable substrates for this coupling but the yields stayed low, even when the reaction was conducted in a micro reactor system. For both of them **204** proofed to be the best catalyst.

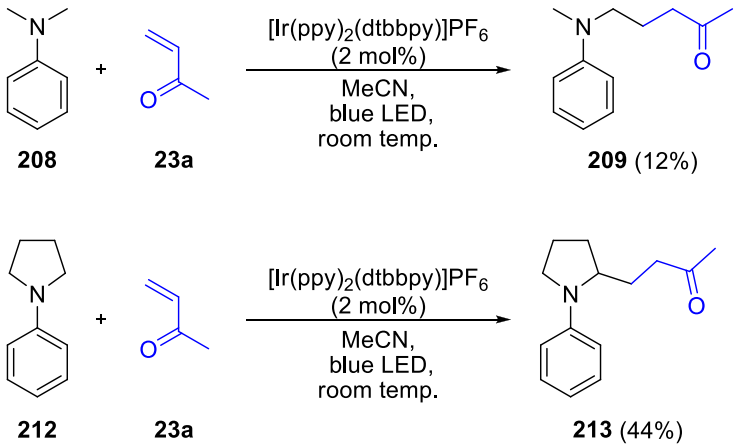

Scheme 106. Photocatalytic conjugate addition using aniline derivatives.

In conclusion we were able to further enhance yield and scope of this unprecedented photocatalytic *N*-α-activation of *tert.* amines and their coupling to Michael acceptors. The yields were in a moderate to good range using 2-phenyl-tetrahydroisoquinoline (**2a**) but decreased when other *tert.* amines were applied.

In the second project a photocatalytic way to functionalize γ-butyrolactones was investigated and established. This work was based on an oxidative Mannich reaction developed by Doyle *et al.* who used a rhodium catalyst to drive this reaction forward.[130] Different silyl ethers were tested for their suitability in this novel photoreaction. TBS-protected furan **238** proofed to be best. Up to 28% yield where obtainable when TBS-furan (**238**, 1 equiv.), trimethylaniline (**234**, 2. equiv) and $[Ir(ppy)_2(dtbbpy)]PF_6$ (**204**·PF_6, 5 mol%) as photoredoxcatalyst were mixed and irradiated without degassing in a micro reactor at a pumping rate of 0.66 mL/h which correlates to a retention time of 2 h 40 min.

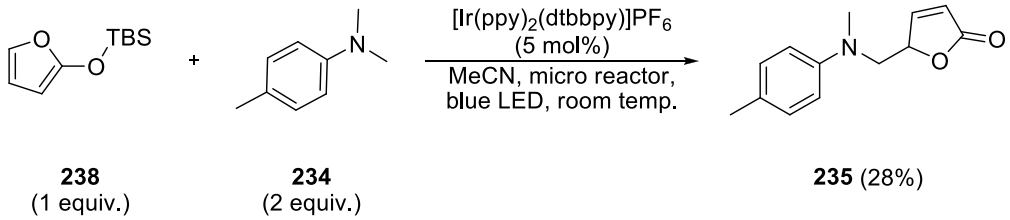

Scheme 107. Photocatalytic Vinylogous Mannich Reaction silyl ether **238** and aniline **234**.

Stephenson et al. published a very similar approach regarding the same class of substrates right after these promising first results;[131] therefore this topic was not further pursued. In contrast to the method developed by Stephenson *et al.* and the rhodium catalyzed reaction developed by Doyle *et al*. our approach does not need a sacrificial electron donor or acceptor apart from ubiquitous oxygen, making this process very environmentally begin.

As third project it was intended to develop a total synthesis for the natural product jamtine (**239**) involving a photocatalytic key step.

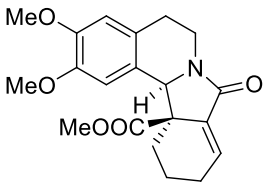

239

Figure 15. Structure of jamtine.

Retrosynthetic analysis led to the conclusion that the coupling of a β-ketoester to an isoquinoline derivative seemed most promising. However, no method could be found to oxidatively couple those two to yield an intermediate for the synthesis of jamtine, neither under photocatalytic condition nor under non photocatalytic conditions (Scheme 108 A).

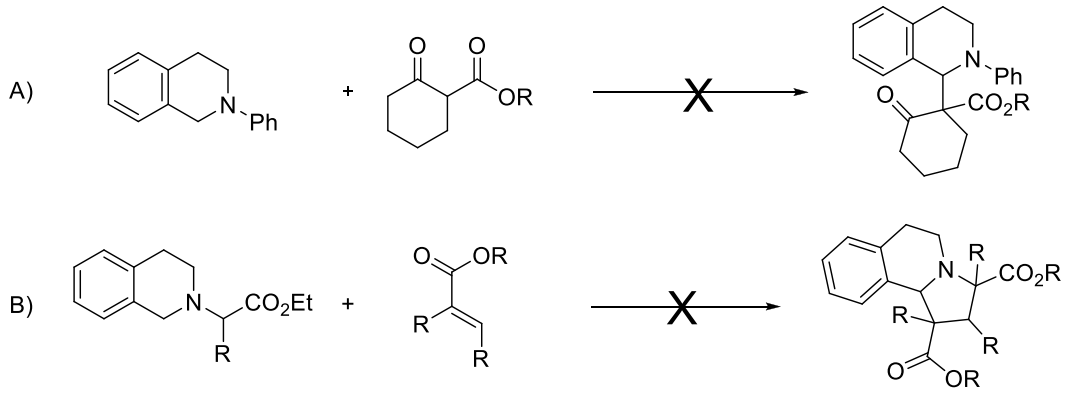

Scheme 108. Envisioned photocatalytic key steps for the synthesis of jamtine (**239**).

Also revising the strategy to [3+2] photocycloadditions using either Xiao´s[132] or Rueping´s[133] conditions did not succeed (Scheme 108 B).Therefore no novel synthesis for jamtine (**239**) could be developed. Most likely steric hindrances and the formation of quaternary carbon centers are the reason for the failure of reaction type A) and B). Further considerations to synthesize jamtine let to longer reaction sequences. Because Simpkins *et al.* were already able to furnish this natural product enantio-selectively in six steps, no more efforts were made to synthesize jamtine.[134]

In the fourth project presented in this thesis a photocatalytic method to open pyrrole derived cyclopropane **273** and functionalize it with methyl vinyl ketone (**23a**) in an unprecedented way was developed (Scheme 109). However, currently only one example of this transformation is known. Further substrates have to be discovered.

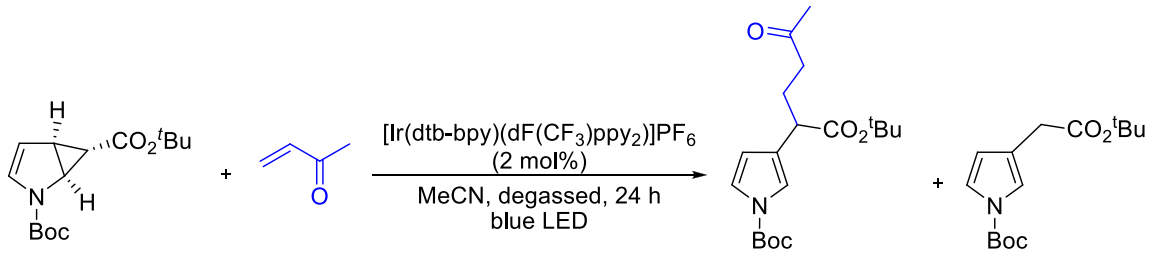

273 (1 equiv.) **23a** (3 equiv.) **276** (27%) **277** (49%)

Scheme 109. Photocatalytic cyclopropane opening and functionalization.

The best results were obtained by addition of three equivalents of MVK (**23a**) and [Ir{dF(CF_3)ppy}$_2$(dtbbpy)]PF_6 (**216**·PF_6, 2 mol%) as photocatalyst in dry MeCN yielding up to 27% of branched product **199** and 47% of open cyclopropane **200** (Scheme 109).

As final project a photoredox catalyst based on $[Ir(ppy)_2(dtbbpy)]PF_6$ (**204**·PF_6) that was immobilized on silica particles was developed. Ligand **317** was synthesized in 3 steps with an overall yield of 18% and complex **322** was furnished in 79% yield subsequently (Scheme 110).

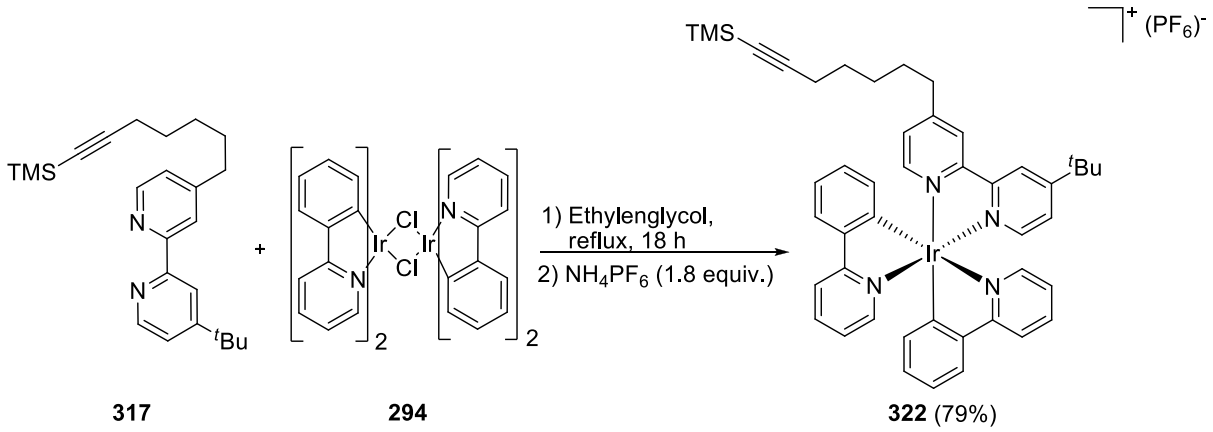

Scheme 110. Synthesis of photocatalyst **322**.

Catalyst **322** as well as the deprotected one exhibited nearly the same photophysical as well as electrochemical properties as unfunctionalized $[Ir(ppy)_2(dtbbpy)]PF_6$ (**204**·PF_6). After deprotection with TBAF, the catalyst was coupled with azide functionalized silica particles in a Huisgen cycloaddition yielding complex **327** (Figure 16). The highest obtained catalyst loading on the particles was 35 µmol/g.

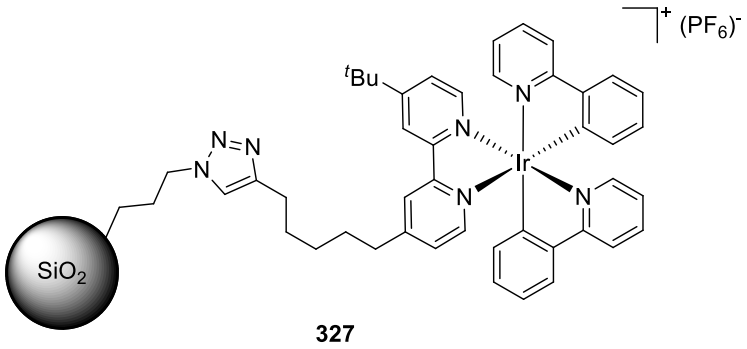

Figure 16. Photoredox catalyst immobilized on silica particles.

The immobilized catalyst was employed in the photochemical deoxygenation of diphenylmethanol, converted to an oxalic ester. This reaction, developed by Reiser *et al.*, is advantageous because of its short reaction time and the low amount of catalyst needed.

Table 29. Deoxygenation reaction and recycling studies with immobilized photoredox catalyst **327**.

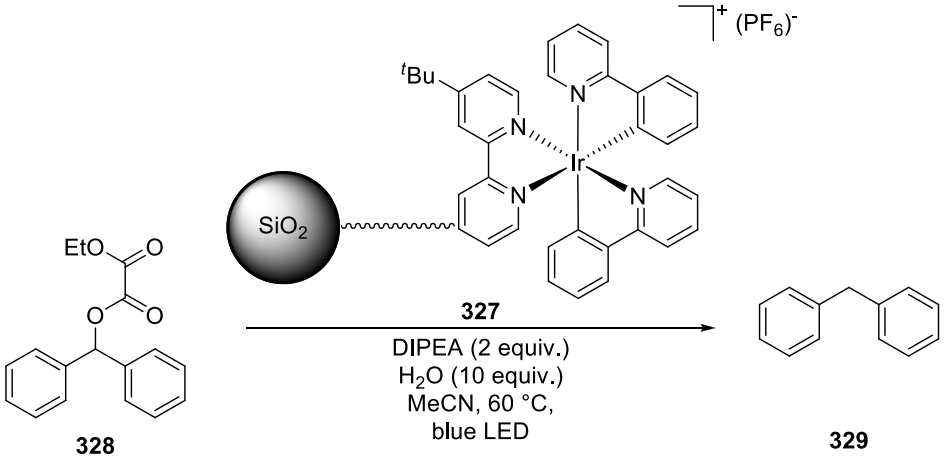

run	catalyst (mol%)	ester (mmol)	time	yield[a)]	catalyst recovered
1	0.1	0.45	4 h	92%	18 mg
2	0.1	0.32	4 h	29%	11 mg
3	0.1	0.2	22 h	15%	6 mg
4	0.1	0.1	22 h	0%	0 mg

[a)] Determined by GC, average of 3 measurements, naphthalene was used as internal standard.

The catalyst could be recycled for 3 consecutive runs although the decrease in activity was high. In the first run 92% of the deoxygenized product **329** was obtained and 72% of catalyst **327** could be recovered. The second run yielded 29% of product **329.** 61% of catalyst **327** were regained. Only 15% of product **329** were obtained in the third run and only a small amount of catalyst could be recovered which was inactive in the following experiment.

With the help of these experiments it could be shown that an immobilized photoredox catalyst can be synthesized *via* this route. The tether bearing photocatalysts exhibited the same photophysical and electrochemical properties as $[Ir(ppy)_2(dtbbpy)]PF_6$ (**204**·PF_6) and the immobilized catalyst (**327**) showed in the first run the same catalytic activity in deoxygenation reactions as unbound **204** but the recyclability was poor.

2. Zusammenfassung

Die vorliegende Arbeit beschäftigt sich mit der Photoredoxkatalyse mit sichtbarem Licht. Es wurden verschiedene Reaktionen, unter anderem 1,4-Additionen an Michael System und oxidative Mannich Reaktionen, untersucht und ein immobilisierbarer Photoredoxkatalysator entwickelt.

Im ersten Projekt wurden die Ausbeuten und die Substratbreite einer photokatalytischen 1,4-Addition an Michael System, die von Deepak Jadhav und mir zuvor entwickelt worden war, verbessert (Schema 1). Der Einfluss verschiedener Additive, neuer Photoredoxkatalysatoren und neuer Amine auf die Reaktion wurde untersucht. Zusätzlich zur Belichtung in einem Schnappdeckel Glas wurde die Reaktion auch in einem Mikroreaktor durchgeführt.

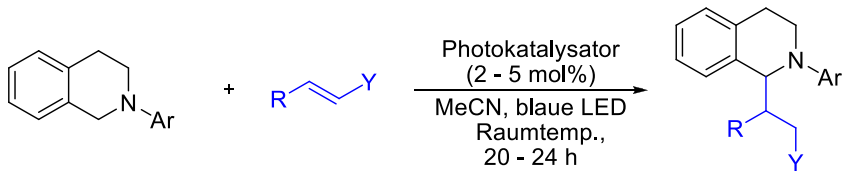

2 **23** **24**

Schema 1. Photokatalytische *N*-α-Funktionalisierung.

Um die Deprotonierung des Radikalkations zum *N*-α-Radikal zu beschleunigen, wurden verschiedenen Basen zur Reaktionsmischung hinzugefügt. Allerdings konnte keine der Basen die Ausbeuten verbessern, im Gegenteil, sie verschlechterten die Ausbeute. Der Ampholyt Wasser hatte bis zu einer Zugabe von 5 vol% keinen Einfluss auf die Reaktion, wurde mehr Wasser zur Reaktionsmischung hinzugefügt verringerten sich die Ausbeute und es konnte somit positiver Effekt von Wasser auf die Reaktion festgestellt werden. Die Ausbeute der Kupplung von Phenylpyrrolidin (**212**) und Methylvinylketon (**23a**) konnte durch die Zugabe von Cäsiumfluorid (1 äquiv.) und Isopropanol (10 äquiv.) leicht verbessert werden in Verbindung mit $Ru(bpy)_3Cl_2$ (**1**·Cl_2) als Photokatalysator. Da die Ausbeute sich dadurch nur gering erhöhte, wurde dieser Weg nicht weiter verfolgt.

Tetrabutylammonium decawolframat (TBADT, **190**), $Cu(dap)_2Cl$ (**195**), $[Ir(ppy)_2(dtbbpy)]PF_6$ (**204**·PF_6) und$[Ir\{dF(CF_3)ppy\}_2(dtbbpy)]PF_6$ (**216**·PF_6) wurden auf ihre Aktivität als Photoredoxkatalysatoren für die *N*-α-Aktivierung untersucht. Die ersten beiden Katalysatoren, **190** und **195**, zeigten keinerlei Aktivität in dieser Reaktion, die beiden letzteren, **204** und **216**, hingegen schon und führten zu ähnlichen Ausbeuten. Da jedoch Photokatalysator **216** deutlich aufwändiger in der Herstellung und teurer ist, wurden mit ihm keine weiteren 1,4-Additionen durchgeführt. Je nach Substrat erzielte

entweder $Ru(bpy)_3Cl_2$ (**1**·Cl_2) oder $[Ir(ppy)_2(dtbbpy)]PF_6$ (**204**·PF_6) bessere Ausbeuten. Eine Übersicht darüber gibt Tabelle 1.[129]

Tabelle 1. Vergleich der Ausbeuten mit $Ru(bpy)_3Cl_2$ (**1**·Cl_2) und $[Ir(ppy)_2(dtbbpy)]PF_6$ (**204**·PF_6).

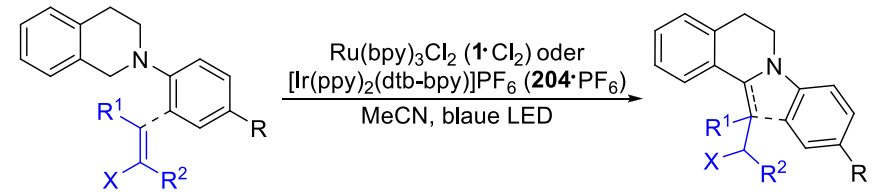

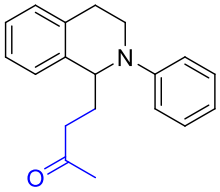	**24a**: Kat **1**: 58% Kat **204**: 68%
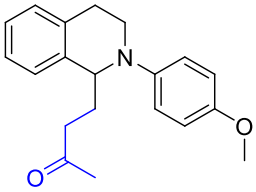	**24b:** Kat **1**: 63% Kat **204**: 37%
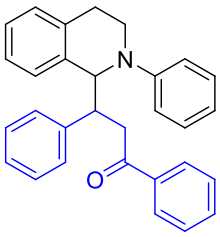	**24c:** Kat **1**: 61% Kat **204**: 83%
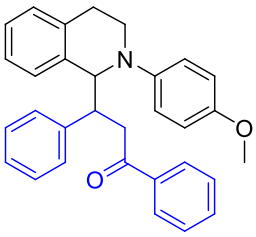	**24d**: Kat **1**: 43% Kat **204**: 33%
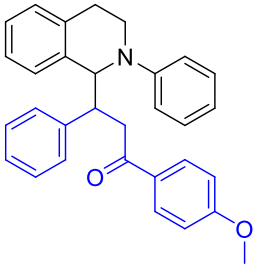	**24e:** Kat **1**: 56% Kat **204**: 93%
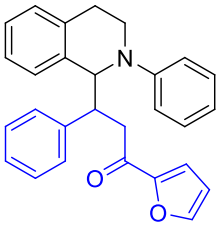	**24f**: Kat **1**: 53% Kat **204**: 66%
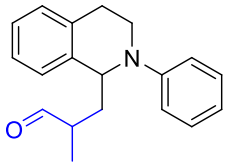	**24g**: Kat **1**: 50% Kat **204**: 50%
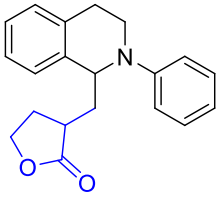	**24h:** Kat **1**: 31% Kat **204**: 33%
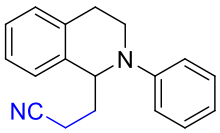	**24i**: Kat **1**: 27% Kat **204**: 31%
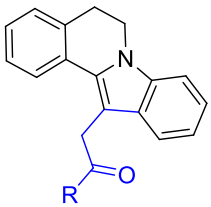	**28a** (R = Me): Kat **1**: 28% Kat **204**: 14% **28b** (R = Ph): Kat **1**: 35% Kat **204**: 18%

Die Ausbeuten mit Katalysator **204** fielen im Vergleich zu Katalysator **1** geringer aus, wenn andere Isochinolinederivate außer 2-phenyl-1,2,3,4-tetrahydroisochinolin (**2a**) eingesetzt wurden (vgl. Tabelle 1, **24b**, **24d**, **28a**, **28b**). Wurde hingegen Katalysator **204** in Reaktionen von Isochinolin **2a** und aliphatischen α,β-ungesättigten Ketonen, Aldehyden und Nitrilen eingesetzt, wurden die

gleichen oder leicht verbesserte Ausbeuten wie mit $Ru(bpy)_3Cl_2$ (**1**·Cl_2) erzielt (vgl. Tabelle 1, **24a**, **24g**, **24h**, **24i**). Mit Katalysator **204** wurden, im Gegensatz zu Katalysator **1**, teilweiße signifikant höhere Ausbeuten für Chalkonderivate erzielt (vgl. Tabelle 1, **24c**, **24e**, **24f**). In einem Fall konnte die Ausbeute sogar von 56% mit $Ru(bpy)_3Cl_2$ (**1**·Cl_2) auf 93% mit $[Ir(ppy)_2(dtbbpy)]PF_6$ (**204**·PF_6) gesteigert werden (vgl. Tabelle 1, **24e**).

Die Unterschiede in den Ausbeuten können mit den verschiedenen Redoxpotentialen von **1** und **204** erklärt werden. **204** hat ein niedrigeres Oxidationspotential beim Übergang vom angeregten Zustand zur Ir^{II}-Spezies weshalb die Oxidation von Isochinolin zum entsprechenden Radikalkation nicht so gut abläuft wie bei **1**. Auf der anderen Seite hat **204** ein größeres Reduktionspotential, was die Reduktion des α-Carbonylradikals zum Anion stärker begünstigt.

Die photokatalytische 1,4-Addition konnte auch an zwei weitere Anilinederivate, **208** und **212**, durchgeführt werden (Schema 2). Allerdings wurden die Produkte nur in niedrigen Ausbeuten erhalten, auch wenn die Reaktion in einem Mikroreaktor durchgeführt wurde. In beiden Fällen erwies sich **204** als der bessere Katalysator.

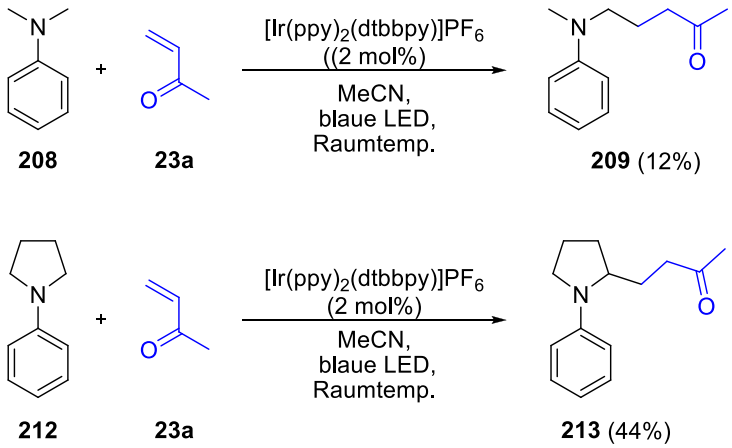

Schema 2. Photokatalytische 1,4-Addition mit Anilinderivaten.

Zusammenfassend war es uns möglich die Ausbeuten dieser bisher unbekannten photokatalytischen 1,4-Addition weiter du erhöhen und die Substratbreite zu vergrößern. Die Ausbeuten lagen im mittleren bis guten Bereich wenn 2-phenyl-tetrahydroisochinolin (**2a**) eingesetzt wurde und nahmen, teilweiße stark, ab bei anderen *tert.* Amine.

Als zweites Projekt wurde eine photokatalytische Methode zur Funktionalisierung von γ-Butyrolactonen entwickelt (Schema 3). Diese Arbeit basiert auf oxidative Mannich Reaktion die von Doyle *et al.* mithilfe eines Rhodiumkatalysators durchgeführt wurden.[130] Verschiedene Silylether wurden eingesetzt, wobei sich das TBS-geschütze Furan **238** als am besten erwies. Produkt **235** konnte in bis zu 28% Ausbeute erhalten werden, wenn eine Mischung aus TBS-Furan (**238**, 1 äquiv.), Trimethylanilin (**234**, 2 äquiv.) und $[Ir(ppy)_2(dtbbpy)]PF_6$ (**204**·PF_6) in Acetonitril ohne entgasen durch einen Mikroreaktor, unter Bestrahlung mit blauem Licht, mit einer Geschwindigkeit von 0.66 mL/h gepumpt wurde, was einer Retentionszeit von 2 h 40 min entspricht.

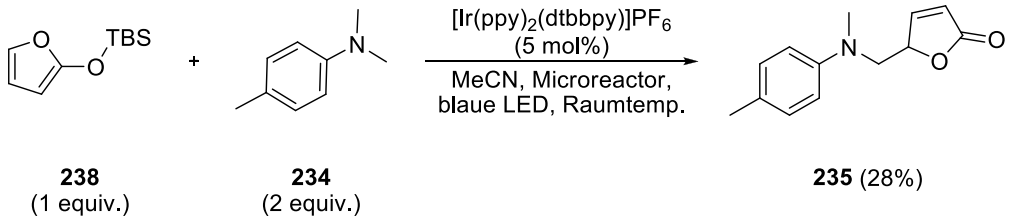

Schema 3 Photokatalytische Vinyloge Mannich Reaktion.

Kurz nach diesen vielversprechenden ersten Ergebnissen, publizierten Stephenson *et al.* nahezu die gleiche Reaktion.[131] Daher wurden die Arbeiten an diesem Projekt eingestellt. Im Gegensatz zur photokatalytischen Methode von Stephenson und der rhodiumkatalysierten von Doyle, benötigt unser Ansatz weder einen Elektrondonor noch Akzeptor außer Luftsauerstoff, was unsere Methode äußerst Nachhaltig macht.

Im dritten Projekt wurde versucht, eine Synthese für den Naturstoff Jamtin (**239**) zu entwickeln die einen photokatalytischen Schlüsselschritt einschließen sollte.

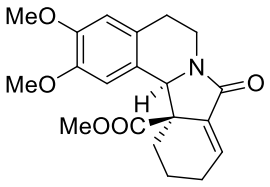

Figur 1. Struktur von Jamtin (**239**).

Nach der retrosynthetischen Analyse erschien die Kupplung von β-Ketoestern an Isochinolinderivate am aussichtsreichsten. Jedoch konnte weder eine photochemische noch nicht photochemische Methode entwickelt werden mit der ein passendes Zwischenprodukt für die Synthese von Jamtin dargestellt werden konnte (Schema 4 A).

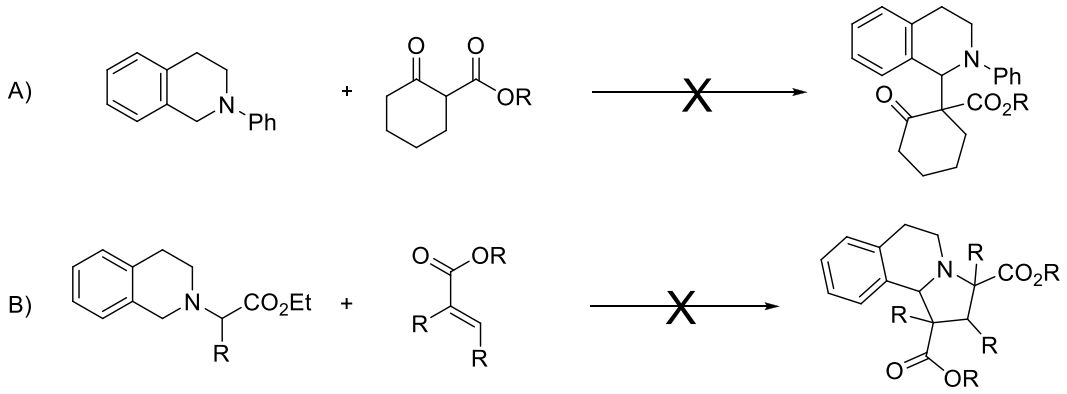

Schema 4. Mögliche photokatalytische Schlüsselschritte in der Synthese von Jamtin (**239**).

Auch eine neue Strategie, bei der eine [3+2] Cycloaddition der Schlüsselschritt sein sollte, führte nicht zum Erfolg. Sowohl mit Reaktionsbedingungen nach Xiao[132] und Rüping[133] konnte nicht das gewünschte Produkt erhalten werden (Schema 4 B). Höchstwahrscheinlich sind sterische Abschirmung und die Darstellung eines quartären Kohlenstoffs die Gründe warum Strategie A) und B) nicht funktioniert haben. Alle weiteren Überlegungen, Jamtin zu synthetisieren, führten zu längeren Reaktionssequenzen die nicht durchgeführt wurden, da Simpkins *et al.* bereits eine enantioselektive Totalsynthese in sechs Schritten vorgestellt haben.[134]

Das vierte Projekt beschäftigt sich mit der Öffnung und Funktionalisierung von Cyclopropanen. Es gelang, Cyclopropan **273** photochemisch zu öffnen und mit Methylvinylketon (**23a**), in einer bisher unbekannten weise, zu funktionalisieren (Schema 5). Jedoch kann diese Reaktion bisher nur an einem Molekül durchgeführt werden und weitere Substrate müssen entdeckt werden.

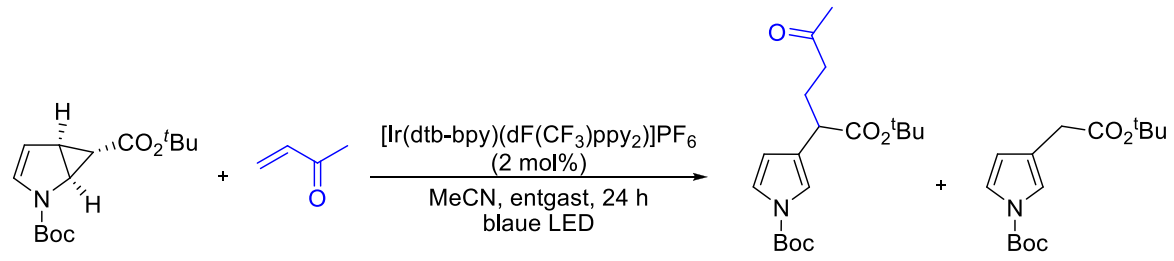

273 (1 äquiv.) + **23a** (3 äquiv.) → **276** (27%) + **277** (49%)

Schema 5. Photokatalytische Öffnung und Funktionalisierung von Cyclopropanen.

Die besten Ausbeuten wurden erzielt wenn **273** (1 äquiv.) mit Methylvinylketon (**23a** 3 äquiv.) und [Ir{dF(CF_3)ppy}$_2$(dtbbpy)]PF_6 (**216**·PF_6, 2 mol%) in trockenem Acetonitril gelöst, entgast und belichtet wurden. So konnten bis zu 27% des Additionsprodukt **276** und bis zu 49% des geöffneten Cyclopropans **277** erhalten werden (Schema 5).

Als letztes Projekt wurde ein auf $[Ir(ppy)_2(dtbbpy)]PF_6$ (**204**·PF_6) basierender Photokatalysator synthetisiert, der auf Siliziumdioxidpartikeln immobilisiert werden konnte. Ligand **317** konnte in drei Schritten und einer Gesamtausbeute von 18% dargestellt werden. Der daraus resultierende Photokatalysator **322** konnte mit einer Ausbeute von 79% synthetisiert werden.

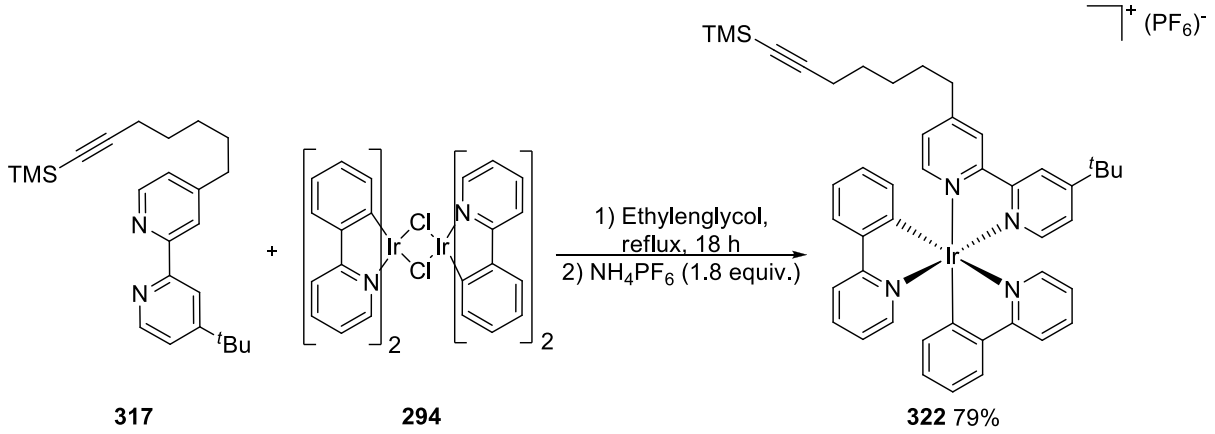

Schema 6. Synthese von Photokatalysator **322**.

Sowohl Katalysator **322** als auch der ungeschützte Katalysator **323** zeigten nahezu die gleichen photophysischen und elektrochemischen Eigenschaften wie **204**. Nach der Entschützung mit TBAF, wurde der Katalysator mit azidfunktionalisierten Silicapartikeln durch eine Huisgen Cycloaddition verbunden. Die Beladung lag bei bis zu 35 µmol/g.

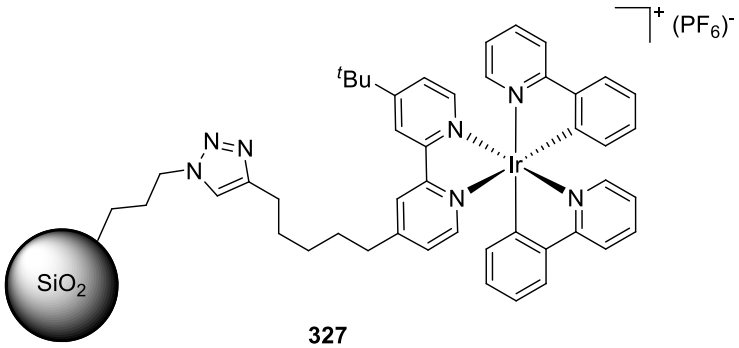

Figur 2. Immobilisierter Photoredoxkatalysator.

Die Anwendbarkeit des immobilisierte Photokatalysator wurde in der Desoxygenierung von Diphenylmethanol, welches in einen Oxalsäureester umgewandelt wurde, getestet. Der Vorteil dieser von Reiser *et al.* entwickelten Reaktion liegt in der kurzen Reaktionszeit und der kleinen Menge an benötigtem Katalysator.

Tabelle 2. Desoxygenierungen mit immobilisiertem Photokatalysator.

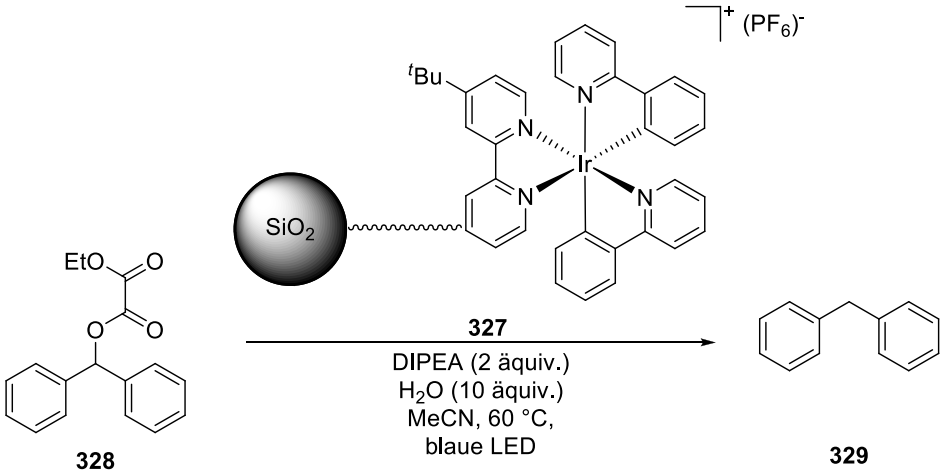

Lauf	Katalysator (mol%)	Ester (mmol)	Zeit	Ausbeute [a]	wiedergewonnener Katalysator
1	0.1	0.45	4 h	92%	18 mg
2	0.1	0.32	4 h	29%	11 mg
3	0.1	0.2	22 h	15%	6 mg
4	0.1	0.1	22 h	0%	0 mg

[a] Bestimmt mittels GC, durchschnitt von 3 Messungen, Naphtalin diente als interner Standard.

Der Katalysator konnte für drei aufeinander folgende Reaktionen recycelt werden, dennoch war der Verlust an katalytischer Aktivität hoch. Im ersten Durchgang wurden 92% des Desoxygenierungsprodukts erhalten und 72% des Katalysators wurden wiedergewonnen. Die Ausbeute des zweiten Laufs lag bei 29% und 61% des eingesetzten Katalysators wurden recycelt. Im dritten Lauf wurden nur noch 15% von Produkt **329** dargestellt und nur eine kleine Menge des Katalysators wurde zurückgewonnen, welche im folgenden Lauf keine katalytische Aktivität mehr zeigte.

Durch diese Experimente konnte gezeigt werden, dass sich ein immobilisierbarer Photokatalysator auf diese Weiße herstellen lässt, der dieselben photophysikalischen und elektrochemischen Eigenschaften aufweist wie $[Ir(ppy)_2(dtbbpy)]PF_6$ (**204**·PF_6). Im ersten Lauf zeigte der heterogene Katalysator sogar die gleiche Aktivität wie homogen zugesetzter **204**. allerdings ließ die Aktivität danach stark nach.

3. References

[129] Kohls, P.; Jadhav, D.; Pandey G.; Reiser O. *Org. Lett.* **2012**, *14*, 672.

[130] Catino, A. J.; Nichols, J. M.; Nettles, B. J.; Doyle. M. P. *J. Am. Chem. Soc.*, **2006**, *128*, 5648.

[131] Freeman, D. B.; Furst, L.; Condie, A. G.; Stephenson C. R. J *Org. Lett.* **2012**, *14*, 94.

[132] Zou, Y. Q.; Lu, L. Q.; Fu, L.; Chang, N. J.; Rong, J.; Chen, R. J.; Xiao W. J.; *Angew. Chem. Int. Ed.* **2011**, *50*, 7171.

[133] Rueping, M.; Leonori D.; Poisson, T. *Chem. Commun.* **2011**, *47*, 9615.

[134] Simpkins N. S.; Gill C. D. *Org. Lett.* **2003**, *5,* 535.

D. Experimental

1. General

Solvents and chemicals

All commercially available chemicals were purchased in high quality and were used without further purification except for methyl vinyl ketone (**23a**) which was distilled prior to use. Absolute THF, Et_2O and DCM were taken from a MB-SPS solvent purification system. Other absolute solvents were prepared by established laboratory procedures. Ethyl acetate, hexanes (40/60) and DCM for chromatography where distilled prior to use. Reactions with moisture and oxygen sensitive reagents were carried out in flame dried glassware under an atmosphere of predried nitrogen.

Thin layer chromatography was performed with TLC precoated aluminum sheets (Merck Silica gel 60 F_{254}, 0.2 mm layer thickness. Visualization was done with UV light (λ = 254 nm and 366 nm) and staining with Vanillin (1.25 g Vanillin, 8 mL conc. sulfuric acid, 25 mL conc. acetic acid, 215 mL methanol), $KMnO_4$ solution (1.0 g $KMnO_4$, 2 g Na_2CO_3, 100 mL water), or ninhydrin (300 mg ninhydrin, 5 mL conc. acetic acid, 35 mL isopropyl alcohol).

Column chromatography was performed with silica gel (Merck, Geduran 60, 0.063-0.200 mm particle size) and flash silica gel 60 (Merck, 0.040-0.063 mm particle size).
Automated column chromatography was performed with a Varian Intelliflash 310 purification system using reusable columns packed with flash silica gel 60 (Merck, 0.040-0.063 mm particle size).

Gas chromatography was performed on a Fisons GC 8000 using a flame ionization detector.

NMR spectroscopy

^{1}H-NMR spectra were recorded on BRUKER Avance 300 (300 MHz) and BRUKER Avance III 400 "Nanobay" (400 MHz) Spectrometer. Chemical shifts were reported as δ, parts per million, relative to the signal of chloroform ($CHCl_3$, 7.26 ppm) or acetonitrile (CH_3CN, 1.94 ppm). Spectra were evaluated in 1st order and coupling constants J are reported in Hertz (Hz). Splitting patterns for the spin multiplicity in the spectra are given as follows: s = singlet, d = doublet, t = triplet, q = quartet, dd = doublet of a doublet, ddd = doublet of a doublet of a doublet, dt = doublet of a triplet, m = multiplet.

^{13}C-NMR spectra were recorded on BRUKER Avance 300 (75 MHz) and BRUKER Avance III 400 "Nanobay" (100 MHz) Spectrometer. Chemical shifts for ^{13}C NMR were reported as δ, parts per million, relative to the center line signal of chloroform ($CHCl_3$, 77.0 ppm) or acetonitrile (CH_3CN, 1.4 ppm and 118.3 ppm). Multiplicities of the signals were assigned with DEPT 135.

ATR-IR spectroscopy was carried out on a Biorad Excalibur FTS 3000 spectrometer, equipped with a Specac Golden Gate Diamond Single Reflection ATR-System. Solid and liquid compounds were measured neatly and the wave numbers are reported as cm^{-1}.

Mass spectrometry was performed in the Central Analytic Department of the University of Regensburg on Finnigan MAT 95, ThermoQuest Finnigan TSQ 7000, Agilent Q-TOF 6540 UHD and Finnigan MAT SSQ 710 A.

Elemental analysis was measured on a Vario EL III or Mikro-Rapid CHN (Heraeus) (Microanalytic section of the University of Regensburg).

ICP-OES was measured on a Spectroflame EOP (Spectro).

Cyclic voltammetry measurements were carried out on an Autolab PGSTAT 302N set-up at 20 °C in acetonitrile containing tetrabutyl ammonium tetrafluoroborate as the supporting electrolyte under an argon atmosphere with use of a conventional undivided electrochemical cell, a glassy carbon working electrode, platinum wire as the counter electrode and silver wire as the reference electrode. The solvent was degassed by vigorous argon bubbling prior to the measurements. Redox potentials were referenced against ferrocene as an internal standard. All values are reported in reference to the SCE electrode.

Phase contrast microscopy was measured on a Nikon Diaphot phase-contrast microscope with an inverted set up and a 20x / 0.4 Objective.

Light sources:

LED plate: Six blue light emitting diodes (LED, 3 W, λ_{max}=455 nm) produced by LUXEON, purchased from Conrad.de, were mounted on a heat sink. A LUMOtech LEDlight 1 -20 VA Universal was used as power supply unit.

Micro reactor: Eight blue light emitting diodes (LED, 3 W, λ_{max}=455 nm) by Oslon LUXEON.

LED Stick: One Cree XP-E (3 W) LED; royal blue: λ_{max}=450 - 465 nm, green: λ_{max}= 520 – 535 nm.

2. Synthesis

2.1 Literature known substances

The following substances were prepared according to literature procedures and the spectroscopic data matched well with literature reports:

2-phenyl-1,2,3,4-tetrahydroisoquinoline (**2a**),[135] 2-(4-methoxyphenyl)-1,2,3,4-tetrahydroisoquinoline (**2b**),[135] 2-(3,4-dihydroisoquinolin-2(1H)-yl)benzaldehyde,[136] (E)-4-(2-(3,4-dihydroisoquinolin-2(1H)-yl)phenyl)but-3-en-2-one (**27a**),[137] (E)-3-(2-(3,4-dihydroisoquinolin-2(1H)-yl)phenyl)-1-phenylprop-2-en-1-one (**27b**),[137] tetra-butylammonium decatungstate (TBADT, $(n\text{-}Bu_4N)_4W_{10}O_{32}$, **190**),[138] $[Ir(ppy)_2(dtbbpy)]PF_6$ (**204**·PF_6),[139] 1-phenylpyrrolidine (**212**),[140] 1-phenylpiperidine (**214**),[140] $[Ir\{dF(CF_3)ppy\}_2(dtbbpy)]PF_6$ (**216**·PF_6),[141] (furan-2-yloxy)triisopropylsilane (**230**),[142] 5-((methyl(phenyl)-amino)methyl)furan-2(5H)-one (**232**),[143] 5-((methyl(p-tolyl)amino)methyl) furan-2(5H)-one (**235**),[143] (furan-2-yl-oxy)trimethylsilane (**13**),[144] *tert*-butyl(furan-2-yloxy) dimethylsilane (**238**),[145] diethyl 2-(3,4-dihydroisoquinolin-2(1H)-yl)malonate (**265**),[146] $Ru(bpz)_3Cl_2$ (**275**·Cl_2),[147], 4-(trimethyl-silyl)but-3-yn-1-ol (**300**),[148] (4-iodobut-1-ynyl)trimethylsilane (**298**),[149] tetrakis(2-phenylpyridine-C^2,N')(μ-dichloro)-diiridium (**294**),[139] (3-azidopropyl)triethoxysilane (**325**).[150]

2.2 General Procedures

General procedure A for photoinduced conjugate addition of *tert.* amines to enone systems with $Ir(dtb\text{-}bpy)(ppy)_2PF_6$:

A dry snap cap vial equipped with a magnetic stir bar and a septum was charged with a 1,2,3,4-tetrahydroisoquinoline derivative, enone and $[Ir)(ppy)_2(dtbbpy]PF_6$ in acetonitrile. The solution was degassed using three freeze-pump-thaw cycles[151] and stirred at room temperature at a distance of approximately 3 cm from a blue light emitting diode (LED) (λ_{max}=455 nm). The photochemical reaction was monitored by TLC analysis. After completion the solvent was removed under reduced pressure. The residue was purified by silica gel column chromatography using hexanes : ethyl acetate solvent systems to yield the desired 1,4 addition product.

General procedure B for oxygen free photoreaction in a LTF-VL micro reactor system:

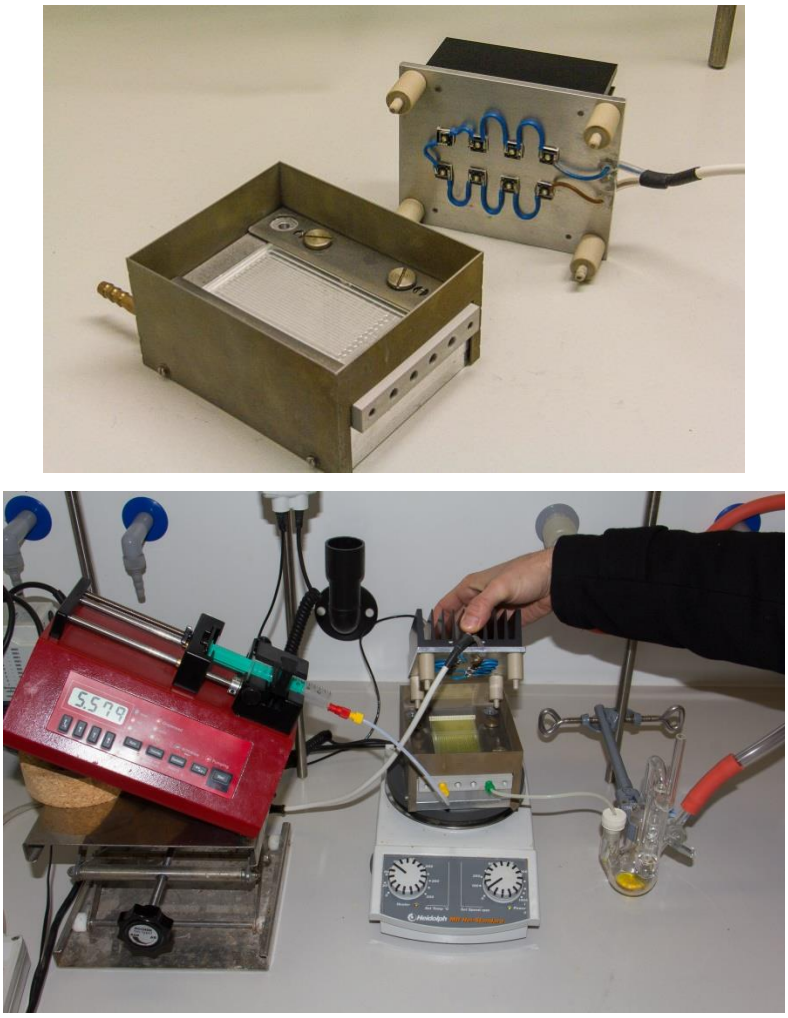

Figure 17. Set up for oxygen free reactions in an LTF micro reactor.

The inlet of the reactor was fitted with PTFE tubing ending in connection for luer lock to attach a syringe. The PTFE tubing on the outlet was pierced through a septum. The septum was mounted to one neck of a two-neck Schlenk flask, a bubbler was fitted to the other neck to prevent over pressure. The Schlenk flask, tubing and micro reactor were purged with nitrogen for 10 min to exclude all oxygen.

In a dry Schlenk flask (one neck) the reaction solution was prepared and degassed using three freeze pump thaw cycles. It is very important that all solid compounds are fully dissolved; otherwise the micro reactor might clog. After backfilling the flask with nitrogen, the reaction solution was taken up in a syringe and 2 mL of nitrogen gas. The outlet of the syringe was attached to the luer lock and the nitrogen counter current flow through the micro reactor was stopped. The syringe was placed in a syringe pump that was standing with one end on a cork ring so the nitrogen bubble in the syringe was rising to the plunger. This way, all of the reaction solution is pushed through the reactor and

collected in the two neck Schlenk flask. The reaction solution was pumped through the micro reactor at the indicated speed and irradiated with eight royal blue LEDs. Afterwards the solution was collected in the Schlenk flask and subjected to purification or analytic as indicated.

General procedure C for photoreactions in a LTF micro reactor system without inert atmosphere:
The inlet of the reactor was fitted with PTFE tubing ending in connection for luer lock to attach a syringe. The PTFE tubing from the outlet ended in an Erlenmeyer flask or a round bottom flask. The system was dried prior to the reaction by purging it with dry nitrogen. All reactants and reagents were fully dissolved in the indicated solvent in a snap cap vial. The reaction solution was taken up in a syringe and 2 mL of air. The outlet of the syringe was attached to the luer lock and the syringe was placed in a syringe pump that was standing with one end on a cork ring so the air bubble in the syringe was rising to the plunger. This way, all of the reaction solution is pushed through the reactor and collected in the flask. The reaction solution was pumped through the micro reactor at the indicated speed and irradiated with eight royal blue LEDs.

2.3 Photochemical conjugate additions

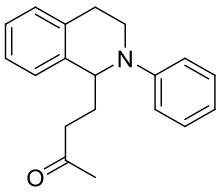

4-(2-phenyl-1,2,3,4-tetrahydroisoquinolin-1-yl)butan-2-one (**24a**): According to general procedure A 2-phenyl-1,2,3,4-tetrahydroisoquinoline (**2a**) (64 mg, 0.3 mmol, 1.0 equiv.), methyl vinyl ketone (**23a**) (75 µL, 0.9 mmol, 3.0 equiv.) and [Ir(ppy)$_2$(dtbbpy]PF$_6$ (**204**·PF$_6$) (6 mg, 6 µmol, 2 mol%) were irradiated in acetonitrile (3 mL) for 24 h. The pure product was obtained by purification on SiO_2 (19:1 hexanes : EtOAc) as brown oil (57 mg, 0.2 mmol, 68%). Analytics were in good accordance with literature.[137]

Experiments in Chapter 1.4, Table 4:

The below mentioned compounds were dissolved in 3 mL of acetonitrile in a snap cap vial fitted with a septum and degassed using three freeze pump thaw cycles. The clear solution was irradiated with a royal blue LED for 24 h. After the reaction was completed the reaction mixture was transferred to a round bottom flask and concentrated in vacuo. 1,2-Dicyanobenzen as internal standard and $CDCl_3$ were added and a ^{1}H-NMR spectrum was recorded.

entry	2-phenyl-1,2,3,4-tetrahydroisoquinoline (2a)	methyl vinyl ketone (23a)	[Ir(ppy)$_2$(dtbbpy]PF$_6$ (**204**·PF$_6$)	additive	1,2-Dicyanobenzen	yield / [%]
1	1 equiv. (63 mg, 0.3 mmol)	3 equiv. (75 µL, 0.9 mmol)	0.5 mol% (1 mg, 2 µmmol)	-	28 mg, 0.2 mmol	52 mg, 0.2 mmol, 62%
2	1 equiv. (63 mg, 0.3 mmol)	3 equiv. (75 µL, 0.9 mmol)	1 mol% (3 mg, 3 µmmol)	-	22 mg, 0.2 mmol	55 mg, 0.2 mmol, 66%
3	1 equiv. (63 mg, 0.3 mmol)	3 equiv. (75 µL, 0.9 mmol)	5 mol% (14 mg, 15 µmmol)	-	20 mg, 0.2 mmol	31 mg, 0.1 mmol, 38%
4	1 equiv. (63 mg, 0.3 mmol)	3 equiv. (75 µL, 0.9 mmol)	1 mol% (3 mg, 3 µmmol)	NaOAc (47 mg, 0.3 mmol)	20 mg, 0.2 mmol	54 mg, 0.2 mmol, 64%
5	1 equiv. (63 mg, 0.3 mmol)	3 equiv. (75 µL, 0.9 mmol)	1 mol% (3 mg, 3 µmmol)	K_2CO_3 (52 mg, 0.4 mmol)	20 mg, 0.2 mmol	38 mg 0.1 mmol, 46%

Experiments in Chapter 1.5, Table 5:

According to general procedure B the below mentioned reagents were dissolved in acetonitrile containing the indicated amount of water. After the reaction was completed the reaction mixture was transferred to a round bottom flask and concentrated in vacuo. 1,2-Dicyanobenzen as internal standard and $CDCl_3$ were added and a ^{1}H-NMR spectrum was recorded.

entry	2-phenyl-1,2,3,4-tetrahydroisoquinoline (2a)	methyl vinyl ketone (23a)	[Ir](ppy)$_2$(dtbbpy]PF$_6$ (**204**·PF$_6$)	water	pump rate	1,2-Dicyanobenzen	yield / [%]
1	1 equiv. (43 mg, 0.2 mmol)	3 equiv. (50 µL, 0.6 mmol)	2 mol% (4 mg, 4 µmmol)	0%	1 mL/h	7 mg, 0.05 mmol	26 mg, 0.1 mmol, 46%
2	1 equiv. (46 mg, 0.2 mmol)	3 equiv. (50 µL, 0.6 mmol)	2 mol% (4 mg, 4 µmmol))	5%	1 mL/h	20 mg, 0.2 mmol	29 mg, 0.1 mmol, 46%
3	1 equiv. (43 mg, 0.3 mmol)	3 equiv. (50 µL, 0.6 mmol)	2 mol% (4 mg, 4 µmmol)	10%	1 mL/h	20 mg, 0.2 mmol	0%

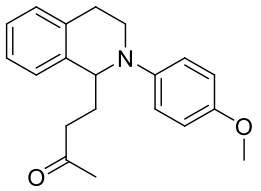

4-(2-(4-methoxyphenyl)-1,2,3,4-tetrahydroisoquinolin-1-yl)butan-2-one (24b): According to general procedure A 2-(4-methoxyphenyl)-1,2,3,4-tetrahydroisoquinoline (**2b**) (47 mg, 0.2 mmol, 1.0 equiv.), methyl vinyl ketone (**23a**) (50 µL, 0.6 mmol, 3.0 equiv.) and [Ir](ppy)$_2$(dtbbpy]PF$_6$ (**204**·PF$_6$) (9 mg, 10 µmol, 5 mol%) were irradiated in 3 mL acetonitrile for 24 h. The pure product was obtained as brown oil (23 mg, 0.07 mmol, 37%). after purification on silica gel (19:1 hexanes : EtOAc).
Analytics were in good accordance with literature.[137]

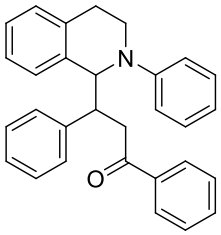

1,3-diphenyl-3-(2-phenyl-1,2,3,4-tetrahydroisoquinolin-1-yl)propan-1-one (24c): According to general procedure A 2-phenyl-1,2,3,4-tetrahydroisoquinoline (**2a**) (64 mg, 0.3 mmol, 1.0 equiv.), *trans*-benzylidenacetophenone (**23b**) (68 mg, 0.3 mmol, 1.1 equiv.) and [Ir](ppy)$_2$(dtbbpy]PF$_6$ (**204**·PF$_6$) (14 mg, 15 µmol, 5 mol%) were irradiated in 3 mL acetonitrile for 24 h. The pure product was obtained as white solid (106 mg, 0.2 mmol, 83%) after purification on silica gel (19:1 hexanes : EtOAc). Analytics were in good accordance with literature.[137]

Experiments in Chapter 1.4, Table 6:

Further experiments in a snap cap vial: The below mentioned compounds were dissolved in 3 mL of acetonitrile in a snap cap vial fitted with a septum and degassed using three freeze pump thaw cycles. The clear solution was irradiated with a royal blue LED for 24 h. After the reaction was completed the reaction mixture was transferred to a round bottom flask and concentrated in vacuo. 3-nitrobenzaldehyde as internal standard and $CDCl_3$ were added and a ^{1}H-NMR spectrum was recorded.

entry	**2-phenyl-1,2,3,4-tetrahydroisoquinoline (2a)**	**chalcone (23b)**	**[Ir](ppy)$_2$(dtbbpy]PF$_6$ (204·PF$_6$)**	**3-nitro-benz-aldehyde**	**yield / [%]**
1	1 equiv. (63 mg, 0.3 mmol)	1.1 equiv. (69 mg, 0.3 mmol)	1 mol% (3 mg, 3 µmmol)	20 mg, 0.1 mmol	61 mg, 0.2 mmol, 48%
2	1 equiv. (65 mg, 0.3)mmol	1.1 equiv. (73 mg, 0.4 mmol	2 mol% (7 mg, 7 µmol)	26 mg, 0.2 mmol	95 mg, 0.2 mmol, 66%
3	1 equiv. (63 mg, 0.3 mmol)	1.1 equiv. (69 mg, 0.33 mmol)	5 mol% (14 mg, 15 µmol)	23 mg, 0.2 mmol	116 mg, 0.3 mmol, 91%
4	1 equiv. (62 mg, 0.3 mmol)	1.1 equiv. (69 mg, 0.3 mmol)	10 mol% (27 mg, 30 µmol)	17 mg, 0.1 mmol	42 mg, 0.1 mmol, 34%
5	2 equiv. (63 mg, 0.3 mmol)	1 equiv. (31 mg, 0.2 mmol)	5 mol% (14 mg, 15 µmol)	31 mg, 0.2 mmol	48 mg 0.1 mmol, 77%
6	1 equiv. (63 mg, 0.3 mmol)	1.5 equiv. (93 mg, 0.5 mmol)	5 mol% (14 mg, 15 µmol)	21 mg, 0.1 mmol	104 mg, 0.3 mmol, 83%
7	1 equiv. (63 mg, 0.3 mmol)	3 equiv. (187 mg, 0.9 mmol)	5 mol% (14 mg, 15 µmol)	30 mg, 0.2 mmol	83 mg, 0.2 mmol, 67%

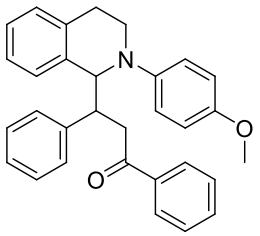

3-(2-(4-methoxyphenyl)-1,2,3,4-tetrahydroisoquinolin-1-yl)-1,3-diphenylpropan-1-one (14d): According to general procedure A 2-(4-methoxyphenyl)-1,2,3,4-tetrahydroisoquinoline (**2b**) (46 mg, 0.2 mmol, 1.0 equiv.), *trans*-benzylidenacetophenone (**23b**) (57 mg, 0.3 mmol, 1.4 equiv.) and [Ir](ppy)$_2$(dtbbpy]PF$_6$ (**204**·PF$_6$) (10 mg, 11 µmol, 5.5 mol%) were irradiated in 3 mL acetonitrile for 24 h. The pure product was obtained as white solid (28 mg, 0.06 mmol, 33%) after purification on silica gel (19:1 hexanes : EtOAc). Analytics were in good accordance with literature.[137]

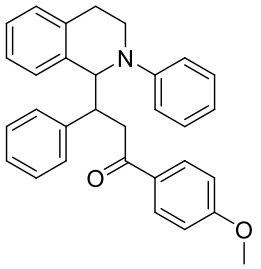

1-(4-methoxyphenyl)-3-phenyl-3-(2-phenyl-1,2,3,4-tetrahydroisoquinolin-1-yl)propan-1-one (24e): According to general procedure A 2-phenyl-1,2,3,4-tetrahydroisoquinoline (**2a**) (62 mg, 0.3 mmol, 1.0 equiv.), (E)-1-(4-methoxyphenyl)-3-phenylprop-2-en-1-one (**23c**) (96 mg, 0.4 mmol, 1.4 equiv.) and $[Ir(ppy)_2(dtbbpy]PF_6$ (**204**·PF_6) (18 mg, 20 µmol, 7 mol%) were irradiated in 3 mL acetonitrile for 24 h. The pure product was obtained as pale brown solid (123 mg, 0.3 mmol, 93%) after purification on silica gel (18.5:1.5 hexanes : EtOAc). Analytics were in good accordance with literature.[137]

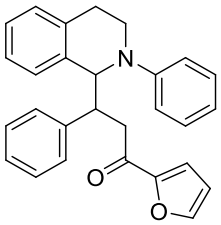

1-(furan-2-yl)-3-phenyl-3-(2-phenyl-1,2,3,4-tetrahydroisoquinolin-1-yl)propan-1-one (24f): According to general procedure A 2-phenyl-1,2,3,4-tetrahydroisoquinoline (**2a**) (35 mg, 0.2 mmol, 1.0 equiv.), (E)-1-(furan-2-yl)-3-phenylprop-2-en-1-one (**23d**) (34 mg, 0.2 mmol, 1.0 equiv.) and $[Ir(ppy)_2(dtbbpy]PF_6$ (**204**·PF_6) (9 mg, 10 µmol, 5 mol%) were irradiated in 3 mL acetonitrile for 24 h. The pure product was obtained as white solid (45 mg, 0.1 mmol, 66%) after purification on silica gel (19:1 hexanes : EtOAc). Analytics were in good accordance with literature.[137]

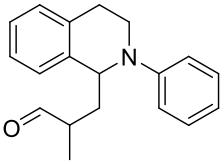

2-methyl-3-(2-phenyl-1,2,3,4-tetrahydroisoquinolin-1-yl)propanal (24g): According to general procedure A 2-phenyl-1,2,3,4-tetrahydroisoquinoline (**2a**) (63 mg, 0.3 mmol, 1.0 equiv.), methacrolein (**23e**) (75 µL, 0.9 mmol, 3.0 equiv.) and $[Ir(ppy)_2(dtbbpy]PF_6$ (**204**·PF_6) (6,9mg, 8 µmol, 2 %) were irradiated in acetonitrile for 24 h. The pure product was obtained as yellow oil (42 mg, 0.15 mmol, 50%) after purification on silica gel (19:1 hexanes : EtOAc). Analytics were in good accordance with literature.[137]

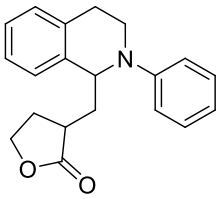

3-((2-phenyl-1,2,3,4-tetrahydroisoquinolin-1-yl)methyl)dihydrofuran-2(3H)-one (24h): According to general procedure A 2-phenyl-1,2,3,4-tetrahydroisoquinoline (**2a**) (65 mg, 0.3 mmol, 1.0 equiv.), 3-methylenedihydrofuran-2(3H)-one (**23f**) (80 µL, 0.92 mmol, 3.0 equiv.) and [Ir(ppy)$_2$(dtbbpy]PF$_6$ (**204**·PF$_6$) (14 mg, 16 µmol, 5 mol%) were irradiated in acetonitrile for 24 h. The pure product was obtained as brown oil (32 mg, 0.1 mmol, 34%) after purification on silica gel (5:1 hexanes : EtOAc). Analytics were in good accordance with literature.[137]

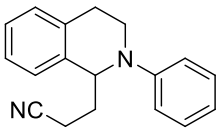

3-(2-phenyl-1,2,3,4-tetrahydroisoquinolin-1-yl)propanenitrile (24i): According to general procedure A 2-phenyl-1,2,3,4-tetrahydroisoquinoline (**2a**) (62 mg, 0.3 mmol, 1.0 equiv.), acrylonitrile (**23g**) (48 µL, 0.9 mmol, 3.0 equiv.) and [Ir(ppy)$_2$(dtbbpy]PF$_6$ (**204**·PF$_6$) (13 mg, 13 µmol, 5 mol%) were irradiated in acetonitrile for 24 h. The pure product was obtained as red solid (24 mg, 0.1 mmol, 31 %) after purification on silica gel (5:1 hexanes : EtOAc). Analytics were in good accordance with literature.[137]

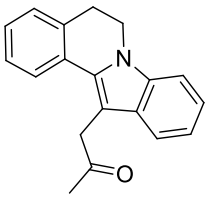

1-(5,6-dihydroindolo[2,1-a]isoquinolin-12-yl)propan-2-one (28a): (E)-4-(2-(3,4-dihydroisoquinolin-2(1H)-yl)phenyl)but-3-en-2-one (**27a**) (71 mg, 0.3 mmol, 1.0 equiv.) and [Ir(ppy)$_2$(dtbbpy]PF$_6$ (**204**·PF$_6$) (12 mg, 13 µmol, 5 mol%) were dissolved in 3 mL acetonitrile and degassed using three freeze-pump-thaw cycles. The mixture was irradiated by blue LEDs for 24 h. Pure product was obtained as yellow oil (12 mg, 0.04 mmol, 14%) after purification on silica gel (4:1 DCM : hexanes). Analytics were in good accordance with literature.[137]

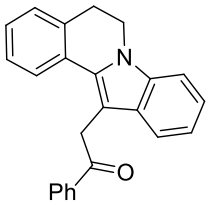

2-(5,6-dihydroindolo[2,1-a]isoquinolin-12-yl)-1-phenylethanone (28b): (E)-4-(2(E)-3-(2-(3,4-dihydroisoquinolin-2(1H)-yl)phenyl)-1-phenylprop-2-en-1-one (**27b**) (181 mg, 0.5 mmol, 1.0 equiv.) and $[Ir(ppy)_2(dtbbpy]PF_6$ (**204**·PF_6) (24 mg, 26 µmol, 5 mol%) were dissolved in 3 mL acetonitrile and degassed using three freeze-pump-thaw cycles. The mixture was irradiated by blue LEDs for 24 h. Pure product was obtained as colorless oil (32 mg 0.1 mmol, 18%) after purification on silica gel (19:1 hexanes : EtOAc). Analytics were in good accordance with literature.[137]

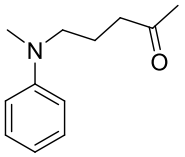

5-(methyl(phenyl)amino)pentan-2-one (209): According to general procedure A N,N-dimethylaniline (**208**) (39 µL, 0.3 mmol, 1 equiv.), methyl vinyl ketone (**23a**) (75 µL, 0.9 mmol, 3.0 equiv.) and $[Ir(ppy)_2(dtbbpy]PF_6$ (**204**·PF_6) (6 mg, 6 µmol, 2 %) were irradiated in acetonitrile (3 mL) for 24 h. The pure product was obtained as brown oil (7 mg, 0.03 mmol, 12%) after purification on silica gel (19:1 hexanes : EtOAc).

R_f (9:1 hexanes : EtOAc) = 0.18.

^{1}H-NMR (300 MHz, $CDCl_3$): δ = 7.18 (dd, *J* = 8.9, 7.2 Hz, 2H), 6.66 (dd, *J* = 7.9, 4.0 Hz, 3H), 3.31 – 3.24 (m, 2H), 2.86 (s, 3H), 2.42 (t, *J* = 7.0 Hz, 2H), 2.07 (s, 3H), 1.87 – 1.74 (m, 2H).

^{13}C-NMR (75 MHz, $CDCl_3$): δ = 208.5, 149.5, 129.4, 116.4, 112.4, 51.9, 40.8, 38.3, 30.1, 21.2.

HRMS: (EI-MS) *m/z* calculated for $C_{12}H_{17}NO$ [$M^{+\bullet}$]: 191.1310, found 191.1313.

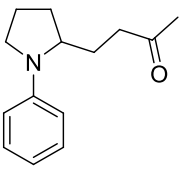

4-(1-phenylpyrrolidin-2-yl)butan-2-one (212): According to general procedure A 1-phenylpyrrolidine (**212**) (64 mg, 0.43 mmol, 1.0 equiv.), methyl vinyl ketone (**23a**) (107 µL, 1.3 mmol, 3.0 equiv.) and $[Ir(dtb\text{-}bpy)(ppy)_2]PF_6$ (**204**·PF_6) (8 mg, 9 µmol, 2 mol%) were irradiated by blue LED in 4.5 mL acetonitrile for 24 h. The pure product was obtained as brown oil (26 mg, 0.12 mmol, 28 %) after purification on silica gel (19:1 hexanes : EtOAc).

Experiments in Chapter 1.6 Table 9:

According to general procedure B 1-phenylpyrrolidine (**212**) (43 µL, 0.3 mmol, 1.0 equiv. (entry 1-6) or 50 µL 0.4 mmol, 1 equiv. (entry 7)), methyl vinyl ketone (**23a**) (75 µL, 0.9 mmol, 3.0 equiv. (entry 1-6) or 86 µL, 1.0 mmol, 3 equiv. (entry 7)) and the below mentioned reagents were dissolved in 3 mL acetonitrile. After the reaction was completed the reaction mixture was transferred to a round bottom flask and concentrated.

^{1}H-NMR-Analysis: 3-nitrobenzaldehyde was added to the residue as internal standard and taken up in $CDCl_3$. A ^{1}H-NMR spectra was recorded and analyzed.

Purification on silica gel was performed on a Varian Intelliflash 310 using a SF15-12g column; beforehand a dryload was prepared of the residue.

entry	catalyst	pump rate	additive	3-nitrobenzaldehyde	Yield 213
1	**1**·Cl_2 5 mol% (11 mg, 15 µmol)	0.33 mL/h		32 mg (0.2 mmol)	17%[a] 11 mg, 0.05 mmol
2	**1**·Cl_2 5 mol% (11 mg, 15 µmol)	0.33 mL/h	CsF 1 equiv. (46 mg, 0.3 mmol) iPrOH 10 equiv. (0.23 mL, 3.0 mmol)		28%[b] 18 mg, 0.08 mmol
3	**1**·Cl_2 5 mol% (11 mg, 15 µmol)	0.25 mL/h	CsF 1 equiv. (46mg, 0.3 mmol) iPrOH 10 equiv. (0.23 mL, 3.0 mmol)		7%[b] 5 mg, 0.02 mmol
4	**1**·Cl_2 5 mol% (11 mg, 15 µmol)	15 h	CsF 1 equiv. (46 mg, 0.3 mmol) iPrOH 10 equiv. (0.23 mL, 3.0 mmol)		15%[b] 10 mg, 0.05 mmol
5	**204**·PF_6 5 mol% (14 mg, 15 µmol)	0.5 mL/h			27%[b] 17 mg, 0.08 mmol
6	**204**·PF_6 5 mol% (14 mg, 15 µmol)	0.33 mL/h		15 mg (0.1 mmol)	32%[a] 21 mg, 0.1 mmol
7	**204**·PF_6 2 mol% (6 mg, 7 µmol)	1 mL/h			44%[b] 33 mg, 0.15 mmol

a) Yield determined by ^{1}H-NMR analysis; b) isolated yield

Experiments in Chapter 1.7, Table 10:

According to general procedure B 1-phenylpyrrolidine (**212**) (43 µL, 0.3 mmol, 1.0 equiv.), methyl vinyl ketone (**23a**) (75 µL, 0.9 mmol, 3.0 equiv.), $[Ir\{dF(CF_3)ppy\}_2(dtbbpy)]PF_6$ (**216**·PF_6) and the below mentioned reagents were dissolved in 3 mL acetonitrile, degassed and pumped through a micro reactor system while irradiated by eight LEDs. After the reaction was completed the reaction mixture was transferred to a round bottom flask and a dryload was prepared. Purification on silica gel was performed on a Varian Intelliflash 310 using a SF15-12g column.

entry	147	pump speed	retention time	additive	yield 213
1	1 mol% (3 mg, 3 µmol)	0.33 mL/h	5 h 10 min	-	20% 13 mg, 0.06 mmol
2	2 mol% (7 mg, 6 µmol)	0.33 mL/h	5 h 10 min	-	35% 23 mg, 0.10 mmol
3	5 mol% (17 mg, 15 µmol)	0.33 mL/h	5 h 10 min	-	39% 25 mg, 0.12 mmol
4	5 mol%. (17 mg, 15 µmol)	0.16 mL/h	10 h 20 min	air	0%
5	2 mol% (7 mg, 6 µmol)	0.50 mL/h	3 h 30 min	$LiBF_4$ (1.2 equiv.) 0.36 mL (1 M solution in MeCN)	traces
6	2 mol% (7 mg, 6 µmol)	0.33 mL/h	5 h 10 min	$ZnCl_2$ (1.3 equiv.) (5 mg, 0.4 mmol)	traces
7	2 mol% (7 mg, 6 µmol)	0.33 mL/h	5 h 10 min	$AlCl_3$ (1.3 equiv.) (5 mg, 0.4 mmol)	traces
8	2 mol% (7 mg, 6 µmol)	0.33 mL/h	5 h 10 min	$Ce(SO_4)_2$ (1.3 equiv.) (16 mg, 0.4 mmol)	traces

R_f (9:1 hexanes : EtOAc) = 0.5.

IR (neat): 2949, 2876, 1711, 1597, 1504, 1455, 1361, 1260, 1158, 1035, 991, 868, 748, 695, 641, 595 cm^{-1}.

^{1}H-NMR (300 MHz, $CDCl_3$): δ = 7.28 – 7.18 (m, 2 H), 6.71 – 6.60 (m, 3 H), 3.79 – 3.68 (m, 1 H), 3.49 – 3.39 (m, 1 H), 3.22 – 3.09 (m, 1 H), 2.49 (t, *J* = 7.4 Hz, 2 H), 2.14 (s, 3 H), 2.09 – 1.89 (m, 4 H), 1.77 (dd, *J* = 6.7, 1.9 Hz, 1 H), 1.67 – 1.53 (m, 1 H).

^{13}C-NMR (75 MHz, $CDCl_3$): δ = 208.6, 147.5, 129.4, 115.7, 112.1, 57.6, 48.7, 40.6, 30.3, 30.1, 27.3, 23.6.

HRMS: (EI-MS) *m/z* calculated for $C_{14}H_{19}NO$ [$M^{+\bullet}$]: 217.1467, found 217.1468.

2.4 Photocatalytic Oxidative Mannich Reactions

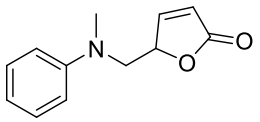

5-((methyl(phenyl)amino)methyl)furan-2(5H)-one (232): According to general procedure C (furan-2-yl-oxy)trimethylsilane[144] (**13**) (34 µl, 0.2 mmol, 1.0 equiv.), N,N-dimethylaniline (**208**) (50 µl, 0.4 mmol, 2.0 equiv.) and $[Ir(dtb\text{-}bpy)(ppy)_2]PF_6$ (**204**·PF_6) (4 mg, 4 µmol, 2 mol%) were dissolved in acetonitrile (2 mL). The solution was pumped through a micro reactor (pump rate: 2 mL/h; retention time 50 min) and irradiated with blue LED. After the reaction the solvent was evaporated and 3-nitrobenzaldehyde (81 mg, 0.5 mmol) was added to the residue as internal standard. According to ^{1}H-NMR analysis 2 mg (0.01 mmol, 5%) of product formed. The ^{1}H-NMR spectrum is good accordance with literature.[152]

R_f (4:1 hexanes : ethyl acetate) = 0.82.

^{1}H-NMR (400 MHz, $CDCl_3$): δ = 7.49 (dd, *J* = 5.7, 1.0 Hz, 1H), 7.26 (t, *J* = 8.0 Hz, 2H), 6.77 (t, *J* = 7.3 Hz, 1H), 6.72 (d, *J* = 8.3 Hz, 2H), 6.13 (dd, *J* = 5.7, 1.8 Hz, 1H), 5.31 – 5.21 (m, 1H), 3.72 – 3.64 (m, 2H), 3.02 (s, 3H).

^{13}C-NMR (100 MHz, $CDCl_3$) δ = 171.6, 153.5, 147.3, 128.4, 121.1, 116.4, 111.3, 81.0, 54.0, 38.

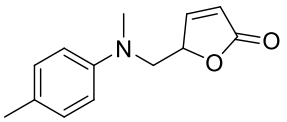

5-((methyl(p-tolyl)amino)methyl)furan-2(5H)-one (235): According to general procedure C (furan-2-yl-oxy)trimethylsilane[144] (**13**) (34 µl, 0.2 mmol, 1.0 equiv.), N,N,4-trimethylaniline (**234**) (58 µl, 0,4 mmol, 2 equiv.) and [Ir(dtb-bpy)(ppy)2]PF6 (**204**·PF_6) (4 mg, 4 µmol, 2 mol%) were dissolved in acetonitrile (2 mL). The solution was pumped through a micro reactor at a rate of 2 mL/h (retention time: 50 min) and irradiated with blue LEDs. Pure product was obtained as brown oil (23 mg, 0.01 mmol, 6%) after purification on silica gel (4:1 hexanes : EtOAc). The ^{1}H-NMR spectrum is good accordance with literature. [152]

Experiment in Chapter 2, Table 13:

According to general procedure C (furan-2-yl-oxy)trimethylsilane[142] (**13**) (34 µl, 0.2 mmol, 1.0 equiv.), N,N,4-trimethylaniline (**234**) (58 µl, 0,4 mmol, 2 equiv.) and [Ir(dtb-bpy)(ppy)2]PF6 (**204**·PF_6) (4 mg, 4 µmol, 2 mol%) were dissolved in acetonitrile (2 mL). The solution was pumped through a micro reactor and irradiated with blue LEDs. After the reaction the solvent was evaporated and 3-nitrobenzaldehyde (15 mg, 0.1 mmol) was added to the residue as internal standard. According to ^{1}H-NMR analysis 5 mg (0.02 mmol, 12%) of product formed.

Experiments in Chapter 2, Scheme 69:

According to general procedure C (furan-2-yloxy)triisopropylsilane[142] (**230**) (53 µl, 0.2 mmol, 1 equiv.), N,N,4-trimethylaniline (**234**) (58 µl, 0,4 mmol, 2 equiv.) and [Ir(dtb-bpy)(ppy)2]PF6 (**204**·PF_6) (9 mg, 10 µmol, 5 mol%) were dissolved in acetonitrile (2 mL). The solution was pumped through a micro reactor and irradiated with blue LEDs. After completion, the solvent was evaporated, 3-nitrobenz-aldehyde was added to the residue as internal standard and a ^{1}H-NMR spectra was recorded.

entry	**pump rate**	**retention time**	**3-nitrobenz-aldehyde**	**Yield 235**
1	4 mL/h	25 min	15 mg (0.1 mmol)	0%
2	1 mL/h	1 h 40 min	15 mg (0.1 mmol)	9% (4 mg, 0.02 mmol)
3	0.66 mL/h	2 h 30 min	15 mg (0.1 mmol)	17% (8 mg, 0.03 mmol)
4	0.3 mL/h	5 h 10 min	15 mg (0.1 mmol)	16% (7 mg, 0.03 mmol)

Experiments in Chapter 2, Table 14:

According to general procedure C *tert*-butyl(furan-2-yloxy) dimethylsilane[145] (**238**) (43 µl, 0.2 mmol, 1 equiv.), N,N,4-trimethylaniline (**234**) (58 µl, 0,4 mmol, 2 equiv.) and [Ir(dtb-bpy)(ppy)2]PF6 (**204**) were dissolved in acetonitrile (2 mL). The solution was pumped through a micro reactor at a rate of 0.66 mL/h (retention time: 2 h 30 min) and irradiated with blue LEDs. After completion, the solvent was evaporated, 3-nitrobenzaldehyde was added to the residue as internal standard and a ^{1}H-NMR spectra was recorded.

entry	**$[Ir(dtb\text{-}bpy)(ppy)_2]PF_6$ ($204\cdot PF_6$)**	**3-nitrobenz-aldehyde**	**Yield 235**
1	1 mol% (2 mg, 2 µmol)	19 mg (0.1 mmol)	18% (8 mg, 0.04 mmol)
2	2 mol% (4 mg, 4 µmmol)	30 mg (0.2 mmol)	18% (8 mg, 0.04 mmol)
3	5 mol% (9 mg, 10 µmol)	16 mg (0.1 mmol)	28% (12 mg, 0.05 mmol)

R_f (4:1 hexanes : ethyl acetate) = 0.88.

^{1}H-NMR (400 MHz, $CDCl_3$): δ =7.43 (dd, J = 5.7, 1.5 Hz, 1H), 7.02 (d, J = 9.0, 2H), 6.6-6.54 (m, 2H), 6.08 (dd, J = 5.7, 2.0 Hz, 1H), 5.21 (m, 1H), 3.60 (d, J = 5.9, 2H), 2.95 (s, 3H), 2.21 (s, 3H).

^{13}C-NMR (100 MHz, $CDCl_3$): δ = 154.6, 146.3, 130.0, 126.8, 122.1, 112.7, 82.0, 55.4, 39.7, 20.2.

2.5 Photocatalytic Cyclopropane Functionalization

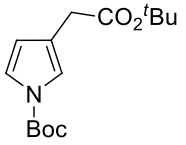

tert-butyl 3-(2-tert-butoxy-2-oxoethyl)-1H-pyrrole-1-carboxylate (277): (1S,5S,6S)-di-tert-butyl 2-azabicyclo[3.1.0]hex-3-ene-2,6-dicarboxylate (**273**) (84 µL, 0.3 mmol, 1.0 equiv.), methyl vinyl ketone (**23a**) (75 µL, 0.9 mmol, 3.0 equiv) and [Ir{dF(CF_3)ppy}$_2$(dtbbpy)]PF_6 (**216**·PF_6) (7 mg, 6 µmol, 2 mol%) were dissolved in acetonitrile (3 mL) in a Schlenk tube and degassed by three freeze pump thaw cycles. After internal irradiation with the help of an LED mounted to a glass rod that was immersed in the reaction solution, a dryload was prepared. Purification on silica gel was performed on a Varian Intelliflash 310 using a SF15-12g column starting with pure hexanes for 5 min and then raising the ethyl acetate amount by 1%/min. The pure product was obtained in 47% (40 mg, 0.14 mmol) yield.

R_f (9:1 hexanes : EtOAc) = 0.52.

IR (neat): 3022, 2983, 2022, 1724, 1370, 1215, 1150, 746, 666, 491 cm^{-1}.

^{1}H-NMR (300 MHz, $CDCl_3$): δ = 7.21 (dd, *J* = 3.4, 1.8 Hz, 1H), 6.09 (t, *J* = 3.3 Hz, 1H), 6.07 – 6.04 (m, 1H), 3.78 (d, *J* = 0.5 Hz, 2H), 1.57 (s, 9H), 1.44 (s, 9H).

^{13}C-NMR (75 MHz, $CDCl_3$): δ = 170.2, 149.3, 128.1, 121.5, 113.8, 109.9, 83.5, 80.7, 36.0, 28.1, 28.0.

HRMS: (EI-MS) *m/z* calculated for $C_{15}H_{24}NO_5$ [$MH^{+\bullet}$]: 282.1700, found 282.1701.

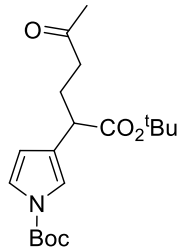

tert-butyl 3-(1-tert-butoxy-1,5-dioxohexan-2-yl)-1H-pyrrole-1-carboxylate (276): (1S,5S,6S)-di-tert-butyl 2-azabicyclo[3.1.0]hex-3-ene-2,6-dicarboxylate (**273**) (84 µL, 0.3 mmol, 1.0 equiv.), methyl vinyl ketone (**23a**) (75 µL, 0.9 mmol, 3.0 equiv) and [Ir{dF(CF_3)ppy}$_2$(dtbbpy)]PF_6 (**216**·PF_6) (7 mg, 6 µmol, 2 mol%) were dissolved in acetonitrile (3 mL) in a Schlenk tube and degassed by three freeze pump thaw cycles. After internal irradiation with the help of an LED mounted to a glass rod that was immersed in the reaction solution, a dryload was prepared. Purification on silica gel was performed on a Varian Intelliflash 310 using a SF15-12g column starting with pure hexanes for 5 min and then raising the ethyl acetate amount by 1%/min. The pure product was obtained in 27% (29 mg, 0.08 mmol) yield.

R_f (9:1 hexanes : EtOAc) = 0.20.

IR (neat): 3751, 2982, 2273, 2023, 1984, 1888, 1716, 1511, 1455, 1369, 1249, 1156, 524, 465 cm^{-1}.

^{1}H-NMR (300 MHz, $CDCl_3$): δ = 7.21 – 7.17 (m, 1H), 6.12 – 6.07 (m, 2H), 4.15 (t, *J* = 7.3 Hz, 1H), 2.56 (t, *J* = 7.5 Hz, 2H), 2.24 (ddd, *J* = 23.5, 15.1, 7.8 Hz, 2H), 2.11 (d, *J* = 2.8 Hz, 3H), 1.56 (s, 9H), 1.40 (s, 9H).

^{13}C-NMR (75 MHz, $CDCl_3$): δ = 208.3, 172.3, 149.4, 132.7, 121.7, 112.1, 110.1, 83.7, 80.8, 44.6, 41.7, 30.1, 28.1, 28.1, 25.3.

HRMS: (EI-MS) *m/z* calculated for $C_{19}H_{30}NO_5$ [$MH^{+\bullet}$]: 353.2118, found 352.2119.

2.6 Photoredoxcatalyst on Solid Support

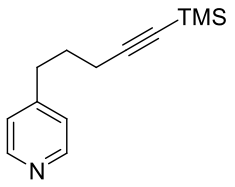

4-(5-(trimethylsilyl)pent-4-ynyl)pyridine (302): According to a procedure by Quing *et al*.[153] Diisopropylamine (0.7 mL, 4.7 mmol, 1.2 equiv.) was dissolved in dry THF (7 mL) under a nitrogen atmosphere at -78 °C (cooling bath: CO_2 (s) in ^{i}PrOH). *N*-Butyllithium (1.6 M solution in hexane, 3.0 mL, 4.7 mmol) was added dropwise. The mixture was stirred at -78 °C for 5 min and then allowed to warm to ambient temperature. The mixture was again cooled to -78 °C and picoline (**297**) (0.42 mL, 4.3 mmol, 1.1 equiv.), dissolved in THF (8 mL) was added. The reaction mixture was stirred at -78 °C for 5 min, then allowed to warm to 0 °C. In the following the mixture was cooled to -78 °C and (4-iodobut-1-ynyl)trimethylsilane[124] (**298**) (1.00 g, 4.0 mmol, 1 equiv.) was added as solution in THF (8 mL). The mixture was stirred overnight at ambient temperatures. After concentration in vacuo, the residue was dissolved in 50 mL DCM and washed with water (3 x 25 mL). The aqueous phase was extracted with DCM (50 mL) and the combined organic phases were dried over $MgSO_4$ and the solvent was removed in vacuo. The pure product was obtained in 66% (572 mg, 2.6 mmol) yield after purification on silica gel (1:1 hexanes : EtOAc).

R_f (hexanes : EtOAc 1:3) = 0.53.

^{1}H-NMR (300 MHz, $CDCl_3$): δ = 8.40 (dd, *J* = 4.5, 1.6 Hz, 2H), 7.02 (dd, *J* = 4.4, 1.6 Hz, 2H), 2.68 – 2.58 (m, 2H), 2.15 (t, *J* = 7.0 Hz, 2H), 1.74 (dt, *J* = 8.7, 7.0 Hz, 2H), 0.11 – 0.04 (m, 9H).

^{13}C-NMR (101 MHz, $CDCl_3$): δ = 150.6, 149.9, 124.1, 106.4, 85.8, 34.1, 29.1, 19.3, 0.2.

HRMS: (EI-MS) *m/z* calculated for $C_{13}H_{18}NSi$ [$M^{+\bullet}$-$H^{\bullet}$]: 216.1209, found 216.1210.

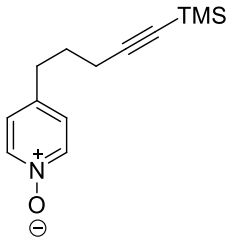

4-(5-(trimethylsilyl)pent-4-ynyl)pyridine 1-oxide (311): The synthesis adapted from *Tzschucke et al*.[154] 4-(5-(trimethylsilyl)pent-4-ynyl)pyridine (**302**) (200 mg, 0.9 mmol, 1 equiv.) was dissolved in acetic acid (2 mL). After the addition of hydrogen peroxide (30% (m/m) H_2O_2 in water, 150 µL, 1.1 mmol, 1.2 equiv.) the mixture was heated to 70 °C for 26 h. The mixture was cooled to ambient temperature and sat. $NaHCO_3$ (20 mL) were added. After extraction with DCM (3 x 10 mL) the

combined organic phases were dried over $MgSO_4$ and concentrated in vacuo. The semi stable product was obtained as red oil in 90% (193 mg, 0.8 mmol) yield and used for the following reactions without further purification.

^{1}H-NMR (300 MHz, $CDCl_3$): δ = 8.49 (d, *J* = 6.0, 1H), 8.13 (d, J = 7.1, 1H), 7.14 – 7.07 (m, 2H), 2.75 – 2.69 (m, 2H), 2.28 – 2.22 (m, 2H), 1.88 – 1.77 (m, 2H), 0.18 (s, 9H).

^{13}C-NMR (101 MHz, $CDCl_3$): δ = 149.9, 139.0, 126.3, 105.8, 86.24, 33.1, 29.0, 19.2, 0.3.

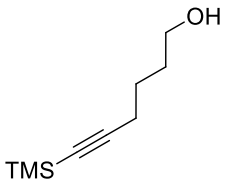

6-(trimethylsilyl)hex-5-yn-1-ol (314): The synthesis was adapted from Overman *et al.*[148] Under inert atmosphere hex-5-yn-1-ol (**313**) (3 mL, 26.9 mmol, 1 equiv.) was dissolved in dry THF (60 mL) at 0 °C. After the addition of ethylmagnesium bromide[155] (as solution in THF, 7.35 g, 55.1 mmol, 2 equiv.) the solution was warmed to ambient temperatures for 5 min and then cooled to 0 °C. After the addition of chlorotrimethylsilane (7 mL, 55.1 mmol, 2 equiv.), the solution was stirred overnight at ambient temperatures. After concentration in vacuo the product was purified by bulb to bulb distillation (bp: 96 °C @ 4 mbar) to obtained the product as colorless oil (2.36 g, 13.9 mmol, 50%). The ^{1}H-NMR spectra is good accordance with literature.[156]

^{1}H-NMR (300 MHz, $CDCl_3$): δ = 3.68 (t, *J* = 6.1 Hz, 2H), 2.27 (t, J = 6.9, 2H), 1.71 – 1.59 (m, 4H), 0.19 – 0.10 (m, 9H).

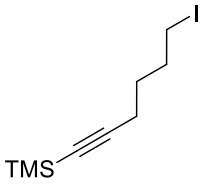

(6-iodohex-1-ynyl)trimethylsilane (315): The synthesis was adapted from de Meijere *et al.*[124] 6-(trimethylsilyl)hex-5-yn-1-ol (**314**) (1.0 g, 5.9 mmol, 1 equiv.), imidazole (0.74 g, 10.9 mmol, 1.9 equiv.), and triphenylphosphine (2.69 g, 10.3 mmol, 1.8 equiv.) were dissolved in diethyl ether (15 ml) and acetonitrile (10,5 ml) at 0 °C to give a colorless solution. Iodine (3.54 g, 14.0 mmol, 2 equiv.) was added in small portions and the mixture was stirred at 0 °C for 2 h. The brown solution was diluted with diethyl ether (100 mL) and washed with sat. $Na_2S_2O_3$ solution until the organic phase was colorless and dried over MgSO4. The solvent was evaporated and a dryload was prepared. After purification on silica gel (pure hexanes) the product was obtained in 69% (1.14 g, 4.1 mmol) yield. The ^{1}H-NMR spectra is good accordance with literature.[157]

R_f (pure hexanes) = 0.5

^{1}H-NMR (300 MHz, $CDCl_3$): δ 3.22 (t, *J* = 6.9 Hz, 2H), 2.26 (t, *J* = 7.0 Hz, 2H), 2.00 – 1.87 (m, 2H), 1.67 – 1.54 (m, 2H), 0.15 (s, 9H).

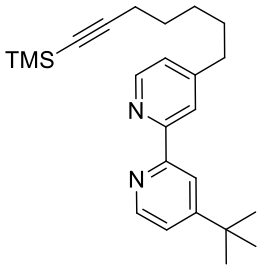

4-tert-butyl-4'-(7-(trimethylsilyl)hept-6-ynyl)-2,2'-bipyridine (317): Diisopropylamine (0.34 mL, 2.4 mmol, 1.2 equiv.) was dissolved in dry THF (5 mL) in a flame dried Schlenk flask under a nitrogen atmosphere and cooled to -78 °C. *N*-Butyllithium (1.6 M solution in hexane, 1.5 mL, 2.4 mmol, 1.2 equiv.) was added dropwise, the solution was warmed to ambient temperatures and stirred for 5 min. After cooling to -78 °C, 4-tert-butyl-4'-methyl-2,2'-bipyridine (**316**) (0.5 g, 2.2 mmol, 1.1 equiv.), dissolved in THF (5 mL), was added *via* syringe pump within 30 min. During the addition the mixture turned black. 15 min after the complete addition, (6-iodohex-1-ynyl)trimethylsilane (**315**) (0.56 g, 2.0 mmol) dissolved in THF (5 mL), was added. The solution was warmed to ambient temperatures and stirred overnight. After concentration in vacuo, the residue was dissolved in DCM (50 mL) and washed with water (3 x 50 mL). The aqueous phase was extracted with DCM (2 x 50 mL). The combined organic phases were dried over $MgSO_4$ filtered and a dryload was prepared. Purification on silica gel (4:1 to 2:1 hexanes : EtOAc) yielded 51% of **317** (0.43 g, 1.1 mmol) as brown oil.

R_f (hexanes : EtOAc 1:1) = 0.56

IR (neat): 2963, 2941, 2862, 2197, 2166, 2134, 2019, 1994, 1976, 1943, 1593, 1546, 1460, 1377, 1248, 1075, 994, 900, 837, 758, 695, 669, 638, 611, 557, 529 cm^{-1}.

^{1}H-NMR (300 MHz, $CDCl_3$): δ = 8.57 (td, *J* = 5.1, 0.6 Hz, 2H), 8.42 (dd, *J* = 1.9, 0.6 Hz, 1H), 8.22 (d, *J* = 0.9 Hz, 1H), 7.30 (dd, *J* = 5.3, 2.0 Hz, 1H), 7.12 (dd, *J* = 5.0, 1.7 Hz, 1H), 2.75 – 2.65 (m, 2H), 2.21 (t, *J* = 6.9 Hz, 2H), 1.77 – 1.62 (m, 2H), 1.61 – 1.40 (m, 4H), 1.38 (s, 9H), 0.12 (s, 9H).

^{13}C-NMR (75 MHz, $CDCl_3$): δ = 161.2, 156.5, 156.3, 152.7, 149.1, 123.9, 121.5, 121.0, 118.4, 107.4, 84.7, 35.5, 35.1, 30.7, 30.0, 28.5, 19.9, 0.3.

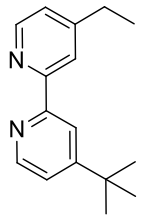

4-tert-butyl-4'-ethyl-2,2'-bipyridine (318): KO^{t}Bu (83 mg, 0.7 mmol, 2 equiv.) and diisopropylamine (0.1 ml, 0.7 mmol, 2 equiv.) were dissolved in dry THF (2 mL) under a nitrogen atmosphere to give a colorless solution. The solution was cooled to -30 °C (acetone/dry ice) and *n*-butyllithium (1.6 M solution in hexane, 0.46 mL, 0.7 mmol, 2 equiv.) was added. The solution was stirred for 30 min, then it was cooled to -50 °C. At this temperature, 4-tert-butyl-4'-methyl-2,2'-bipyridine (**316**) (80 mg, 0.35 mmol, 1 equiv.) dissolved in dry THF (2 mL) was added. After stirring for 2 h, the mixture was cooled to -78°C and MeI (0.13 mL, 2.1 mmol) was added. The solution was warmed to ambient temperatures and stirred overnight. The reaction was quenched by addition of water (25 mL). The aqueous phase was extracted with DCM (3 x 25 mL). The combined organic phases were dried over $MgSO_4$, filtered and a dryload was prepared. Purification on silica gel (3:1 hexanes : EtOAc) yielded 79% of **318** (67 mg, 1.1 mmol).

^{1}H-NMR (300 MHz, $CDCl_3$): δ = 8.61 – 8.50 (m, 2H), 8.43 – 8.37 (m 1H), 8.25 – 8.18 (m, 1H), 7.32 – 7.27 (m, 1H), 7.15 – 7.08 (m, 1H), 2.71 (q, *J* = 7.6 Hz, 2H), 1.36 (s, 9H), 1.28 (t, *J* = 7.6 Hz, 3H).

^{13}C-NMR (75 MHz, $CDCl_3$): δ = 160.0, 155.2, 153.0, 148.0, 147.0, 123.5, 122.3, 121.0, 119.9, 117.2, 34.0, 29.6, 27.4, 13.4.

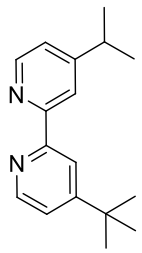

4,4'-di-tert-butyl-2,2'-bipyridine (319): KO^{t}Bu (83 mg, 0.7 mmol, 3 equiv.) and diisopropylamine (0.1 ml, 0.7 mmol, 3 equiv.) were dissolved in dry THF (2 mL) under a nitrogen atmosphere to give a colorless solution. The solution was cooled to -30 °C (acetone/dry ice) and *n*-butyllithium (1.6 M solution in hexane, 0.46 mL, 0.7 mmol, 3 equiv.) was added. The solution was stirred for 30 min, and then it was cooled to -50 °C. At this temperature, 4-tert-butyl-4'-ethyl-2,2'-bipyridine (**318**) (60 mg, 0.3 mmol, 1 equiv.) dissolved in dry THF (2 mL) was added. After stirring for 2 h, the mixture was cooled to -78 °C and MeI (0.13 mL, 2.1 mmol, 9 equiv.) was added. The solution was warmed to ambient temperature and stirred overnight. The reaction was quenched by addition of water (25 mL). The aqueous phase was extracted with DCM (3 x 25 mL). The combined organic phases were

dried over $MgSO_4$, filtered and a dryload was prepared. Purification on silica gel (2:1 hexanes : EtOAc) yielded 65% of **319** (41 mg, 0.2 mmol).

^{1}H-NMR (300 MHz, $CDCl_3$): δ = 8.59 – 8.56 (m, 2H), 8.43 – 8.39 (m, 1H), 8.27 – 8.22 (m, 1H), 7.29 (dd, *J* = 5.2, 2.0 Hz, 1H), 7.19 – 7.12 (m, 1H), 3.07 – 2.62 (m, 1H), 1.37 (s, 9H), 1.30 (d, *J* = 6.9 Hz, 6H).

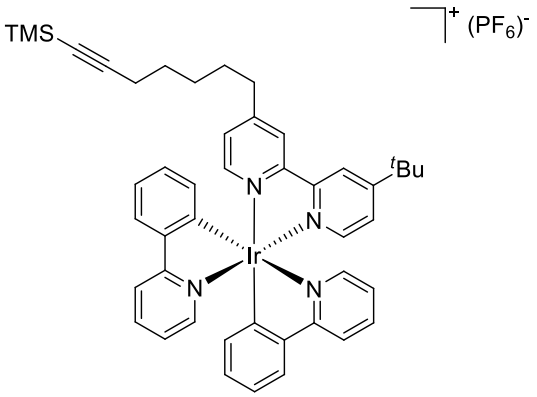

Bis(2-phenylpyridine-C^2,N')(4-tert-butyl-4'-(7-(trimethylsilyl)hept-6-ynyl)-2,2'-bipyridine)iridium hexafluorophosphate (322): Similar to a procedure by Malliaras *et al*.[139] Tetrakis(2-phenylpyridine-C^2,N')(μ-dichloro)-diiridium (**294**)[139] (156 mg, 0.15 mmol, 0.5 equiv.) and 4-tert-butyl-4'-(7-(trimethylsilyl)hept-6-ynyl)-2,2'-bipyridine (**317**) (110 mg, 0.3 mmol, 1 equiv.) were dissolved in ethylene glycol (10 mL) under an atmosphere of nitrogen and heated to 150 °C for 18 h. The mixture was diluted with water (150 mL) and extracted with hexanes (2 x 50 mL). The aqueous phase was heated to 75°C for 30 min and NH_4PF_6 (600 mg, 3.6 mmol, 24 equiv.) in water (5 mL) was added. The yellow precipitated was filtered of and dried in a desiccator over P_4O_{10}. Recrystallization in hot toluene yielded **x150x** as yellow crystals (202 mg, 0.2 mmol, 79%). The TMS-protection group was often removed during recrystallization giving rise to product **322**.

HRMS: (ESI MS) *m/z* calculated for $C_{46}H_{50}IrN_4Si$ [$M^{+\bullet}$]: 879.3430, found 879.3424.

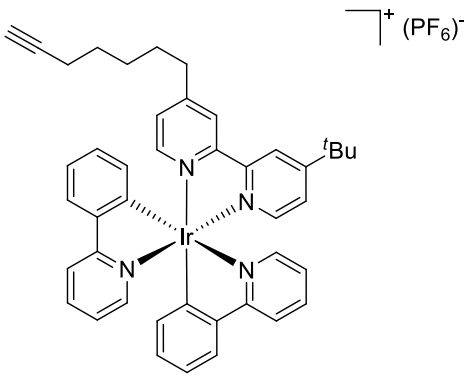

Bis(2-phenylpyridine-C^2,N')(4-tert-butyl-4'-(hept-6-ynyl)-2,2'-bipyridine)-2,2'-bipyridine)iridium hexafluorophosphate (323): Bis(2-phenylpyridine-C^2,N')(4-tert-butyl-4'-(7-(trimethylsilyl)hept-6-ynyl)-2,2'-bipyridine)iridium hexafluorophosphate (**322**) (50 mg, 0.06 mmol, 1 equiv.) was dissolved

in THF (1 ml) to give a yellow solution. Tetra-*n*-butylammonium fluoride (19 mg, 0.07 mmol, 1.3 equiv.) was added in small portions. The solution turned black instantly. The mixture was stirred overnight and DCM (10 mL) were added. The organic phase was washed with water (2 x 5 mL) and concentrated in vacuo to give rise a yellow powder.

IR (neat): 3913, 3676, 3113, 3058, 3029, 2875, 2643, 2550, 2419, 2246, 2230, 2213, 2091, 2046, 2034, 2019, 2004, 1606, 1583, 1550, 1477, 1420, 1314, 1368, 1162, 1127, 1081, 1061, 1030, 913, 879, 832, 758, 727, 694, 669, 630, 556 cm^{-1}.

^{1}H-NMR (300 MHz, acetone): δ = 8.93 – 8.82 (m, 2H), 8.23 (d, *J* = 8.3 Hz, 2H), 8.02 – 7.86 (m, 6H), 7.80 (t, *J* = 6.9 Hz, 2H), 7.71 (dd, *J* = 5.9, 1.9 Hz, 1H), 7.57 (dd, *J* = 5.6, 1.6 Hz, 1H), 7.15 (dd, *J* = 10.4, 4.3 Hz, 3H), 7.06 – 6.99 (m, 2H), 6.91 (t, *J* = 7.4 Hz, 2H), 6.39 – 6.30 (m, 2H), 2.92 – 2.79 (m, 3H), 2.35 – 2.26 (m, 2H), 1.73 (dt, *J* = 15.2, 7.7 Hz, 2H), 1.59 – 1.46 (m, 3H), 1.41 (s, 9H).

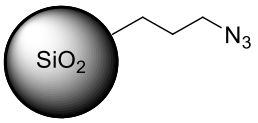

Azide silica particles (326): (3-azidopropyl)triethoxysilane (**325**) (0.5 mL, 2.1 mmol, 1 equiv.), tetraethyl orthosilicate (2.,4 mL, 10.7 mmol, 5 equiv.), and ammonia (5 mL, 42.8 mmol, 10 equiv.) were dissolved in water (50 mL) to give a colorless solution. After heating to 80 °C for 16 h the solution was filtered and the precipitate was washed with water and acetone. Yield: 889.3 mg;

Elemental analysis: 9.4767% Nitrogen => Loading: 2.26 mmol/g.

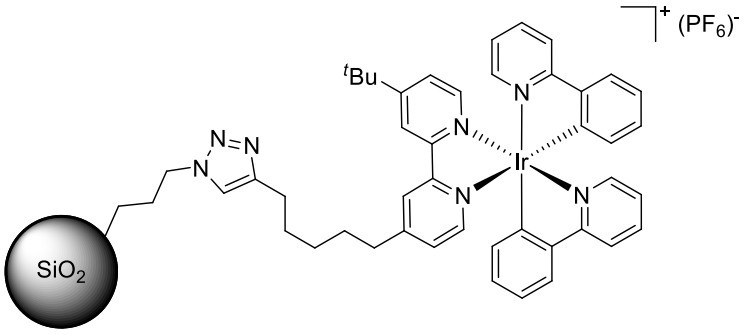

Silica bound photoredox catalyst (327): Under an atmosphere of nitrogen azide-particles (**326**) (116 mg, 0.2 mmol, 2 equiv.), CuI (9 mg, 0.05 mmol, 20 mol%), and DIPEA (40 µL, 0.2 mmol, 2 equiv.) were dissolved in degassed DCM (2 mL). Bis(2-phenylpyridine-C^2,N')(4-tert-butyl-4'-(hept-6-ynyl)-2,2'-bipyridine)-2,2'-bipyridine)iridium hexafluorophosphate (**323**) (94 mg, 0.1 mmol, 1 equiv.), dissolved in DCM (2 mL) was added and the mixture was stirred for 3 days. The particles were filtered off and washed several times with DCM. Yield: 24.2 mg

ICP measurement: 7 µmol/l => Loading: 35 µmol/g

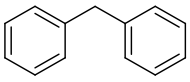

Diphenylmethane (329): $[Ir(ppy)_2(dtbbpy)]PF_6$ (**204**·PF_6), (1.8 mg, 2.0 µmol, 0.1 mol%), benzhydryl ethyl oxalate (**328**) (57 mg, 0.2 mmol), DIPEA (68 µL, 0.4 mmol, 2 equiv.), water (36 µL, 2.0 mmol, 10 equiv.) and naphthalene (25.6 mg, 0.2 mmol, 1 equiv.) were dissolved in acetonitrile (2.0 mL) in a pressure tube. The solution was irradiated without degassing with an LED stick overnight at ambient temperatures and afterwards for 45 min at 60 °C. The mixture was filtered through a syringe filter and analyzed by gas chromatography (start: 100 °C, 0 min; rate: 20 K/min; end: 300 °C, 2 min). Average yield of three runs: 91%

$[Ir(ppy)_2(dtbbpy)]PF_6$ (**204**·PF_6), (1.8 mg, 2.0 µmol, 0.1 mol%), benzhydryl ethyl oxalate (**328**) (57 mg, 0.2 mmol), DIPEA (68 µL, 0.4 mmol, 2 equiv.), water (36 µL, 2.0 mmol, 10 equiv.), naphthalene (25.6 mg, 0.2 mmol, 1 equiv.) and SiO2 (50,5 mg, 0,840 mmol) were dissolved in acetonitrile (2.0 mL) in a pressure tube and irradiated without degassing with an LED stick overnight at ambient temperatures and afterwards for 45 min at 60°C. The mixture was filtered through a syringe filter and analyzed by gas chromatography (start: 100 °C, 0 min; rate: 20 K/min; end: 300 °C, 2 min). Average yield of three runs: 90%

Experiments with silica bound catalyst A (loading: 35 µmol/g)

Table 26, entry 1: Catalyst **327** (16 mg, 0.55 µmol, 0.5 mol%), benzhydryl ethyl oxalate (**328**) (31 mg, 0.11 mmol, 1 equiv.), DIPEA (37 µL, 0.22 mmol, 2 equiv.), water (20 µL, 1.1 mmol, 10 equiv.) and naphthalene (14 mg, 0.1 mmol, 1 equiv.) were dissolved in acetonitrile (1.0 mL) and irradiated without degassing with an LED stick for 1.5 h at ambient temperatures. The mixture was filtered through a syringe filter and analyzed by gas chromatography (start: 100 °C, 0 min; rate: 20 K/min; end: 300 °C, 2 min). Average yield of three runs: 0%. Recovered catalyst: 4 mg.

Table 26, entry 2: Catalyst **327** (4 mg, 0.14 µmol, 0.1 mol%), benzhydryl ethyl oxalate (**328**) (40 mg, 0.14 mmol, 1 equiv.), DIPEA (48 µL, 0.36 mmol, 2 equiv.), water (25 µL, 1.4 mmol, 10 equiv.) and naphthalene (18 mg, 0.14 mmol, 1 equiv.) were dissolved in acetonitrile (1.0 mL) and irradiated without degassing with an LED stick for 1.5 h at 60 °C. The mixture was filtered through a syringe filter and analyzed by gas chromatography (start: 100 °C, 0 min; rate: 20 K/min; end: 300 °C, 2 min). Average yield of three runs: 48%. Recovered catalyst: 0 mg.

Experiments with silica bound catalyst B (loading: 18 µmol/g)

Table 27, entry 1: Catalyst **327** (25 mg, 0.45 µmol, 0.1 mol%), benzhydryl ethyl oxalate (**328**) (128 mg, 0.45 mmol, 1 equiv.), DIPEA (153 µL, 0.9 mmol, 2 equiv.), water (81 µL, 4.5 mmol, 10 equiv.) and naphthalene (58 mg, 0.45 mmol, 1 equiv.) were dissolved in acetonitrile (4.0 mL) and irradiated without degassing with an LED stick for 4 h at 60 °C. The mixture was filtered through a syringe filter and analyzed by gas chromatography (start: 100 °C, 0 min; rate: 20 K/min; end: 300 °C, 2 min). Average yield of three runs: 92%. Recovered catalyst: 18 mg.

Table 27, entry 2: Catalyst **327** (18 mg, 0.32 µmol, 0.1 mol%), benzhydryl ethyl oxalate (**328**) (91 mg, 0.32 mmol, 1 equiv.), DIPEA (110 µL, 0.64 mmol, 2 equiv.), water (58 µL, 3.2 mmol, 10 equiv.) and naphthalene (41 mg, 0.32 mmol, 1 equiv.) were dissolved in acetonitrile (3.0 mL) and irradiated without degassing with an LED stick for 4 h at 60 °C. The mixture was filtered through a syringe filter and analyzed by gas chromatography (start: 100 °C, 0 min; rate: 20 K/min; end: 300 °C, 2 min). Average yield of three runs: 29%. Recovered catalyst: 11 mg.

Table 27, entry 3: Catalyst **327** (11 mg, 0.2 µmol, 0.1 mol%), benzhydryl ethyl oxalate (**328**) (57 mg, 0.2 mmol, 1 equiv.), DIPEA (68 µL, 0.4 mmol, 2 equiv.), water (36 µL, 2.0 mmol, 10 equiv.) and naphthalene (26 mg, 0.2 mmol, 1 equiv.) were dissolved in acetonitrile (2.0 mL) and irradiated without degassing with an LED stick for 22 h at 60 °C. The mixture was filtered through a syringe filter and analyzed by gas chromatography (start: 100 °C, 0 min; rate: 20 K/min; end: 300 °C, 2 min). Average yield of three runs: 15%. Recovered catalyst: 6 mg.

Table 27, entry 4: Catalyst **327** (6 mg, 0.1 µmol, 0.1 mol%), benzhydryl ethyl oxalate (**328**) (28 mg, 0.1 mmol, 1 equiv.), DIPEA (34 µL, 0.2 mmol, 2 equiv.), water (18 µL, 1.0 mmol, 10 equiv.) and naphthalene (13 mg, 0.1 mmol, 1 equiv.) were dissolved in acetonitrile (1.0 mL) and irradiated without degassing with an LED stick for 22 h at 60 °C. The mixture was filtered through a syringe filter and analyzed by gas chromatography (start: 100 °C, 0 min; rate: 20 K/min; end: 300 °C, 2 min). Average yield of three runs: 0%. Recovered catalyst: 0 mg.

3. References

[135] Li, Z.; Li, C. J. *J. Am. Chem. Soc.*, **2005**, *127* , 6968–6969.

[136] Kraus, G. A.; Gupta, V.; Kohut, M.; Singh, N. *Bioorg. Med. Chem. Lett.*, **2009**, *19*, 5539-5542.

[137] Kohls, P.; Jadhav, D.; Pandey G.; Reiser O. *Org. Lett.* **2012**, *14*, 672.

[138] Tanielian, C. *Coord. Chem. Rev.* **1998**, *178–180*, 1165.

[139] Slinker, J. D.; Gorodetsky, A. A.; Lowry, M. S.; Wang, J.; Parker, S.; Rohl, R.; Bernhard, S.; Malliaras G. G. *J. Am. Chem. Soc.* **2004**, *126*, 2763.

[140] Kwong, F. A.; Klapars, A.; Buchwald, S. L. *Org. Lett.* **2002**, 4, 581 - 584

[141] Lowry, M. S.; Goldsmith, J. I.; Slinker, J. D.; Rohl, R.; Pascal, R.A.; Malliaras, G. G.; Bernhard S. *Chem. Mater.* **2005**, *17*, 5712

[142] Rosso, G. B.; Pilli, R. A., *Tetrahedron Letters*, **2006**, *47*, 185.

[143] Shen, Y.; Tan, Z.; Chen, D.; Feng, X.; Li,M.; Guo, C.-C.; Zhu, C. *Tetrahedron* **2009**, *65*, 158.

[144] Boeckman, R. K.; Pero, J. E.; Boehmler, D. J. *J. Am. Chem. Soc.* **2006**, *128*, 11032.

[145] Curti, C.; Battistini, L.; Zanardi, F.; Rassu, G.; Zambrano, V.; Pinna L.; Casiraghi G. *J. Org. Chem.* **2010**, *75*, 8681.

[146] Rueping, M.; Leonori D.; Poisson, T. *Chem. Commun.* **2011**, *47*, 9615.

[147] Ross, H. B.; Boldaji, M.; Rillema, D., P.; Blanton, C. B.; White, R. P. *Inorg. Chem.* **1989**, *28*, 1013.

[148] Overman, E. L.; Brown, M. J.; McCann, S. F. *Org. Synth.* **1990**, *68*, 182.

[149] Bräse, S.; Wertel, H.; Frank, D.; Vidović, D.; de Meijere, A. *Eur. J. Org. Chem.***2005**, *19*, 4167–4178.

[150] Nakazawa, J.; Smith, B. J.; Stack, T. D. P. *J. Am. Chem. Soc.*, **2012**, *134*, 2750.

[151] http://chem.chem.rochester.edu/~nvd/pages/how-to.php?page=degas_solvents

[152] Catino, A. J.; Nichols, J. M.; Nettles, B. J.; Doyle. M. P. *J. Am. Chem. Soc.*, **2006**, *128*, 5648.

[153] Sun, J.-Y.; Qiu, X.-L.; Meng, W.-D.; Qing, F.-L. *Tetrahedron* **2006**, *62*, 8702.

[154] Duric, S.; Tzschucke, C. C. *Organic Letters* **2011**, *13*, 2310.

[155] Skattebøl, L.; Jones, E. R. H.; Whiting, M. C. *Org. Synth* **1959**, *39*, 56.

[156] Stork, G., Tang, P. C.; Casey, M.; Goodman, B.; Toyota, M. *J. Am. Chem. Soc.* **2005**, *127*, 16255.

[157] Kita, Y.; Okunaka, R.; Honda, T.; Shindo, M.; Taniguchi, M.; Kondo, M.; Sasho M. *J. Org. Chem.* **1991**,*56*, 119.

E. Appendix

1. NMR Spectra

^{1}H-NMR spectra: upper image

^{13}C-NMR spectra (DEPT 135 integrated): lower image

Solvent and frequency are stated each spectrum.

Calculated superimposed spectra of 2-phenyl-1,2,3,4-tetrahydroisoquinoline (**2a**, red line) and 4-(2-phenyl-1,2,3,4-tetrahydroisoquinolin-1-yl)butan-2-one (**24a**, green line)

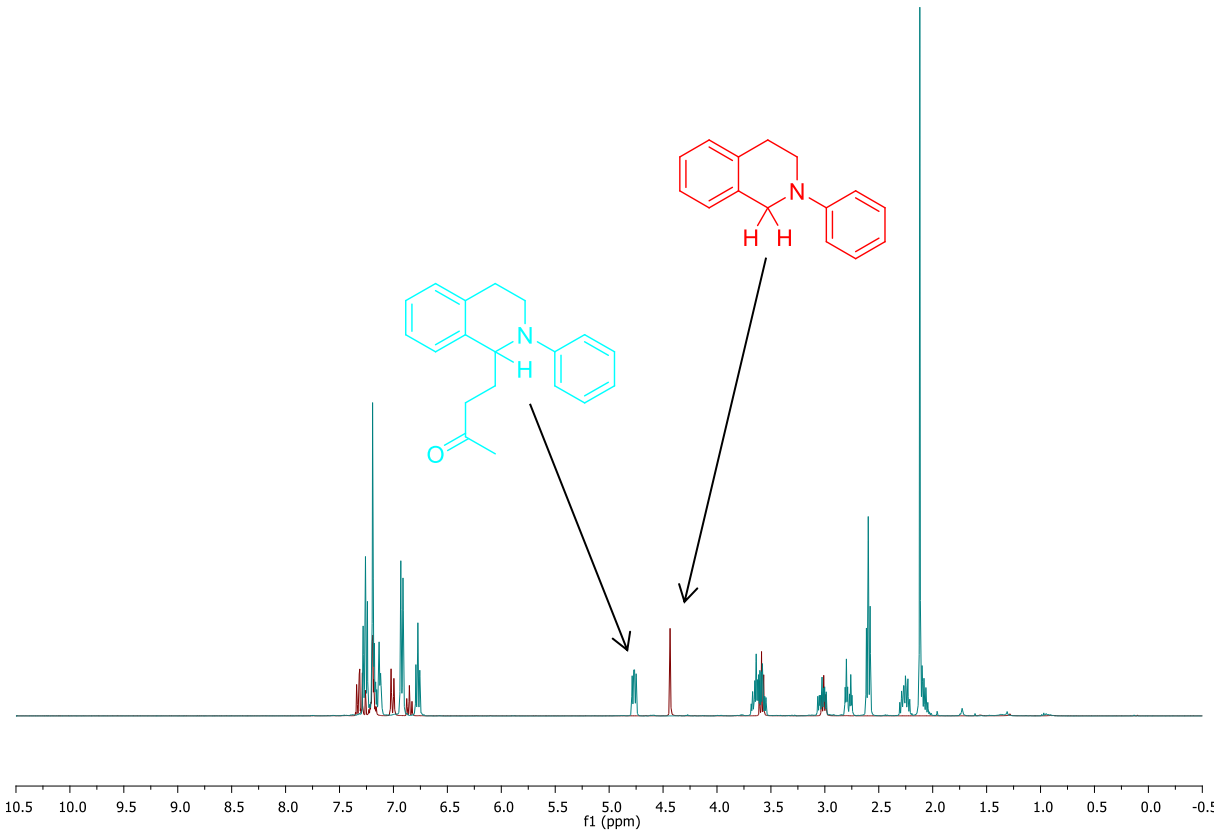

Spectra of the crude reaction mixture with 1,2-Dicyanobenzen as internal standard of the reaction in Chapter 1.4, table 4, entry 2 (1 equiv. isoquinoline **2a**, 3 equiv. MVK (**23a**), 1 mol% **204**·PF_6)

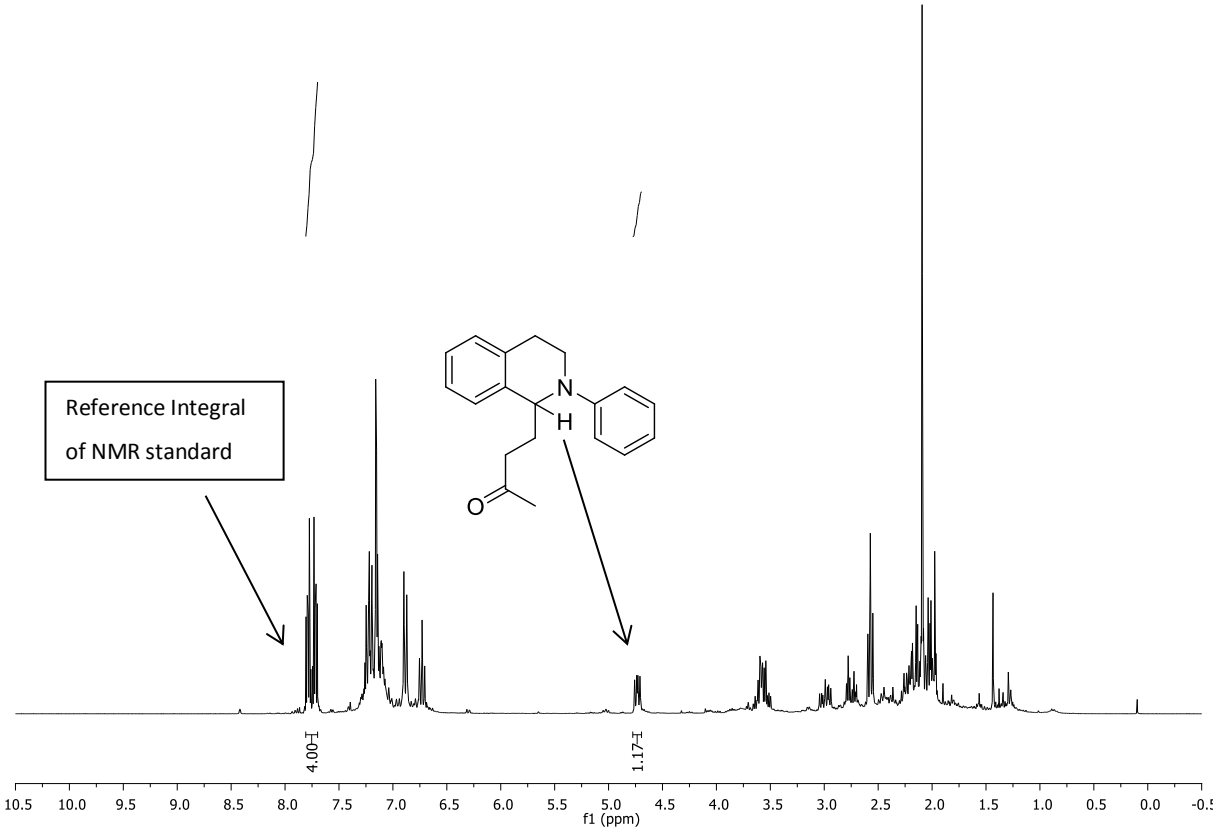

5-(methyl(phenyl)amino)pentan-2-one (209)

300 MHz, $CDCl_3$

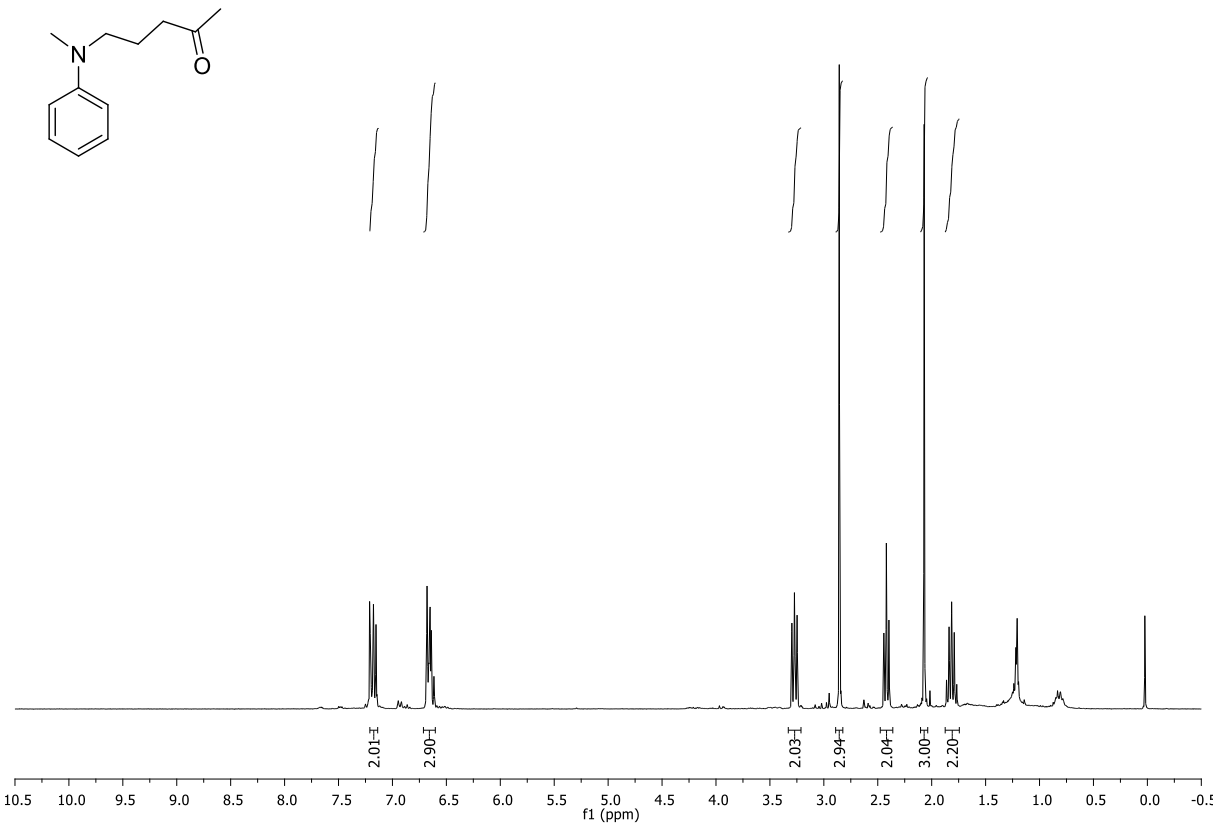

75 MHz, $CDCl_3$

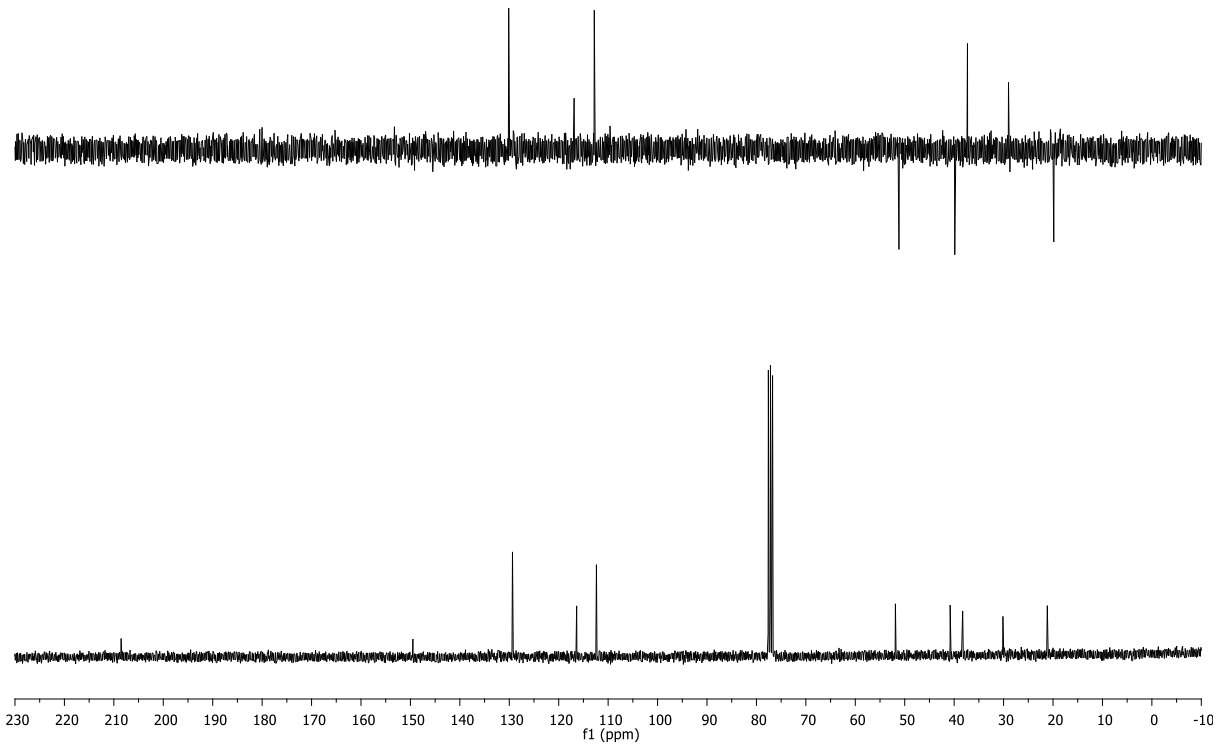

4-(1-phenylpyrrolidin-2-yl)butan-2-one (213)

300 MHz, $CDCl_3$

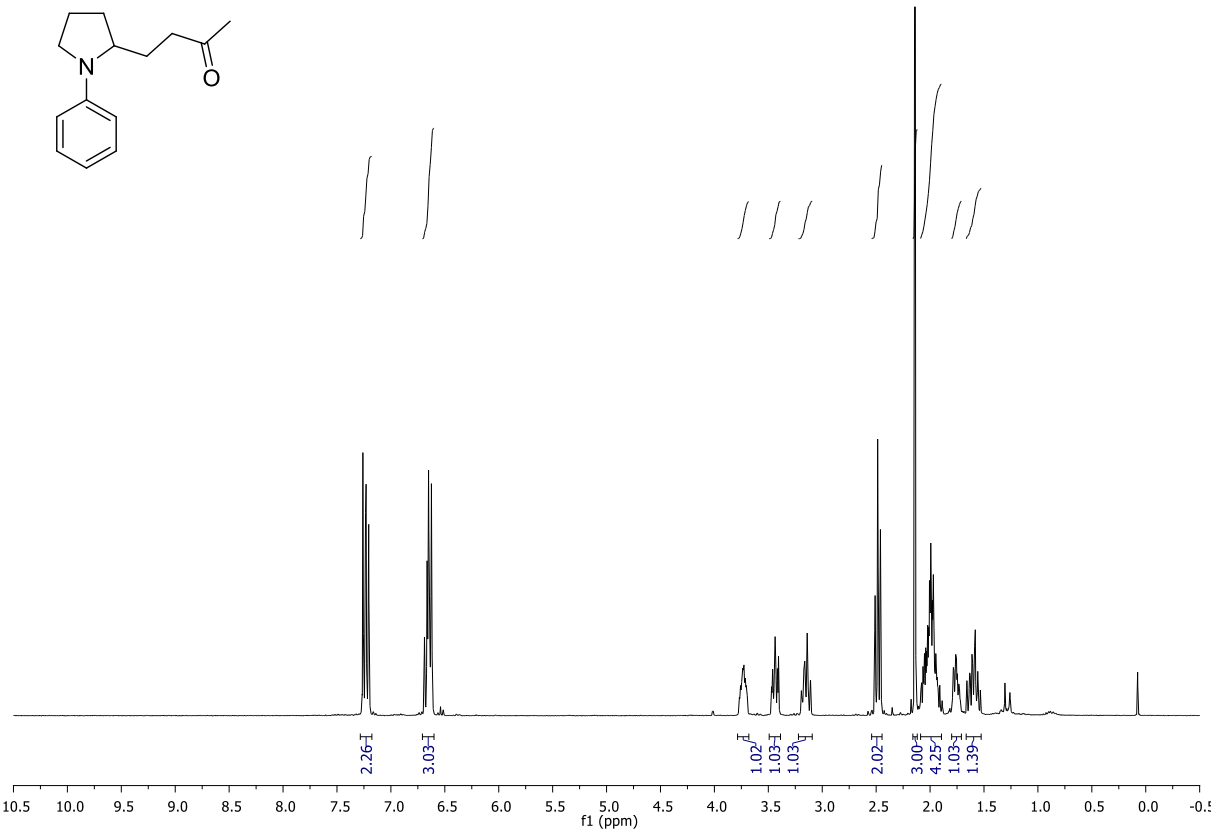

75 MHz, $CDCl_3$

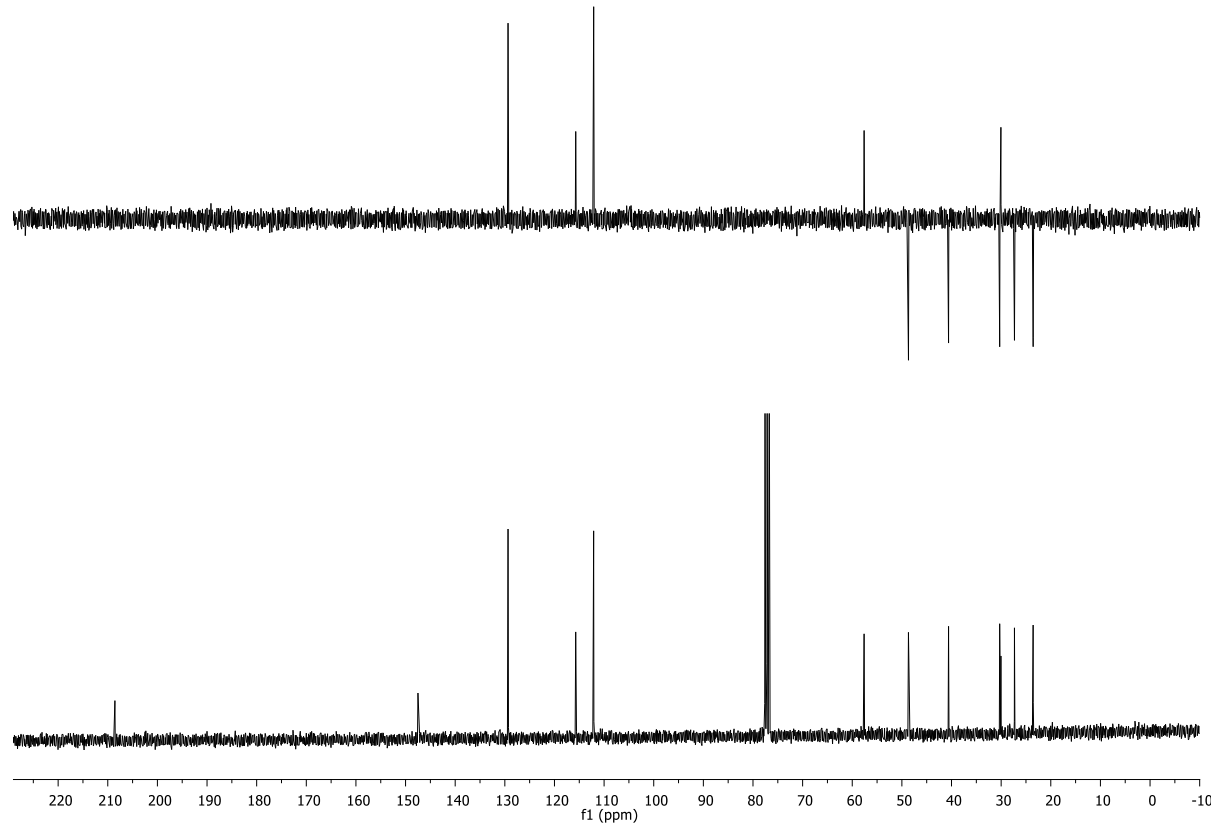

5-((methyl(phenyl)amino)methyl)furan-2(5H)-one (232)

400 MHz, $CDCl_3$

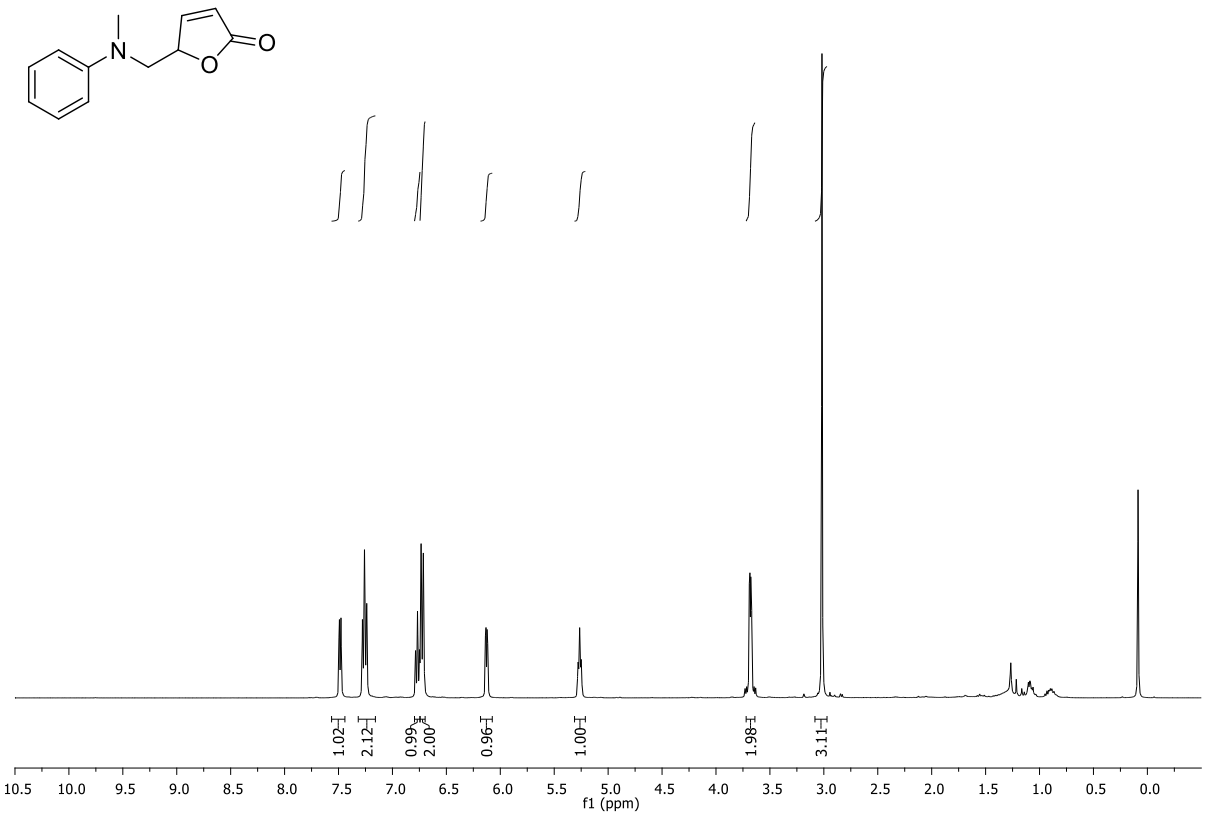

100 MHz, $CDCl_3$

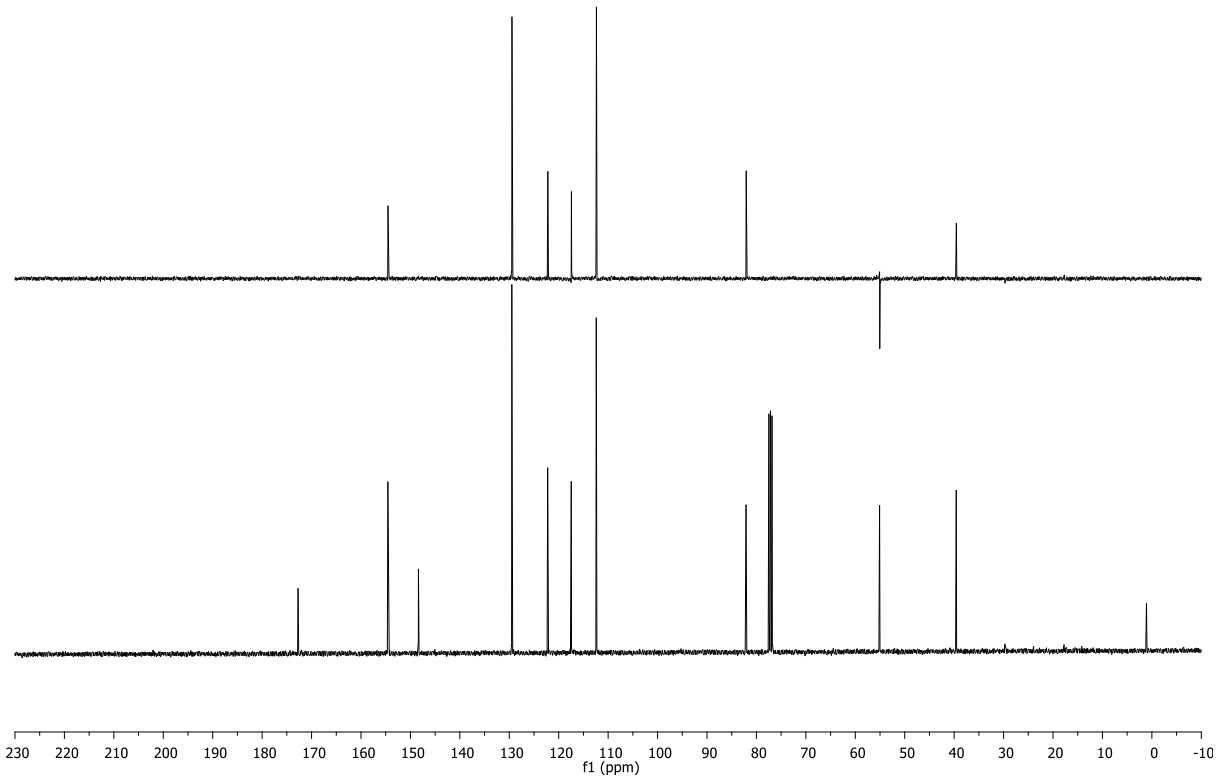

5-((methyl(p-tolyl)amino)methyl)furan-2(5H)-one (235)

400 MHz, $CDCl_3$

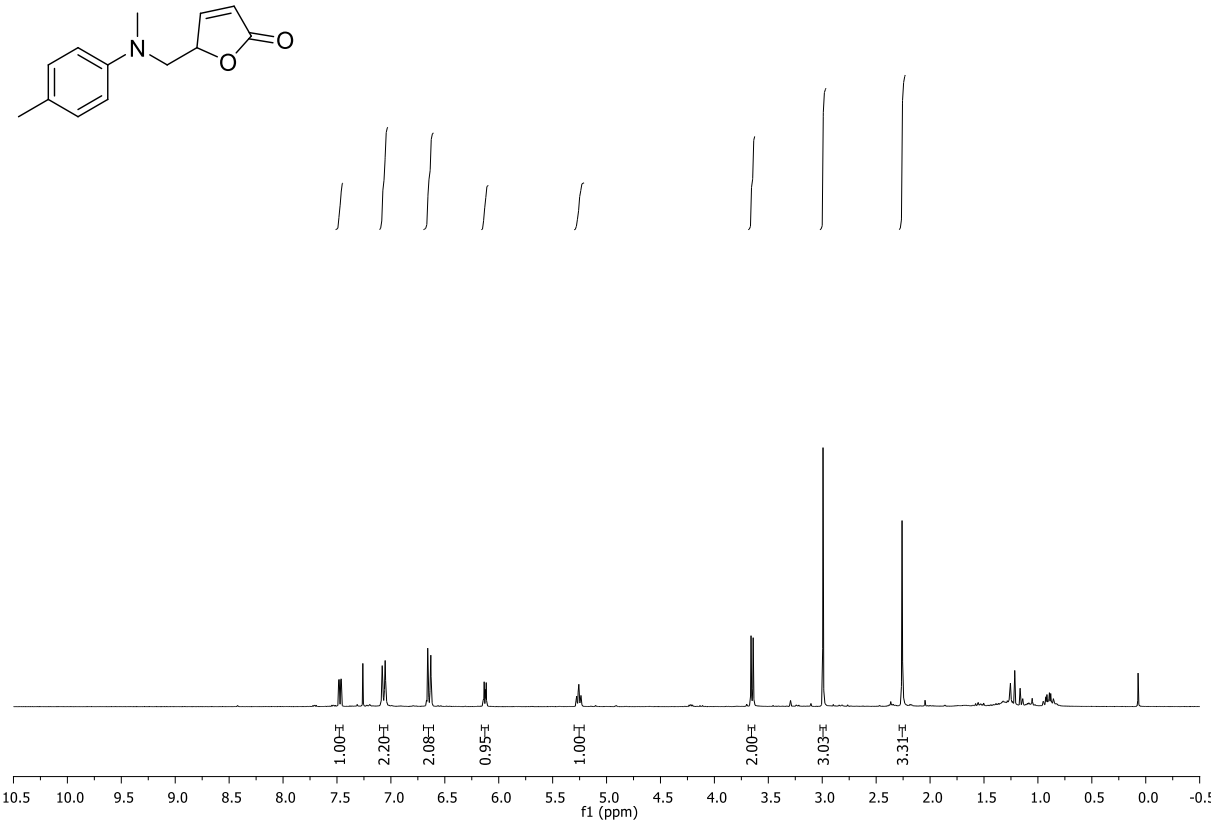

100 MHz, $CDCl_3$

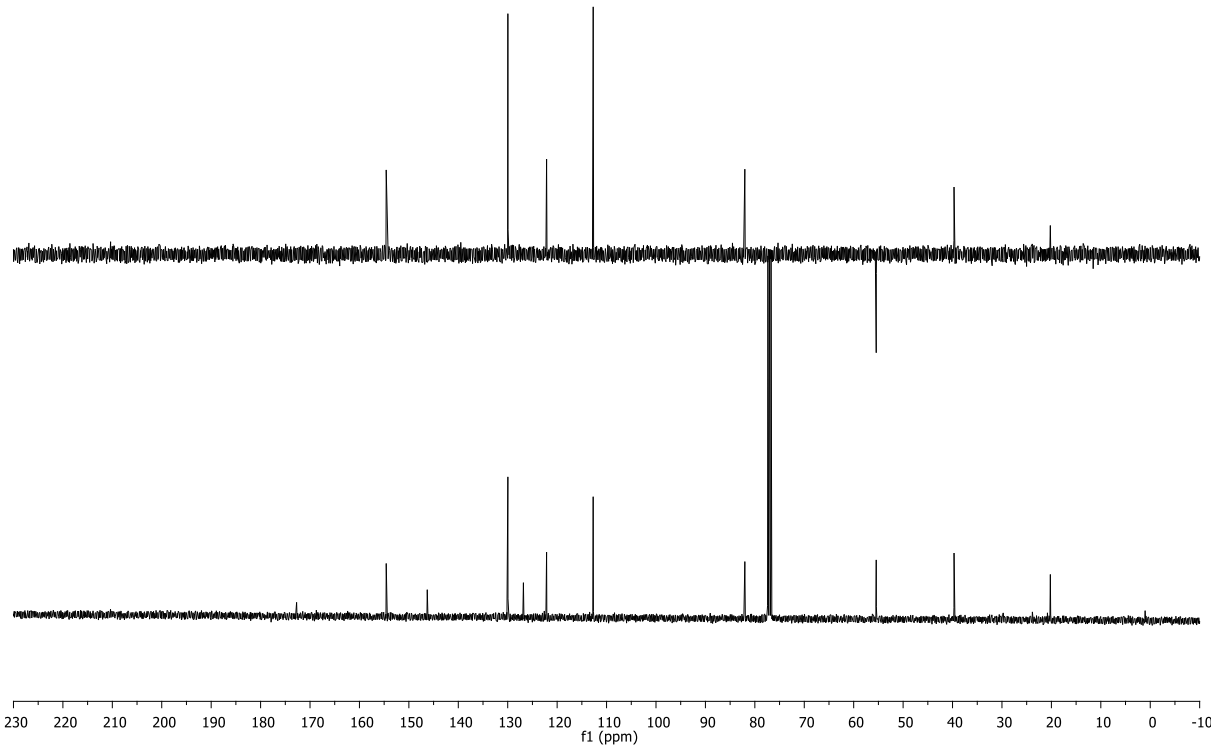

tert-butyl 3-(2-tert-butoxy-2-oxoethyl)-1H-pyrrole-1-carboxylate (277)

300 MHz, $CDCl_3$

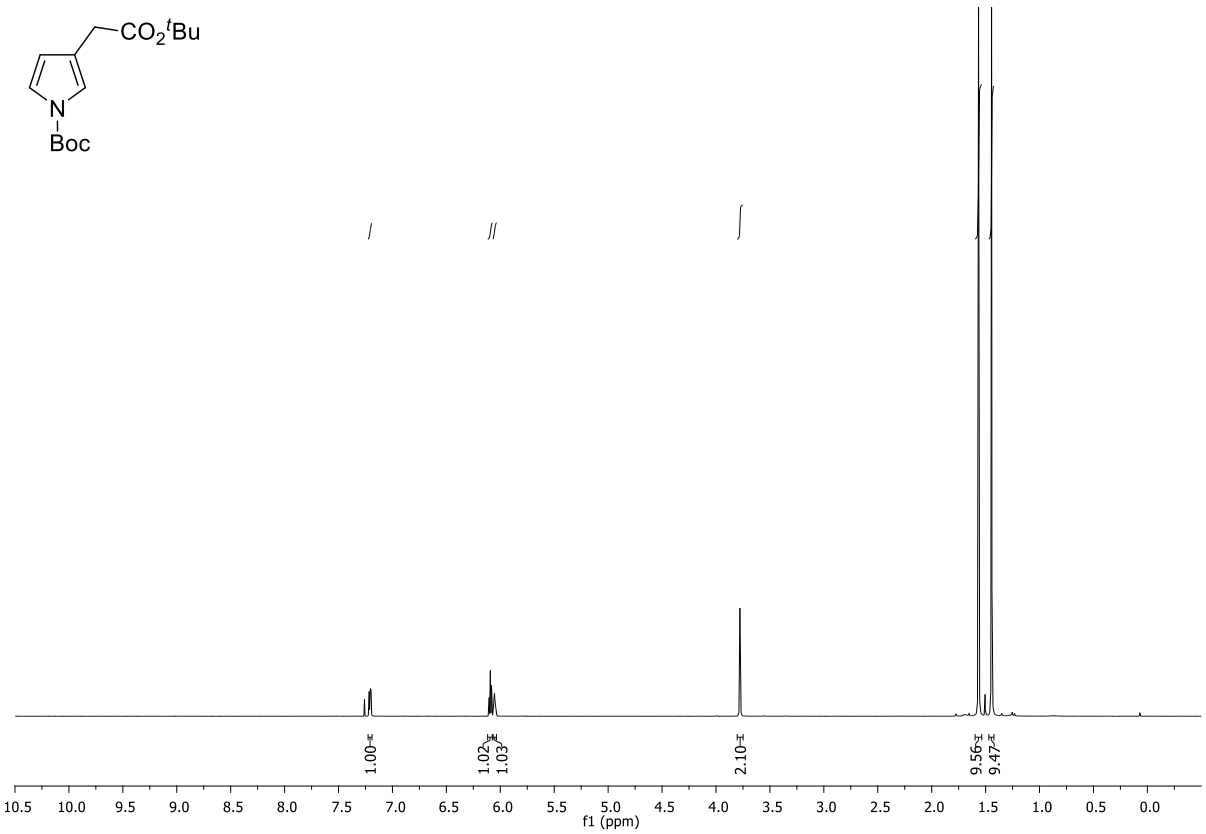

75 MHz, $CDCl_3$

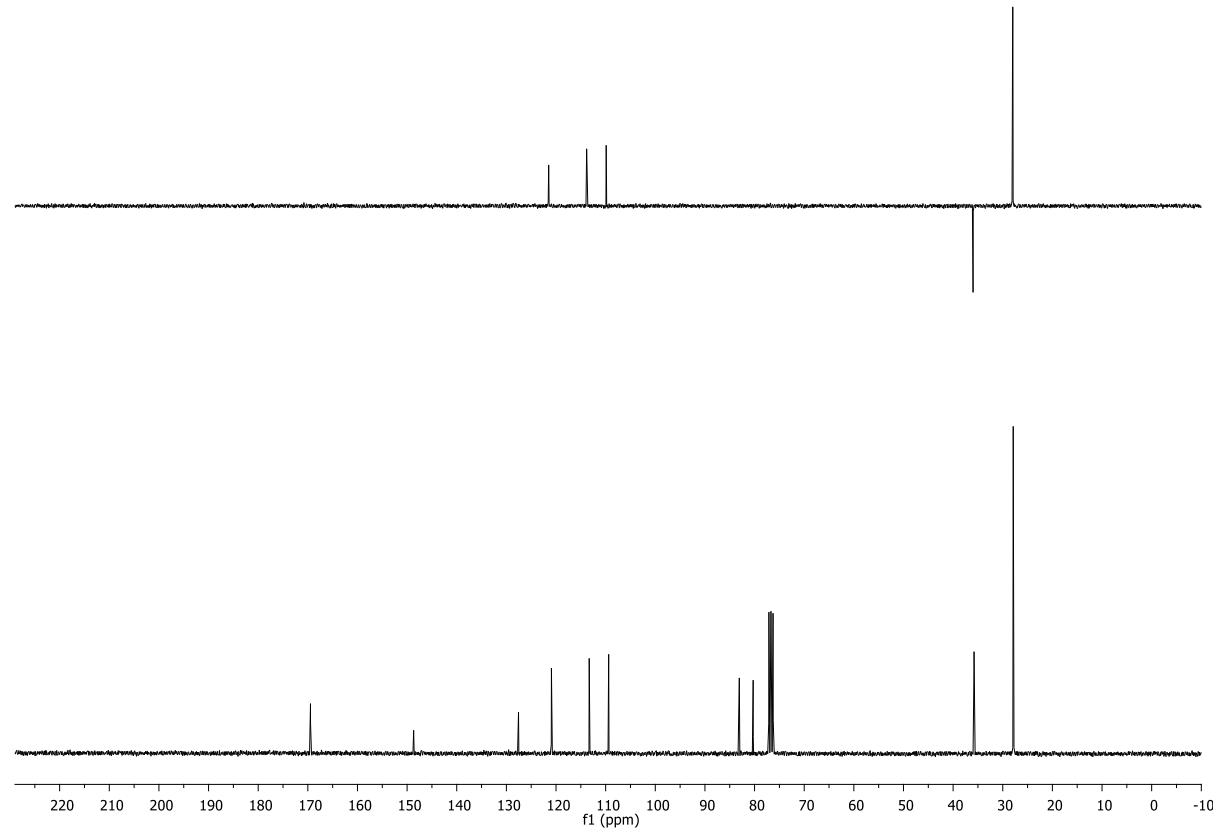

tert-butyl 3-(1-tert-butoxy-1,5-dioxohexan-2-yl)-1H-pyrrole-1-carboxylate (276)

300 MHz, $CDCl_3$

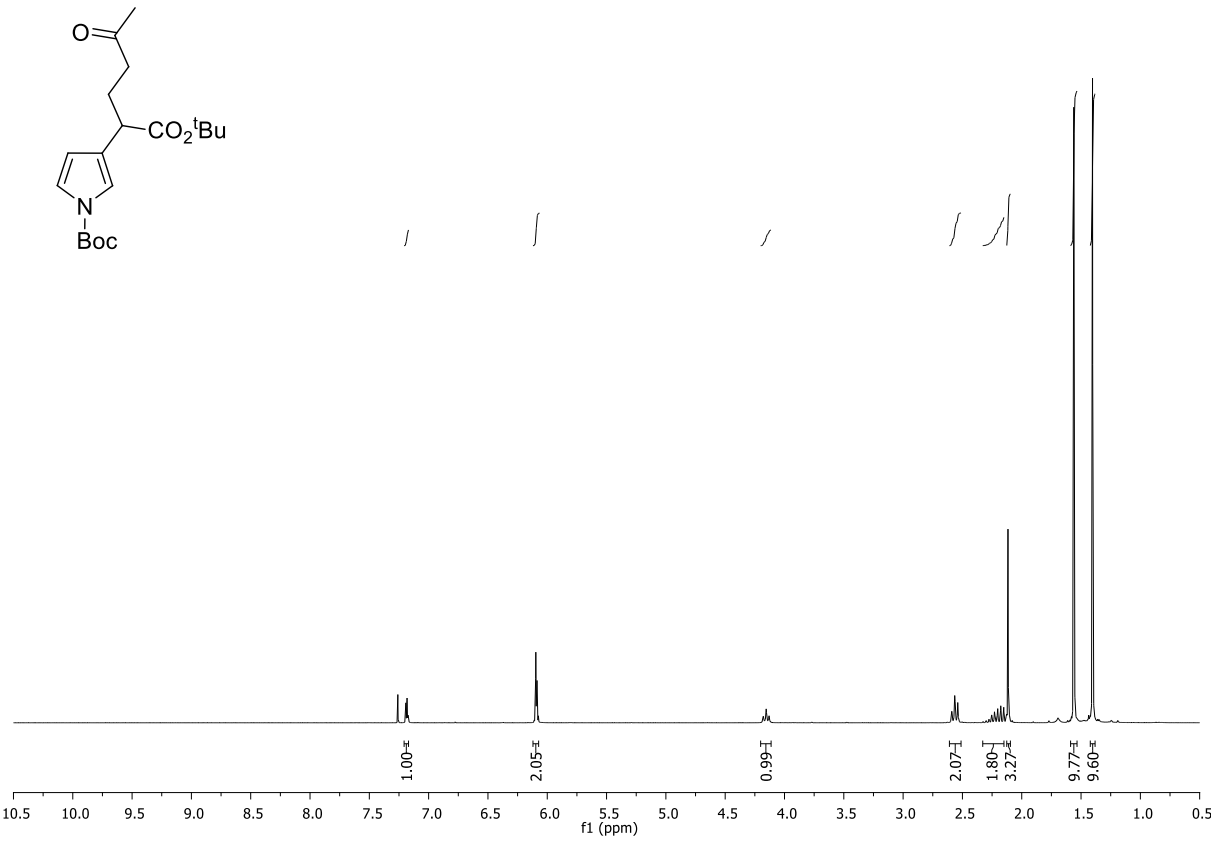

75 MHz, $CDCl_3$

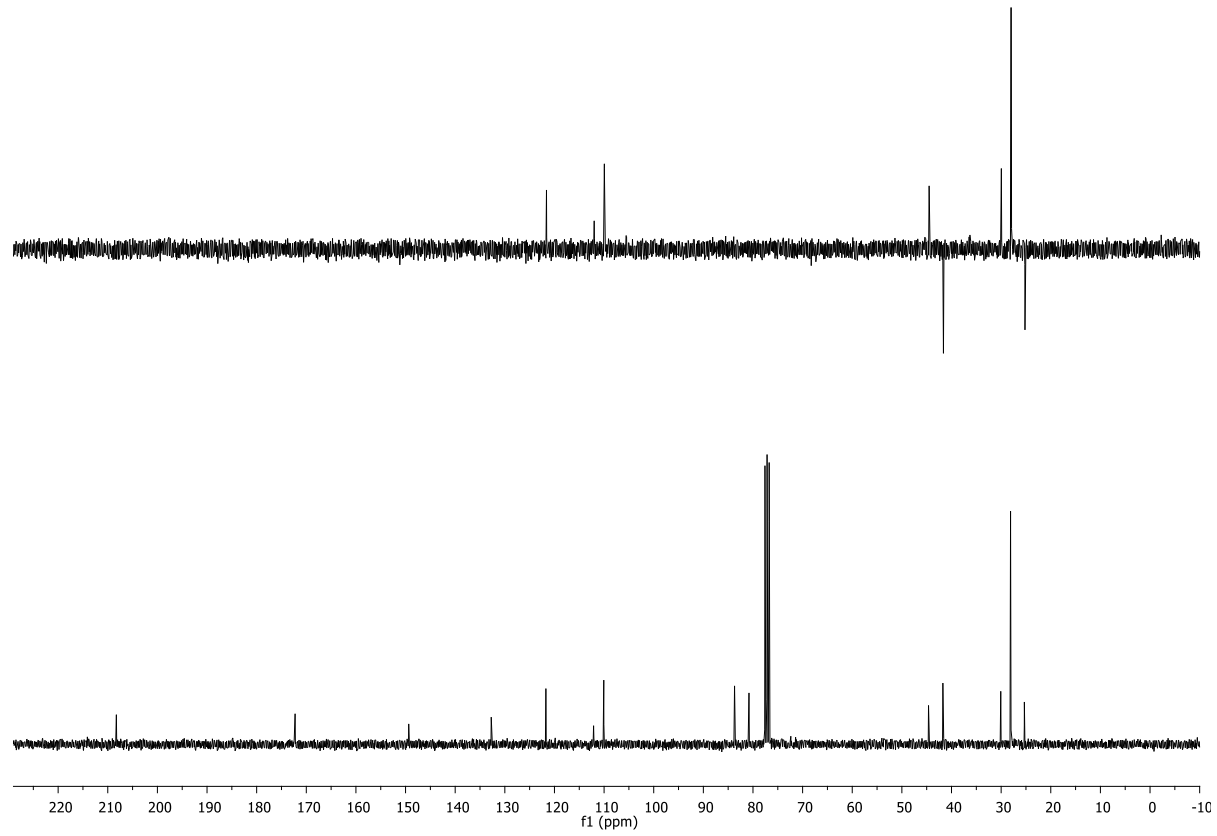

4-(5-(trimethylsilyl)pent-4-ynyl)pyridine (302)

300 MHz, $CDCl_3$

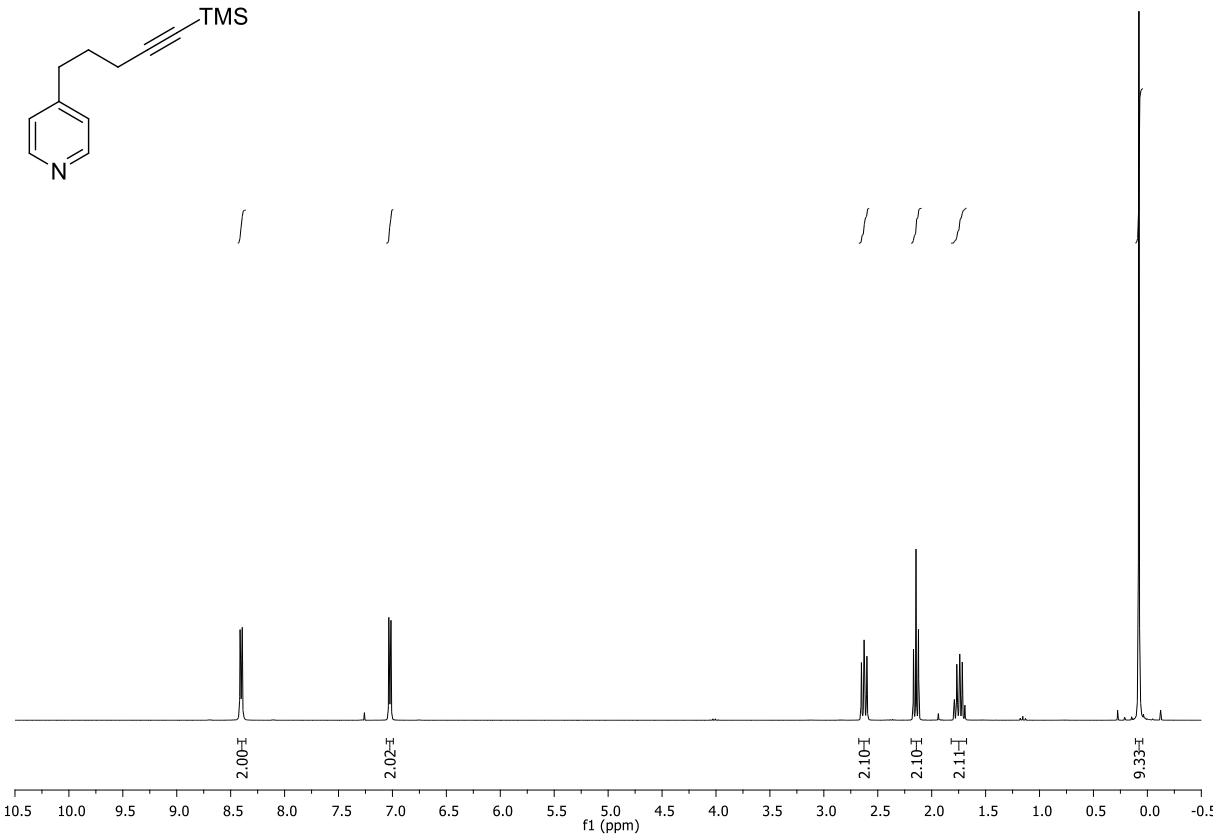

101 MHz, $CDCl_3$

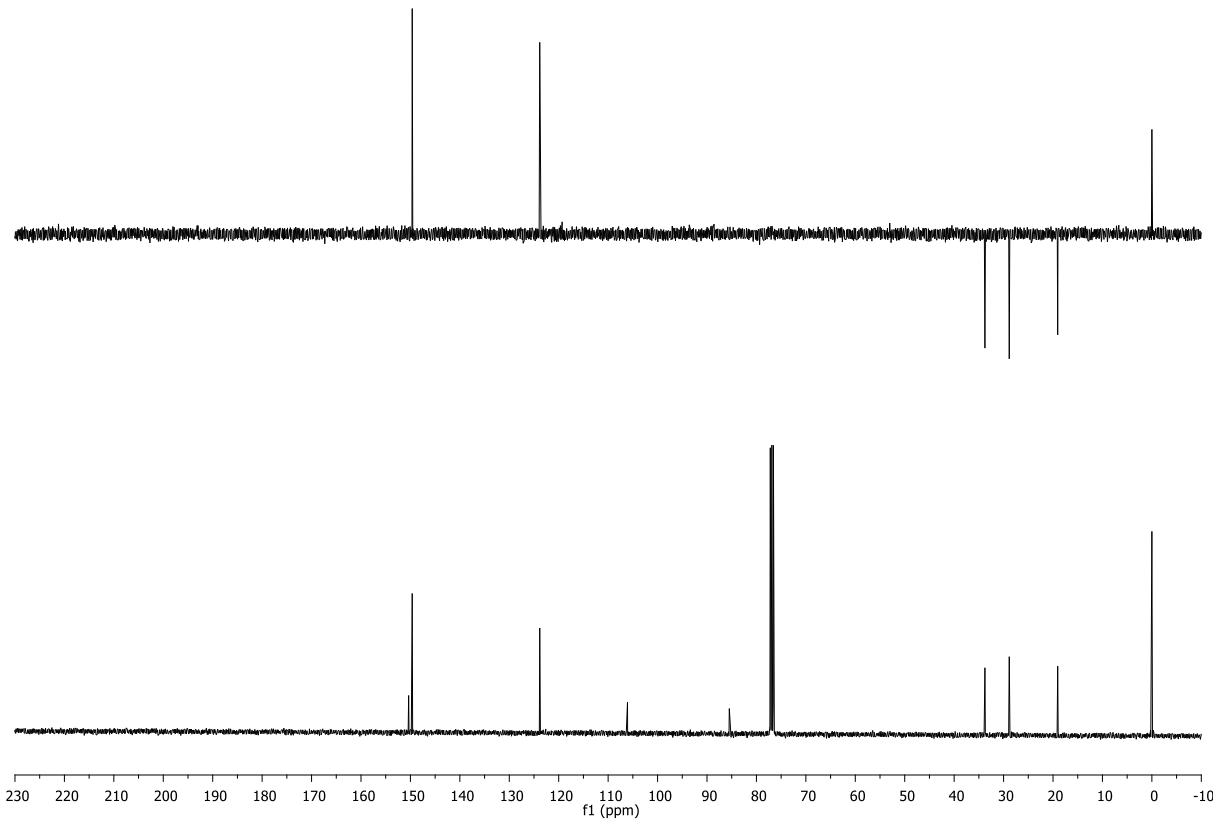

4-(5-(trimethylsilyl)pent-4-ynyl)pyridine 1-oxide (311)

300 MHz, $CDCl_3$

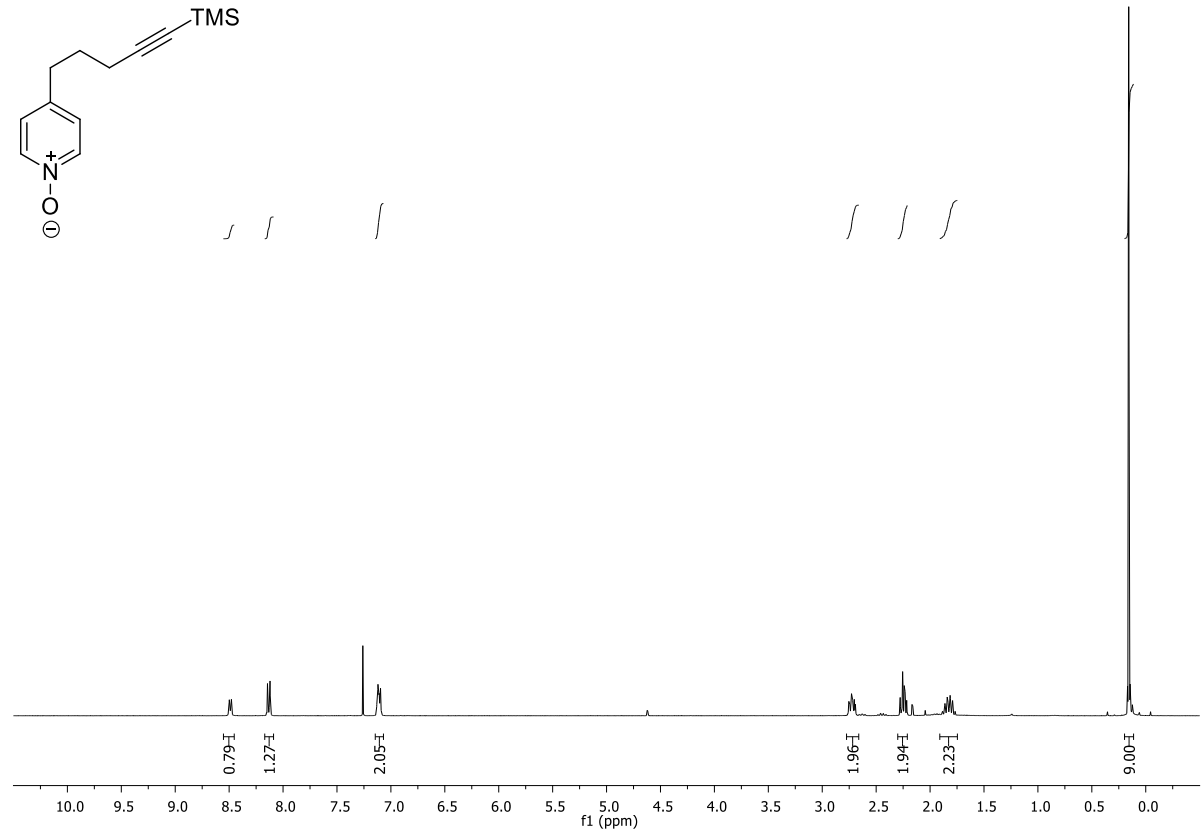

101 MHz, $CDCl_3$

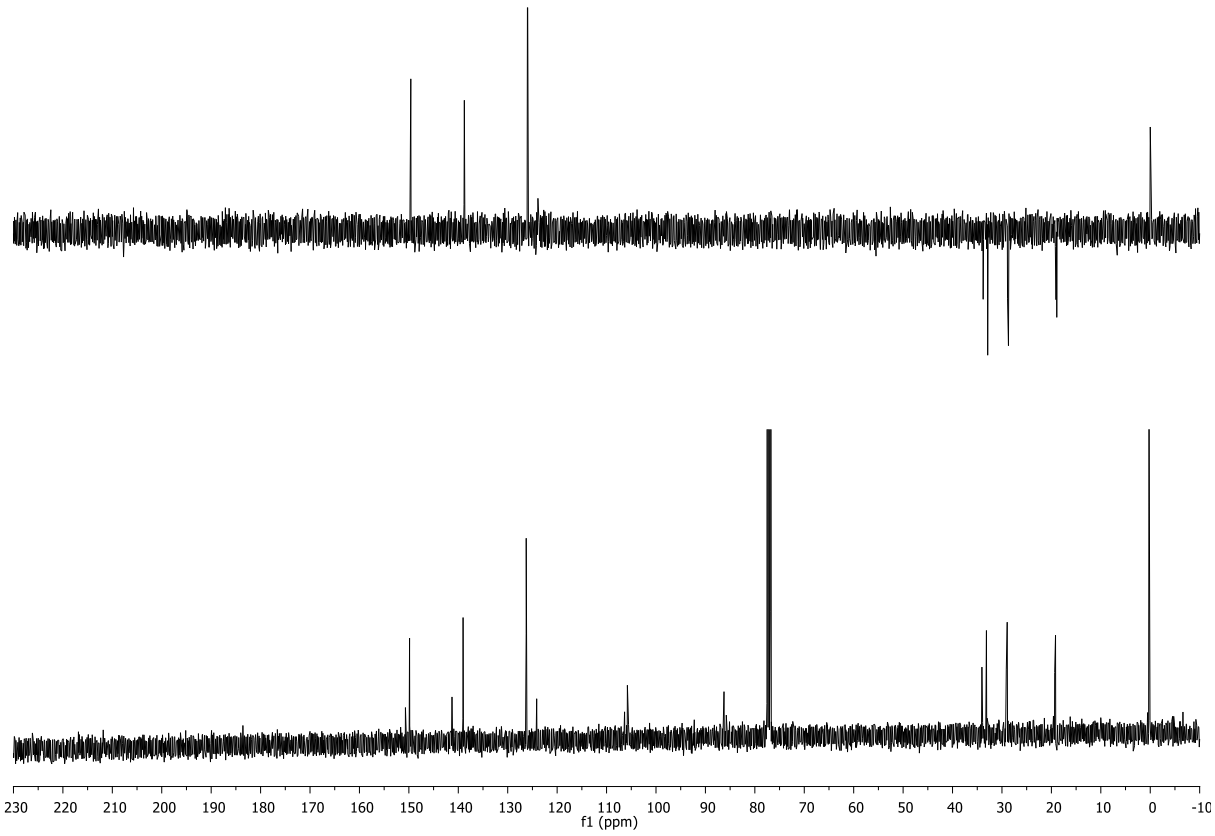

6-(trimethylsilyl)hex-5-yn-1-ol (314)

300 MHz, $CDCl_3$

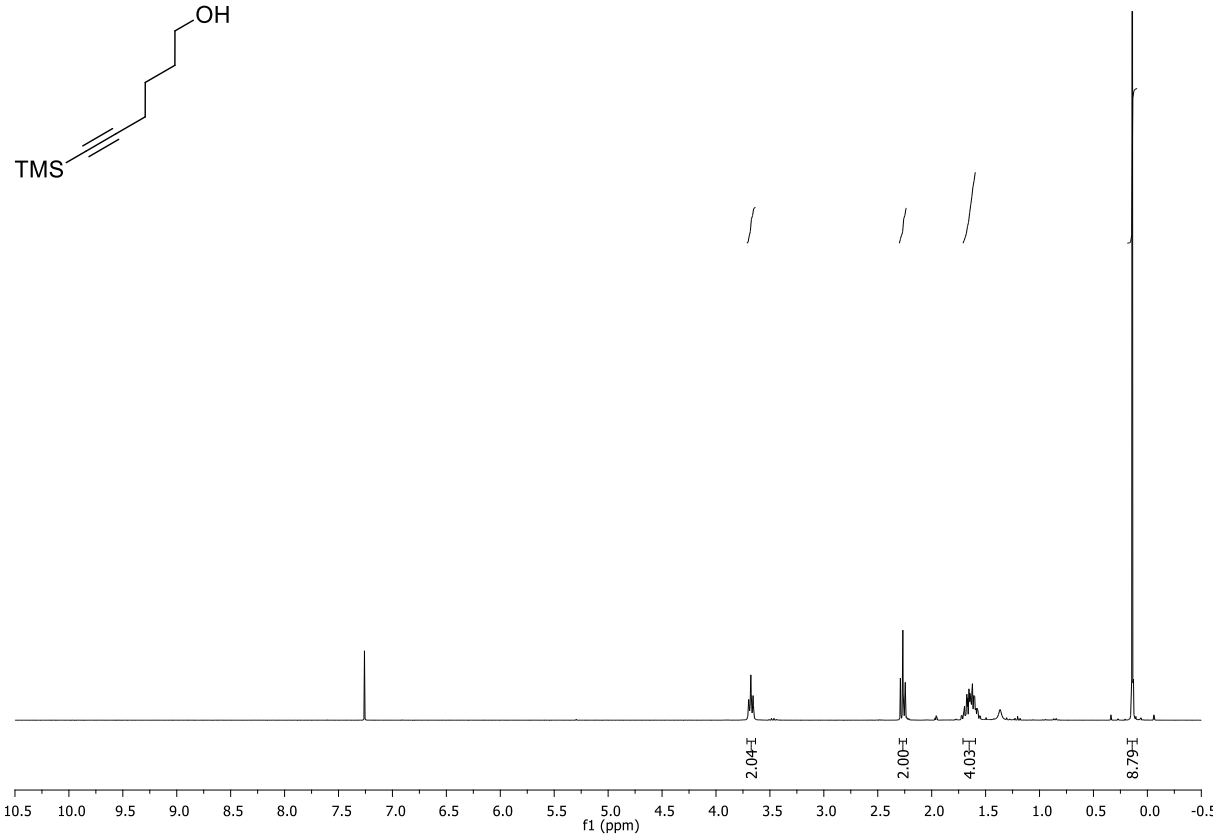

(6-iodohex-1-ynyl)trimethylsilane (315)

300 MHz, $CDCl_3$

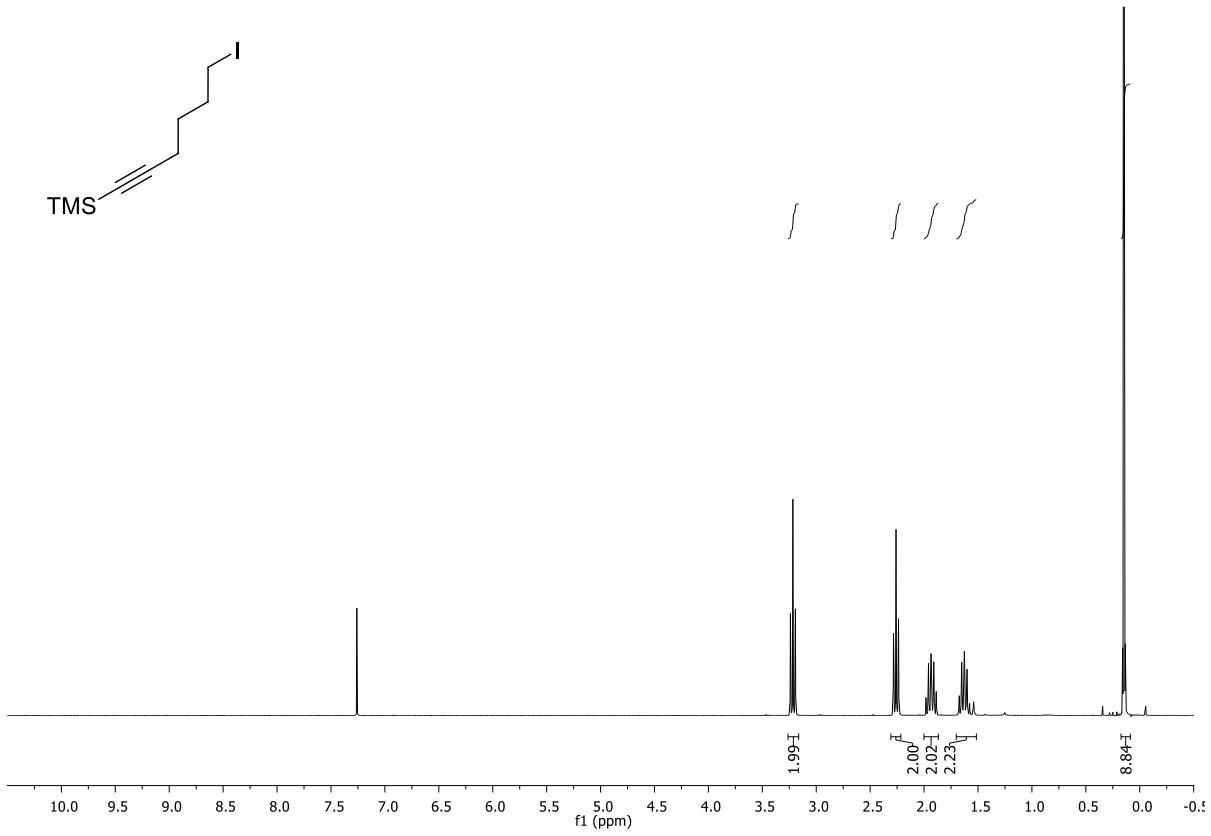

4-tert-butyl-4'-(7-(trimethylsilyl)hept-6-ynyl)-2,2'-bipyridine (317):

300 MHz, $CDCl_3$

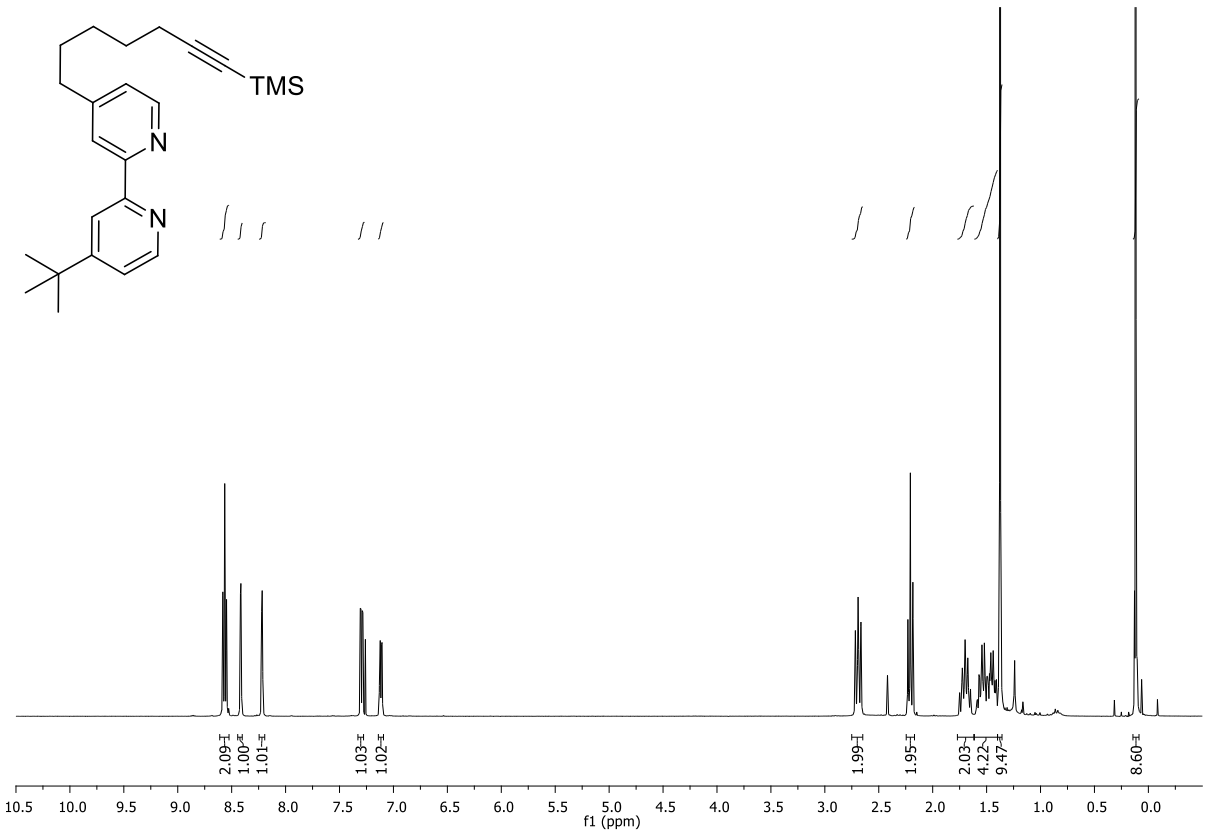

75 MHz, $CDCl_3$

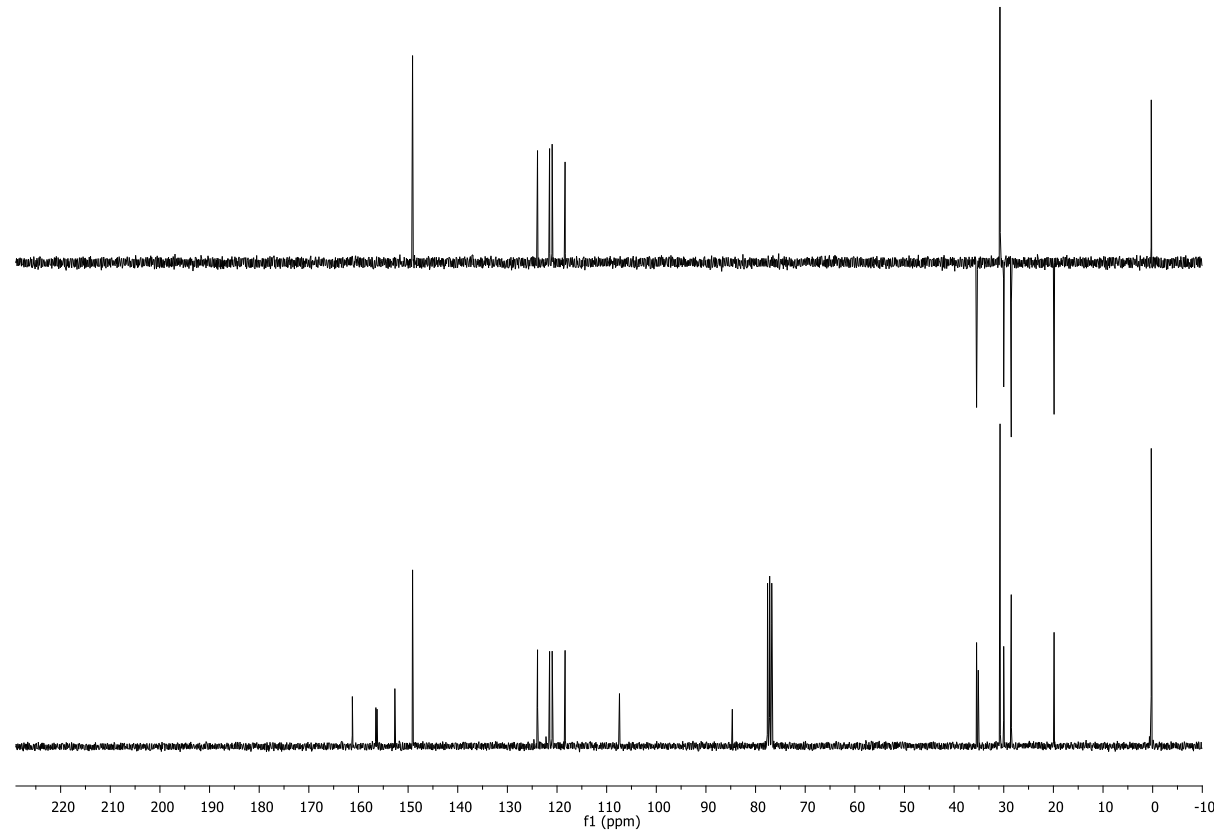

4-tert-butyl-4'-ethyl-2,2'-bipyridine (318)

300 MHz, $CDCl_3$

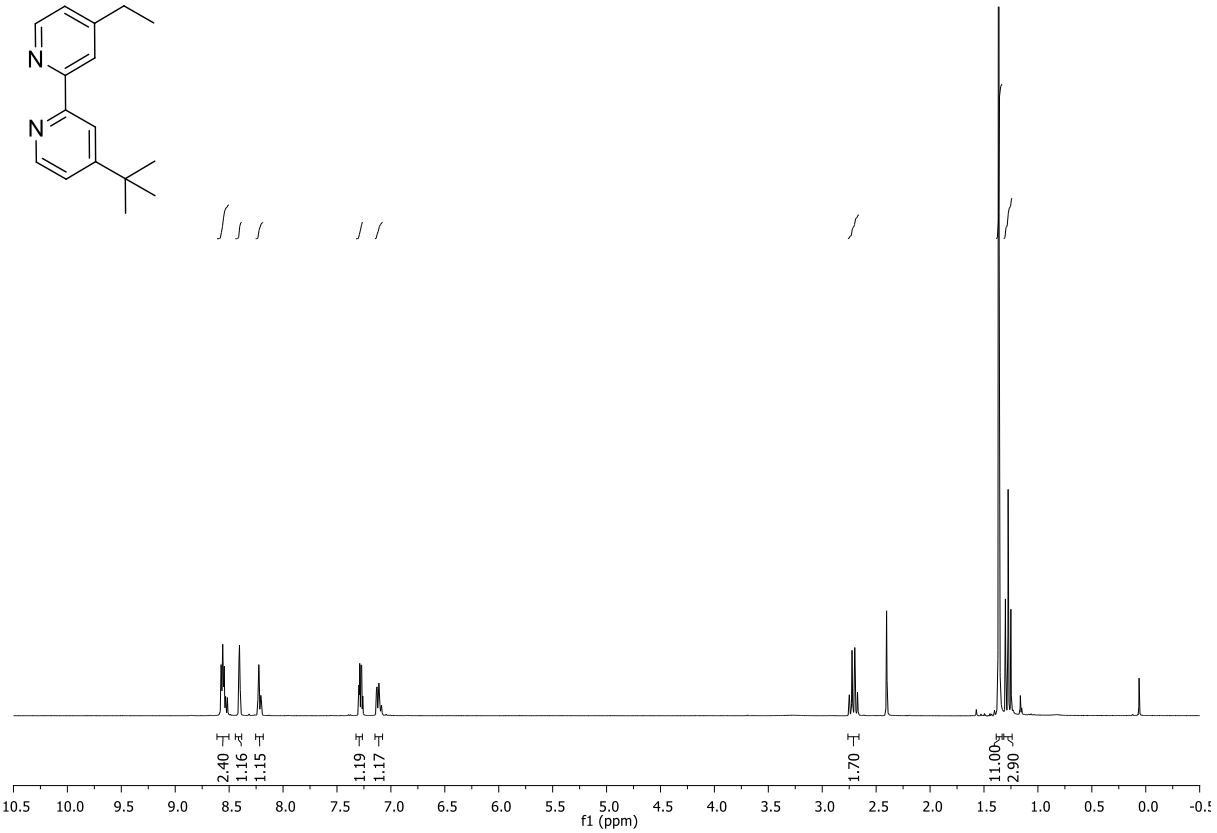

75 MHz, $CDCl_3$

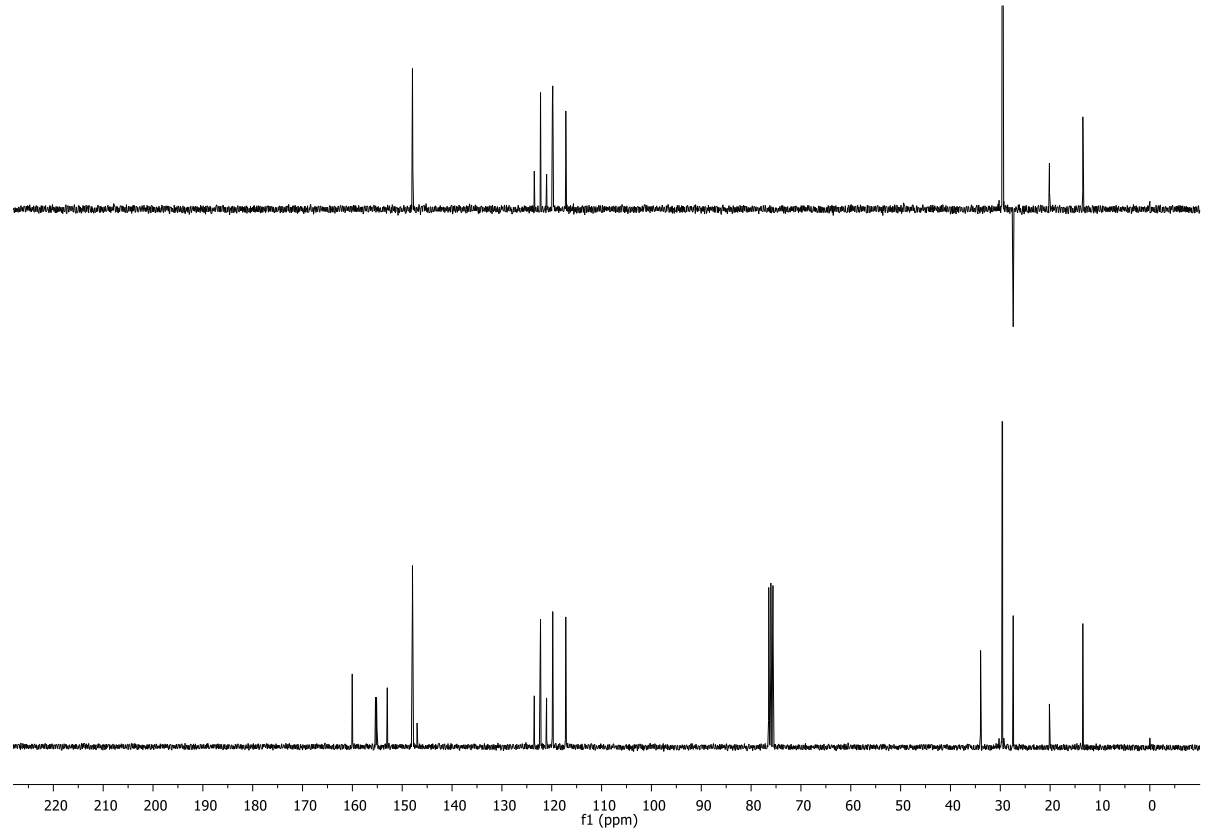

4,4'-di-tert-butyl-2,2'-bipyridine (319)

300 MHz, $CDCl_3$

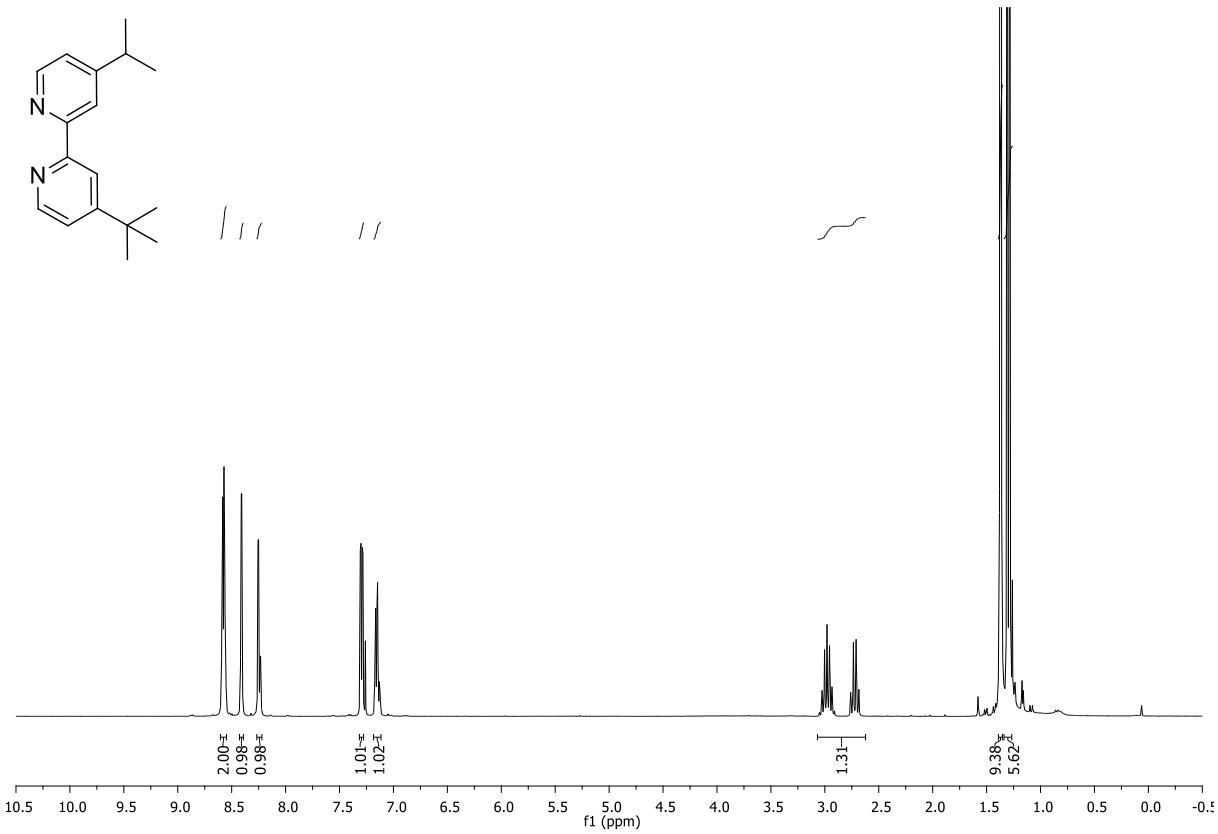

Bis(2-phenylpyridine-C^2,N')(4-tert-butyl-4'-(hept-6-ynyl)-2,2'-bipyridine)-2,2'-bipyridine)iridium hexafluorophosphate (323)

300 MHz, acetone

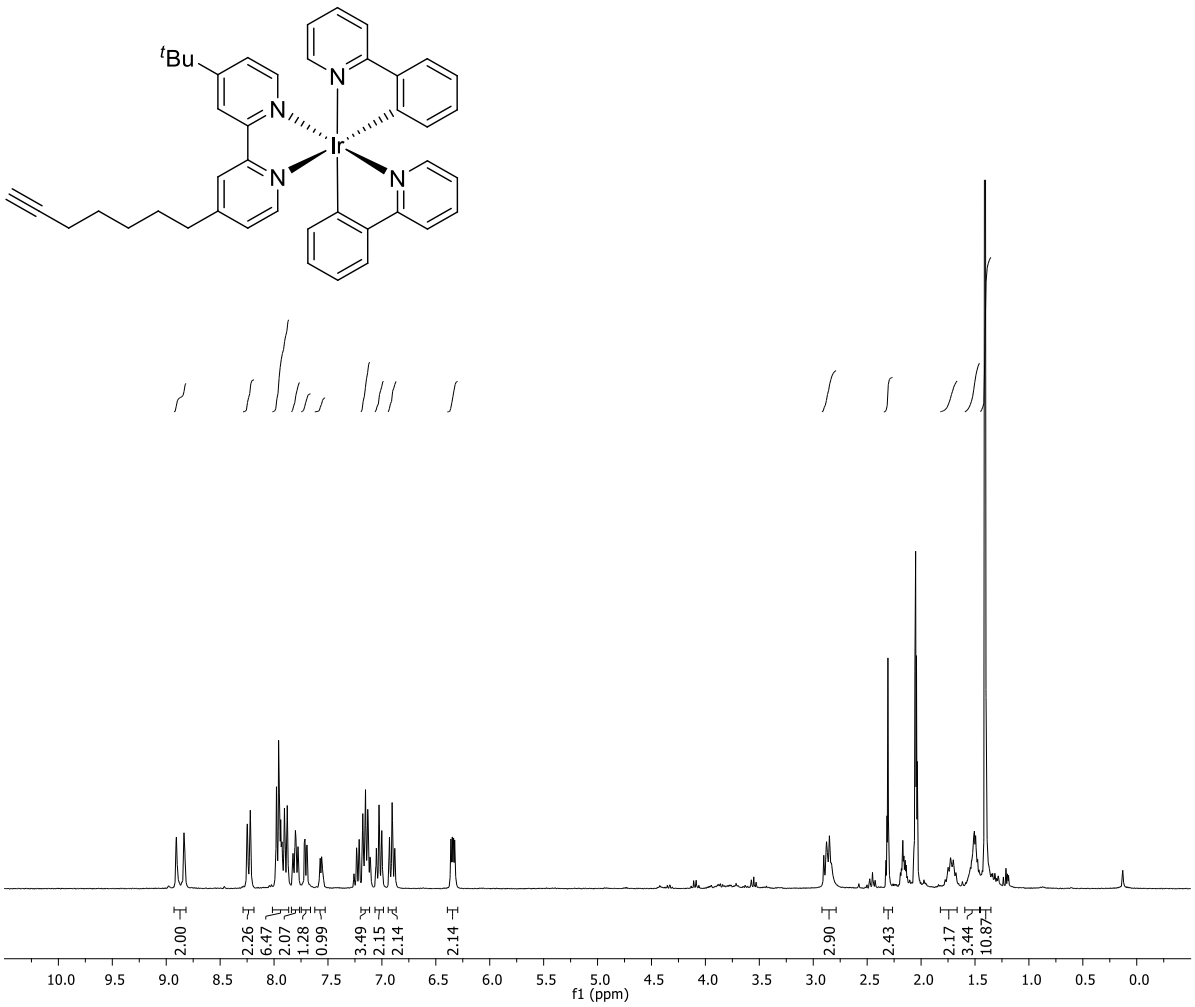

2. GC Spectra

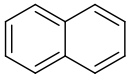 retention time: 3.59 min

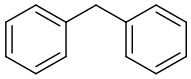 retention time: 5.12 min

one out of three runs is shown here. The given yield in Chapter 5.4 is the average of three runs. Calibration was provided by Viktor Kais.

Scheme 104 without silica: one out of three runs is shown here:

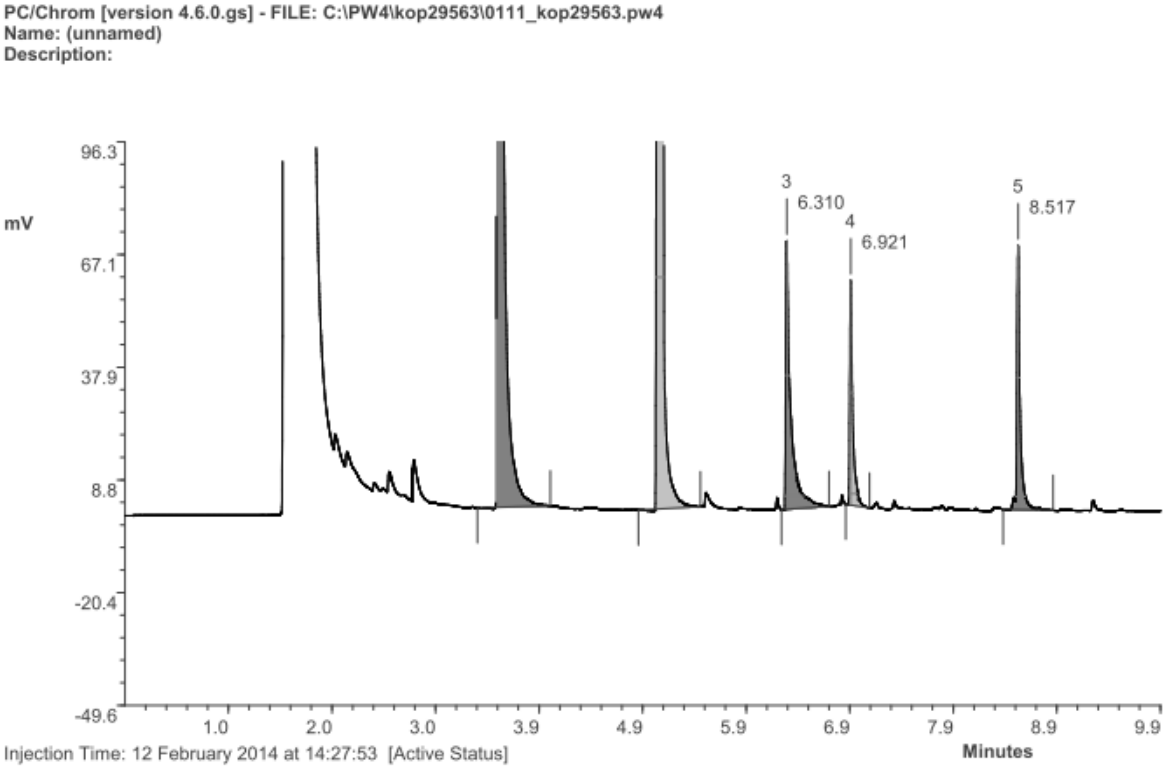

Peak	RT	Area	%Ar	Conc.(Ar)	Height	M	Units	Name
1	3.584	3362.658	44.13	Not Calculated	1198.987	1		
2	5.118	3772.156	49.50	Not Calculated	1199.402	1		
3	6.310	228.728	3.00	Not Calculated	69.428	1		
4	6.921	113.793	1.49	Not Calculated	58.062	1		
5	8.517	143.121	1.88	Not Calculated	68.302	1		

Scheme 104 with silica:

PC/Chrom [version 4.6.0.gs] - FILE: C:\PW4\kop29563\0109_kop29563.pw4
Name: (unnamed)
Description:

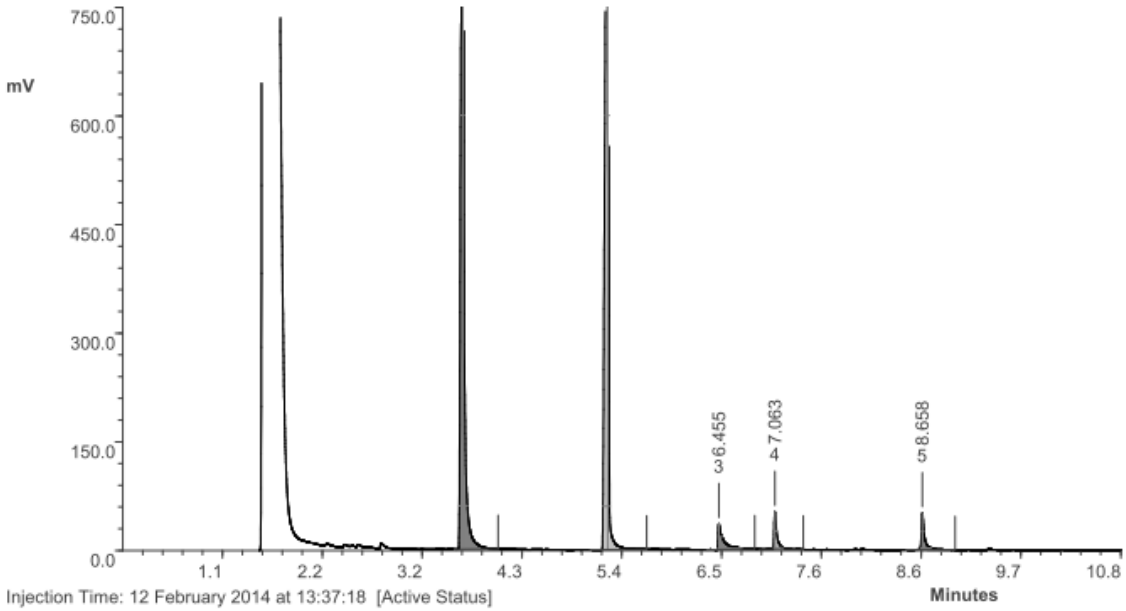

Injection Time: 12 February 2014 at 13:37:18 [Active Status]
Type: AUTOINJ Injection Number: 109 Channel: Channel A Acquisition Rate: 16Hz
Method File: C:\PW4\kop29563\0001_kop29563.mth Baseline noise: (not calculated)
Standard File: (none) Sequence File: C:\PW4\kop29563\kop29563.seq

Peak	RT	Area	%Ar	Conc.(Ar)	Height	M	Units	Name
1	3.683	3049.193	44.89	Not Calculated	1198.921	1		
2	5.254	3368.838	49.59	Not Calculated	1199.370	1		
3	6.455	142.246	2.09	Not Calculated	35.229	1		
4	7.063	115.935	1.71	Not Calculated	51.566	1		
5	8.658	116.987	1.72	Not Calculated	50.276	1		

Table 26 run 1:

PC/Chrom [version 4.6.0.gs] - FILE: C:\PW4\kop29563\0113_kop29563.pw4
Name: (unnamed)
Description:

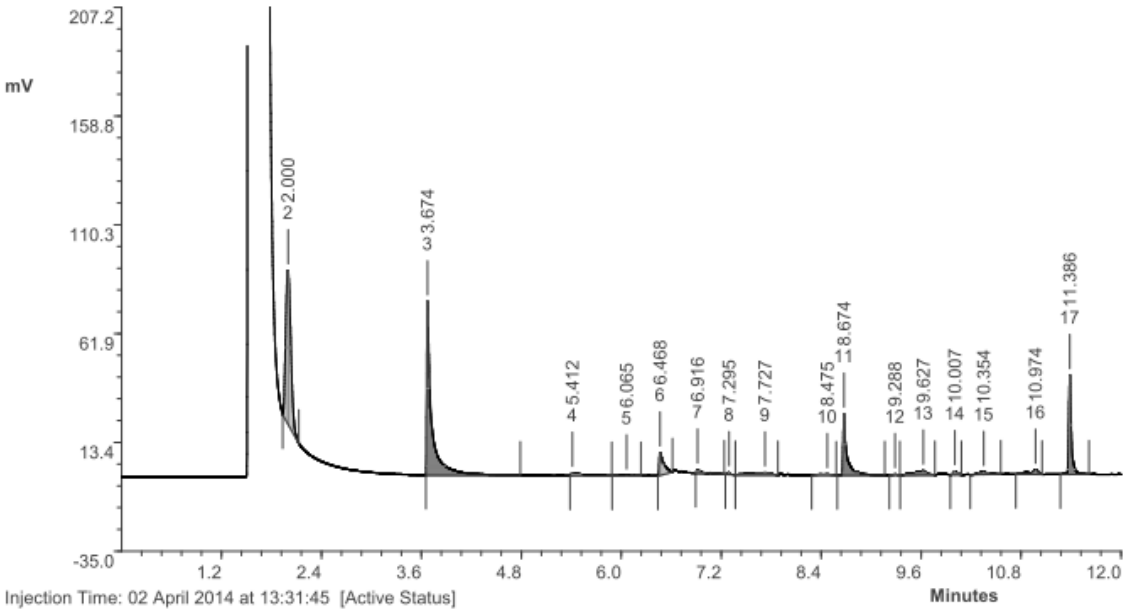

Injection Time: 02 April 2014 at 13:31:45 [Active Status]
Type: AUTOINJ Injection Number: 113 Channel: Channel A Acquisition Rate: 16Hz
Method File: C:\PW4\kop29563\0001_kop29563.mth Baseline noise: (not calculated)
Standard File: (none) Sequence File: C:\PW4\kop29563\kop29563.seq

Peak	RT	Area	%Ar	Conc.(Ar)	Height	M	Units	Name
1	1.522	72.081	7.40	Not Calculated	256.553	0		
2	2.000	290.971	29.86	Not Calculated	68.393	0		
3	3.674	306.559	31.46	Not Calculated	77.308	0		
4	5.412	12.241	1.26	Not Calculated	1.267	0		
5	6.065	1.539	0.16	Not Calculated	0.150	0		
6	6.468	39.217	4.02	Not Calculated	10.172	0		
7	6.916	6.946	0.71	Not Calculated	1.539	0		
8	7.295	1.530	0.16	Not Calculated	0.927	0		
9	7.727	13.193	1.35	Not Calculated	1.010	0		
10	8.475	5.055	0.52	Not Calculated	0.526	0		
11	8.674	84.906	8.71	Not Calculated	27.372	0		
12	9.288	0.999	0.10	Not Calculated	0.387	0		
13	9.627	17.028	1.75	Not Calculated	1.833	0		
14	10.007	4.938	0.51	Not Calculated	1.527	0		
15	10.354	9.505	0.98	Not Calculated	1.086	0		
16	10.974	13.099	1.34	Not Calculated	1.927	0		
17	11.386	94.562	9.70	Not Calculated	44.230	0		

Table 26 run 2:

PC/Chrom [version 4.6.0.gs] - FILE: C:\PW4\kop29563\0117_kop29563.pw4
Name: (unnamed)
Description:

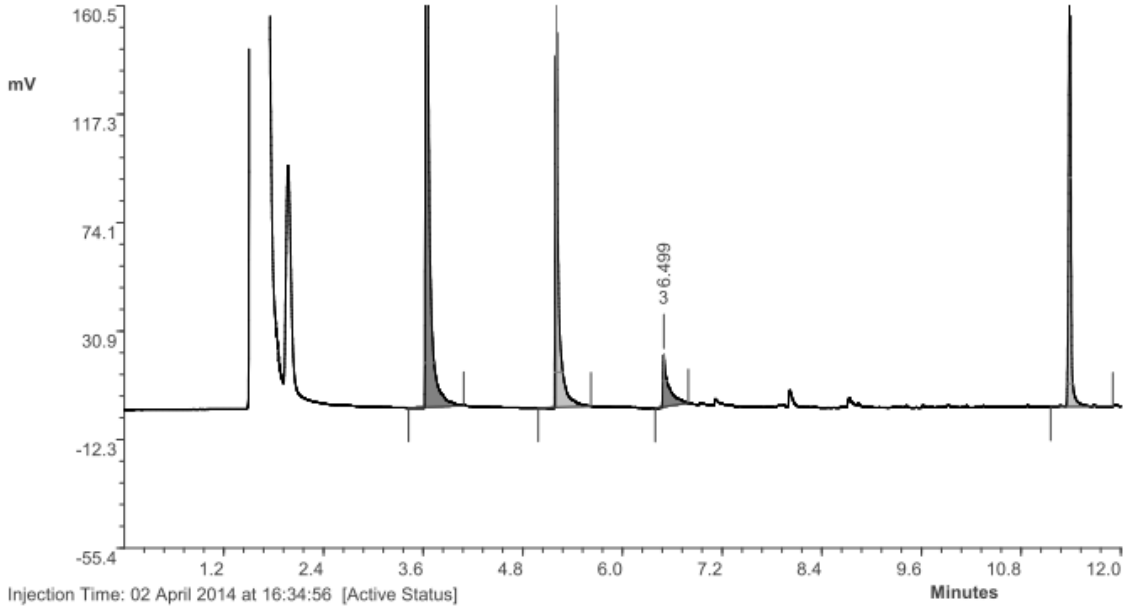

Injection Time: 02 April 2014 at 16:34:56 [Active Status]
Type: AUTOINJ Injection Number: 117 Channel: Channel A Acquisition Rate: 16Hz
Method File: C:\PW4\kop29563\0001_kop29563.mth Baseline noise: (not calculated)
Standard File: (none) Sequence File: C:\PW4\kop29563\kop29563.seq

Peak	RT	Area	%Ar	Conc.(Ar)	Height	M	Units	Name
1	3.641	876.759	47.76	Not Calculated	351.493	1		
2	5.202	525.815	28.64	Not Calculated	279.391	1		
3	6.499	93.269	5.08	Not Calculated	20.510	1		
4	11.389	339.837	18.51	Not Calculated	182.350	1		

Table 27, run 1:

PC/Chrom [version 4.6.0.gs] - FILE: C:\PW4\kop29563\0121_kop29563.pw4
Name: (unnamed)
Description:

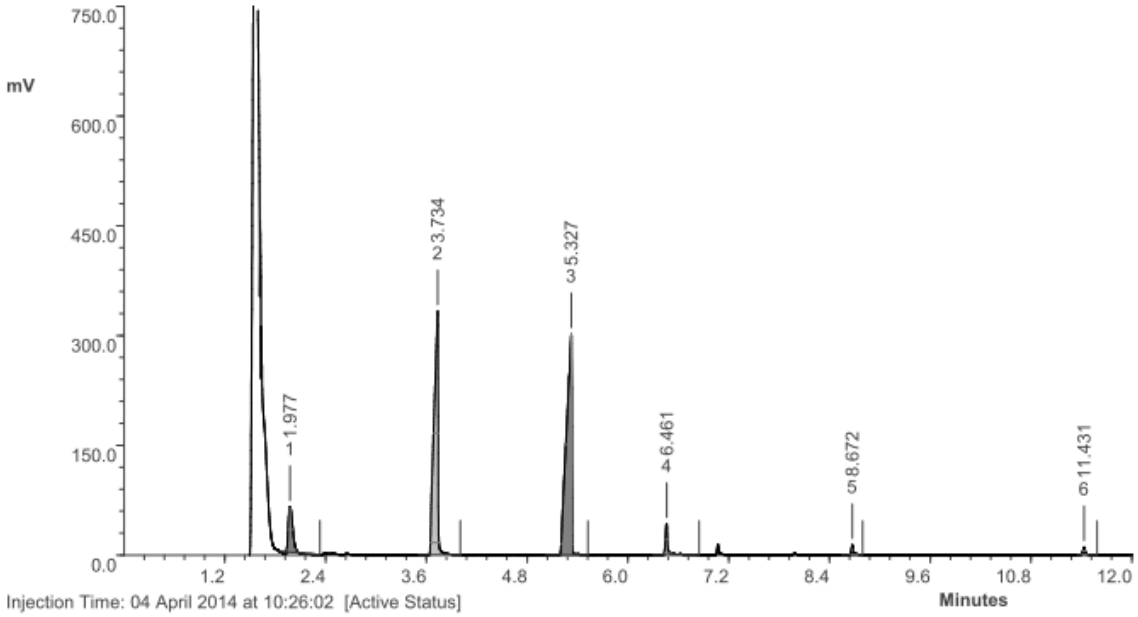

Injection Time: 04 April 2014 at 10:26:02 [Active Status]
Type: AUTOINJ Injection Number: 121 Channel: Channel A Acquisition Rate: 16Hz
Method File: C:\PW4\kop29563\0001_kop29563.mth Baseline noise: (not calculated)
Standard File: (none) Sequence File: C:\PW4\kop29563\kop29563.seq

Peak	RT	Area	%Ar	Conc.(Ar)	Height	M	Units	Name
1	1.977	200.164	7.29	Not Calculated	61.495	1		
2	3.734	1122.848	40.92	Not Calculated	332.800	1		
3	5.327	1299.410	47.35	Not Calculated	301.204	1		
4	6.461	80.099	2.92	Not Calculated	41.976	1		
5	8.672	22.320	0.81	Not Calculated	13.447	1		
6	11.431	19.407	0.71	Not Calculated	10.398	1		

Table 27, run 2:

PC/Chrom [version 4.6.0.gs] - FILE: C:\PW4\kop29563\0124_kop29563.pw4
Name: (unnamed)
Description:

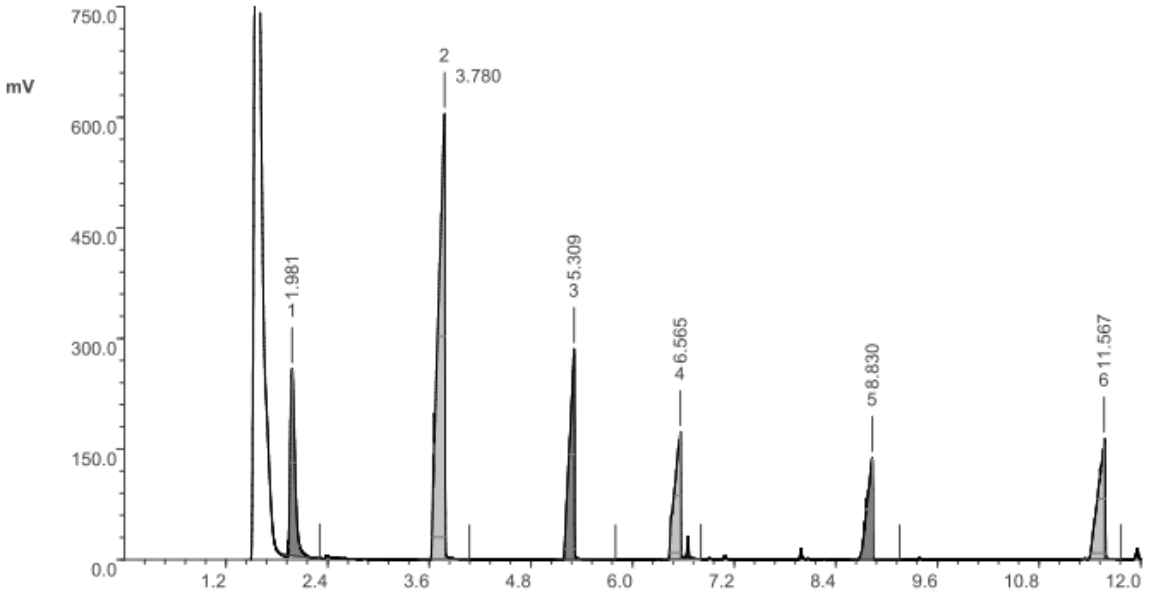

Injection Time: 08 April 2014 at 10:39:47 [Active Status]
Type: AUTOINJ Injection Number: 124 Channel: Channel A Acquisition Rate: 16Hz
Method File: C:\PW4\kop29563\0001_kop29563.mth Baseline noise: (not calculated)
Standard File: (none) Sequence File: C:\PW4\kop29563\kop29563.seq

Peak	RT	Area	%Ar	Conc.(Ar)	Height	M	Units	Name
1	1.981	984.518	12.64	Not Calculated	252.665	1		
2	3.780	3174.751	40.77	Not Calculated	604.033	1		
3	5.309	1124.331	14.44	Not Calculated	285.372	1		
4	6.565	919.094	11.80	Not Calculated	171.867	1		
5	8.830	625.461	8.03	Not Calculated	137.396	1		
6	11.567	958.702	12.31	Not Calculated	163.689	1		

Table 27, run 3:

PC/Chrom [version 4.6.0.gs] - FILE: C:\PW4\kop29563\0127_kop29563.pw4
Name: (unnamed)
Description:

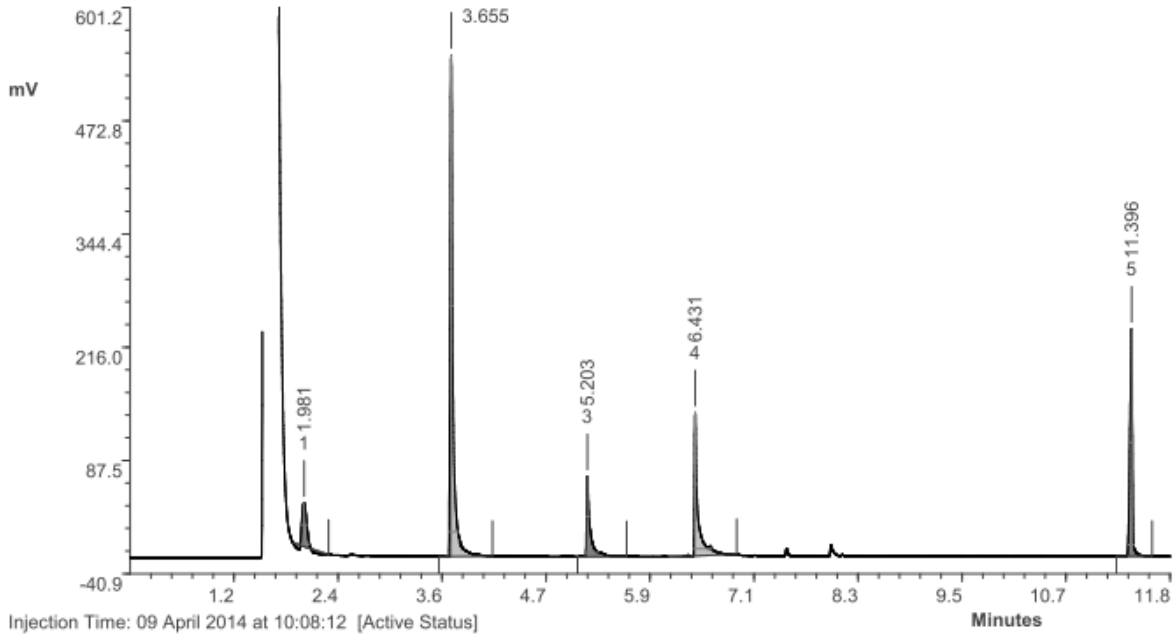

Injection Time: 09 April 2014 at 10:08:12 [Active Status]
Type: AUTOINJ Injection Number: 127 Channel: Channel A Acquisition Rate: 16Hz
Method File: C:\PW4\kop29563\0001_kop29563.mth Baseline noise: (not calculated)
Standard File: (none) Sequence File: C:\PW4\kop29563\kop29563.seq

Peak	RT	Area	%Ar	Conc.(Ar)	Height	M	Units	Name
1	1.981	137.575	5.25	Not Calculated	48.868	1		
2	3.655	1290.044	49.20	Not Calculated	568.669	1		
3	5.203	248.963	9.50	Not Calculated	90.815	1		
4	6.431	442.943	16.89	Not Calculated	162.375	1		
5	11.396	502.368	19.16	Not Calculated	257.407	1		

3. List of Abbreviations

A	acceptor
ATR	attenuated total reflection
Bn	benzyl
Boc	tert-butyloxycarbonyl
bp	boiling point
bpy	2,2'-bipyridine
bpz	2,2'-bipyrazine
CAN	ceric ammonium nitrate
conc.	concentrated
CT	charge transfer
d	day(s)
D	donor
dap	dianisol phenantrolin
DCM	dichloromethane
DDQ	2,3-dichloro-5,6-dicyano-1,4-benzoquinone
$dF(CF_3)ppy$	2-(2,4-difluorophenyl)-5-trifluoromethylpyridine
DIPEA	N,N-diisopropylethylamine
DMA	dimethylacetamide
DMF	dimethylformamide
d. r.	diastereomeric ratio
dtbbpy	4,4'-di-tert-butyl-2,2'-bipyridine
EA	ethyl acetate
ee	enantiomeric excess
Et	ethyl
FT	Fourier transformation
GC	gas chromatography
h	hour
HRMS	high resolution mass spectrometry
^{i}Pr	*iso*-propyl
^{i}PrOH	iso-propyl alcohol
IR	infrared spectroscopy
LAH	lithium aluminum hydride
LC	liquid chromatography
LDA	Lithium diisopropylamide
LMCT	ligand to metal charge transfer
Me	methyl
min	minute(s)
MLCT	metal to ligand charge transfer
mp	melting point
MS	mass spectrometry
MeCN	acetonitrile
MeI	methyl iodine
MV	methyl viologen
MVK	Methyl vinyl ketone
NBS	N-Bromosuccinimide
NMP	N-methylpyrrolidone
NMR	nuclear magnetic resonance
PE	petroleum ether
ph	phenyl
POM	polyoxometalates
ppm	parts per million
ppy	2-phenypyridine
quant.	quantitative
R	arbitrary residue
ref.	reference
sat.	saturated
SCE	saturated calomel electrode
TBAB	tetrabutylammonium bromide
TBADT	tetrabutylammonium decatungstate
TBHP	*tert*-butyl hydroperoxide
*t*Bu	*tert*-butyl

temp.	temperature
Tf	trifluoromethanesulfonate
TFA	trifluoroacetic acid
THF	tetrahydrofurane
TLC	thin layer chromatography
UV	ultra violet
vis.	visible
X	halogen atom

4. List of Publications

[1] Kohls, P.; Jadhav, D.; Pandey G. and Reiser O. **Visible Light Photoredox Catalysis: Generation and addition of N -Aryltetrahydroisoquinoline-Derived α-Amino Radicals to Michael Acceptors**, *Org. Lett.* **2012**, *14*, 672 – 675.

[2] Reiser, O.; Kachkovskyi, G.; Kais, V.; Kohls, P.; Paria, S.; Pirtsch, M.; Rackl, D.; Seo, H. **Homogeneous visible light-mediated photoredox catalysis other than ruthenium and iridium.** In *Chemical Photocatalysis* König B. Ed.; Walter de Gruyter: Berlin, Boston, **2013,** 247.

[3] Panlilioa, B. G.; Macabeo, A. P. G.; Knorn, M.; Kohls, P.; Richomme, P.; Kouam, S. F.; Gehle, D.; Krohn, K.; Franzblau, S. G.; Zhang, Q.; Aguinaldo, A. M. **A lanostane aldehyde from Momordica charantia**, *Phytochemistry Letters* **2012**, *5*, 682 – 684.

[4] Vidar, W. S.; Macabeo, A. P. G.; Knorn, M.; Kohls, P.; Aguinaldo, A. M. **Polymethoxylated flavones from Micromelum compressum**, *Biochemical Systematics and Ecology*, **2013**, *50*, 48.

[5] Lirio, S. B.; Macabeo, A. P. G.; Paragas, E. M.; Knorn, M.; Kohls, P.; Franzblau, S. G.; Wang, Y. Aguinaldo, A. M. **Antitubercular constituents from Premna odorata Blanco**, *Journal of Ethnopharmacology*, **2014**, *154*, 471 - 474.

5. Congresses and Scientific Meetings

Oral Contributions:

[1] GRK 1626 Kick-Off Meeting, Wildbad Kreuth (Germany),
April 2010:
Photoinduced 1,4-Addition of tertiary Amines and Michael Systems.

[2] 2nd INDIGO PhD Research Conference and Intensive Course, Donaustauf (Germany),
October 2010:
Visible Light Photoredox Catalysis: α-Coupling of Isoquinolines with Michael acceptors.

[3] GRK 1626 Annual Report Meeting, Prüfening (Germany),
April 2011:
Photocatalytical Conjugate Addition.

[4] 3rd INDIGO PhD Research Conference and Intensive Course, Chennai (India),
February 2012:
Photoredox Catalysis: Conjugate Addition.

[5] Industrial Green Chemical World Convention (IGCW), Mumbai (India),
December 2013:
Visible Light photons as a reagent in organic synthesis.

[6] GRK 1626 Annual Report Meeting, Kloster Kostenz (Germany),
April 2014:
Photochemical *N*-α-Activation

Poster Contributions:

[1] 12th Belgian Organic Synthesis Symposium, Namur (Belgium), July 2010:
Photoinduced Conjugate Additions Of Tertiary Amines.

[2] GDCh Conference „Photochemistry 2010“, Erlangen (Germany), September 2010:
Photoinduced Conjugate Additions Of Tertiary Amines.

[3] European Symposium on Organic Chemistry 2011, Chersonissos (Greece), July 2011
Carbon – Carbon Bond Formations by Photocatalytic Conjugate Addition.

[4] GDCh Wissenschaftsforum, Bremen (Germany), September 2011:
Photoinduced Conjugate Additions of Tertiary Amines.

[5] 4th EuChemMS Conference, Prague (Czech Republic), August 2012:
Visible light photoredox catalysis with N-α-radicals as intermediates.

[6] European Symposium on Organic Chemistry 2013, Marseilles (France), July 2013:
Visible light photoredox catalysis with N-α-radicals as intermediates.

6. Curriculum Vitea

M. Sc. **Paul Simon Kohls**

Unterislinger Weg 26
93053 Regensburg
p_kohls@hotmail.com

Personal Details:

date and place of birth:	June, 3rd 1985 in Aalen (Germany)
nationality:	German

Professional Record:

since 10/2010 **Research Assistant and Doctoral Student, University of Regensburg, Germany**
in the group of Prof. Dr. Oliver Reiser with the main focus on *Photocatalysis with visible light*. Including a three month research stay at NCL Pune (India) in the group of Dr. Ganesh Pandey.

Education:

10/2008 – 09/2010	**Master of Science, University of Regensburg, Germany**
	(M. Sc.) in Chemistry (Overall Grade: 1,3)
10/2005 – 09/2008	**Bachelor of Science, University of Regensburg,. Germany**
	(B. Sc.) in Chemistry (Overall Grade: 2,4)
07/2004 – 03/2005	**Basic Military Service**
	at Engineering School, München and PzGrenBtl. 52, Rothenburg/Fulda
09/1995 – 06/2004	**Allgemeine Hochschulreife (**equivalent to A-level**)**, **Aalen, Germany**
	at Kopernikus Gymnasium Wasseralfingen, (Overall Grade: 2,8)
07/2001 – 06/2002	**Highschool Exchange Year, Prairie du Chien, Wi, USA**
	at Prairie du Chien High-School

Scholarships and Awards:

12/2013	Nomination for the **Green Innovation Award 2013** given by **Industrial Green Chemical World**.
06/2011 – 05/2013	**Research Scholarship** according to the **Bayrischen Elitenförderungsgesetz** and **Member** of the **Elitenetzwerk Bayern**
since 2012	**Travel grant** by and **Membership** of the Indian-German Graduate School of Advanced Organic Synthesis for a Sustainable Future (**INDIGO**).
since 2010	**Research Scholarship** by and **Membership** of DFG research training group GRK 1626 *Chemical Photocatalysis.*

F. Acknowledgment - Danksagung

I am deeply grateful to Prof. Dr. Oliver Reiser for offering me a place in his research group, this challenging topic, our discussions on chemical problems, the opportunity to go abroad and all his support during my work.

Thanks to Dr. Peter Kreitmeier, Roxane Harteis, Helena Konkel, Brigitte Eichenseer, Georg Adolin and Klaus Döring, for your constant support, synthesizing starting materials, and for all your help on everyday problems. The same is true for our secretaries Young Rothermund, Hedwig Ohli and especially Antje Weigert.

All the coworkers in the analytical and NMR-department I would like to thank for the measurement of the compounds. Special thanks to Regina Hoheisel for the CV measurements and the good atmosphere in her lab.

Special thanks to my lab mates Julian Bodensteiner, Allan Patrick Macabeo, Matthias Knorn and Christian Faderl for the great lab atmosphere, the help and discussions on chemical and practical problems and the talks about non-chemical stuff! Steelpanther for life!

Thanks to Ludwig, Andreas O., Daniel R., Roland, Quirin, Soraia, Benni, Verena, Matze, Jimmy, Andreas B., Andreas K., Corina, Tom E., Sabine, Viktor, Saerom, Hana, Tom R., Daniel D., Francesca and all other current and former members of the Reiser group for the great atmosphere, the after work sessions and the barbeques. Especially I am very grateful to Daniel Rackl, Viktor Kais, Georgyi Kachkovskyi, Ludwig Pilsl, Klaus Harrar, Sebastian Wittmann and Michael Schwarz for their help and discussions on chemistry during this thesis.

Thanks to Ludwig Pilsl for providing the cyclopropanes, to Daniel Rackl for providing the bipyridine intermediate and the synthetic discussions about its functionalization and to Viktor Kais for providing a suitable screening reaction for the immobilized photoredox catalyst including the oxalic ester and the GC-calibrations.

For proof reading of this thesis I have to thank my lab mate Christian Faderl, Daniel Rackl, Sabine Kerres, Thomas Rawner and especially Sabine Möhle for their spent time and helpful remarks.

Matthias Neumann, Johannes Franz and Kirsten Zeitler deserve sincere thanks for great discussions on photochemistry and good advice.

I would like to thank all my Bachelor students and Forschungspraktikanten Christian Faderl, Matthias Lochner, Sai Puneet Desai, Sabine Möhle, Benjamin Kastl, Tobias Kahoun and Cornelia Herman for their work in the lab and their fruitful input.

I am grateful to Dr. Ganesh Pandey for offering me the chance to work in his labs at the NCL Pune and also to Deepak Jadhav, Priyanka Adate, Sandeep Tiwari, Ramakrishna Laha and Ankur Pandey for helping me getting stated and showing me the Indian way of life.

For financial support, great seminar days and for granting me a scholarship to start my PhD thesis I have to thank the GRK 1626 Chemical Photocatalysis. Furthermore I have to thank the Bavarian State for granting me a “Forschungstipendium nach dem Bayrischen Elitenförderungsgesetz.“ to pursue my PhD studies. Money was also provided by the INDIGO Network for my research stay in India and the GDCh to attend conferences which is also gratefully acknowledged.

My friends Quirin, Roland, Matthias, Christian, Dennis, Stefan, Steffen, Michel, Florian, Eva, Bernie, Lu and Micha deserve my gratitude for the great time we spend and all the stuff we did together.

Und zu guter letzt möchte ich ganz herzlich meiner Familie und meiner Freundin Sabine danken!
Für die ganze Unterstützung und die Geduld die ich in den letzten Jahren von euch erfahren durfte und dass ihr mich immer an mich geglaubt habt! Danke!

G. Declaration

Herewith I declare that this present thesis is a presentation of my original work prepared single-handed. Wherever contributions from others are involved, all of them are marked clearly, with reference to the literature, license, and acknowledgement of collaborative research.

Regensburg, 24.03.2015

Paul Kohls